Large-momentum effective theory

Xiangdong Ji[*]

Maryland Center for Fundamental Physics, Department of Physics, University of Maryland, College Park, Maryland 20742, USA
and Tsung-Dao Lee Institute, Shanghai Jiao Tong University, Shanghai 200240, China

Yizhuang Liu[†]

Tsung-Dao Lee Institute, Shanghai Jiao Tong University, Shanghai 200240, China
and Institute of Theoretical Physics, Jagiellonian University, 30-348 Kraków, Poland

Yu-Sheng Liu[‡]

Tsung-Dao Lee Institute, Shanghai Jiao Tong University, Shanghai 200240, China

Jian-Hui Zhang[§]

Center of Advanced Quantum Studies, Department of Physics, Beijing Normal University, Beijing 100875, China

Yong Zhao[¶]

Physics Department, Brookhaven National Laboratory Building 510A, Upton, New York 11973, USA
and Physics Division, Argonne National Laboratory, Lemont, Illinois 60439, USA

(published 30 August 2021)

Since the parton model was introduced by Feynman more than 50 years ago, much has been learned about the partonic structure of the proton through a large body of high-energy experimental data and dedicated global fits. However, limited progress has been made in calculating partonic observables such as the parton distribution function (PDFs) from the fundamental theory of strong interactions, quantum chromodynamics (QCD). Recently some advocated for a formalism, large-momentum effective theory (LaMET), through which one can extract parton physics from the properties of the proton traveling at a moderate boost factor such as $\gamma \sim 2$–5. The key observation behind this approach is that Lorentz symmetry allows the standard formalism of partons in terms of light-front operators to be replaced by an equivalent one with large-momentum states and time-independent operators of a universality class. With LaMET, the PDFs, generalized PDFs or generalized parton distributions, transverse-momentum-dependent PDFs, and light-front wave functions can all be extracted in principle from lattice simulations of QCD (or other nonperturbative methods) through standard effective field theory matching and running. Future lattice QCD calculations with exascale computational facilities could help one to understand the experimental data related to the hadronic structure, including those from the upcoming electron-ion colliders dedicated to exploring the partonic landscape of the proton. Here the progress made in the past few years in the development of the LaMET formalism and its applications is reviewed, with an emphasis on a demonstration of its effectiveness from initial lattice QCD simulations.

CONTENTS

[*]xji@umd.edu
[†]yizhuang.liu@uj.edu.pl
[‡]mestelqure@gmail.com
[§]zhangjianhui@bnu.edu.cn
[¶]yong.zhao@anl.gov

I. INTRODUCTION

The proton and neutron, collectively called the nucleon, are the basic building blocks of visible matter in the Universe today. Ever since they were discovered in laboratories nearly a century ago (Rutherford, 1919; Chadwick, 1932), their fundamental properties have been explored: from the determination of the spin through the specific heat of liquid hydrogen (Dennison, 1927) to the measurement of the magnetic moments (Estermann, Frisch, and Stern, 1933) to the extraction of their electromagnetic sizes through elastic electron scattering (Hofstadter, 1956). The most revealing discovery, however, came from the electron deep-inelastic scattering (DIS) on the proton and nuclei at Stanford Linear Accelerator Center (SLAC) in the late 1960s, in which the constituents of the proton and neutron, quarks (and later gluons), were discovered (Bloom *et al.*, 1969). Soon after, quantum chromodynamics (QCD), a quantum field theory (QFT) based on "color" SU(3) gauge symmetry, was established as the fundamental theory of strong interactions (Fritzsch, Gell-Mann, and Leutwyler, 1973; Gross and

Wilczek, 1973; Politzer, 1973), and of the internal structure of the nucleon as well (Thomas and Weise, 2001).

During the last 50 years, significant progress has been made in understanding the nucleon's internal structure in both experiment and theory. Multiple experimental facilities have been built to study high-energy collisions involving protons and nuclei, from which a large amount of experimental data has been accumulated. Based on the QCD factorization theorems (Collins, 2011a), which were derived from perturbative QCD analyses beyond Feynman's parton model (Feynman, 1972), the parton distribution functions (PDFs), which characterize the longitudinal-momentum distributions of quarks and gluons in hadrons moving at infinite momentum, have been obtained from global fits to these data (Harland-Lang *et al.*, 2015; Ball *et al.*, 2017; Gao, Harland-Lang, and Rojo, 2018; Hou *et al.*, 2019). A recent result of the phenomenological proton PDFs is shown in Fig. 1, where x is the momentum fraction of the proton carried by partons. The PDFs provide a comprehensive description of the quark and gluon content of the nucleon. On the theoretical frontier, the Euclidean path-integral formalism of QCD, combined with the lattice regularization and Monte Carlo simulations (Wilson, 1974), has offered a systematic way of performing *ab initio* calculations of nonperturbative strong interactions. The rapid rise in computational power and the development of intelligent numerical algorithms have made such a lattice QCD approach extremely successful in computing hadron spectroscopy, the strong coupling, hadronic form factors, etc., and even scattering phase shifts (Briceño, Dudek, and Young, 2018; Tanabashi *et al.*, 2018; Aoki *et al.*, 2020).

Despite these impressive achievements, we have not been able to systematically explain the partonic structure of the proton from first principles; more explicitly, we have not made fundamental progress in computing the quark and gluon distributions starting from the QCD Lagrangian; see Sec. I.C for a summary. There is actually a good reason behind it: The standard formulation of parton physics in literature (Sterman, 1993; Collins, 2011a) is accomplished
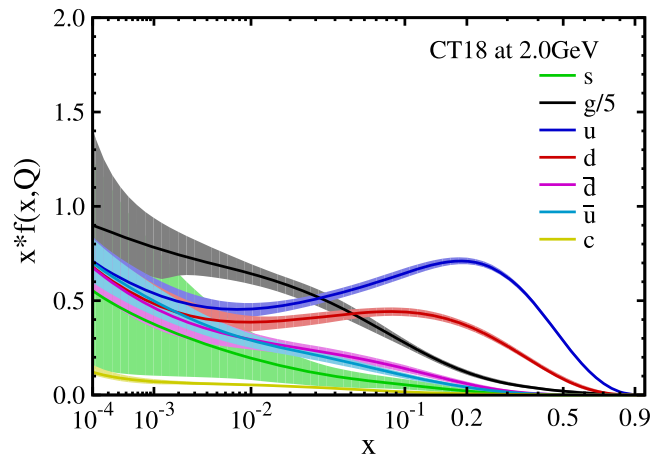

FIG. 1. Phenomenological parton distributions obtained by the CTEQ-TEA Collaboration (CT18) from fits to global high-energy scattering data, where $0 \leq x \leq 1$ is the fraction of the proton's infinite momentum carried in a parton. From Hou *et al.*, 2019.

through the *dynamical correlators* of quark and gluon fields on the light front (LF) defined by $t - z = $ const, which has the important feature of being independent of the proton's momentum. On the other hand, lattice QCD is formulated in the Euclidean space with imaginary time and cannot be used to directly calculate the dynamical correlations that depend on real time. The standard lattice approach to parton physics has been to calculate the lower moments of parton distributions, which are matrix elements of local operators (Lin *et al.*, 2018). However, limitations to the first few moments prohibit practitioners from reliably reproducing the x-dependent structure shown in Fig. 1, other than by fitting model functional forms. Over the years, Hamiltonian diagonalization in LF quantization (LFQ) (Brodsky, Pauli, and Pinsky, 1998) and Schwinger-Dyson equations (Maris and Roberts, 2003) have been proposed to solve the nucleon structure as Minkowskian approaches. Although significant advances have been made phenomenologically, a systematic approximation to calculating the nucleon PDFs is still missing.

A few years ago, some of us proposed a general approach to calculating x-dependent parton distributions based on Feynman's original idea about partons: They are the infinite-momentum limit of static properties of the proton at large momentum, and therefore are intrinsically Euclidean quantities accessible through lattice QCD (Ji, 2013, 2014; Ji, Zhang, and Zhao, 2013). Accordingly, parton physics in an intermediate range of $x_{\min} \sim 0.1 < x < x_{\max} \sim 0.9$ can be calculated from the physical properties of the proton at a moderately large momentum, such as that with a Lorentz boost factor $\gamma = 2$–5. The theory has been named large-momentum effective theory (LaMET) because a rigorous connection between the infinite-momentum frame (IMF) partons and quarks and gluons at a finite momentum requires a proper accounting of the ultraviolet (UV) modes with large momentum in effective field theory (EFT) and systematic power counting.

The basic principle for LaMET comes from an implicit observation in the naive parton model: The structure of the proton is approximately independent of its momentum so long as it is much larger than a typical strong-interaction scale Λ_{QCD} or its mass. For example, the quark momentum distribution at moderate x in the proton at $P = |\vec{P}| = 5$ GeV is not unlike that at $P = 50$ GeV or 5 TeV. One might call this phenomenon *large-momentum symmetry*, the nature of which is similar to that of the electronic structure of the hydrogen atom not being sensitive to the proton mass so long as it is much larger than that of the electron. The asymptotic behavior of the proton structure might be controlled by an expansion in Λ_{QCD}/P, but a justification would require a better understanding of the underlying dynamics. Assuming this, Feynman replaced the protons probed at large but finite momenta in high-energy scattering with the one at infinite momentum $P = \infty$, which corresponds to the leading term in the Λ_{QCD}/P expansion, and therefore the idealized concepts of the proton in the IMF and its constituents (*partons*) were born.

In QFTs, however, the existence of the $P = \infty$ limit depends on their UV behavior. In general, the infinite-momentum limit does not commute with the UV cutoff limit $\Lambda_{UV} \to \infty$. While the physical limit is $(\Lambda_{UV} \gg P) \to \infty$, the parton model and subsequent QCD factorization theorems use $(P \gg \Lambda_{UV}) \to \infty$, keeping all PDFs with the finite support $|x| \leq 1$, where negative x is for antiquarks. Thus, partons are an idealized concept that does not exist in the real world. Because of asymptotic freedom, the previously mentioned differences can be calculated in perturbative QCD. Therefore, LaMET is an effective theory for partons that uses the ordinary field theoretical calculations $(\Lambda_{UV} \gg P) \to \infty$ and systematically takes into account noncommuting $P \to \infty$ limits through EFT matching and running, and finite P effects by power corrections. Thus, the PDFs defined in the IMF or on the LF can be accessed at moderate x from the structure calculations at P of approximately a few GeVs.

The first application of LaMET was to the total gluon helicity ΔG in the polarized proton, a quantity of significant experimental interest at the polarized RHIC (Bunce *et al.*, 2000), but one that had not been within theoretical reach for many years. Ji, Zhang, and Zhao (2013) showed that, from a large-momentum matrix element of the gluon spin operator in a physical gauge, ΔG can be obtained through an EFT matching. Following this success, LaMET was applied to the collinear quark PDFs (Ji, 2013). The latter application has generated considerable theoretical as well as numerical activities, particularly for the flavor nonsinglet u-d distributions in the proton and other hadrons. A general LaMET framework was subsequently introduced by Ji (2014). More recently the approach was extended to the gluons as well (Li, Ma, and Qiu, 2019; Zhang, Ji *et al.*, 2019). Therefore, the PDFs can now be computed directly in lattice QCD at a specific Feynman variable x without using LFQ. The partonic landscape of the proton is extremely rich and LaMET holds the promise of computing parton physics beyond the collinear PDFs.

In recent years, tremendous progress has been made in formulating new parton observables for the proton. In particular, two parallel concepts have been developed in characterizing the transverse structure of the proton. The first is the generalized parton distributions (GPDs) (Müller *et al.*, 1994; Ji, 1997b; Radyushkin, 1998). The GPDs combine the features of the proton's elastic form factors, which provide the transverse-space density of partons (Miller, 2007), and Feynman PDFs, and then interpolate them. Given the joint longitudinal-momentum and transverse-space distributions, one can construct the orbital angular momentum (OAM) of partons (Ji, 1997b). In general, the GPDs can be used to generate momentum-dissected transverse-space images of the proton (Burkardt, 2000). A new class of experimental processes, deeply virtual exclusive processes, including deeply virtual Compton scattering (DVCS) in which the final state is a diffractive real photon plus a recoiling proton, has been found to measure them (Ji, 1997a, 1997b). The second concept is the transverse-momentum-dependent (TMD) PDFs (or TMDPDFs), in which the parton's transverse momentum is explicit (Collins and Soper, 1981; Collins, 2011a). Much theoretical progress has been made in recent years regarding their proper definitions, factorizations, and spin correlations (Collins and Rogers, 2013, 2017; Echevarría, Idilbi, and Scimemi, 2013). TMDPDFs can be measured in

experimental processes by observing the transverse momentum of the final-state particles.

Over the years, it has gradually become clear that a dedicated experimental facility to fully explore the partonic landscape of the proton is required. To meet this requirement, the U.S. nuclear science community has proposed building a high-energy, high-luminosity Electron-Ion Collider (EIC) (Aprahamian *et al.*, 2015), which was recently approved by the U.S. Department of Energy. The new collider accelerates electrons to 10–30 GeV and ions (including the proton and heavy nuclei all the way up to Pb or U) up to 100 GeV per nucleon, realizing the center-of-mass collision energy $E_{\text{c.m.}}$ from 40 to 170 GeV. The corresponding electron energy in fixed-target experiments would be 100 GeV to 10 TeV. The beams are polarized, with high luminosity up to 10^{33-34} collisions/cm^2 s, which are critical for studying exclusive processes such as DVCS. The kinematic range of the collisions covers the Bjorken x_B (which coincides with the parton momentum fraction x in the naive parton model discussed in Sec. II) down to sub-10^{-4}, and Q^2 as high as 10^4 GeV^2. Much of the EIC science was discussed in a dedicated study (Accardi *et al.*, 2016).

The EIC and lattice QCD efforts will not stop at the precision parton physics of the proton. We need to develop ways or languages to describe the nucleon as a strongly coupled relativistic quantum system, in much the same way as we understand the quantum Hall effects in condensed matter physics. Without a deep understanding of the mechanisms of strongly coupled QCD physics, we cannot claim a fundamental understanding of the structure of the proton and neutron, in particular, the origin of their masses and spins. This is one of the most challenging goals facing the standard model of particle and nuclear physics today.

This review systematically exposes the idea, formalism, and results of the LaMET approach to parton physics. We do not claim the review to be exhaustive, because the field is rapidly developing. References in the related fields are not meant to be complete either, and we apologize for any important omissions. Closely related reviews on lattice parton physics were given by Zhao (2018) and Cichy and Constantinou (2019). There have been studies on the effectiveness of LaMET in various models (Gamberg *et al.*, 2015; Jia and Xiong, 2016; Broniowski and Ruiz Arriola, 2017, 2018; Nam, 2017; Radyushkin, 2017d; Hobbs, 2018; Xu *et al.*, 2018; Bhattacharya, Cocuzza, and Metz, 2019a, 2019b; Ji, Liu, and Zahed, 2019; Ma, Zhu, and Lu, 2019; Del Debbio, Giani, and Monahan, 2020; Kock, Liu, and Zahed, 2020; Son, Tandogan, and Polyakov, 2020), some of which we mention in the following for illustrative purposes. There have also been papers questioning the validity of the LaMET method (Carlson and Freid, 2017; Rossi and Testa, 2017, 2018), some of which were clarified later in the literature (Briceño, Hansen, and Monahan, 2017; Ji, Zhang, and Zhao, 2017; Radyushkin, 2019b). We do not discuss them here. We have used *proton* in most places in the text to emphasize its importance in nuclear and particle physics. However, the discussions apply equally to the neutron and other hadrons as well.

The plan for this review is as follows. In the remainder of the Introduction, we explain the nature of parton physics as an effective description of the internal structure of the proton at large momentum, as well as other existing methods in the literature for solving the parton structure. In Sec. II, we introduce the LaMET method starting from the momentum renormalization group equation (RGE) of physical observables in a moving hadron, followed by the matching between momentum distributions and PDFs. We then formulate an EFT expansion to compute parton physics from theoretical methods suitable for the structure of a large-momentum proton. In Sec. III, we discuss some important details for collinear PDFs: renormalization of the nonlocal operators, particularly power divergences in lattice regularization, and matching to all orders in perturbation theory. Section IV is devoted to applications to general collinear-parton observables including GPDs, parton distribution amplitudes, and higher-order parton correlations. We also discuss applications for the OAM of the partons in a polarized proton. In Sec. V, we consider the application to TMDPDFs, a new class of parton observables. We study matching of the quasi-TMDPDFs to the physical ones and explore the lattice calculation of the soft function. Finally, Sec. VI summarizes the recent lattice calculations relevant to LaMET applications, and the conclusion is given in Sec. VII. The review is completed with a List of Symbols and Abbreviations and an appendix on notations and conventions.

A. Partons through infinite-momentum states

Although partons have become a ubiquitous language for high-energy scattering, their role as effective degrees of freedom of QCD for describing the internal structure of the nucleon is less emphasized in the literature. In applications within QCD factorization theorems, they are (following Feynman) objects arising from the limit of infinite momentum, with the potential UV divergences regulated and renormalized after the limit. Thus, the partons are an idealized concept, referring to the quark and gluon Fock components of the nucleon or other hadrons only in the context of IMF and LF gauge $A^+ = (A^0 + A^z)/\sqrt{2} = 0$. They are in the same category of concepts as the infinitely heavy quark in heavy-quark effective field theory (HQET) (Manohar and Wise, 2000). To motivate LaMET, it is important to understand the origin and the nature of the partons.

Built from the knowledge of electron scattering in nonrelativistic systems (atoms and molecules) (West, 1975), Feynman introduced the *naive parton model* to describe DIS on the proton and to explain the observed phenomenon of Bjorken scaling (Bjorken and Paschos, 1969; Feynman, 1969, 1972).

Shown in Fig. 2 is the DIS process in which a virtual photon with large momentum q^μ is absorbed by a proton of momentum P^μ and mass M. The invariant variables are $Q^2 = -q^\mu q_\mu$ and $P \cdot q = M\nu$, and Bjorken $x_B = Q^2/(2P \cdot q)$ fixed in the scaling (or Bjorken) limit $Q^2 \to \infty$, $P \cdot q \to \infty$. The inclusive DIS cross section can be factored into a product of leptonic and hadronic tensors, where the former is associated with the electromagnetic current of the lepton while the latter contains all information about the electromagnetic interaction with the target proton.
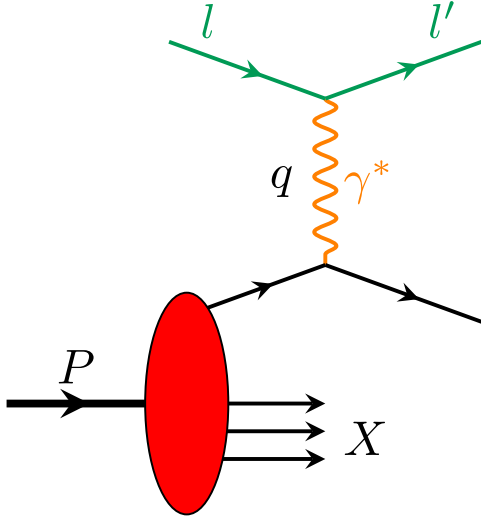
FIG. 2. Deep-inelastic scattering in which partons are probed in the proton in the Bjorken limit.

To learn about the proton structure, it is best to consider the scattering in the Breit frame where

$$q^\mu = (0, 0, 0, -Q),$$

$$P^\mu = \left(\sqrt{\frac{Q^2}{4x_B^2} + M^2}, 0, 0, \frac{Q}{2x_B} \right), \qquad (1)$$

and the virtual photon has zero energy. The probe is sensitive only to the spatial structure, as in nonrelativistic electron scattering. However, relativity now constrains the proton to move at a large momentum $P^z = Q/(2x_B)$ with boost factor $\gamma = Q/(2x_B M)$, which approaches $P^z = \infty$ in the Bjorken limit.

Feynman made intuitive assumptions about the proton structure and scattering mechanism without QFT subtleties (Feynman, 1972): The proton structure at different large P^z should be similar and can be approximated by that at $P^z = \infty$, or in the IMF. The interactions between constituents (partons) are infinitely time dilated, and the wave-function configurations are frozen. The proton in high-energy scattering can be seen as being made of noninteracting partons, each with a longitudinal momentum xP^z with $0 < x < 1$.

The internal structure of nonrelativistic systems is independent of their overall momentum. However, relativistic systems are different, as they least experience the Lorentz contraction. The structures of such systems are inextricably mixed with the overall motion, and their dependence on the external momentum is a dynamical problem. On the other hand, if the internal structure depends on a particular hadron scale Λ_{QCD}, the protons at all large momenta with $P^z \gg \Lambda_{QCD}$ have a similar structure corresponding to the $P^z \to \infty$ limit. This means that if $f(k^z, P^z)$ is the constituent momentum-k^z distribution in a proton of momentum P^z, it might be analytical at $P^z = \infty$ and admits the following Taylor series expansions in $1/P^z$:

$$f(k^z, P^z) = f(x) + f_2(x)(\Lambda_{QCD}/P^z)^2 + \cdots, \qquad (2)$$

where $x = k^z/P^z$. If so, one may find a large-momentum symmetry of the proton properties up to power corrections $\mathcal{O}(1/P^z)$ (we sometimes omit the upper index z for simplicity), and $f(x)$ is the parton distribution.

This picture can be shown to hold in certain simple QFT models, where the dynamical frame dependence of wave functions for composite systems can be studied straightforwardly. There are many interesting examples of two-dimensional systems for which solutions can be found. One of the much studied cases is large-N_c QCD, also called the 't Hooft model ('t Hooft, 1974), in which the bound states have a well-defined large-momentum limit. The wave functions can be expanded in $1/P$, with the corrections starting from $(1/P)^2$. The momenta of the constituents k and $P - k$ scale in this limit. When plotted as a function of $x = k/P$, the change in the wave function with the magnitude of the momentum can be found in Figs. 6–9 of Jia *et al.* (2017). This is the type of example in which Feynman's intuition applies.

However, such a intuition fails in many $(3 + 1)$-dimensional QFTs, including QCD. When a bound state travels at increasingly large momenta, more and more high-momentum modes of a field theory are needed to build up its internal structure. Lorentz contraction indicates that the range of constituent momentum important for the structure also increases. If these high-momentum modes do not decouple effectively from the low-momentum ones, large logarithms of the form $\ln P$ will develop in the structural quantities. Hence, a singularity (cut) at $P = \infty$ can exist in these theories, making $P \to \infty$ limit ill defined and the large-momentum expansion impossible. This situation is intimately related to UV properties of the theories, for which the limits of taking the UV cutoff $\Lambda_{UV} \to \infty$ and $P \to \infty$ do not commute. While the physically relevant one is $(\Lambda_{UV} \gg P) \to \infty$, partons in QCD factorizations are obtained in the other limit $(\Lambda_{UV} \ll P) \to \infty$ when the UV divergences are ignored. Thus, one can formally write the parton distribution as

$$f(x, \Lambda_{UV}) = \frac{1}{2} \int \frac{d\lambda}{2\pi} e^{ix\lambda} \langle P^z = \infty | \psi^\dagger(z)\psi(0) | P^z = \infty \rangle, \qquad (3)$$

where $\lambda = \lim_{P^z \to \infty, z \to 0}(zP^z)$ and ψ is a quantum field.

Historically, the IMF limit of field theories was first studied at the level of diagrammatic rules for perturbation theory (Weinberg, 1966). It was found that taking $P \to \infty$ by ignoring the UV divergences considerably simplifies the perturbation theory rules: Many time-ordered diagrams vanish and only a few have finite contributions. Moreover, scattering in this limit resembles that in nonrelativistic quantum mechanics, and the wave-function description becomes useful. The Fock states define the partons that have the proper kinematic support $(0 < x < 1)$. After the limit is taken, all physical quantities are now independent of P, and large-momentum symmetry is exact before UV divergences are regulated. Therefore, it is the "naive" limit $(\Lambda_{UV} \ll P \to \infty)$ that corresponds to Feynman's naive parton model.

In the standard QCD study of high-energy scattering, the previously mentioned concept of partons as effective degrees

of freedom has been used implicitly. The PDFs are defined in terms of the naive $P = \infty$ limit and are used to match the experimental cross sections, resulting in QCD factorization theorems (Collins, 2011a).

B. Partons through light-front correlators

In the literature and in textbooks, parton distributions are not traditionally represented in terms of the Euclidean matrix elements, as in Eq. (3). Rather, they are represented by the so-called LF correlators of quantum fields ("operator formalism") (Brodsky, Pauli, and Pinsky, 1998; Collins, 2011a). A more explicit formulation in terms of collinear quantum fields and the effective Lagrangian is made in soft-collinear effective theory (SCET) (Bauer *et al.*, 2001; Bauer and Stewart, 2001; Bauer, Pirjol, and Stewart, 2002).

There is a physical way to see that the parton description of high-energy scattering results in the light-front correlations. Consider DIS in the rest frame of the proton, where the virtual photon has momentum

$$q^\mu = \left(\nu, 0, 0, -\sqrt{\nu^2 + 2x_B M \nu}\right). \tag{4}$$

In the Bjorken limit $\nu \to \infty$, although the invariant mass Q of the photon goes to infinity the photon momentum becomes actually lightlike in the sense that it approaches the light front. Therefore, in the inclusive DIS cross section, the separation of the two electromagnetic currents in the hadronic tensor, which is Fourier conjugate to the photon momentum, also approaches the light-cone direction.

Thus, it appears natural that all the structural physics of the proton in the IMF can also be expressed in terms of time-dependent LF correlators or correlations of quantum fields on the LF. Formally, this is simple to see if one writes

$$|P \to \infty\rangle = U(\Lambda_\infty)|P = 0\rangle. \tag{5}$$

The boost operator $U(\Lambda_\infty)$ can be applied to the static nonlocal operators in the ordinary momentum distributions. In doing so, all static correlations become light-cone ones. The boost process is then similar to shifting the Hamiltonian evolution in quantum mechanics from the Schrödinger to the Heisenberg picture, where time dependence is then in the operators.

To express light-cone correlations, it is convenient to introduce two conjugate lightlike (or light-cone) vectors $p^\mu = (\Lambda, 0, 0, \Lambda)$ and $n^\mu = (1/2\Lambda, 0, 0, -1/2\Lambda)$ with the following properties: $n^2 = p^2 = 0$ and $n \cdot p = 1$, where Λ is a parameter. Any four-vector can then be expanded as

$$k^\mu = k \cdot n p^\mu + k \cdot p n^\mu + k_\perp^\mu. \tag{6}$$

In particular, the momentum P^μ of a proton moving in the z direction can be expressed as

$$P^\mu = p^\mu + (M^2/2)n^\mu, \tag{7}$$

where M is the proton mass.

Using the previous notation, one can express the unpolarized quark distribution in the proton as (Collins, 2011a)

$$q(x) = \frac{1}{2} \int \frac{d\lambda}{2\pi} e^{i\lambda x} \langle P|\bar{\psi}(0)\slashed{n}W(0, \lambda n)\psi(\lambda n)|P\rangle_c, \tag{8}$$

where ψ is the quark field and W is a gauge link defined as

$$W(x_2, x_1)$$
$$= \mathcal{P} \exp\left[-ig \int_0^1 dt(x_2 - x_1)_\mu A^\mu[x_1 + (x_2 - x_1)t]\right] \tag{9}$$

to ensure gauge invariance, with $\mathcal{P}$ denoting the path ordering. c indicates the connected contributions only, and is suppressed in the rest of this review. It is a property of gauge theories in which the charge fields are not gauge invariant, and the physical distributions must include a beam of collinear gauge particles. Note that Eq. (8) is true for any momentum P (a residual momentum symmetry), particularly in the rest frame of the nucleon. The x support of Eq. (8) is $[-1, 1]$. For negative x, one defines the antiquark distribution with $-q(-x) \equiv \bar{q}(x)$. Equation (8) is more familiar in the literature than Feynman's original formulation of PDFs. In the single quark target, one finds that $q(x) = \delta(x - 1)$.

To expose the partons in Eq. (8), one can follow the QCD light-front quantization (Chang and Ma, 1969; Kogut and Soper, 1970; Drell and Yan, 1971) suggested by Dirac in 1949 (Dirac, 1949). In LFQ (Brodsky, Pauli, and Pinsky, 1998), one defines the LF coordinates as

$$\xi^\pm = (\xi^0 \pm \xi^3)/\sqrt{2}, \tag{10}$$

where ξ^+ is the LF "time" and ξ^- is the LF "spatial coordinate." And any four-vector A^μ will now be written as $(A^+, A^-, \vec{A}_\perp)$. Dynamical degrees of freedom are defined on the $\xi^+ = 0$ plane with arbitrary ξ^- and $\vec{\xi}_\perp$, with conjugate momentum k^+ and $\vec{k}_\perp$. Dynamics is generated by the light-cone Hamiltonian $H_{LC} = P^-$. For a free particle with three-momentum $(k^+, \vec{k}_\perp)$ and mass m, the on-shell LF energy is $k^- = (\vec{k}_\perp^2 + m^2)/(2k^+)$.

For QCD, one can define the Dirac matrices $\gamma^\pm = (\gamma^0 \pm \gamma^3)/\sqrt{2}$ and the projection operators for the quark fields as $P_\pm = (1/2)\gamma^\mp\gamma^\pm$, so that any ψ can be decomposed into $\psi = \psi_+ + \psi_-$ with $\psi_\pm = P_\pm\psi$, where ψ_+ is considered a dynamical degree of freedom. For the gauge field, A^+ is fixed by the LF gauge $A^+ = 0$. $A_\perp$ are dynamical degrees of freedom. ψ_- and A^- are dependent variables that can be expressed in terms of ψ_+ and $A_\perp$ using equations of motion (Kogut and Soper, 1970).

The physics of the LF correlations becomes manifest if one introduces the following canonical expansion:

$$\psi_+(\xi^+ = 0, \xi^-, \vec{\xi}_\perp)$$
$$= \int \frac{d^2k_\perp}{(2\pi)^3} \frac{dk^+}{2k^+} \sum_\sigma [b_\sigma(k)u(k, \sigma)e^{-i(k^+\xi^- - \vec{k}_\perp \cdot \vec{\xi}_\perp)}$$
$$+ d_\sigma^\dagger(k)v(k, \sigma)e^{i(k^+\xi^- - \vec{k}_\perp \cdot \vec{\xi}_\perp)}], \tag{11}$$

where $b^\dagger(k)$ and $d^\dagger(k)$ [$b(k)$ and $d(k)$] are quark and antiquark creation (annihilation) operators, respectively. σ is the light-cone helicity of the quarks, which can be either $+1/2$ or $-1/2$. Covariant normalization is adopted for the particle states and the creation and annihilation operators, i.e.,

$$
\begin{aligned}
&\{b_\sigma(k), b_{\sigma'}^\dagger(k')\} \\
&= \{d_\sigma(k), d_{\sigma'}^\dagger(k')\} \\
&= (2\pi)^3 \delta_{\sigma\sigma'} 2k^+ \delta(k^+ - k'^+) \delta^{(2)}(\vec{k}_\perp - \vec{k}'_\perp). \quad (12)
\end{aligned}
$$

Substituting Eq. (12) into Eq. (8), one finds the following quark distribution:

$$
q(x) = \frac{1}{2x} \sum_\sigma \int \frac{d^2\vec{k}_\perp}{(2\pi)^3} \langle P|b_\sigma^\dagger(x,\vec{k}_\perp)b_\sigma(x,\vec{k}_\perp)|P\rangle / \langle P|P\rangle \quad (13)
$$

for $x > 0$, and similarly for $x < 0$ one gets the antiquark distribution. The factor $1/x$ comes from the normalization of the creation and annihilation operators. The previously mentioned matrix element should be interpreted as the matrix element in a wave packet state, in the limit of a state of definite momentum (Collins, 2011a). This way, one recovers the physical meaning of PDFs in the LF correlator (operator) formalism.

C. Other approaches to parton structure

Calculating the partonic structure of the hadrons from QCD has always been an important goal in hadronic physics. There have been two main approaches apart from various phenomenology and models: light-front quantization and lattice QCD. We now give a review of LFQ and lattice approaches that differs from the main subject of this review.

Although LFQ explicitly uses the parton degrees of freedom, it has not been successful in practical calculations. LF perturbation theory, like the standard Hamiltonian perturbation theory, breaks Lorentz symmetry manifestly and requires a sophisticated renormalization scheme to restore it. A potential renormalization scheme must deal with the long-range correlations in the ξ^- direction that require functional dependence on the renormalization counterterms (Wilson *et al.*, 1994). Thus, LF perturbation theory has not been used for any calculations beyond one loop, except for the two-loop anomalous magnetic moment in QED (Langnau and Burkardt, 1993). In fact, the common wisdom of using dimensional regularization (DR) for the transverse integrals and cutoff regularization for the longitudinal one has not been proven useful for multiloop calculations, although it has been successfully used to derive the Balitsky-Fadin-Kuraev-Lipatov evolution by Mueller from the quarkonium wave functions (Mueller, 1994).

The enthusiasm for using LFQ in QCD is not about perturbation theory, but rather to solve the hadron states. Discretized LFQ was proposed by Pauli and Brodsky (1985) to make practical calculations for the bound-state problems. This nonperturbative method turns out to be successful for models in the $1+1$ dimension, such as the Schwinger model (McCartor, 1994; Harada, Okazaki, and Taniguchi, 1996), the

$1+1$ QCD (Burkardt, 1989; Srivastava and Brodsky, 2001), the $1+1$ ϕ^4 theory (Harindranath and Vary, 1987), and the sine-Gordon model (Burkardt, 1993). For $(3+1)$-dimensional theories, simple approximations have been considered, like the Tamm-Dancoff approximation (Perry, Harindranath, and Wilson, 1990). For QCD itself, one again has to use severe truncations in the number of Fock states. Some recent works of this type include Vary *et al.* (2010), Jia and Vary (2019), and Lan *et al.* (2019). However, to derive a fully renormalized Hamiltonian is difficult and, moreover, there has been no demonstration thus far showing that the Fock-space truncation actually converges (Wilson *et al.*, 1994). Therefore, a systematic approximation for QCD bound states in LFQ has yet to be found.

Given the rapid development in lattice QCD, it is natural to use it to compute parton physics. However, simulating real-time evolution directly is numerically challenging, which runs into the so-called sign problem or, more generally, the non-deterministic-polynomial-time- (NP-) hard problem. Over the years, a number of methods have been proposed to indirectly calculate the PDFs, which includes well-studied moment methods, the hadronic tensor and Compton amplitude method, coordinate-space factorization, etc. These approaches calculate lattice observables that can be related to the PDFs or structure functions through the operator product expansion (OPE) or the dispersion relation, and thus can be used to probe certain information on the partonic structure of hadrons. However, their aims are mainly to get the lower moments of PDFs and/or segments of certain coordinate correlations, not directly in parton degrees of freedom.

The most-adopted approach on the lattice has been to calculate the moments of PDFs as the matrix elements of local operators (Kronfeld and Photiadis, 1985; Martinelli and Sachrajda, 1987). In the moments approach, one starts with the so-called twist-2 operators (Christ, Hasslacher, and Mueller, 1972)

$$
O^{\mu_1\cdots\mu_n} = \bar{\psi}\gamma^{(\mu_1}iD^{\mu_2}\cdots iD^{\mu_n)}\psi - \text{trace} \quad (14)
$$

in the quark case, where $(\mu_1\cdots\mu_2)$ indicates that all the indices are symmetrized, the trace terms are those with at least one factor of the metric tensor $g^{\mu_i\mu_j}$ multiplied by operators of dimension $(n+2)$ with $n-2$ Lorentz indices, etc. Their matrix elements in the proton state are

$$
\langle P|O^{\mu_1\cdots\mu_n}(\mu)|P\rangle = 2a_n(\mu)(P^{\mu_1}\cdots P^{\mu_n} - \text{trace}), \quad (15)
$$

and the PDFs are related to the local matrix elements through

$$
\begin{aligned}
a_n(\mu) &= \int_{-1}^1 dx\, x^{n-1} q(x,\mu^2) \\
&= \int_0^1 x^{n-1}[q(x,\mu^2) + (-1)^n \bar{q}(x,\mu^2)], \quad (16)
\end{aligned}
$$

with $n = 1, 2, \ldots$. The time-dependent correlation for the PDF in Eq. (8) is recovered by taking all the components as positive in Eq. (15) as follows:

$$
\langle P|O^{+\cdots+}(\mu)|P\rangle = 2a_n(\mu)P^+\cdots P^+, \quad (17)
$$

and packaging all the moments into a distribution. Likewise, for the gluon PDF, its moments are again related as follows to the matrix elements of local operators:

$$O_g^{\mu_1\cdots\mu_n} = -F^{(\mu_1\alpha}iD^{\mu_2}\cdots iD^{\mu_{n-1}}F_\alpha^{\mu_n)}, \qquad (18)$$

with $n = 2, 4, 6, \ldots$.

A large number of lattice QCD calculations of PDF moments have been done thus far with various degrees of control in systematics (Lin *et al.*, 2018); they include discretization errors, physical pion mass, finite volume effects, excited-state contaminations, and proper renormalization. Most of the lattice calculations have been focused on the first and second moments $\langle x \rangle$ (Bali *et al.*, 2014; Green *et al.*, 2014; Alexandrou, Constantinou *et al.*, 2017) and $\langle x^2 \rangle$ (Dolgov *et al.*, 2002; Deka *et al.*, 2009) for the unpolarized distributions, and the zeroth and first moments $\langle 1 \rangle$ (Alexandrou, Constantinou *et al.*, 2017; Gong *et al.*, 2017; Chang *et al.*, 2018; Alexandrou, Bacchio *et al.*, 2019) and $\langle x \rangle$ (Aoki *et al.*, 2010; Abdel-Rehim *et al.*, 2015) for the polarized distributions. However, it has been difficult to calculate higher moments due to power divergences and rapid decay in the signals. Nonetheless, moment calculations can provide a useful calibration for any comprehensive lattice approach to PDFs.

To get more information about the PDFs, researchers proposed calculating the hadronic tensor of DIS in Euclidean space, and analytically continuing the result to Minkowski space (Liu and Dong, 1994; Liu *et al.*, 1999; Liu, 2000, 2016, 2017, 2020). Since numerical methods for analytical continuation are known to be difficult for precise control (similar to the previously mentioned NP-hard or sign problem), the approach is useful mainly for the nucleon low-lying excitations. It is challenging to obtain parton physics this way.

A similar approach called "OPE without OPE" was suggested by Aglietti *et al.* (1998) and Martinelli (1999); see also Dawson *et al.* (1998), Capitani, Gockeler, Horsley, Oelrich *et al.* (1999), and Capitani, Gockeler, Horsley, Petters *et al.* (1999). The point is that the Compton amplitude in the nondispersive region can be calculated in the Euclidean space (Ji and Jung, 2001). Through the dispersion relation and Taylor expansion at $\nu = P \cdot q = 0$, one can extract the higher moments of structure functions from the lattice Compton amplitude. Recent work on parton structure from this approach was conducted by Chambers *et al.* (2017), Hannaford-Gunn *et al.* (2020), and Horsley *et al.* (2020). A similar method has been adopted for Compton amplitude with heavy-light currents (Detmold and Lin, 2006). This approach has been used to calculate the second moment of the pion distribution amplitude (Detmold *et al.*, 2018, 2020).

The current-current correlators can also be studied through the OPE in the coordinate space without momentum insertion into the currents (Braun and Müller, 2008). The spatial correlation at small distances can be used to calculate higher moments of distribution amplitudes of the mesons. A number of lattice studies were performed by Braun *et al.* (2015), Bali, Braun *et al.* (2018), and Bali *et al.* (2019). A similar strategy was suggested more recently by Ma and Qiu (2018a) for

parton distributions and has been used in lattice simulations (Sufian *et al.*, 2019, 2020). The pseudo-PDF has been proposed based on the equal-time correlation (or the quasi-PDF in Fourier space) used in LaMET (Radyushkin, 2017a, 2019c) and uses a coordinate-space factorization or OPE at small distance as in Braun and Müller (2008). Because of its close connection with the quasi-PDF, we discuss comparisons of the pseudo-PDF data analysis method with that for the quasi-PDF in Sec. III.C.

There have been pioneering studies on moments of the "quasi" quark TMDPDFs on lattice (Hagler *et al.*, 2009; Musch *et al.*, 2011, 2012; Engelhardt *et al.*, 2016; Yoon *et al.*, 2017). The staple-shaped gauge-link operators have been used to connect the quark fields separated in the spatial direction to simulate the moments of the TMDPDF. The ratios of these moments are presumed to be independent of the unknown soft function and may be compared with experimental data. However, a rigorous relation of these constructions to the physical moments of TMDPDFs had not been investigated before LaMET, particularly the relationship between the large-momentum limit and the rapidity cutoff, which is an essential ingredient of TMD physics. A comparison of this approach to LaMET is made in Sec. V.B.

II. LARGE-MOMENTUM EFFECTIVE THEORY

As explained in Sec. I.A, Feynman's partons originated from describing the structure of a bound state traveling at large momentum P. On the other hand, in QCD factorizations they appear to be effective degrees of freedoms arising in the infinite-momentum limit disregarding UV divergences. Reconciling these two pictures results in LaMET for the parton structure of hadrons.

We start by considering the structure of the proton at finite momentum. We define the ordinary momentum distributions of the constituents while trying to illustrate their dependence on the proton momentum. We demonstrate that the large-P momentum dependence follows a RGE, similar to the well-known RGE for partons. In Sec. II.C, we show that momentum distributions at large P are related to PDFs through a matching between different orders of $P \to \infty$ and UV cutoff limits. This matching process has a standard EFT explanation: Parton physics or observables can be obtained from an effective theory in which $P \ll \Lambda_{\rm UV}$ are calculated nonperturbatively in the so-called $\mathcal{P}$ space (Messiah, 1979) after "integrating out" degrees of freedom between P and ∞ (or $\mathcal{Q} = 1 - \mathcal{P}$ space) through perturbation theory. Therefore, the LaMET approach to partons is in some sense similar to lattice QCD as an EFT approach for continuum field theories, in which all active degrees of freedom ($\mathcal{P}$ space) are bounded by $|k| \le \pi/a$, where a is lattice spacing, whereas those at $|k| \ge \pi/a$ ($\mathcal{Q}$ space) are taken into account through perturbative coefficients and higher-dimensional operators.

In Sec. II.D, we outline the formalism of LaMET for a general parton observable. The method can in principle also be used to calculate any LF correlations in terms of large-momentum external states (see, in particular, the application to a soft function in Sec. V). The strategy is also applicable for the components of the LF wave functions. Thus, LaMET offers a practical and systematic way to carry out the program

of LFQ. Instead of working with the LF coordinates directly, one uses the instant form of dynamics and large momentum or boost factor γ as a regulator for the LF divergences. In a certain sense, the quantization using tilted light-cone coordinates (Lenz *et al.*, 1991) is similar to the spirit of the LaMET approach.

At present, the only systematic approach to solve non-perturbative QCD is lattice field theory (Wilson, 1974). Therefore, a practical implementation of LaMET can be done through lattice calculations. It can also be done with other bound-state methods using Euclidean approaches, such as the instanton liquid model (Schäfer and Shuryak, 1998). While LFQ may provide an attractive physical picture for the proton, the Euclidean equal-time formulation is more practical for carrying out the calculations, and LaMET serves to bridge them.

A. Structure of the proton at finite momentum

In relativistic theories, the internal structure of a composite system is frame dependent (we always refer to the total momentum eigenstates), and we are interested in the properties of the proton at a momentum much larger than its rest mass.

We start from the quark momentum density in a fast-moving proton, assuming that it moves in the z direction. A straightforward definition is

$$N_P(\vec{k}) = \sum_\sigma \langle P | b_\sigma^\dagger(\vec{k}) b_\sigma(\vec{k}) | P \rangle / \langle P | P \rangle, \qquad (19)$$

where the quark helicity, color, and other implicit indices are summed over. Equation (19) should be compared with the parton density in Eq. (13). To make it gauge invariant, it is convenient to consider the definition from a coordinate-space correlator

$$N_{P,W}(\vec{k}) = \frac{1}{2} \int \frac{d^3\xi}{(2\pi)^3} e^{-i\vec{k}\cdot\vec{\xi}} \langle P | \bar{\psi}(0) \gamma^0 W(0, \vec{\xi}) \psi(\vec{\xi}) | P \rangle, \quad (20)$$

where the Dirac matrix γ^0 ensures that it is a number density. It is a static quantity without time dependence and can be calculated in Euclidean field theories, in contrast to Eq. (8) for partons. The gauge invariance is ensured by the Wilson line $W(0, \vec{\xi})$ between the quark fields separated by $\vec{\xi}$, which is defined in the fundamental representation of the color SU(3) group. There are infinitely many choices for the Wilson line, generating infinitely many momentum densities. For example, one can choose a straight-line link between 0 and $\vec{\xi}$. One can also let the Wilson line run from the fields along the z direction for a long distance (if not infinity) before joining them together along the transverse direction (a staple).

For its connection to the PDFs, we consider a transverse-momentum-integrated, longitudinal-momentum distribution

$$N_P(k^z) = \int d^2\vec{k}_\perp N_{P,W}(\vec{k})$$
$$= \frac{1}{2} \int \frac{dz}{2\pi} e^{-ik^z z} \langle P | \bar{\psi}(0) \gamma^0 W(0, z) \psi(z) | P \rangle, \quad (21)$$

where we ignore the question of convergence at large $|\vec{k}_\perp|$. Now the gauge link $W(0, z)$ is naturally taken as a straight line as follows:

$$W(0, z) = \exp\left(-ig \int_0^z A^{z'}(z') dz'\right)$$
$$= \exp\left(ig \int_\infty^0 A^{z'}(z') dz'\right) \exp\left(ig \int_z^\infty A^{z'}(z') dz'\right)$$
$$= W^\dagger(\infty, 0) W(\infty, z), \qquad (22)$$

where in the second line we have split the gauge link into two, going from z to infinity and coming back from infinity to zero. We can define a "gauge-invariant" quark field

$$\Psi(\vec{\xi}) = W(\infty, \vec{\xi}) \psi(\vec{\xi}), \qquad (23)$$

and the previously mentioned density becomes

$$N_P(k^z) = \frac{1}{2} \int \frac{dz}{2\pi} e^{-ik^z z} \langle P | \bar{\Psi}(0) \gamma^0 \Psi(z) | P \rangle, \qquad (24)$$

where again we have not considered UV divergences. The previously defined momentum distribution has been called *quasi-PDF*, but it is really a physical momentum distribution in a proton of momentum P.

In the rest frame of the proton, $N_{P=0}(k^z)$ is symmetric in positive and negative k^z, probably peaks around $k^z = 0$, and decays as $k^z \to \pm\infty$. Owing to the perturbative QCD effects, it decays algebraically at large k^z instead of exponentially. Because of this property, the high moments of the distribution, $\int dk^z (k^z)^n N_0(k^z)$ with $n > 0$, have the standard QFT UV divergences.

As P becomes nonzero and large, the peak $N_P(k_z)$ will be around αP^z, where α is a constant of order 1. The density at negative k^z becomes smaller, but not zero. This is due to the so-called backward-moving particles from the large-momentum kick in perturbation theory. For the same reason, the density at $k^z > P^z$ is not zero either.

$N_P(k^z)$ has a renormalization scale dependence because the quark fields must be renormalized. One can choose DR and modified minimal subtraction ($\overline{\text{MS}}$) scheme. Any other regularization scheme can be converted into this one perturbatively. For $z \neq 0$, the only renormalization necessary is the quark wave function (with anomalous dimension γ_F) in the $A^z = 0$ gauge because the linear divergence associated with the gauge link vanishes in the $\overline{\text{MS}}$ scheme. More extensive discussions on the renormalization issue, particularly about nonperturbative renormalization, are made in Sec. III.

As an example showing how the parton momentum density depends on P, we depict in Fig. 3 the quark wave-function amplitude of a meson in the 't Hooft model [(1 + 1)-dimensional QCD with $N_c \to \infty$] ('t Hooft, 1974), the square of which yields the quark momentum density. In this model, a meson of momentum P^μ can be built as
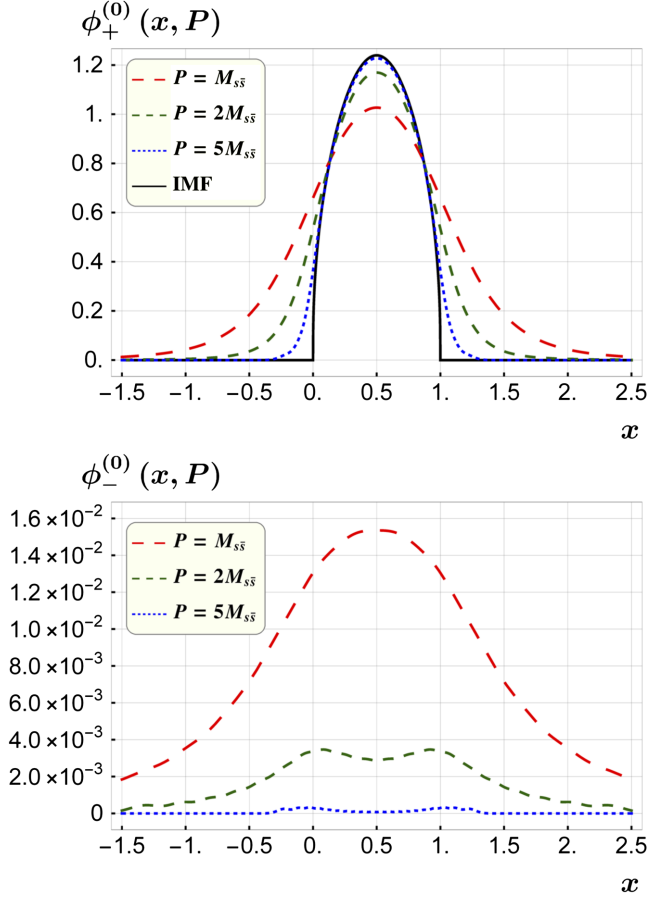
$\phi_+^{(0)}(x, P)$

$\phi_-^{(0)}(x, P)$

FIG. 3. Wave-function amplitudes of a meson in the 't Hooft model at different external momenta. From Jia *et al.*, 2017.

$$|P_n^\mu\rangle = \int \frac{dk}{2\pi|P|}[M(k-P,k)\phi_n^+(k,P) + M^\dagger(k,k-P)\phi_n^-(k,P)]|0\rangle, \qquad (25)$$

where $M(p,k) = \sum_i d_{-p}^i b_k^i / \sqrt{N_c}$ and $M^\dagger(p,k) = \sum_i b_k^{i\dagger} d_{-p}^{i\dagger} / \sqrt{N_c}$ are annihilation and creation operators for quark-antiquark pairs. The corresponding wave-function amplitudes $\phi_n^+(k,P)$ and $\phi_n^-(k,P)$ satisfy a pair of equations first derived by Bars and Green (1978).

The previously defined meson bound state has a well-defined large-momentum limit. The wave functions can be expanded in $1/P$, with the corrections starting from $(1/P)^2$. The momenta of the constituents k and $P - k$ scale in this limit. When plotted as a function of $x = k/P$, the change in the wave function with the magnitude of the momentum is shown in Fig. 3.

B. Momentum renormalization group

Here we consider how to calculate the external momentum P dependence of physical observables discussed in Sec. II.B. The dependence is related to the boost properties of the operators under consideration, namely, their commutation relations with the boost generators $\hat{K}^i$. We argue that in the large-momentum limit one has a *momentum RGE*, which is a differential equation relating properties of the system at different momenta. Momentum RGE will be, in the end, related to the renormalization properties of the observables on the LF.

Consider a generic operator $\hat{O}$ and its matrix element in a state with momentum P:

$$O(P) = \langle P|\hat{O}|P\rangle. \qquad (26)$$

We calculate the momentum dependence by writing $|P\rangle = \exp[-i\omega(P)\hat{K}]|P = 0\rangle$, where $\hat{K}$ is the boost operator along the momentum direction and ω is a boost parameter depending on P. Taking a derivative with respect to the boost parameter gives

$$\frac{dO(P)}{dP} = i\frac{d\omega(P)}{dP}\langle P|[\hat{O},\hat{K}]|P\rangle. \qquad (27)$$

The rhs of Eq. (27) depends on the commutator $[\hat{O},\hat{K}]$, i.e., the boost properties of the operator. For a scalar operator, the commutation relation vanishes and $O(P)$ is frame independent. For a vector operator, the commutation relation resembles that of an energy-momentum four-vector, and the result is the standard Lorentz transformation of a four-vector. For nonlocal operators, the commutation relation requires the elementary formula

$$[J^{\mu\nu}, \phi_i(x)] = i[l^{\mu\nu}\delta_{ij} + S_{ij}^{\mu\nu}]\phi_j(x), \qquad (28)$$

where $l^{\mu\nu} = i(x^\mu\partial^\nu - x^\nu\partial^\mu)$ is the OAM operator and $S^{\mu\nu}$ is the intrinsic spin matrix. Thus, one of the fields is now $\phi_i(t = \sinh\omega z, 0, 0, \cosh\omega z)$, which generates a time-dependent correlation function.

In the large-momentum limit, because of asymptotic freedom the P dependence is calculable in perturbation theory and Eq. (27) simplifies. One obtains the momentum or boost RGE (Ji, 2014)

$$\frac{dO(P)}{dP} = \lim_{\Delta P\to 0}[O(P+\Delta P) - O(P)]/\Delta P \qquad (29)$$

$$\overset{P\gg M}{\to} C[\alpha_s(P)] \otimes O(P) + \mathcal{O}(M^2/P^2), \qquad (30)$$

where $C[\alpha_s(P)]$ is a perturbative expansion in the strong coupling α_s. The circled times symbol can be a simple multiplication or a certain form of convolution, depending on the observable $O(P)$ studied. The proof of Eq. (30) is nontrivial, and it can be analyzed on a case-by-case basis. There can be mixings among a set of independent operators with the same quantum numbers. The momentum RGEs are similar to those for scale transformation and that for the coarse graining of a Hamiltonian. That the two are connected in some cases may be traced to Lorentz symmetry.

As an example of the momentum RGE, we calculate the quark momentum distribution in a perturbative quark state using Eq. (24). Since it is gauge invariant, we can calculate it in any gauge (for example, the Feynman gauge). The one-loop diagrams in QCD are shown in Fig. 4. There are two sources of UV divergences: one is the logarithmic divergences from the vertex and self-energy diagrams, and the other is the linear divergence in the self-energy of the Wilson line. For the
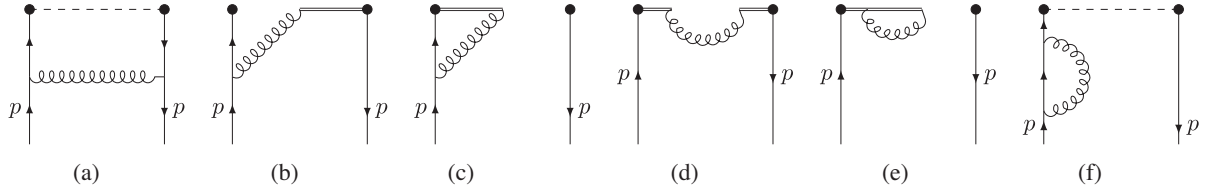
FIG. 4. One-loop diagrams for the quasi-PDF in a free quark state in the Feynman gauge. The conjugate diagrams of (b), (c), (e), and (f) do contribute but are not shown here.

moment, we use the transverse-momentum cutoff Λ_{UV} as the UV regulator. Using $y = k^z/P^z$, the one-loop result reads for a large-momentum quark (Xiong *et al.*, 2014)

$$\tilde{q}^{(1)}(y, P^z, \Lambda_{\mathrm{UV}})$$

$$= \frac{\alpha_s C_F}{2\pi} \begin{cases} \frac{1+y^2}{1-y}\ln\frac{y}{y-1} + 1 + \frac{\Lambda_{\mathrm{UV}}}{(1-y)^2 P^z}, & y > 1, \\[2mm] \frac{1+y^2}{1-y}\ln\frac{(P^z)^2}{m^2} + \frac{1+y^2}{1-y}\ln\frac{4y}{1-y} \\[1mm] \quad - \frac{4y}{1-y} + 1 + \frac{\Lambda_{\mathrm{UV}}}{(1-y)^2 P^z}, & 0 < y < 1, \\[2mm] \frac{1+y^2}{1-y}\ln\frac{y-1}{y} - 1 + \frac{\Lambda_{\mathrm{UV}}}{(1-y)^2 P^z}, & y < 0, \end{cases} \quad (31)$$

where we have ignored all power-suppressed contributions and keep the leading P^z dependence only. There is an additional contribution of the form $\delta Z_1(\Lambda_{\mathrm{UV}}/P^z)\delta(y-1)$.

The previous result has several interesting features:

- The distribution does not vanish outside $[0, 1]$. The radiative gluon can carry a large negative momentum fraction, resulting in a recoiling quark carrying larger momentum than the parent quark, and thus $y > 1$. The same gluon can also carry a momentum larger than P^z, making the active quark have $y < 0$.

- While this effect is easy to understand perturbatively, it is surprising that a scaling contribution remains outside $[0, 1]$ in the IMF. As the proton travels faster, one might think any constituent has a momentum k^z that is positive from the Lorentz transformation. However, the order of limits matters because, no matter how large the parent-quark momentum is, there are always quarks with much larger momentum, i.e., $k^z \gg P^z \gg \Lambda_{\mathrm{QCD}}$. In this sense, Feynman's parton model does not describe the exact properties of the momentum distribution in a large-momentum nucleon.

- The contribution outside $[0, 1]$ at one loop is entirely perturbative because of the absence of any infrared (IR) divergence. This is no longer true at the two-loop level, but the contribution depends only on the same one-loop IR physics in $[0, 1]$.

- The distribution for y in $[0, 1]$ has a term depending on $\ln P^z$. This dependence reflects that the quark substructure is resolved as a function of P^z, an interesting feature of boost. This dependence is perturbative in the sense that the derivative is IR safe:

$$P^z \frac{d\tilde{q}(y, P^z, \Lambda_{\mathrm{UV}})}{dP^z} = \frac{\alpha_s C_F}{\pi}\left[\left(\frac{1+y^2}{1-y}\right)_+ - \frac{3}{2}\delta(1-y)\right]. \quad (32)$$

Apart from the δ-function term, the rhs is similar to the one-loop quark splitting function in Dokshitzer-Gribov-Lipatov-Altarelli-Parisi (DGLAP) evolution (Gribov and Lipatov, 1972; Altarelli and Parisi, 1977; Dokshitzer, 1977). Therefore, one might suspect that the momentum dependence is closely related to the familiar renormalization scale evolution in the PDFs. In fact, the physics is just the other way around: It is the hadron-momentum dependence of the physical momentum distribution that generates the DGLAP evolution in the infinite-momentum limit. One can derive an all-order momentum RGE for the momentum distribution function. Momentum RGE also provides a method to sum over the large logarithms of the momentum.

- There is a singularity at $y = 1$. This singularity is generated from soft-gluon radiation. This singularity combined with the virtual contribution yields a finite result.

- There is a linear divergence in the cutoff regulator, leading to $\Lambda_{\mathrm{UV}}/P^z$ term, which is absent in DR. Thus, to keep $1/(P^z)^2$ power counting, it is important to work in a renormalization scheme where this term does not exist.

We can also move on to study the hadron-momentum RGEs of other structural properties considered in Sec. II.A. In particular, the RGE for TMD distributions will lead to the familiar rapidity RGE in the literature. We reserve these discussions for Sec. V.

C. Effective field theory matching to PDFs

As we see in Sec. II.B, the momentum distributions of the constituents (now called quasi-PDFs in the literature) in a proton at large P differ from the PDFs or LF distributions in many ways. In particular, the momentum fraction y in a physical momentum distribution is not limited to $[0, 1]$ due to backward-moving particles, which is the case even in the $P \to \infty$ limit. In fact, the infinite-momentum limit is not analytical, due to the presence of $\ln P$.

However, partons are effective objects arising from a different limit $\Lambda_{\mathrm{UV}} \ll P \to \infty$. There is also an important computational advantage in taking the naive limit $P \gg \Lambda_{\mathrm{UV}}$ in perturbative calculations: Feynman integrals have one fewer four-momentum. Therefore, this limit of QFTs serves as a reference system where the structure of the bound states is manifestly independent of the hadron momentum and is similar to scale-invariant critical points at which second-order phase transitions occur in condensed matter systems. However, the theory in the naive IMF limit introduces additional UV divergences.

Therefore, the partons in QCD are similar to the infinitely heavy quarks in HQET (Manohar and Wise, 2000). In certain QCD systems, heavy quarks such as the bottom quark are present, and their masses are much larger than the typical

QCD scale Λ_{QCD}. In this case, one might study the dependence on the heavy-quark mass by expanding around $m_Q = \infty$. This expansion will generally produce a power series in $1/m_Q$. However, the limits of taking $\Lambda_{\text{UV}} \to \infty$ and infinite heavy-quark-mass limits are not interchangeable, due to the presence of the large logarithms $\ln m_Q$. In an EFT approach, one takes the $m_Q \to \infty$ limit first; this will result in a new theory with different UV behavior but without the heavy-quark mass, and symmetries among different heavy-quark systems become manifest. The renormalization of the extra UV divergences yields a RGE that can be used to resum large quark-mass logarithms.

Therefore, the momentum distribution at large P differs from the parton distributions only in the order of limits; their IR nonperturbative physics is the same. In asymptotically free theories such as QCD, differences (or discontinuities) in taking the limits of $P \gg \Lambda_{\text{UV}}$ and $\Lambda_{\text{UV}} \gg P \to \infty$ are perturbatively calculable, as only the high-momentum modes matter. The differences are called *matching coefficients*. Therefore, one is able to write the following power expansion for the momentum-dependent distribution (quasi-PDF) in terms of the PDF (Xiong *et al.*, 2014; Izubuchi *et al.*, 2018; Ma and Qiu, 2018a, 2018b):

$$\tilde{q}(y, P^z, \mu) = \int_{-1}^{1} \frac{dx}{|x|} C\left(\frac{y}{x}, \frac{\mu}{xP^z}\right) q(x, \mu)$$

$$+ \mathcal{O}\left(\frac{\Lambda_{\text{QCD}}^2}{(yP^z)^2}, \frac{\Lambda_{\text{QCD}}^2}{[(1-y)P^z]^2}\right), \quad (33)$$

where the power correction is suppressed by the parton momentum yP^z and the spectator momentum $(1-y)P^z$ (Ji *et al.*, 2020). This expansion may also be called a factorization formula, as the quasi-PDF contains all the IR physics in the PDF and C involves only UV physics. As we extensively discuss in Sec. III, this factorization formula is true to all orders in perturbation theory. Equation (33) allows us to calculate the LF parton physics from the momentum distribution at large P. Since the expansion parameter is $\Lambda_{\text{QCD}}^2/(yP^z)^2$ and $\Lambda_{\text{QCD}}^2/[(1-y)P^z]^2$, for intermediate y one might not need large P^z to neglect the power corrections.

The previously mentioned relation between the two quantities has a simple explanation in terms of the Lorentz boost: Consider the spatial correlation along z shown in Fig. 5 in a large-momentum state. It can be seen as approaching the LF one in the rest frame of the proton. In other words, we are using a near-LF correlation to approximate a LF correlation. Accordingly, we can invert Eq. (33) recursively to express the PDF in terms of quasi-PDF with their differences being taken care of through the perturbative matching $\tilde{C}$ and power corrections as follows:

$$q(x, \mu) = \int_{-\infty}^{\infty} \frac{dy}{|y|} \tilde{C}\left(\frac{x}{y}, \frac{\mu}{yP^z}\right) \tilde{q}(y, P^z, \mu)$$

$$+ \mathcal{O}\left(\frac{\Lambda_{\text{QCD}}^2}{(xP^z)^2}, \frac{\Lambda_{\text{QCD}}^2}{[(1-x)P^z]^2}\right). \quad (34)$$

Equation (34) has an EFT interpretation: The parton physics is calculated in an effective field theory with physical
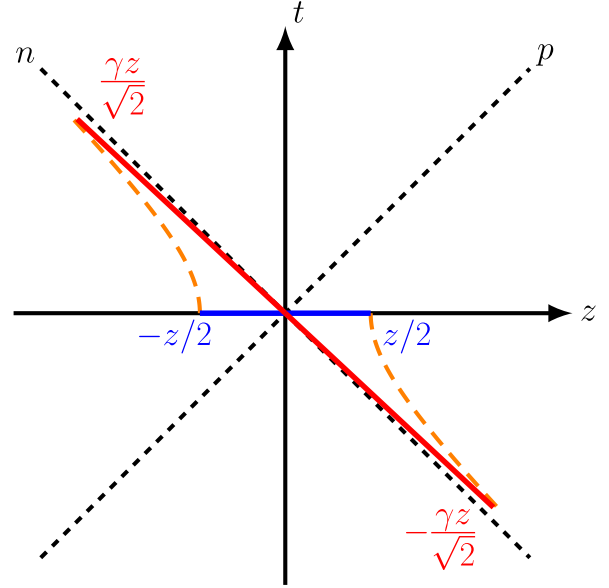

FIG. 5. Line segment in the z direction in the frame of a large-momentum hadron. Through the Lorentz boost, it is equivalent to a line segment of length $\sim \gamma z$ close to the light one in the hadron state of zero momentum. Here $\gamma z/\sqrt{2}$ is the length of projection of the boosted line segment to the light-cone direction n. Thus, we call the dimensionless variable $\lambda = zP^z \sim \gamma zM$ as the quasi light-cone distance.

momentum scale from 0 to P, whereas the physics from degrees of freedom from P to ∞ can be integrated out to generate the perturbative coefficients $\tilde{C}$ and the high-order terms in $1/(P^z)^2$. In contrast to HQET, the full QCD degrees of freedom are used in LaMET calculations. In other words, the effective Lagrangian of LaMET is the standard QCD one, while the large momentum P for expansions appears only in the external states.

D. Recipe for parton physics in LaMET

The principle of LaMET is to simulate the time dependence of parton observables through external states at large momentum. Thus, we can generalize the discussions in Sec. II.C to any type of physical observable for the large-momentum proton, which are generally called quasiparton observables. Examples given later include transverse-momentum-dependent distributions and LF wave functions.

Consider any Euclidean quasiobservable O that depends on a large hadron momentum P^z and UV cutoff $\Lambda_{\text{UV}} \gg P^z$. Using asymptotic freedom, we can systematically expand the P^z dependence as follows:

$$O(P^z, \Lambda_{\text{UV}}) = Z\left(\frac{P^z}{\Lambda_{\text{UV}}}, \frac{P^z}{\mu}\right) \otimes o(\mu) + \mathcal{O}\left(\frac{\Lambda_{\text{QCD}}^2}{(P^z)^2}\right) + \cdots, \quad (35)$$

where the crossed times symbol refers to a convolution if appropriate and Z factorizes all the perturbative dependence on P^z and does not contain any IR divergence. The quantity $o(\mu)$ is defined in a theory with $P^z \to \infty$, exactly as in

Feynman's parton model. In fact, $o(\mu)$ is a LF correlation containing all the IR collinear and soft singularities. The important point of the expansion is that it may converge at moderately large P^z, say, a few GeV, allowing access to quantities needed for large P^z (a few TeV). One can also use the large boost factor $\gamma = P^z/M$ as the expansion parameter $1/\gamma$.

The momentum dependence of the quasiobservables can be studied through momentum RGEs. If we define the anomalous dimension through

$$\gamma_P(\alpha_s) = \frac{1}{Z}\frac{\partial Z}{\partial \ln P^z}, \tag{36}$$

it follows that

$$\frac{\partial O(P^z)}{\partial \ln P^z} = \gamma_P(\alpha_s) \otimes O(P^z) \tag{37}$$

up to power corrections. One can resum large logarithms involving P^z using Eq. (37).

When taking $P^z \to \infty$ first in $O(P^z)$ before a UV regularization is imposed, one recovers from $\hat{O}$ the light-cone operator $\hat{o}$ by construction. On the other hand, the physical matrix element is calculated at a large P^z, with UV regularization such as the lattice cutoff imposed first. Thus, the difference between the matrix elements of $\hat{o}$ and $\hat{O}$ is a matter of the order of the limits. This is the standard setup for an EFT. The different limits do not change the IR physics. In fact, the factorization in terms of Feynman diagrams can be proved order by order as in the renormalization program, as discussed in Sec. III.

The parton physics can be calculated more directly by reversing Eq. (35) to produce the following EFT expansion:

$$o(\mu) = \tilde{Z}\left(\frac{P^z}{\Lambda_{\mathrm{UV}}}, \frac{P^z}{\mu}\right) \otimes O(P^z, \Lambda_{\mathrm{UV}}) + \mathcal{O}\left(\frac{\Lambda_{\mathrm{QCD}}^2}{(P^z)^2}\right) + \cdots. \tag{38}$$

Thus, to compute any parton observable defined by an operator made of LF dynamical fields $\hat{o}$, one constructs a time-independent version $\hat{O}$ that, under an infinite Lorentz boost, approaches $\hat{o}$. One then calculates the matrix element of $\hat{O}$ in a hadron with large momentum P^z using whatever approach (lattice QCD is an obvious choice for the time-independent operator $\hat{O}$) and then uses Eq. (38) to systematically approximate the parton observable. Usually the matrix element of $\hat{O}$ depends on P^z as well as all the lattice UV artifacts. In principle, the latter does not affect the EFT expansion and will be canceled out by the matching coefficient $\tilde{Z}$ and higher-order terms in the expansion. However, in practical applications, such as the quasi-PDF calculations, a nonperturbative renormalization is still necessary to remove all the power divergences to ensure a continuum limit.

E. Universality

LaMET provides a framework to systematically compute partonic observables on the LF from the properties of a large-momentum proton. However, the relationship is not one to

one. There can be infinitely many possible Euclidean operators in the large-momentum proton that generate the same LF observable. This is because the large-momentum physical states have built-in collinear (as well as soft) parton modes, and upon acting on a Euclidean operator they help to *project out* the leading LF physics. All operators projecting out the same LF physics form a *universality class*. Accordingly, in the operator formulation for parton physics such as SCET, one uses LF operators to project out parton physics off the external states of any momentum, including $P = 0$.

Concepts such as the universality class have been used in critical phenomena in condensed matter physics, where systems with different microscopic Hamiltonians can have the same scaling properties near their critical points. Critical phenomena correspond to the IR fixed points of the scale transformation and are dominated by physics at long-distance scales. In this case, parton physics arises from the infinite-momentum limit ($P = \infty$), which is a UV fixed point of the momentum RGEs. It is the longitudinal short-distance (or large-momentum) physics that is relevant at the fixed point. However, the short distance here does not mean that everything is perturbative. The part that is nonperturbative characterizes the partonic structure of the proton. The critical region near $P = \infty$ acts as a filter to select only the physics that is relevant, so universality classes emerge.

In the case of unpolarized PDFs, the initial proposal in LaMET starts with the matrix element of the following operator (Ji, 2013):

$$O_1(z) = \bar{\psi}(0)\gamma^z W(0, z)\psi(z). \tag{39}$$

However, one could alternatively start with (Constantinou and Panagopoulos, 2017; Radyushkin, 2017b)

$$O_2(z) = \bar{\psi}(0)\gamma^0 W(0, z)\psi(z), \tag{40}$$

and the leading contributions in the large-momentum expansion would be the same. One could also consider any linear combination of the two. Jia *et al.* (2018) did the calculations with these two operators in the 't Hooft model, and the results have been compared at different hadron momenta. For lattice simulations, an important issue is about the operator mixing, which depends on the specific choice of operators in the universality class.

Another example of Euclidean operators for PDFs is the following current-current correlators in a pure space separation:

$$O_3(z) = J^\mu(0)J^\nu(z), \tag{41}$$

where J^μ is an electromagnetic current. This type of correlator was first considered by Braun and Müller (2008) and Bali *et al.* (2018) for the calculation of pion distribution amplitude (DA) and recently has been suggested for calculating PDFs with generalized bilocal "currents" (Ma and Qiu, 2018a). When the matrix elements are calculated in the large-momentum states, $O(z)$ falls into the same universality class as the operators in Eqs. (39) and (40). Instead of using light quarks as the intermediate propagator in $O(z)$, one can have a number of

other choices for LaMET applications, including scalars (Aglietti *et al.*, 1998; Abada *et al.*, 2001) and heavy quarks (Detmold and Lin, 2006). One can similarly work with quark bilinear operators in any physical gauge that becomes the light-front one in the large-momentum limit (Gupta, Daniel, and Grandy, 1993).

Another important example of universality class is the gluon helicity contribution to the spin of the proton, as we discuss in detail in Sec. IV.D. The gluon spin operator $\vec{E} \times \vec{A}$ is gauge dependent. However, in physical gauges where the transverse degrees of freedom are dynamical, the matrix element is the same in the large-momentum limit. Therefore, one can potentially choose different gauges to perform calculations at finite momentum on the lattice, such as the Coulomb gauge $\vec{\nabla} \cdot \vec{A} = 0$, the axial gauge $A^z = 0$, or the temporal gauge $A^0 = 0$. Different gauge choices will have different UV properties ($\ln P$) and hence different matching conditions. However, the IR part of the matrix element is the same (Hatta, Ji, and Zhao, 2014).

At a practical level, it is useful to determine which operator has the fastest convergence in the LaMET expansion. The current-current correlators use the light-quark propagator to simulate the lightlike Wilson line (sometimes called light ray). The quasi-PDF approach not only starts from a quantity with a clear physical meaning (a momentum distribution) but also generates the needed Wilson line simply by rotating a spacelike one (shown in Fig. 5). Thus, it is plausible that the quasi-PDF will mathematically provide a faster large-P convergence than the other choices.

III. RENORMALIZATION AND MATCHING FOR PDFs

In this section, we consider the LaMET application for calculating the simplest collinear PDFs, which have been the most extensively studied in the literature so far. Although universality allows one to extract the collinear PDFs from the matrix elements of a wide class of operators evaluated at large momentum, we focus on physical observables closely resembling the collinear PDFs, i.e., the quark and gluon momentum distributions or the quasi-PDFs. We also discuss the coordinate-space factorization approach in which the pseudo-PDF and current-current correlators have been studied.

We mainly review the technical progress made in renormalization and matching using the quasi-PDFs. The matching can be done in principle at the bare matrix element level since a factorization formula like Eq. (33) is valid for both bare and renormalized momentum distributions. All the UV divergences in the bare quasi-PDF can be factorized into the matching coefficient C, and the latter automatically renormalizes the bare lattice matrix elements, so the continuum limit can be taken afterward. However, such a matching coefficient then has to be calculated in lattice perturbation theory, which is computationally challenging and converges slowly (Lepage and Mackenzie, 1993). The quasi-PDF contains linear power divergence under UV cutoff regularization due to the Wilson-line self-energy (Ji, 2013; Xiong *et al.*, 2014), which makes it impossible to take the continuum limit with fixed-order calculations in lattice perturbation theory. Although the latter problem can be improved by resumming the linear and

possibly the logarithmic divergences, it is usually preferred to nonperturbatively renormalize the quasi-PDFs on the lattice, after which a continuum limit can be taken and a perturbative matching can be done in the continuum theory. To this end, a thorough understanding of the renormalizability of Wilson-line operators defining the quasi-PDFs is required. In addition to renormalization, the applications of LaMET rely on the validity of the large-momentum factorization formula (33), which can be proven in perturbation theory to all orders by showing that the collinear divergences are the same in the momentum distributions and light-cone PDFs.

We begin in Sec. III.A with the proof of multiplicative renormalizability of the Wilson-line operators that define the quasi-PDFs. We first work in the continuum theory with the $\overline{\text{MS}}$ scheme, then generalize the conclusion to lattice theory. In Sec. III we next outline the factorization theorem for momentum distributions to all orders in perturbation theory and state the form of convolution between the matching coefficient and the PDF. In Sec. III.C we show that the factorization theorem has an equivalent form in coordinate space that can be used as an alternate route to extract PDFs from lattice matrix elements. Finally, we discuss the nonperturbative renormalization of quasi-PDFs on the lattice and their matching to the $\overline{\text{MS}}$ PDF in Sec. III.D.

A. Renormalization of nonlocal Wilson-line operators

The momentum distributions of the proton are defined from equal-time nonlocal Wilson-line operators of the form of Eq. (21). In this section, we review the renormalization of these spacelike nonlocal operators [the renormalization of lightlike nonlocal operators defining the PDFs was given by Collins and Soper (1982b) and Collins (2011a)]. We first discuss their renormalization in DR using an auxiliary field approach, then discuss similar gluon operators. We then consider power divergences in the momentum cutoff type of UV regularization. The conclusion is that they are all multiplicatively renormalizable with a finite number of mixings with other operators.

1. Renormalization of nonlocal quark operators

We are interested in operators of the following kind:

$$O_\Gamma(z) = \bar{\psi}\left(\frac{z}{2}\right)\Gamma W\left(\frac{z}{2}, -\frac{z}{2}\right)\psi\left(-\frac{z}{2}\right). \qquad (42)$$

Since the Wilson line $W(z_1, z_2)$ is a path-ordered integral of gauge fields, it is not obvious that such operators are multiplicatively renormalizable. The renormalization of non-lightlike Wilson loops and Wilson lines was studied in the early literature (Dotsenko and Vergeles, 1980; Craigie and Dorn, 1981), and the all-order proof of their multiplicative renormalizability was first made using diagrammatic methods (Dotsenko and Vergeles, 1980; Craigie and Dorn, 1981) and then the functional formalism of gauge theories (Dorn, 1986). The same conclusion was also conjectured to hold for the quark bilinear operator $O_\Gamma(z)$, whose renormalization takes the following form (Musch *et al.*, 2011; Ishikawa *et al.*, 2016; Chen, Ji, and Zhang, 2017):

$$O_\Gamma^B(z, \Lambda) = Z_{\psi,z}(\Lambda, \mu) e^{\delta m(\Lambda)|z|} O_\Gamma^R(z, \mu), \qquad (43)$$

where B and R stand for bare and renormalized operators, respectively, and all the fields and couplings in $O_\Gamma^B(z, \Lambda)$ are bare ones that depend on the UV cutoff Λ. $\delta m(\Lambda)$ is the "mass correction" of the Wilson line, which includes all the linear power divergences of its self-energy. $Z_{\psi,z}(\Lambda, \mu)$ includes all the logarithmic divergences from wave-function and vertex renormalizations.

An early two-loop study of the quasi-PDF in the $\overline{\text{MS}}$ scheme indeed indicated the multiplicative renormalizability of $O_\Gamma(z)$ (Ji and Zhang, 2015). The first rigorous proof of Eq. (43) was given in the auxiliary "heavy-quark" field formalism (Green, Jansen, and Steffens, 2018; Ji, Zhang, and Zhao, 2018), which was used to prove the renormalizability of Wilson lines (Samuel, 1979; Arefeva, 1980; Gervais and Neveu, 1980; Dorn, 1986). This formalism is defined by extending the QCD Lagrangian to include the auxiliary heavy-quark fields $Q, \bar{Q}$ and their gauge interaction as follows:

$$\mathcal{L} = \mathcal{L}_{\text{QCD}} + \bar{Q}_0 i n_z \cdot D_0 Q_0, \qquad (44)$$

where the subscript 0 denotes bare quantities. $n_z^\mu = (0, 0, 0, 1)$ is the direction vector of the spacelike Wilson line $W(z, 0)$, $D_0^\mu = \partial^\mu + i g_0 A_0^\mu$, and Q_0 is a color-triplet scalar Grassmann field in the fundamental representation of SU(3). Note that if we replace n_z^μ with the timelike vector $n_t^\mu = (1, 0, 0, 0)$, then Eq. (44) yields the leading-order HQET Lagrangian.

In the theory defined by Eq. (44), the Wilson line can be expressed as the following connected two-point function of the heavy-quark fields:

$$\langle Q_0(\xi) \bar{Q}_0(\eta) \rangle_Q = S_0^Q(\xi, \eta), \qquad (45)$$

where ξ and η are space-time coordinates and $\langle \cdots \rangle_Q$ stands for integrating out the auxiliary fields. Equation (45) is valid up to the determinant of $i n_z \cdot D_0$, which is a constant and can be absorbed into the normalization of the generating functional (Mannel, Roberts, and Ryzak, 1992). The Green's function $S_0^Q(\xi, \eta)$ satisfies

$$i n_z \cdot D_0(\xi) S_0^Q(\xi, \eta) = \delta^{(4)}(\xi - \eta), \qquad (46)$$

which has the solution

$$S_0^Q(\xi, \eta) = W(\xi^3, \eta^3) \theta(\xi^3 - \eta^3) \delta(\xi^0 - \eta^0) \delta^{(2)}(\vec{\xi}_\perp - \vec{\eta}_\perp) \quad (47)$$

with a proper choice of boundary condition. In this way, the Wilson-line operator $O_\Gamma^B(z)$ can be replaced by the following product of two local composite operators averaged over all the heavy-quark field configurations (Dorn, 1986):

$$O_\Gamma^B(z) = \int d^4\xi \, \delta(\xi^3 - z)$$
$$\times \left\langle \bar{\psi}_0\left(\frac{\xi}{2}\right) Q_0\left(\frac{\xi}{2}\right) \Gamma \bar{Q}_0\left(-\frac{\xi}{2}\right) \psi_0\left(-\frac{\xi}{2}\right) \right\rangle_Q, \quad (48)$$

where the UV regulator is suppressed.

Consequently, the renormalization of $O_\Gamma^B(z)$ is reduced to that of the two local "heavy-to-light" currents

$$J^B = \bar{Q}_0 \psi_0. \qquad (49)$$

The renormalizability of this auxiliary field theory has been proven using the standard functional techniques for gauge theories (Dorn, 1986). After fixing the covariant gauge and introducing the ghost fields, the theory including the auxiliary heavy quark has a residual Becchi-Rouet-Stora-Tyutin (BRST) symmetry, from which one can derive the Ward-Takahashi identities to show that all the UV divergences of the Green's functions can be subtracted using a finite number of local counterterms. In analogy, the same method has also been used to prove the all-order renormalization of HQET in perturbation theory (Bagan and Gosdzinsky, 1994).

According to Dorn (1986), the heavy-quark Lagrangian can be renormalized in a covariant gauge as

$$\mathcal{L} = \mathcal{L}_{\text{QCD}}[g_0, \psi_0, A_0, c_0] + \bar{Q}_0 i n_z \cdot D_0 Q_0$$
$$= \mathcal{L}_{\text{QCD}}[g, \psi, A, c] + \mathcal{L}_{\text{c.t.}}[g, \psi, A, c]$$
$$+ Z_Q \bar{Q}(i n_z \cdot \partial - i \delta m) Q - g Z_1^{QQg} \bar{Q} n_z \cdot A_a t^a Q, \quad (50)$$

where $\mathcal{L}_{\text{c.t.}}[g, \psi, A, c]$ are the QCD counterterms and the bare fields and coupling are related to the renormalized ones through

$$\psi_0 = Z_\psi^{1/2} \psi, \quad A_0 = Z_A^{1/2} A, \quad Q_0 = Z_Q^{1/2} Q, \quad g_0 = Z_g g. \quad (51)$$

The heavy-quark-gluon vertex renormalization constant Z_1^{QQg} is related to Z_g through the Slavnov-Taylor identities of the auxiliary field theory (Dorn, 1986) as follows:

$$Z_g = Z_1^{QQg} Z_A^{-1/2} Z_Q^{-1}. \qquad (52)$$

The $i\delta m$ can be regarded as the mass correction of the heavy quark except that it is imaginary. For Dirac fermions, the mass correction is logarithmically divergent and proportional to the bare mass as a result of chiral symmetry; for HQET, the mass correction of the heavy quark is proportional to the UV cutoff, i.e., linearly divergent, which is also expected for the auxiliary field here. Since the proof of renormalizability for this auxiliary field theory is carried out in the $\overline{\text{MS}}$ scheme with DR ($d = 4 - 2\epsilon$), all power divergences vanish, as does δm. Nevertheless, δm may include $\mathcal{O}(\Lambda_{\text{QCD}})$ contributions due to the renormalon ambiguities that are known to exist in HQET (Beneke and Braun, 1994; Bigi *et al.*, 1994).

Since the auxiliary field theory is renormalizable, the renormalization of the operator product in Eq. (48) amounts to the renormalizations of the two heavy-to-light currents. Using the standard techniques in quantum field theory (Collins, 1986), one can show recursively that the overall UV divergence of the insertion of J^B into Green's functions is absorbed into a renormalization factor Z_J to all orders in perturbation theory as follows:

$$J^B = Z_J J^R = Z_\psi^{1/2} Z_Q^{1/2} Z_V J^R, \qquad (53)$$

where Z_V is the vertex renormalization constant of the heavy-to-light current. The renormalization of heavy-to-light currents in HQET has been calculated up to three-loop order in perturbative QCD (Shifman and Voloshin, 1987; Politzer and Wise, 1988; Broadhurst and Grozin, 1991; Ji and Musolf, 1991; Chetyrkin and Grozin, 2003). More recently it was argued that the anomalous dimension of the heavy-to-light current is identical to that in HQET to all orders (Braun, Chetyrkin, and Kniehl, 2020), which is also the case for the "heavy-to-gluon" current that is discussed later, so the renormalization factors for the spacelike and timelike Wilson-line operators should be exactly the same.

Using the previous results, we can show that

$$
\begin{aligned}
O_\Gamma^B(z) &= Z_J^2 \int d^4\xi \, \delta(\xi^3 - z) \left\langle \bar{J}^R\left(\frac{\xi}{2}\right) \Gamma J^R\left(-\frac{\xi}{2}\right) \right\rangle_Q \\
&= Z_J^2 e^{\delta m |z|} O_\Gamma^R(z),
\end{aligned}
\tag{54}
$$

where δm arises from the determinant of $(in_z \cdot \partial - \delta m)$ in Eq. (50). In this way, we identify that $Z_{\psi,z} = Z_J^2$ in Eq. (43), which is independent of Γ. At one-loop order (Stefanis, 1984),

$$
Z_{\psi,z} = 1 + \frac{\alpha_s C_F}{4\pi} \frac{3}{\epsilon_{\rm UV}},
\tag{55}
$$

where the UV regulator $\epsilon_{\rm UV}$ is to be distinguished from the IR regulator $\epsilon_{\rm IR}$ in DR.

The multiplicative renormalizability of $O_\Gamma^B(z)$ has also been proven with a recursive analysis of all-order Feynman diagrams (Ishikawa *et al.*, 2017). In addition to Eq. (43), it was found that $O_\Gamma^B(z)$ does not mix with gluons or quarks of other flavors. This can also be easily understood within the auxiliary field formalism, as the flavor-changing heavy-to-light current does not mix with other operators (Green, Jansen, and Steffens, 2020).

Finally, under lattice regularization we can still use the previous techniques to prove Eq. (54), where the mass correction δm is now nonvanishing and equal to the lattice UV cutoff $1/a$ multiplied by a perturbative series in the coupling constant α_s.

2. Renormalization of nonlocal gluon operators

Using the same heavy-quark auxiliary field formalism, it has also been proven that the Wilson-line operators for the gluon quasi-PDF are multiplicatively renormalizable (Zhang, Ji *et al.*, 2019), which is echoed by the diagrammatical proof given by Li, Ma, and Qiu (2019).

According to LaMET, the gluon quasi-PDF can be defined as (Ji, 2013)

$$
\tilde{g}(x, P^z) = N \int \frac{d\lambda}{4\pi x (P^z)^2} e^{i\lambda x} \langle P | O_g(z) | P \rangle,
\tag{56}
$$

where N is a normalization factor and

$$
O_g^B(z) = g_{\perp,\mu\nu} F_{0,a}^{n_1\mu}\left(\frac{z}{2}\right) W^{ab}\left(\frac{z}{2}, -\frac{z}{2}\right) F_{0,b}^{n_2\nu}\left(-\frac{z}{2}\right),
\tag{57}
$$

with $F_{0,a}^{n\mu} = n_\rho F_{0,a}^{\rho\mu}$ and n_1^μ, n_2^μ being either n_z^μ or n_t^μ. a, b are color indices in the adjoint representation. The transverse metric tensor

$$
g_\perp^{\mu\nu} = g^{\mu\nu} - n_t^\mu n_t^\nu / n_t^2 - n_z^\mu n_z^\nu / n_z^2,
\tag{58}
$$

and $N = (n_z \cdot P / n_t \cdot P)^{(n_1 + n_2) \cdot n_t}$. For lattice implementation, $O_g^B(z)$ can also be defined as (Dorn, 1986; Zhang, Ji *et al.*, 2019)

$$
O_g^B(z) = 2 g_\perp^{\mu\nu} \text{tr}\left[F_{0,\mu}^{n_1}\left(\frac{z}{2}\right) W\left(\frac{z}{2}, -\frac{z}{2}\right) F_{0,\nu}^{n_2}\left(-\frac{z}{2}\right) W\left(-\frac{z}{2}, \frac{z}{2}\right) \right],
\tag{59}
$$

where $F^{\mu\nu} = F_a^{\mu\nu} t^a$ and W are in the fundamental representation. As in Eq. (48), we can express $O_g^B(z)$ as a product of two local composite operators:

$$
\begin{aligned}
\tilde{O}_g^B(z) &= \int d^4\xi \, \delta(\xi^3 - z) \\
&\quad \times g_{\perp,\mu\nu} \left\langle F_{0,a}^{n_1\mu}\left(\frac{\xi}{2}\right) Q_0^a\left(\frac{\xi}{2}\right) \bar{Q}_0^b\left(-\frac{\xi}{2}\right) F_{0,b}^{n_2\nu}\left(-\frac{\xi}{2}\right) \right\rangle_Q \\
&\equiv \int d^4\xi \, \delta(\xi^3 - z) g_\perp^{\mu\nu} \left\langle J_{n_1\mu}^B\left(\frac{\xi}{2}\right) \bar{J}_{n_2\nu}^B\left(-\frac{\xi}{2}\right) \right\rangle_Q,
\end{aligned}
\tag{60}
$$

where the auxiliary heavy-quark fields are in the adjoint representation and

$$
J_B^{\mu\nu} = F_{0,a}^{\mu\nu} Q_0^a, \qquad \bar{J}_B^{\mu\nu} = \bar{Q}_0^a F_{0,a}^{\mu\nu}.
\tag{61}
$$

The renormalization of $J_B^{\mu\nu}$ and $\bar{J}_B^{\mu\nu}$ is more involved than the quark case, as they can mix with other composite operators of the same or fewer dimensions. In DR, BRST symmetry allows $J_B^{\mu\nu}$ to mix with (Dorn, 1986; Zhang, Ji *et al.*, 2019)

$$
J_{2B}^{\mu\nu} = (n_z^\nu F_{0,a}^{\mu n_z} - n_z^\mu F_{0,a}^{\nu n_z}) Q_0^a / n_z^2,
\tag{62}
$$

$$
J_{3B}^{\mu\nu} = (-in_z^\mu A_{0,a}^\nu + in_z^\nu A_{0,a}^\mu)[(in_z \cdot D_0 - i\delta m) Q_0]^a / n_z^2.
\tag{63}
$$

Their renormalization matrix is given by (Dorn, 1986)

$$
\begin{pmatrix} J_B^{\mu\nu} \\ J_{2B}^{\mu\nu} \\ J_{3B}^{\mu\nu} \end{pmatrix} = \begin{pmatrix} Z_{11} & Z_{12} & Z_{13} \\ 0 & Z_{22} & Z_{23} \\ 0 & 0 & Z_{33} \end{pmatrix} \begin{pmatrix} J_R^{\mu\nu} \\ J_{2R}^{\mu\nu} \\ J_{3R}^{\mu\nu} \end{pmatrix},
\tag{64}
$$

where $J_{2B}^{\mu\nu}$ is gauge invariant while $J_{3B}^{\mu\nu}$ is gauge dependent and proportional to the equation of motion (EOM) for the auxiliary field. The Green's functions of the EOM operator will result in a δ function

$$
[in_z \cdot D_0(\xi) - i\delta m] \langle Q_0(\xi) \bar{Q}_0(0) \rangle_Q = \delta^{(4)}(\xi)
\tag{65}
$$

that contributes a contact term $\delta(z)$ only after integrating over the auxiliary fields. As long as $z \neq 0$, such mixing vanishes in all Green's functions of $O_g^B(z)$, so we can ignore the mixing between $J_B^{\mu\nu}$ and $J_{3B}^{\mu\nu}$ in the renormalization of $O_g^B(z)$.

At $z = 0$, $O_g^B(z)$ becomes a local operator and is known to mix with BRST-exact and EOM operators (Collins and Scalise, 1994), whose renormalization can be performed in the standard way.

Note that when contracted with n_z as

$$J_{2B}^{n_z\mu} = J_B^{n_z\mu} = F_{0,a}^{n_z\mu}Q_0^a,$$

$$J_{3B}^{n_z\mu} = i\left(-A_0^{\mu,a} + \frac{n_z^\mu}{n_z^2}n_z \cdot A_0^a\right)[(in_z \cdot D_0 - i\delta m)Q_0]_a, \quad (66)$$

the $J_B^{n_z\mu}$ mixes only with the EOM operator $J_{3B}^{n_z\mu}$. As previously argued, we can ignore such mixing for $z \neq 0$. Moreover, this degeneracy also leads to relations among elements in the renormalization matrix (Dorn, 1986),

$$Z_{11} + Z_{12} = Z_{22}, \qquad Z_{13} = Z_{23}. \quad (67)$$

When contracted with n_t,

$$J_B^{n_t\mu} = F_{0,a}^{n_t\mu}Q_0^a,$$
$$J_{2B}^{n_t\mu} = n_z^\mu F_{a,0}^{n_t n_z}Q_0^a/n_z^2,$$
$$J_{3B}^{n_t\mu} = i\frac{n_z^\mu}{n_z^2}n_t \cdot A_0^a[(in_z \cdot D_0 - i\delta m)Q_0]_a. \quad (68)$$

As one can see, $J_{2B}^{n_t\mu}$ and $J_{3B}^{n_t\mu}$ vanish after contraction with $g_\perp^{\mu\nu}$, so $J_B^{n_t\mu}$ with the transverse Lorentz index μ is multiplicatively renormalizable.

To summarize, for $z \neq 0$ and the transverse Lorentz index μ, both $J_B^{n_z\mu}$ and $J_B^{n_t\mu}$ are multiplicatively renormalizable in coordinate space, thus proving the following renormalizability of the gluon Wilson-line operator $O_g^B(z)$:

$$O_g^B(z) = Z_J Z_{\bar{J}} \int d^4\xi\, \delta(\xi^3 - z)g_\perp^{\mu\nu}\left\langle J_{n_1\mu}^R\left(\frac{\xi}{2}\right)\bar{J}_{n_2\nu}^R\left(-\frac{\xi}{2}\right)\right\rangle_Q$$

$$= e^{\delta m|z|}Z_J Z_{\bar{J}} O_g^R(z), \quad (69)$$

where

$$J_B^{n_1\mu} = Z_J J_R^{n_1\mu} = (Z_Q^g)^{1/2}Z_A^{1/2}Z_V^g J_R^{n_1\mu}, \quad (70)$$

$$\bar{J}_B^{n_2\nu} = Z_{\bar{J}} J_R^{n_2\nu} = (Z_Q^g)^{1/2}Z_A^{1/2}Z_{\bar{V}}^g J_R^{n_2\mu}, \quad (71)$$

with Z_V^g and $Z_{\bar{V}}^g$ the renormalization constants for the vertex involving one gluon and one heavy-quark field. The wave-function renormalization constant for the auxiliary heavy quark Z_Q^g is different than in the quark case as it is in the adjoint representation.

In addition, since $J_B^{n_z\mu}$ and $J_B^{n_t\mu}$ do not mix with heavy-to-light quark currents due to the mismatch of quantum numbers, this implies that the nonlocal gluon Wilson-line operator does not mix with the singlet quark one under renormalization.

For the polarized gluon quasi-PDF, its definition is the same as Eq. (56) except that the gluon Wilson-line operator becomes

$$\Delta O_g^B(z) = \epsilon_{\perp,\mu\nu}F_{0,a}^{n_1\mu}(z)W^{ab}(z,0)F_{0,b}^{n_2\nu}(0), \quad (72)$$

where $\epsilon_\perp^{\mu\nu} = \epsilon^{03\mu\nu}$. Since $\epsilon_\perp^{\mu\nu}$ contracts only with the transverse Lorentz indices, one can use the same proof for $O_g^B(z)$ to show that $\Delta O_g^B(z)$ is also multiplicatively renormalizable and does not mix with the singlet quark case (Zhang, Ji *et al.*, 2019).

Finally, one can also prove that Eq. (69) is valid under lattice regularization with δm linearly divergent (Zhang, Ji *et al.*, 2019). This completes the proof of renormalizability of the gluon Wilson-line operators.

One-loop renormalization.—Now we demonstrate the previous result using an explicit one-loop example. For the nonlocal Wilson-line operators to be multiplicatively renormalizable, it is important that all linear divergences associated with diagrams other than the Wilson-line self-energy cancel out among themselves. To see this, a gauge symmetry preserving regularization is crucial. We use DR and keep poles around $d = 3$ to identify the linear divergences (Wang, Zhang *et al.*, 2019; Zhang, Ji *et al.*, 2019).

The one-loop vertex correction to the heavy-to-gluon current is shown in Fig. 6. Each diagram contributes

$$I_a^{\rho\nu} = \frac{\alpha_s C_A}{\pi}\left[\frac{1}{4-d}\frac{3}{4}F_a^{\rho\nu}Q_a + \text{finite terms}\right],$$

$$I_b^{\rho\nu} = \frac{\alpha_s C_A}{\pi}\left[\frac{1}{d-4}(A_a^\nu n_z^\rho - A_a^\rho n_z^\nu)n_z \cdot \partial Q_a/n_z^2\right.$$

$$\left. + \frac{\pi\mu}{d-3}(n_z^\rho A_a^\nu - n_z^\nu A_a^\rho)Q_a + \text{finite terms}\right],$$

$$I_c^{\rho\nu} = \frac{\alpha_s C_A}{\pi}\left\{\frac{1}{d-4}\left[\frac{1}{2}(F_a^{\rho n_z}n_z^\nu - F_a^{\nu n_z}n_z^\rho)Q_a/n_z^2\right.\right.$$

$$\left. + \frac{1}{4}F_a^{\rho\nu}Q_a + \frac{1}{2}(A_a^\rho n_z^\nu - A_a^\nu n_z^\rho)n_z \cdot \partial Q_a/n_z^2\right]$$

$$\left. - \frac{\pi\mu}{d-3}(n_z^\rho A_a^\nu - n_z^\nu A_a^\rho)Q_a + \text{finite terms}\right\}. \quad (73)$$

Figures 7(b) and 7(c) both include a linear divergence that is evident as the $\mu/(d-3)$ term, but they cancel among themselves. This guarantees that the overall UV divergence in the vertex correction is logarithmic, and the renormalization of the heavy-to-gluon current is thus multiplicative. Combining the one-loop results in Eq. (73) with the wave-function renormalizations, we have

$$Z_{11} = 1 + \frac{\alpha_s C_A}{4\pi}\frac{1}{\epsilon_{\rm UV}}, \qquad Z_{12} = 1 - \frac{\alpha_s C_A}{4\pi}\frac{1}{\epsilon_{\rm UV}},$$

$$Z_{13} = Z_{23} = 1 - \frac{\alpha_s C_A}{4\pi}\frac{1}{\epsilon_{\rm UV}}, \qquad Z_{22} = 0, \quad (74)$$

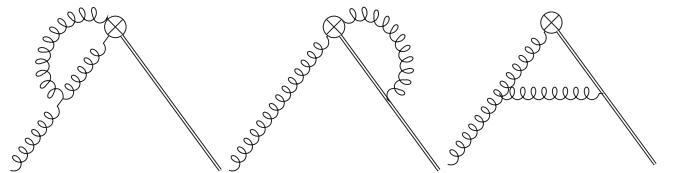
FIG. 6. One-loop vertex corrections to the heavy-to-gluon current.

where $C_A = N_c = 3$ for QCD. If we ignore the mixing to the EOM operator,

$$Z_V^{J^{n_z \nu}} = Z_V^{J^{\nu n_z}} = 0,$$

$$Z_V^{J^{n_t i}} = Z_V^{J^{i n_t}} = Z_V^{J^{ij}} = Z_V^{J^{ji}} = 1 + \frac{\alpha_s C_A}{4\pi} \frac{1}{\epsilon_{\text{UV}}}, \quad (75)$$

where $i, j = 1, 2$. As a result, the one-loop current renormalization constant is

$$Z_{J^{n_z \nu}} = Z_{J^{\nu n_z}} = 1 + \frac{\alpha_s}{4\pi} \left(\frac{1}{6} C_A - \frac{4}{3} n_f T_F \right) \frac{1}{\epsilon_{\text{UV}}},$$

$$Z_{J^{n_t i}} = Z_{J^{i n_t}} = Z_{J^{ij}} = Z_{J^{ji}}$$

$$= 1 + \frac{\alpha_s}{4\pi} \left(\frac{7}{6} C_A - \frac{4}{3} n_f T_F \right) \frac{1}{\epsilon_{\text{UV}}}, \quad (76)$$

where $T_F = 1/2$ and n_f is the number of active quark flavors. The two-loop results were given by Braun, Chetyrkin, and Kniehl (2020).

As one can see, the anomalous dimension of the heavy-to-gluon current is the same for $\mu, \nu = 0, 1, 2$, which is due to SO(2, 1) [or SO(3) in Euclidean space] symmetry around the z axis.

B. Factorization of quasi-PDFs

The key to LaMET applications for collinear-parton physics is the factorization formula that relates the quasi-PDFs to light-cone PDFs (Ji, 2013). Here we use the perturbative properties of the matching coefficients to write the following factorization form in the $\overline{\text{MS}}$ scheme in a manner consistent with a direct EFT calculation of PDFs at any given x (Izubuchi *et al.*, 2018; Wang, Zhang *et al.*, 2019):

$$q_i(x, \mu) = \int_{-\infty}^{\infty} \frac{dy}{|y|} \left[\sum_j \tilde{C}_{q_i q_j} \left(\frac{x}{y}, \frac{\mu}{yP^z} \right) \tilde{q}_j(y, P^z, \mu) \right.$$

$$\left. + \tilde{C}_{qg} \left(\frac{x}{y}, \frac{\mu}{yP^z} \right) \tilde{g}(x, P^z, \mu) \right] + \cdots, \quad (77)$$

$$g(x, \mu) = \int_{-\infty}^{\infty} \frac{dy}{|y|} \left[\sum_j \tilde{C}_{gq} \left(\frac{x}{y}, \frac{\mu}{yP^z} \right) \tilde{q}_j(y, P^z, \mu) \right.$$

$$\left. + \tilde{C}_{gg} \left(\frac{x}{y}, \frac{\mu}{yP^z} \right) \tilde{g}(y, P^z, \mu) \right] + \cdots, \quad (78)$$

where i and j run over quark and antiquark flavors. The ellipsis term includes mass corrections whose analytical forms have been derived to all orders of $M^2/(P^z)^2$ (Chen *et al.*, 2016), and higher-twist contributions of the order of $\mathcal{O}(\Lambda_{\text{QCD}}^2/(xP^z)^2, \Lambda_{\text{QCD}}^2/[(1-x)P^z]^2)$; see Eq. (33). All P^z dependence on the right-hand side cancels out, just like with a renormalization scale.

As explained in Sec. II, the previous factorization is guaranteed on the grounds of physics because the difference between quasi-PDFs and light-cone PDFs is of the order of limits in $P^z \to \infty$ and $\Lambda_{\text{UV}} \to \infty$, and the IR physics in both quantities must be the same. An all-order factorization proof

for the quark quasi-PDF in perturbation theory was first given with a diagrammatical approach (Ma and Qiu, 2018b). The formula has also been derived using the OPE of nonlocal Wilson-line operators (Izubuchi *et al.*, 2018; Ma and Qiu, 2018a; Wang, Zhang *et al.*, 2019). Here we outline a diagrammatic proof similar to that of Ma and Qiu (2018b), showing that the collinear divergences of the quasi-PDFs do factorize and are equal to those of the light-cone PDFs. Since the collinear divergence is a concept in perturbation theory, we show the factorization using a massless external quark state with lightlike momentum $P^\mu = (P^z, 0, 0, P^z)$. While the proof is only for perturbative free quark states, the factorization formulas are widely believed to be true nonperturbatively as well. We use DR to regulate both UV and collinear divergences and consider only bare quantities since UV renormalization does not change the leading collinear divergences.

Before the analysis, we mention that all the soft divergences cancel between the real and virtual contributions to the quasi-PDFs, as discussed in Sec. II.B; thus, we need to focus only on the collinear divergences. To obtain an intuitive understanding of the structure for collinear divergences, we start with the one-loop diagram in Fig. 4(a) in the Feynman gauge. The integral reads

$$\int \frac{d^{4-2\epsilon} k}{(2\pi)^{4-2\epsilon}} \frac{\text{tr}[\not{P} \not{k} \gamma^z \not{k}] \delta(k^z - yP^z)}{(k^2 + i0)^2 [(P-k)^2 + i0]}. \quad (79)$$

The internal quark momentum is $k^\mu = (k^+, k^-, \vec{k}_\perp)$ and the gluon momentum is $P - k$. When k^- and $k_\perp = |\vec{k}_\perp|$ are small, the internal quark and gluon become collinear to the external quark, i.e., $k^\mu \sim (k^+, 0, 0_\perp)$ and $(P-k)^\mu \sim (P^+ - k^+, 0, 0_\perp)$. In this case, the denominators of the quark and gluon propagators $(k^2)^2$ and $(P-k)^2$ both vanish, which leads to collinear divergence. Conversely, for $k^2 = (P-k)^2 = 0$, k must be collinear to P since the condition requires that $k^2 = k \cdot P = P^2 = 0$. For small k^- and $k_\perp$, the δ function is dominated by the k^+ term of $k^z = (k^+ - k^-)/\sqrt{2}$ and reduces to $\sqrt{2}\delta(k^+ - yP^+)$. This is simply the vertex that restricts $k^+ = yP^+$ for the light-cone PDF up to the factor $\sqrt{2}$. Furthermore, for collinear k and $P - k$ the spinor trace in the numerator is dominated by the γ^+ part of $\gamma^z = (\gamma^+ - \gamma^-)/\sqrt{2}$, $\text{tr}[\not{P} \not{k} \gamma^z \not{k}] \sim \text{tr}[\not{P} \not{k} \gamma^+ \not{k}]/\sqrt{2}$. Thus, in the collinear region $k^\mu \sim (k^+, 0, 0, 0)$ the previous integral reduces to that of the light-cone PDF as follows:

$$\int_c \frac{d^{4-2\epsilon} k}{(2\pi)^{4-2\epsilon}} \frac{\text{tr}[\not{P} \not{k} \gamma^+ \not{k}] \delta(k^+ - yP^+)}{(k^2 + i0)^2 [(P-k)^2 + i0]}, \quad (80)$$

where the subscript "c" denotes the collinear region.

This picture naturally arises in a highly boosted hadron state where the quark is approximately on shell. Therefore, as explained in Sec. II.E, although the operator contains no light-cone information, the large-momentum external hadron state can still generate collinear divergences equivalent to those in the light-cone PDFs. By subtracting the full integral for light-cone PDF from that for the quasi-PDF, the logarithmic collinear divergence cancels, and the remaining difference is perturbative and can be absorbed into the matching kernel.

Similarly, for the vertex diagram in Fig. 4(b) the loop integral is proportional to

$$\int \frac{d^{4-2\epsilon}k}{(2\pi)^{4-2\epsilon}} \frac{1}{P^z - k^z} \frac{\text{tr}[\not{P}\gamma^z \not{k}\gamma^z]\delta(k^z - yP^z)}{(k^2 + i0)[(P-k)^2 + i0]}. \quad (81)$$

The entire integral in the collinear region reduces to

$$\int_c \frac{d^{4-2\epsilon}k}{(2\pi)^{4-2\epsilon}} \frac{1}{P^+ - k^+} \frac{\text{tr}[\not{P}\gamma^+ \not{k}\gamma^+]\delta(k^+ - yP^+)}{(k^2 + i0)[(P-k)^2 + i0]}, \quad (82)$$

which is the corresponding integral for the light-cone PDF. One key feature of the diagram is that, while the gauge link probes the z component of the gluon field $A^z = (A^+ - A^-)/\sqrt{2}$, only the A^+ component (longitudinal polarization) contributes to the leading collinear divergence. While attaching a new collinear gluon to the gauge link induces a power suppression from the link propagator of $\mathcal{O}(1/P^z)$, the A^+ component of the collinear gluon radiated from fast-moving color charges receives enhancement from the Lorentz boost factor γ that compensates for the suppression.

This result can be generalized to all orders. As in the one-loop diagrams, in the leading region of collinear divergence there are an arbitrary number of longitudinally polarized A^+ gluons, which are emitted dynamically from the fast-moving state instead of being put in by hand using the lightlike gauge link, in contrast to the standard collinear PDF. The existence of the A^+ gluons increases the level of complication in showing the equivalence of collinear divergences between the quasi-PDFs and light-cone PDFs. For simplification, from now on we work in the light-cone gauge $A^+ = 0$ to eliminate all the A^+ gluons. Therefore, the vertex diagrams no longer contribute to the leading collinear divergence, thus making its structure much simpler.

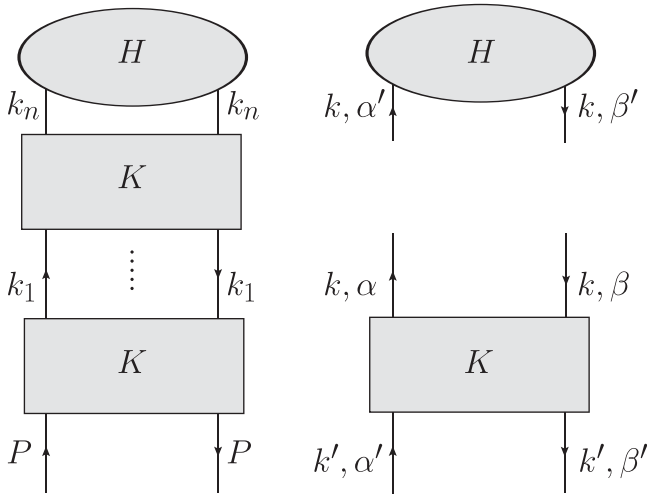In a general diagram, we decompose the potential leading region of the quasi-PDF into the ladder structure shown in Fig. 7. The upper two-particle-irreducible (2PI) kernel that contains the nonlocal operator defining the quasi-PDF is H. The 2PI kernel in the ladder is K. K contains the upper two external quark lines but not the lower ones. The momenta flowing out of the ladders are labeled as k_1 to k_n from bottom to top when there are n 2PI kernels. We write H and K as matrices in spinor and momentum space. $H = H_{\alpha'\beta'}(yP^z; k)$, where k denotes the momentum flowing into H and $K = K_{\alpha\beta;\alpha'\beta'}(k, k')$, where k, k' are the momenta of the upper and lower external legs, respectively. Here $\alpha\beta$ and $\alpha'\beta'$ are the spinor indices for the upper and lower two external legs, respectively. Following the method of Curci, Furmanski, and Petronzio (1980) and Collins (2011a), we find the following:

(1) There are no collinear divergences in the upper part H in the light-cone gauge.

(2) If none of $k_1, \ldots, k_n$ are collinear, there will be no leading collinear divergence. More generally, for the ith 2PI kernel, if either k_{i-1} or k_i is not collinear, then the subintegrals inside the kernel are finite and the kernel does not contribute to leading collinear divergence.

(3) If k_i is not collinear, then there are no collinear divergences for the upper part of the diagram above the ith ladder.

Therefore, the collinear divergences are generated in the momentum regions R_i in which k_1 to k_i are collinear, while k_{i+1} to k_n are not. We can construct counterterms that subtract out the collinear divergences in each of the regions R_i. For this we keep only the $+$ component of k_i in the convergent upper part HK^{n-i}, as in the one-loop example; namely, $k_i \to (k_i^+, 0, 0_\perp)$ in the upper part. This will leave the collinear divergence unchanged. Notice also that $[HK^{n-i}]_{\alpha\beta} = H_{\alpha'\beta'} K^{n-i}_{\alpha'\beta';\alpha\beta}$ should be understood as a 4×4 Dirac matrix with indices $\alpha\beta$, while the lower part is $[K^i \not{P}]_{\alpha\beta} = K^i_{\alpha\beta;\alpha'\beta'} \not{P}_{\alpha'\beta'}$. In the leading region of collinear divergence, HK^{n-i} and $K^i \not{P}$ are proportional to γ^+ and γ^-, respectively. Therefore, to obtain the leading collinear divergence, we can disentangle the spinor traces for the upper and lower parts by contracting them with $\gamma^-/2$ and $\gamma^+/2$ separately. The only communication between them is the k^+ integration. The collinear divergence is contained in the lower part

$$q^i(x, \epsilon_{\text{IR}}) = \int \frac{dk^- d^{d-2}k_\perp}{2(2\pi)^d} \text{tr}[\gamma^+ K^i(xP^+, k^-, k_\perp; P)\not{P}], \quad (83)$$

where $d = 4 - 2\epsilon$, $k^+ = xP^+$, and the subtraction for the region R_i can be written effectively as a convolution

$$\int \frac{dx}{x} \hat{C}^{n-i}(y, x, P^z) q^i(x, \epsilon_{\text{IR}}), \quad (84)$$

where

$$\hat{C}^{n-i}(y, x, P^z) = \tfrac{1}{2}\text{tr}[HK^{n-i}(yP^z; xP^+, 0, 0_\perp)(xP^+)\gamma^-] \quad (85)$$

is the naive matching kernel. Here the y dependence comes from the operator in H. However, the naive matching kernel still suffers from collinear subdivergences that need to be subtracted. This can be achieved using the subtracted matching kernels $C^{n-i}(y, x)$, defined recursively in a way similar to the

FIG. 7. Left panel: ladder decomposition of the quasi-PDF. The upper 2PI kernel H contains the operator defining the quasi-PDF, and the external two legs at the bottom of the diagram are the external large P^z state. Right panel: kernels H and K.

Bogoliubov-Parasiuk-Hepp-Zimmermann relation for UV renormalization (Collins, 2011a). If we sum over n and i, the recursive relation leads to

$$\tilde{q}(y, P^z, \epsilon_{\text{IR}}) = \sum_{n=0}^{\infty} \sum_{i=0}^{n} \int \frac{dx}{x} C^{n-i}(y, x, P^z) q^i(x, \epsilon_{\text{IR}})$$

$$= \int \frac{dx}{x} C(y, x, P^z) q(x, \epsilon_{\text{IR}}), \qquad (86)$$

where $\tilde{q}(y, P^z, \epsilon_{\text{IR}})$ is the quasi-PDF, $C(y, x, P^z) = \sum_{n=0}^{\infty} C^n(y, x, P^z)$ is the all-order matching kernel, and $q(x, \epsilon_{\text{IR}}) = \sum_{i=0} q^i(x, \epsilon_{\text{IR}})$. Based on the definition of $q^i(x, \epsilon_{\text{IR}})$, it is clear that q^i equals the light-cone PDF with i 2PI kernels and that q is the full light-cone PDF with natural support $0 < x < 1$. The light-cone PDF $q(x)$ is independent of the operator defining the quasi-PDF, as it is sensitive only to the explicit form of the collinear divergence. The rhs of Eq. (86) contains all the collinear divergences from the quasi-PDF $\tilde{q}$. Thus, the matching relation for bare quantities is established. A similar matching can be written down for the renormalized quantities, where the renormalization affects only the matching kernel $C(y, x, P^z)$. Note that the explicit solution for $C^{n-i}(y, x, P^z)$, which leads to Eq. (33), can be given based on a subtraction operator defined similar to that given by Collins (2011a). Besides, Eq. (86) can be inverted order by order in α_s, thus proving Eq. (33), which can also be generalized to Eqs. (77) and (78).

Now we present the matching coefficient in the $\overline{\text{MS}}$ scheme at one-loop order. The one-loop expansion of the $\overline{\text{MS}}$ quasi- and light-cone PDFs in a free massless quark state with momentum $p^\mu = (p^z, 0, 0, p^z)$ are

$$\tilde{q}(y, \mu/p^z, \epsilon_{\text{IR}}) = \tilde{q}^{(0)}(y) + \frac{\alpha_s C_F}{2\pi} \tilde{q}^{(1)}(y, \mu/p^z, \epsilon_{\text{IR}}), \quad (87)$$

$$q(x, \epsilon_{\text{IR}}) = q^{(0)}(x) + \frac{\alpha_s C_F}{2\pi} q^{(1)}(x, \epsilon_{\text{IR}}). \qquad (88)$$

At tree level, $\tilde{q}^{(0)}(y) = q^{(0)}(y) = \delta(1 - y)$. At one loop, the $\overline{\text{MS}}$ quasi-PDF and its counterterm are (Izubuchi *et al.*, 2018)

$$\tilde{q}^{(1)}(y, \mu/p^z, \epsilon_{\text{IR}})$$

$$= \begin{cases} \left(\frac{1+y^2}{1-y} \ln \frac{y}{y-1} + 1 + \frac{3}{2y}\right)^{[1,\infty]}_{+(1)} - \frac{3}{2y}, & y > 1, \\[2ex] \left(\frac{1+y^2}{1-y}\left[-\frac{1}{\epsilon_{\text{IR}}} - \ln \frac{\mu^2}{4(p^z)^2} + \ln[y(1-y)]\right]\right. \\ \left. -\frac{y(1+y)}{1-y} + 2\sigma(1-y)\right)^{[0,1]}_{+(1)}, & 0 < y < 1, \\[2ex] \left(-\frac{1+y^2}{1-y} \ln \frac{-y}{1-y} - 1 + \frac{3}{2(1-y)}\right)^{[-\infty,0]}_{+(1)} \\ -\frac{3}{2(1-y)}, & y < 0, \end{cases}$$

$$+ \delta(1-y)\left[\frac{3}{2} \ln \frac{\mu^2}{4(p^z)^2} + \frac{5+2\sigma}{2}\right], \qquad (89)$$

$$\delta\tilde{q}^{(1)}(y, \mu/p^z, \epsilon_{\text{UV}}) = \frac{3}{2\epsilon_{\text{UV}}} \delta(1-y), \qquad (90)$$

where ϵ_{IR} regulates the collinear divergence, $\sigma = 0$ for $\Gamma = \gamma^t$, and $\sigma = 1$ for $\Gamma = \gamma^z$. The plus function at $y = y_0$ with support in a given domain D is defined as

$$\int_D dy [g(y)]^D_{+(y_0)} h(y) = \int_D dy g(y)[h(y) - h(y_0)], \qquad (91)$$

with arbitrary $g(y)$ and $h(y)$. Note that the $\overline{\text{MS}}$ renormalization of the quasi-PDF actually requires a subtle treatment of vector current conservation (Izubuchi *et al.*, 2018). We present results only in a form that is sufficient for our discussion, which differs slightly from that of Izubuchi *et al.* (2018) using the δ functions at $y = \pm\infty$ and from the treatment given by Alexandrou, Cichy *et al.* (2019).

On the other hand,

$$q^{(1)}(x, \epsilon_{\text{IR}}) = \frac{\alpha_s C_F}{2\pi} \frac{(-1)}{\epsilon_{\text{IR}}} \left(\frac{1+x^2}{1-x}\right)^{[0,1]}_{+(1)}, \qquad (92)$$

which is limited to the physical region as expected.

By comparing the quasi-PDFs and light-cone PDFs in Eqs. (89) and (92), we find that both of them have the same collinear divergence or, in other words, they share the same IR physics, thus validating the factorization formula at one-loop order. Setting $p^z = xP^z$ and plugging the one-loop results into Eq. (33), we extract the following matching coefficient for the hadron matrix element that depends only on the perturbative scales μ and P^z:

$$C^{\overline{\text{MS}}}\left(y, \frac{\mu}{xP^z}\right) = \delta(1-y) + \frac{\alpha_s C_F}{2\pi}\left[\tilde{q}^{(1)}\left(y, \frac{\mu}{xP^z}, \epsilon_{\text{IR}}\right)\right.$$

$$\left. - q^{(1)}(y, \epsilon_{\text{IR}})\right]. \qquad (93)$$

The complete one-loop matching coefficients in Eq. (33) in the transverse-momentum cutoff and $\overline{\text{MS}}$ schemes were given by Wang and Zhao (2018), Wang, Zhao, and Zhu (2018), and Wang, Zhang *et al.* (2019). The two-loop results were obtained recently by Chen, Wang, and Zhu (2020a, 2020b, 2020c) and Li, Ma, and Qiu (2020).

C. Coordinate-space factorization of bilinear operators

Although the LaMET application to PDFs concerns the expansion of momentum densities in the $P^z \to \infty$ limit, lattice QCD calculations actually start with a computation of coordinate-space correlations, for example,

$$\tilde{h}(z, P^z) = \frac{1}{N_\Gamma} \langle P^z | O_\Gamma(z) | P^z \rangle, \qquad (94)$$

at all z and a Fourier transform done with respect to $\lambda = zP^z$ at a fixed P^z. Here the normalization factor $N_\Gamma = 2P^z$ for $\Gamma = \gamma^z$, while the normalization factor $N_\Gamma = 2P^t$ for $\Gamma = \gamma^t$. The $\tilde{h}(z, P^z)$ is a function of two independent variables z and P^z, and in LaMET analysis the relevant combinations are quasi-LF distance λ (see Fig. 5) and P^z; hence, $\tilde{h}(\lambda, P^z)$ is called the quasi-LF correlation, which is later distinguished from the LF correlation $h(\lambda, \mu)$.

The coordinate-space factorization approach of Braun, Gornicki, and Mankiewicz (1995) has been suggested as an alternative way to extract the PDFs from $\tilde{h}(z, P^z)$ (Orginos *et al.*, 2017; Radyushkin, 2017a, 2019a), which is closely related to the OPE. Instead of working with variables λ and P^z, one may consider $\tilde{h}$ a function of λ and z^2, i.e., $\tilde{h}(\lambda, z^2)$. The Fourier transform of $\tilde{h}(\lambda, z^2)$ with respect to λ is no longer the momentum distribution of the proton at a fixed momentum. Instead, it is called a pseudodistribution (Radyushkin, 2017a). At small $|z| \ll \Lambda_{QCD}^{-1}$, $\tilde{h}(\lambda, z^2)$ can be factorized into the light-cone correlation (Izubuchi *et al.*, 2018; Radyushkin, 2018a) as follows:

$$\tilde{h}(\lambda, z^2\mu^2) = \int_{-1}^{1} d\alpha \, \mathcal{C}(\alpha, z^2\mu^2) h(\alpha\lambda, \mu) + \cdots, \quad (95)$$

where the ellipsis represents the power corrections in $z^2\Lambda_{QCD}^2$ and the matching coefficient $\mathcal{C}$ is related to C in Eq. (33) by

$$C\left(\eta, \frac{\mu}{xP^z}\right) = \int \frac{d\lambda}{2\pi} e^{i\eta\lambda} \int_{-1}^{1} d\alpha \, e^{-i\lambda\alpha} \mathcal{C}\left(\alpha, \frac{\mu^2\lambda^2}{(xP^z)^2}\right). \quad (96)$$

To illustrate the connection between the factorization in Eq. (95) and the OPE, we take the nonsinglet quark case as an example (Izubuchi *et al.*, 2018; Wang, Zhang *et al.*, 2019). In the $\overline{\text{MS}}$ scheme, the renormalized $O_{\gamma^{\mu_0}}(z, \mu)$ can be expanded in terms of local gauge-invariant twist-2 operators as $z^2 \to 0$ as follows:

$$O_{\gamma^{\mu_0}}(z, \mu) = \sum_{n=0}^{\infty} \left[C_n(\mu^2 z^2) \frac{(iz)^n}{n!} (n_z)_{\mu_1} \cdots (n_z)_{\mu_n} \right.$$
$$\left. \times O^{\mu_0\mu_1\cdots\mu_n}(\mu) + \text{higher twist} \right], \quad (97)$$

where $\mu_0 = 0$ or 3, $C_n = 1 + \mathcal{O}(\alpha_s)$ is the Wilson coefficient, and $O^{\mu_0\mu_1\cdots\mu_n}(\mu)$ is the twist-2 operator in Eq. (14).

Using the hadron matrix elements in Eq. (15) and their relation to the light-cone PDF in Eq. (16), we write the following small-$|z|$ expansion of the hadron matrix element of $O_{\gamma^{\mu_0}}(z, \mu)$ (Izubuchi *et al.*, 2018):

$$\tilde{h}(\lambda, z^2\mu^2) = \langle P|O_{\gamma^{\mu_0}}(z, \mu)|P\rangle/2P^{\mu_0}$$
$$= \sum_{n=0}^{\infty} C_n(z^2\mu^2) \frac{(-i\lambda)^n}{n!} \left[1 + \mathcal{O}\left(\frac{M^2}{(P^z)^2}\right) \right]$$
$$\times \int_{-1}^{1} dx \, x^n q(x, \mu) + \mathcal{O}(z^2\Lambda_{QCD}^2), \quad (98)$$

where the $\mathcal{O}(M^2/(P^z)^2)$ term comes from the kinematic trace contribution and the $\mathcal{O}(z^2\Lambda_{QCD}^2)$ term from higher twist. The Wilson coefficients $C_n(z^2\mu^2)$ have been calculated at one-loop (Izubuchi *et al.*, 2018) and two-loop (Li, Ma, and Qiu, 2020) orders. Comparing Eqs. (95) and (98), we identify

$$\mathcal{C}(\alpha, \mu^2 z^2) \equiv \int \frac{d\lambda}{2\pi} e^{i\lambda\alpha} \sum_n C_n(\mu^2 z^2) \frac{(-i\lambda)^n}{n!}. \quad (99)$$

Since z^2 is fixed in $\mathcal{C}(\alpha, \mu^2 z^2)$, the integration in Eq. (99) is actually over P^z from $-\infty$ to $+\infty$. $\mathcal{C}(\alpha, z^2\mu^2)$ has support $-1 \le \alpha \le 1$, and its one-loop result is

$$\mathcal{C}(\alpha, z^2\mu^2) = \left[1 + \frac{\alpha_s C_F}{2\pi} \left(\frac{3}{2} \ln \frac{z^2\mu^2 e^{2\gamma_E}}{4} + \frac{3}{2} \right) \right] \delta(1 - \alpha)$$
$$+ \frac{\alpha_s C_F}{2\pi} \left\{ \left(\frac{1+\alpha^2}{1-\alpha} \right)_{+(1)}^{[0,1]} \left[-\ln \frac{z^2\mu^2 e^{2\gamma_E}}{4} - 1 \right] \right.$$
$$\left. - \left(\frac{4\ln(1-\alpha)}{1-\alpha} \right)_{+(1)}^{[0,1]} + 2(1+\sigma)(1-\alpha) \right\}$$
$$\times \theta(\alpha)\theta(1-\alpha), \quad (100)$$

which was also calculated and further studied by Ji, Zhang, and Zhao (2017), Radyushkin (2018a, 2018b), Zhang, Chen, and Monahan (2018), and Li, Ma, and Qiu (2020). One can check to ensure that this result is indeed related to one-loop momentum-space matching by Eq. (96). Since we are interested in the relation between the quasi-LF correlation with the matrix element of the light-ray operator $O_{\gamma^+}(\lambda n)$, Eq. (95) can also be obtained by using the light-ray operator expansion given by Balitsky and Braun (1989), Braun, Gornicki, and Mankiewicz (1995), and Braun and Müller (2008).

Using the OPE or a short-distance expansion, Balitsky, Morris, and Radyushkin (2019) and Wang, Zhang *et al.* (2019) also derived in coordinate space and studied at one-loop order the exact factorization formula for the gluon and singlet quark quasi-PDFs, which includes their mixings.

The limits $P^z \to \infty$ in the LaMET expansion and $z \to 0$ in coordinate-space factorization, keeping finite $\lambda = zP^z$, are equivalent. However, in practical lattice QCD calculations, one is limited by the largest momentum P_{max}^z in a specific setup, and the two approaches start to differ.

In the LaMET systematic approximation, one should calculate $\tilde{h}(z, P_{max}^z)$ with all possible z or λ, but in practice the largest $\lambda_{max} = z_{max}P_{max}^z$ is limited by the lattice volume as well as the data quality at large z. Because of QCD confinement, $\tilde{h}(z, P_{max}^z)$ has a correlation length $\sim 1/\Lambda_{QCD}$, leading to an exponential decay at large z (Ji *et al.*, 2020). Therefore, if z_{max} is sufficiently large (e.g., a proton size of ~ 1 fm) for $\tilde{h}(z, P_{max}^z)$ to fall to almost zero, then the truncated Fourier transform of $\tilde{h}(z, P_{max}^z)$ should converge quickly and the truncation effects mainly affect results at small $x \lesssim 1/\lambda_{max}$. If $\tilde{h}(z, P_{max}^z)$ exhibits exponential decay but still has a nonzero value at z_{max}, then one can perform a physically motivated extrapolation beyond z_{max} (Ji *et al.*, 2020) to do the Fourier transform, which removes the unphysical oscillation from truncation and affects only the small-x region. In the momentum space, one can use the LaMET expansion to calculate the PDF point by point in x, with the systematic error controlled by $\Lambda_{QCD}^2/(xP_{max}^z)^2$ and $\Lambda_{QCD}^2/[(1-x)P_{max}^z]^2$, which gives the prediction for a cetain region of x, $[x_{min}, x_{max}]$, with a target error.

In coordinate-space factorization, one expands $\tilde{h}(\lambda, z^2)$ in $z^2\Lambda_{QCD}^2$. For the factorization formula to be valid, z must remain in the perturbative region. For example, an estimate of Ji *et al.* (2020) gave $z_{max} \sim 0.3$–0.4 fm. Although there have

been observations that forming ratios of $\tilde{h}(\lambda, z^2)$ may cancel the higher-twist contributions at $z > 0.4$ fm (Orginos *et al.*, 2017), this cancellation needs be quantified for precise calculations. With a finite range of quasi-LF correlations, the PDFs can be extracted through modeling the x dependence or more advanced techniques such as Bayesian analysis (Bringewatt *et al.*, 2020) or neural network (Cichy, Debbio, and Giani, 2019; Karpie *et al.*, 2019; Del Debbio *et al.*, 2020), which is similar to extracting the PDFs from experimental data (Ma and Qiu, 2018a), although quantifying the systematic error from fitting can be challenging. The coordinate-space factorization can also provide the extraction of the lowest moments of PDFs (Karpie, Orginos, and Zafeiropoulos, 2018; Gao *et al.*, 2020; Joó *et al.*, 2020; Shugert *et al.*, 2020), where the main systematic error is controlled by $z^2 \Lambda_{\text{QCD}}^2$.

Thus far there have been only limited studies about the comparison between quasi-PDF and pseudo-PDF analysis (Alexandrou, Cichy, Constantinou, Green *et al.*, 2020; Bhat *et al.*, 2020). It remains to be seen how systematic errors in the two strategies will be compared and contrasted.

D. Nonperturbative renormalization and matching

The multiplicative renormalizability of the nonlocal Wilson-line operators for quasi-PDFs allows a nonperturbative renormalization on the lattice, after which the continuum limit can be taken. This is an important step in the application of LaMET. One way of doing so is to perform a mass subtraction of the Wilson line first (Musch *et al.*, 2011; Ishikawa *et al.*, 2016; Chen, Ji, and Zhang, 2017; Zhang *et al.*, 2017; Green, Jansen, and Steffens, 2018, 2020) and then renormalize the remnant UV divergences with lattice perturbation theory or another nonperturbative scheme. Another scheme that has gained more popularity in recent years is the regularization-independent momentum subtraction (RI/MOM) scheme (Alexandrou, Cichy *et al.*, 2017; Constantinou and Panagopoulos, 2017; Chen *et al.*, 2018; Stewart and Zhao, 2018; Liu *et al.*, 2020). In the coordinate-space approach when $|z| \ll \Lambda_{\text{QCD}}^{-1}$, the ratios of quasi-LF correlations in different states (Orginos *et al.*, 2017; Radyushkin, 2017a; Braun, Vladimirov, and Zhang, 2019; Li, Ma, and Qiu, 2020) have also been proposed as a renormalization scheme. At large z, the RI/MOM and ratio schemes introduce extra nonperturbative effects at different levels, which may distort the IR property of the original quasi-LF correlations. Because of the suppression of long-range contributions by large P^z in the Fourier transform, this nonperturbative contamination affects mainly the end-point region in x space, while the existing LaMET calculations with the RI/MOM scheme at moderate x, such as those given by Alexandrou *et al.* (2018b) and Lin, Chen *et al.* (2018), suffer less from such systematics. Nevertheless, this complication can be avoided by switching to the hybrid scheme (Ji *et al.*, 2020), where one utilizes the advantages of different schemes at short and large distances. In the following, we discuss the previous schemes in order, with a particular focus on the hybrid renormalization scheme.

Before we proceed, we note that the current-current correlators given by Detmold and Lin (2006), Braun and Müller (2008), and Ma and Qiu (2018a) do not need or have simple renormalization on the lattice, although it might be more costly to simulate them. There is another distinct method based on a redefinition of the quasi-PDF with smeared fermion and gauge fields via the gradient flow (Monahan and Orginos, 2017). The smeared quasi-PDF is free from UV divergences and remains finite in the continuum limit, which can be perturbatively matched to the PDF (Monahan, 2018b). Nevertheless, this method awaits implementation on the lattice.

1. Wilson-line mass-subtraction scheme

Since the mass correction δm includes all the linear UV divergences, it is highly favorable to nonperturbatively subtract it from the quasi-PDFs. It is well known that the Wilson-line renormalization is related to the additive renormalization of the static quark-antiquark potential, i.e., δm, especially in the context of finite temperature field theory. For a rectangle-shaped Wilson loop of dimension $L \times T$ in the spatial and temporal directions, its vacuum expectation value for large T scales as

$$\lim_{T \to \infty} W(L, T) = c(L) e^{-V(L)T}. \qquad (101)$$

The renormalized static potential is

$$V^R(L) = V(L) + 2\delta m, \qquad (102)$$

and δm can be fixed by imposing the condition $V^R(L_0) = 0$ for a particular value of L_0. Alternatively, one can also fit δm from the string potential model as follows:

$$V(L) = \sigma L - \frac{\pi}{12L} - 2\delta m. \qquad (103)$$

In addition to using the static potential to determine δm, it was also proposed to calculate this quantity in the auxiliary heavy-quark field theory with the following condition (Green, Jansen, and Steffens, 2018):

$$\delta m = \frac{d}{dz} \ln \text{Tr} \langle Q(x + zn_z) \bar{Q}(x) \rangle_{\text{QCD}+Q} \Big|_{z=z_0}. \qquad (104)$$

Other suggestions have also been made for a nonperturbative calculation of δm (Ji *et al.*, 2020). For example, one can investigate the asymptotic large-z behavior of the hadron matrix element or the single quark Green's function of the vacuum expectation value of $O_\Gamma(z, a)$ in a fixed gauge. The δm calculated from all these matrix elements will have the following dependence on the lattice spacing a:

$$\delta m = m_{-1}(a)/a + m_0, \qquad (105)$$

where $m_{-1}(a)$ is the coefficient of the power divergence that is independent of the specific matrix element, while $m_0 \sim O(\Lambda_{\text{QCD}})$ is finite and depends on the external state. The determination of m_0 can be nontrivial, and in practical calculations one could adopt a fine-tuning method, such as that for the Wilson-fermion mass, to find the critical value of m_0 at which the final result converges fastest in the large-P^z limit.

After the Wilson-line mass subtraction, there are still logarithmic UV divergences in $O_\Gamma(z, a)$. One can use lattice perturbation theory to match δm-subtracted $O_\Gamma(z, a)$ to the $\overline{\text{MS}}$ scheme (Ishikawa *et al.*, 2016; Constantinou and Panagopoulos, 2017; Xiong, Luu, and Meißner, 2017), but the convergence still needs to be examined at higher orders. Green, Jansen, and Steffens (2018, 2020) nonperturbatively renormalized the logarithmic divergences with RI/MOM–like schemes.

The Wilson-line mass subtraction was implemented on the lattice by Musch *et al.* (2011), Zhang *et al.* (2017), Green, Jansen, and Steffens (2018), Zhang, Jin *et al.* (2019), and Alexandrou, Cichy, Constantinou, Green *et al.* (2020).

2. RI/MOM scheme

The RI/MOM scheme has been widely used in lattice QCD for the renormalization of local composite quark operators that are free from power-divergent mixings (Martinelli *et al.*, 1995). It is essentially a momentum subtraction scheme in QFT and can be nonperturbatively implemented on the lattice. For an arbitrary composite quark bilinear operator O^B that is multiplicatively renormalized as $O^B = Z_O O^R$, the RI/MOM scheme is defined by imposing the following condition on its off-shell quark matrix element at a subtraction scale μ_R:

$$Z_O^{-1} \langle p|O^B|p\rangle|_{p^2 = -\mu_R^2} = \langle p|O|p\rangle_{\text{tree}}. \qquad (106)$$

where the subscript "tree" represents the tree-level matrix element in perturbation theory. If $\mu_R \gg \Lambda_{\text{QCD}}$, Z_O defined in Eq. (106) is in the perturbative region, and we can convert it to the $\overline{\text{MS}}$ scheme order by order in perturbation theory. In this sense, Z_O is not literally nonperturbative, but rather an all-order calculable quantity.

Since the nonlocal quark bilinear operator $O_\Gamma(z)$ has been proven to be multiplicatively renormalizable in the coordinate space, one can also renormalize it in the RI/MOM scheme and then match the result to PDF in the $\overline{\text{MS}}$ scheme (Constantinou and Panagopoulos, 2017; Stewart and Zhao, 2018). On the lattice, the off-shell matrix element of an operator is defined from its amputated Green's function, or vertex function, with off-shell quarks. For the nonlocal Wilson-line operator, the latter is

$$\Lambda_0^\Gamma(z, a, p) \equiv [S_0^{-1}(p, a)]^\dagger \sum_{x, y} e^{ip \cdot (x-y)}$$
$$\times \langle 0|T[\psi_0(x, a) O_\Gamma^B(z, a) \bar\psi_0(y, a)]|0\rangle S_0^{-1}(p, a), \qquad (107)$$

where $S_0(p, a)$ is the bare quark propagator, and the external momentum p is Euclidean on the lattice. Since Green's functions are not gauge invariant, one needs to fix a gauge (usually Landau gauge $\partial \cdot A = 0$ is chosen), and the gauge dependence is expected to be canceled out by the matching or scheme conversion order by order in perturbation theory.

After including the quark wave-function renormalization Z_q, which can be determined independently on the lattice (Martinelli *et al.*, 1995), Eq. (106) is revised as

$$Z_q Z_{O_\Gamma}^{-1} \Lambda_0^\Gamma(z, a, p)|_{p=p_R} = \Lambda_{\text{tree}}^\Gamma(z, a, p) = \Gamma e^{ip_R \cdot z}. \qquad (108)$$

Since $O_\Gamma(z, a)$ is not $O(4)$ covariant, one needs to define the RI/MOM scheme with two scales: one is $\mu_R = |p_R|$, and the other is p_R^z. For convenience we simply denote them as $p = p_R$. To work in the perturbative region and control the lattice discretization effects that are of the order of $\mathcal{O}(a^2 \mu_R^2, a^2(p_R^z)^2)$, one must work in the window $\Lambda_{\text{QCD}} \ll \mu_R \ll a^{-1}$, $p_R^z \ll a^{-1}$, which is attainable if the lattice spacing is small enough.

Since the quarks are off shell, finite mixings with the EOM operators can also appear. As a result, Eq. (108) in general cannot be satisfied as a matrix equation. Instead, one usually needs a projection operator $\mathcal{P}$ to define the off-shell matrix elements, i.e.,

$$\langle p|O_\Gamma^B|p\rangle = \text{tr}[\Lambda_0^\Gamma(z, a, p)\mathcal{P}], \qquad (109)$$

so as to calculate the renormalization factor Z_{O_Γ}.

The bare hadron matrix element $\tilde h_B(z, P^z, a)$ can then be renormalized in coordinate space as

$$\tilde h_R(z, P^z, p_R^z, \mu_R, a) = Z_O^{-1}(z, p_R^z, \mu_R, a)\tilde h_B(z, P^z, a). \qquad (110)$$

In the continuum limit, the renormalized matrix element is independent of the UV regulator, so we should obtain the same result in DR under the RI/MOM scheme, i.e.,

$$\tilde h_R(z, P^z, p_R^z, \mu_R) = \lim_{a \to 0} \tilde h_R(z, P^z, p_R^z, \mu_R, a)$$
$$= \lim_{\epsilon \to 0} Z_O^{-1}(z, p_R^z, \mu_R, \epsilon)\tilde h_B(z, P^z, \epsilon), \qquad (111)$$

which allows us to compute the matching coefficients in continuum perturbation theory. Note that δm vanishes in Z_O due to the use of DR.

By Fourier transforming the previously mentioned renormalized matrix element to momentum space, one can then work out the RI/MOM matching coefficient for the quasi-PDFs (Stewart and Zhao, 2018). One-loop matching coefficients for different spin structures were obtained by Liu *et al.* (2018, 2020) and Stewart and Zhao (2018), and the two-loop result for the unpolarized case was given by Chen, Wang, and Zhu (2020a). Alternatively, one can also first convert the RI/MOM matrix element to the $\overline{\text{MS}}$ or modified $\overline{\text{MS}}$ schemes (Constantinou and Panagopoulos, 2017; Alexandrou, Cichy *et al.*, 2019), then do the Fourier transform and momentum-space matching.

3. Ratio scheme

In the coordinate-space factorization, $|z| \ll \Lambda_{\text{QCD}}^{-1}$ must be small, whereas P^z can be of any value. In this case, the ratio scheme given by Orginos *et al.* (2017) and Radyushkin (2017a) can be an effective choice for lattice renormalization. Consider the ratio

$$\tilde h(\lambda, z^2, a)/\tilde h(0, z^2, a), \qquad (112)$$

where the denominator is a nonperturbative matrix element at $P^z = 0$. Since $\tilde{h}(\lambda, z^2, a)$ and $\tilde{h}(0, z^2, a)$ calculated from the same lattice ensemble are correlated with each other, the error in the ratio can be reduced. The ratio does not need further renormalization on the lattice, so one can directly take the continuum limit as follows:

$$\lim_{a \to 0} \frac{\tilde{h}(\lambda, z^2, a)}{\tilde{h}(0, z^2, a)} = \frac{\tilde{h}(\lambda, z^2)}{\tilde{h}(0, z^2)}, \qquad (113)$$

which was referred to as the "reduced Ioffe-time pseudodistribution" by Orginos *et al.* (2017) and Radyushkin (2017a). In the $\overline{\text{MS}}$ scheme, $\tilde{h}(0, z^2\mu^2)$ has a small-z expansion

$$\tilde{h}(0, z^2\mu^2) = C_0(z^2\mu^2) + \mathcal{O}(z^2M^2, z^2\Lambda_{\text{QCD}}^2), \quad (114)$$

where the lowest moment of the isovector quark PDF a_0 is trivially 1. If we ignore all the power corrections, then $\tilde{h}(0, z^2\mu^2)$ is perturbative and can be regarded as a renormalization factor. Therefore, the ratio in Eq. (113) still satisfies a OPE or factorization formula similar to Eqs. (95) and (98), except that the matching coefficient must be modified correspondingly (Izubuchi *et al.*, 2018; Radyushkin, 2018a) as

$$\mathcal{C}^{\text{ratio}}(\alpha, z^2\mu^2) = \mathcal{C}(\alpha, z^2\mu^2) - \delta(1 - \alpha)C_0(z^2\mu^2). \quad (115)$$

In other variants of the ratio scheme, it has also been suggested that one replaces $\tilde{h}(0, z^2, a)$ with the vacuum matrix element of the nonlocal Wilson-line operator (Braun, Vladimirov, and Zhang, 2019; Li, Ma, and Qiu, 2020), as the UV divergence does not depend on the external state.

4. Hybrid scheme

Since the factorization formula for the quasi-PDF is proven only in the $\overline{\text{MS}}$ scheme, it is not legitimate to use momentum-space factorization for any schemes that differ from $\overline{\text{MS}}$ nonperturbatively. The RI/MOM and ratio schemes fall into this category, as the conversion factors that match them to $\overline{\text{MS}}$ include logarithms of z^2 (Constantinou and Panagopoulos, 2017; Izubuchi *et al.*, 2018), which requires one to run α_s to the IR region when $z \sim \Lambda_{\text{QCD}}^{-1}$. In contrast, the Wilson-line mass-subtraction scheme with wave-function renormalizations is essentially the same as $\overline{\text{MS}}$, so it will not introduce extra IR effects.

However, the Wilson-line mass-subtraction scheme also has disadvantages. On the lattice, due to discretization effects at $z \sim a$, the lattice scheme cannot reproduce the short-distance $\ln z^2$ behavior of the $\overline{\text{MS}}$ matrix elements of the nonlocal operator. Such discretization effects, however, are canceled in the RI/MOM or ratio schemes. To take advantage of both types of schemes, a hybrid scheme was proposed by Ji *et al.* (2020) that provides a viable approach to renormalize the quasi-LF correlations at all z.

To begin with, for $|z| \leq z_S$ where z_S is smaller than the distance at which the leading-twist approximation in the OPE becomes unreliable, one renormalizes the quasi-LF correlation as

$$\frac{\tilde{h}(z, a, P^z)}{Z_X(z, a)}, \qquad (116)$$

where X can be the RI/MOM or ratio scheme.

For $|z| > z_S$, one applies the Wilson-line mass subtraction

$$\tilde{h}(z, a, P^z)e^{-\delta m|z|}Z_{\text{hybrid}}, \qquad (117)$$

where Z_{hybrid} denotes the wave-function and vertex renormalizations, which can be nonperturbatively determined by imposing a continuity condition at $z = z_S$ as follows:

$$Z_{\text{hybrid}}e^{-\delta m|z_S|}\tilde{h}(z, a, P^z) = \frac{\tilde{h}(z, a, P^z)}{Z_X(z_S, a)}, \qquad (118)$$

which leads to

$$Z_{\text{hybrid}}(z_S, a) = e^{\delta m|z_S|}/Z_X(z_S, a). \qquad (119)$$

In this way, one has to calculate only δm. Note that the final result should be independent of z_S, so one should try multiple values and find the optimal one around which the result changes the most slightly.

The perturbative matching for the hybrid renormalized quasi-PDF can be derived accordingly. Taking Z_X as the zero-momentum matrix element in the ratio scheme as an example, the $O(\alpha_s)$ matching has been derived as (Ji *et al.*, 2020)

$$\begin{aligned}
C_{\text{hybrid}}[\xi, \mu^2/(p^z)^2, z_S^2\mu^2] &= C_{\text{ratio}}[\xi, \mu^2/(p^z)^2] \\
&+ \frac{\alpha_s C_F}{2\pi}\frac{3}{2}\left[-\frac{1}{|1 - \xi|_+} + \frac{2\text{Si}[(1 - \xi)\lambda_S]}{\pi(1 - \xi)} + \ln\frac{e^{-2\gamma_E}}{\lambda_S^2}\delta(1 - \xi)\right],
\end{aligned}$$
$$(120)$$

where C_{ratio} was given by Izubuchi *et al.* (2018), $\xi = y/x$, and $\lambda_S = z_S p^z$, with $p^z = xP^z$ the parton momentum. The plus function is defined as

$$\frac{1}{|1 - \xi|_+} \equiv \lim_{\beta \to 0^+}\left[\frac{\theta(|1 - \xi| - \beta)}{|1 - \xi|} + 2\delta(1 - \xi)\ln\beta\right]. \quad (121)$$

Owing to a finite lattice volume and deteriorating signal-to-noise ratios at large z, the available lattice data have to be truncated at z_L. As discussed in Sec. III.C, the quasi-LF correlation has a correlation length $\xi_z \sim \Lambda_{\text{QCD}}^{-1}$ and exhibits an exponential decay at large z (~ 1 fm). If z_L is not sufficiently large and the quasi-LF correlation still has a considerable nonzero value, then a direct Fourier transform truncated at z_L will lead to unphysical oscillations and other systematics in the quasi-PDF.

To improve this situation, it is suggested in the hybrid scheme to perform an extrapolation to $z \to \infty$ (Ji *et al.*, 2020). When P^z is not large and the lattice matrix elements exhibit exponential behavior near z_L, one can use the form $\sim e^{-z/\xi_z}$ to do the extrapolation, although some algebraic behavior can be added on top to better reflect the z dependence. If P^z is large, then the signal-to-noise ratio gets worse, so z_L is smaller. In this case, the quasi-LF correlation is yet to show exponential

decay and is dominated by the leading-twist contributions, so one can use the algebraic decay form to do the extrapolation. Since $\lambda_L = z_L P^z$ can reach reasonably large values with contemporary computing resources, the extrapolation will affect only the small-x region, for which the LaMET expansion is not well under control after all.

To summarize, the hybrid scheme provides a proper renormalization of the quasi-LF correlations at all z, which allows for a controlled calculation of the PDF for $x \in [x_{\min}, x_{\max}]$ through a LaMET expansion in momentum space. Therefore, we expect it to play a dominant role in the LaMET calculation of PDFs in the future.

E. Total gluon helicity ΔG and transversity PDF

Apart from the collinear PDFs, the first application of LaMET is the gluon helicity contribution ΔG to the proton spin (Ji, Zhang, and Zhao, 2013). In the naive sum rule for the proton spin (Jaffe and Manohar, 1990), ΔG is related to the following matrix element of a nonlocal light-cone correlation operator (Manohar, 1991):

$$\Delta G = \langle PS | i \int \frac{dx\,d\lambda}{4\pi x P^+} e^{i\lambda x} F^{+\alpha}(0) W(0, \lambda n) \tilde{F}^+_{\alpha}(\lambda n) | PS \rangle, \quad (122)$$

which in the light-cone gauge $A^+ = 0$ reduces to

$$\Delta G = \langle PS | (\vec{E} \times \vec{A})^z | PS \rangle / (2P^+). \quad (123)$$

Within the LaMET framework, one can start with a static "gluon spin" operator, which is defined as $\vec{E} \times \vec{A}$ fixed in a time-independent gauge that maintains the transverse polarizations of the gluon field in the IMF limit. For example, the Coulomb gauge $\vec{\nabla} \cdot \vec{A} = 0$ and axial gauges $A^z = 0$ and $A^0 = 0$ are viable options (Hatta, Ji, and Zhao, 2014).

In the Coulomb gauge and the $\overline{\text{MS}}$ scheme, the static gluon spin $\Delta \tilde{G}$ in a large on-shell quark state at one-loop order is (Chen *et al.*, 2011; Ji, Zhang, and Zhao, 2013)

$$\Delta \tilde{G}(P^z, \mu)(2S^z) = \langle PS | \epsilon^{ij}_{\perp} F^{i0} A^j | PS \rangle_q |_{\vec{\nabla} \cdot \vec{A} = 0}$$
$$= \frac{\alpha_s C_F}{4\pi} \left[\frac{5}{3} \ln \frac{\mu^2}{m^2} - \frac{1}{9} + \frac{4}{3} \ln \frac{(2P^z)^2}{m^2} \right] (2S^z), \quad (124)$$

where the subscript q denotes a quark and S^μ is the spin vector. The collinear divergence is regulated by the finite quark mass m.

If we follow the procedure used by Weinberg (1966) and take the $P^z \to \infty$ limit before UV regularization (Ji, Zhang, and Zhao, 2013), then

$$\Delta \tilde{G}(\infty, \mu)(2S^z) = \langle PS | \epsilon^{ij}_{\perp} F^{i0} A^j | PS \rangle_q |_{\vec{\nabla} \cdot \vec{A} = 0}$$
$$= \frac{\alpha_s C_F}{4\pi} \left(3 \ln \frac{\mu^2}{m^2} + 7 \right) (2S^z), \quad (125)$$

which is exactly the same as the light-cone gluon helicity $\Delta G(\mu)$ (Hoodbhoy, Ji, and Lu, 1999). Therefore, despite the difference in the UV divergence, the collinear divergences of

$\Delta \tilde{G}(P^z, \mu)$ and $\Delta G(\mu)$ are exactly the same, which allows for a perturbative matching between them.

The complete factorization formula that relates $\Delta \tilde{G}(P^z, \mu)$ to ΔG and $\Delta \Sigma$ is

$$\Delta \tilde{G}(P^z, \mu) = Z_{gg}(P^z/\mu) \Delta G(\mu)$$
$$+ Z_{gq}(P^z/\mu) \Delta \Sigma(\mu) + \cdots, \quad (126)$$

where the ellipsis represents the power corrections suppressed by $1/P^z$ and the matching coefficients Z_{gg} and Z_{gg} have been calculated for the Coulomb gauge at one loop (Ji, Zhang, and Zhao, 2015).

In addition, one can calculate the gluon helicity PDF $\Delta g(x)$ according to the factorization formula in Sec. III, then integrate it over x to obtain ΔG.

At leading twist, in addition to the unpolarized and helicity PDFs that we discussed earlier, there is also the transversity PDF defined as (Jaffe and Ji, 1991, 1992)

$$h_1(x) = \frac{1}{2P^+} \int \frac{d\lambda}{2\pi} e^{-i\lambda x} \langle PS_\perp | \bar{\psi}(0) \gamma^+ \gamma_\perp \gamma_5 \psi(\lambda n) | PS_\perp \rangle. \quad (127)$$

$h_1(x)$ simply counts the number of transversely polarized quarks carrying the momentum fraction x in a transversely polarized proton. The first moment of this distribution corresponds to the so-called tensor charge δq, which is the matrix element of a chiral-odd operator. $h_1(x)$ can be accessed through the transverse-transverse-spin asymmetry in Drell-Yan processes (Ralston and Soper, 1979; Jaffe and Ji, 1991, 1992) or the Collins single-spin asymmetry in semi-inclusive deep-inelastic scattering (SIDIS), where the transversity TMDPDF couples to a chiral-odd TMD-fragmentation function (Collins, 1993). At present, experimental results on the transversity PDF are limited (Barone, Drago, and Ratcliffe, 2002; Kang *et al.*, 2016; Lin, Melnitchouk *et al.*, 2018; Radici and Bacchetta, 2018; Cammarota *et al.*, 2020), especially for the sea quark contributions (Chang and Peng, 2014), so this is one scenario where a lattice QCD calculation can make an important difference.

The LaMET calculation of $h_1(x)$ is straightforward, as the nonlocal operator has the same renormalization as the unpolarized case, and its one-loop matching has been calculated in the $\overline{\text{MS}}$ and RI/MOM schemes at one-loop order (Alexandrou *et al.*, 2018b; Liu *et al.*, 2018). The first lattice calculations of $h_1(x)$ were made by Chen *et al.* (2016), Alexandrou *et al.* (2018b), and Liu *et al.* (2018), which we discuss in more detail in Sec. VI.

IV. GENERALIZED COLLINEAR-PARTON OBSERVABLES

In Sec. III, we extensively discussed the leading-twist collinear PDFs that characterize the 1D structure of the proton in longitudinal-momentum space. There are various other parton observables that provide complementary information. In this section, we focus on observables defined by collinear-parton correlators, in the sense that only the collinear quark and gluon mode contribute, corresponding to the so-called collinear expansion in QCD factorizations (Sterman, 1993; Collins, 2011a). We call them "generalized collinear-parton

observables" (GCPOs) and discuss their calculations through a LaMET framework. Observables defined by parton correlators involving transverse separations, in particular, the TMDPDFs, Wigner functions, and light-front wave functions (LFWFs), are considered later.

Some of the important GCPOs are the GPDs introduced by Müller *et al.* (1994) and rediscovered (Ji, 1997b) due to their connection to the spin structure of the proton. They describe the correlation between the transverse position and longitudinal momentum of partons inside the proton, and thus provide important information for 3D imaging of the proton. A proton spin sum rule was derived in terms of the moments of the GPDs, which has stimulated considerable general interest in the GPDs. It was also found that in the so-called zero skewness limit or when the longitudinal-momentum transfer vanishes, the GPD has a probability interpretation in the impact parameter space (Burkardt, 2000). In a general case, it is related to the quantum phase-space distributions or Wigner functions (Ji, 2003; Belitsky, Ji, and Yuan, 2004). Experimentally, the GPDs can be measured through hard exclusive processes such as DVCS or deeply virtual meson production (DVMP), which were first proposed by Ji (1997a, 1997b). Much effort has been devoted to measuring such processes at completed and ongoing experiments, including HERA, COMPASS, and JLab. For a more comprehensive discussion on the GPDs, see the reviews by Ji (1998, 2004), Diehl (2003), and Belitsky and Radyushkin (2005). Despite the fact that the GPDs have a more complicated kinematic dependence and relation to experimental observables, various fitting methods have been proposed in the literature to fit available DVCS and DVMP data (Favart *et al.*, 2016; Kumericki, Liuti, and Moutarde, 2016). In parallel, one can also extract certain information on the GPDs from lattice calculations of their moments (Gockeler *et al.*, 2004; Hagler *et al.*, 2008; Alexandrou *et al.*, 2020), which is again limited due to the same difficulties as exist in lattice calculations of the PDF moments. For the JLab 12 GeV program and the future EIC, it is important to have first-principle calculations of GPDs with a much better understanding of the physical landscape in different kinematic variables.

A simpler but closely related GCPO is the parton DAs, which are collinear matrix elements of light-cone operators between a hadron state and the QCD vacuum, representing the probability amplitude of finding a given Fock state in the hadron. They can be probed in certain exclusive processes (Brodsky, 2002) and are crucial inputs for processes relevant to measuring fundamental parameters of the standard model and for probing new physics. There is a vast amount of literature on this subject, particularly regarding the pion DA. For a review see Brodsky and Lepage (1989), Grozin (2005), and Braun (2006).

Another type of GCPO involves the higher-twist parton distributions. They are defined by multiparton correlation functions and quantify the proton structure in terms of longitudinal-momentum correlations (Jaffe and Soldate, 1982; Ellis, Furmanski, and Petronzio, 1983; Jaffe and Ji, 1992). Although physically interesting, they are hard to separate theoretically due to mixing with the leading-twist ones (Mueller, 1985; Ji, 1995) and difficult to extract experimentally because they are power suppressed (Ji, 1993).

Higher-twist effects can become important in kinematic regions where the suppression is relaxed. Moreover, some twist-3 distributions (g_T and h_L) are different; they have no leading twist to mix with and are dominant in spin-related observables (Jaffe and Ji, 1992). Twist-3 GPDs are also relevant for studying parton OAM in the proton (Hatta and Yoshida, 2012; Ji, Xiong, and Yuan, 2013; Courtoy *et al.*, 2014) and can be accessed through the DVCS process (Penttinen *et al.*, 2000; Kiptily and Polyakov, 2004).

In principle, all the previously discussed GCPOs can be computed within LaMET. In addition, an accurate LaMET expansion for the leading-twist PDFs requires calculations of quasi higher-twist matrix elements. In the following, we begin with the flavor nonsinglet quark GPDs and hadronic DAs, for which the computational procedure has been well established, then give some generic discussions on higher-twist distributions, followed by a discussion on power-suppressed contributions required to extract the leading-twist quark PDFs, which have been investigated using different approaches but not yet implemented in numerical computations.

A. Generalized parton distributions

The operators defining the GPDs are the same as those defining the PDFs. Thus, the LaMET calculation of PDFs can be straightforwardly generalized to the GPDs by taking into account the nonforward kinematics (Liu *et al.*, 2019b). To illustrate how this works, we take the nonsinglet unpolarized quark GPDs in the nucleon as an example.

The unpolarized quark GPDs are defined through the following matrix element (Ji, 2004):

$$F = \frac{1}{2\bar{P}^+} \int \frac{d\lambda}{2\pi} e^{-ix\lambda} \langle P'S'|O_{\gamma^+}(\lambda n)|PS\rangle$$
$$= \frac{1}{2\bar{P}^+} \bar{u}(P'S') \left[H\gamma^+ + E \frac{i\sigma^{+\mu}\Delta_\mu}{2M} \right] u(PS), \quad (128)$$

where we have suppressed the arguments (x, ξ, t, μ) of F, H, and E for simplicity. The operator

$$O_{\gamma^+}(\lambda n) = \bar{\psi}\left(\frac{\lambda n}{2}\right) \gamma^+ W\left(\frac{\lambda n}{2}, -\frac{\lambda n}{2}\right) \psi\left(-\frac{\lambda n}{2}\right), \quad (129)$$

with $n^\mu = (1/\sqrt{2})(1/\bar{P}^+, 0, 0, -1/\bar{P}^+)$, is the same operator used to define the unpolarized quark PDF, and M is the nucleon mass. The momentum fraction $x \in [-1, 1]$, and

$$\Delta \equiv P' - P, \quad t \equiv \Delta^2, \quad \xi \equiv -\frac{P'^+ - P^+}{P'^+ + P^+} = -\frac{\Delta^+}{2\bar{P}^+}, \quad (130)$$

where without loss of generality we have chosen a Lorentz frame in which the average momentum takes the following form:

$$\bar{P}^\mu \equiv \frac{P'^\mu + P^\mu}{2} = (\bar{P}^0, 0, 0, \bar{P}^z). \quad (131)$$

The skewness parameter $\xi \in [-1, 1]$ since $P^+, P'^+ \geq 0$. There exists another kinematic constraint on ξ that follows from $\vec{\Delta}_\perp^2 \geq 0$:

$$\xi \leq \xi_{\max}(t) = \sqrt{\frac{-t}{-t + 4M^2}}. \qquad (132)$$

In the following, we also assume $\xi > 0$ without loss of generality. With these kinematic constraints, the GPDs can be divided into several kinematic regions that have different physical interpretations. As shown in Fig. 8, in the region $\xi < x < 1$ ($-1 < x < -\xi$) the distribution describes the emission and reabsorption of a quark (antiquark), while in the region $-\xi < x < \xi$ it represents the creation of a quark and antiquark pair. The first region is similar to that present in usual PDFs and referred to as the DGLAP region, whereas the second is similar to that in a meson DA, which is discussed later in this section, and referred to as the Efremov-Radyushkin-Brodsky-Lepage (ERBL) region. The easiest way to see this is in light-cone quantization and light-cone gauge, where the matrix element defining the GPDs can be rewritten in terms of parton creation and annihilation operators; for details see Ji (2004).

The previously defined quark GPDs have a number of remarkable properties [see Ji (1998, 2004), Diehl (2003), and Belitsky and Radyushkin (2005)] that either hold or have similar counterparts for the later-defined quark quasi-GPDs. In addition to being physically significant, these properties also serve as useful checks on calculations related to GPDs.

According to LaMET, the previously defined unpolarized quark GPDs can be determined by calculating the following quasi-GPDs:

$$\tilde{F} = \frac{1}{2\bar{P}^0} \int \frac{d\lambda}{2\pi} e^{iy\lambda} \langle P'S'|O_{\gamma^0}(z)|PS \rangle$$

$$= \frac{1}{2\bar{P}^0} \bar{u}(P'S')\left\{ \tilde{H}\gamma^0 + \tilde{E}\frac{i\sigma^{0\mu}\Delta_\mu}{2M} \right\} u(PS), \quad (133)$$

where we have again suppressed the arguments $(y, \tilde{\xi}, t, \bar{P}^z, \mu)$ of $\tilde{F}$, $\tilde{H}$, and $\tilde{E}$. The operator $O_{\gamma^0}(z) = \bar{\psi}(z/2)\times \gamma^0 W(z/2, -z/2)\psi(-z/2)$ is the same operator as that defining the unpolarized quark quasi-PDF, and $\lambda = z\bar{P}^z$. As in the quasi-PDF case, the momentum fraction y extends from $-\infty$ to ∞. The skewness parameter for the quasi-GPD

$$\tilde{\xi} = -\frac{P'^z - P^z}{P'^z + P^z} = -\frac{\Delta^z}{2\bar{P}^z} = \xi + \mathcal{O}\left(\frac{M^2}{(\bar{P}^z)^2}, \frac{t}{(\bar{P}^z)^2}\right) \quad (134)$$
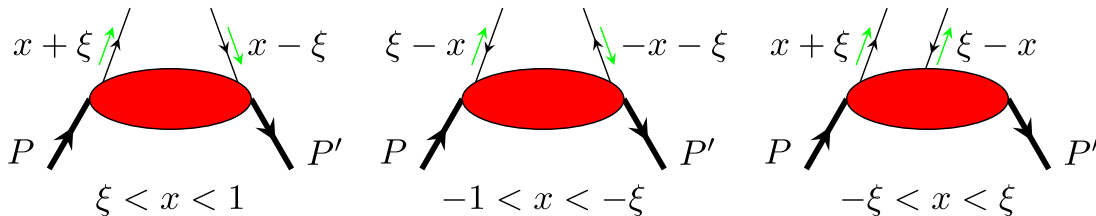
differs from the light-cone skewness ξ by power-suppressed corrections. Moreover, the constraint from $\vec{\Delta}_\perp^2 \geq 0$ becomes (Ji, Schäfer *et al.*, 2015)

$$\tilde{\xi} \leq \frac{1}{2\bar{P}^z}\sqrt{\frac{-t[(\bar{P}^z)^2 + M^2 - t/4]}{M^2 - t/4}}, \qquad (135)$$

which differs from the constraint in Eq. (132) by corrections of $\mathcal{O}(M^2/(\bar{P}^z)^2, t/(\bar{P}^z)^2)$. We can replace $\tilde{\xi}$ with ξ and attribute the difference to generic power-suppressed contributions.

The previously defined quasi-GPDs can be renormalized by observing that their UV divergence depends only on the operators defining them, not on the external states. Since $O_{\gamma^0}(z)$ is multiplicatively renormalized, we can choose the same renormalization factor as for the quasi-PDF (Stewart and Zhao, 2018; Liu *et al.*, 2020) to renormalize the quasi-GPD. After renormalization, the quasi-GPD can then be matched to the usual GPD through a factorization formula.

The factorization of quasi-GPDs was first proposed and verified at one-loop order by Ji, Schäfer *et al.* (2015) and Xiong and Zhang (2015), where a transverse-momentum cutoff and a quark mass were used as the UV and IR regulator, respectively. Later a detailed derivation based on OPE was given by Liu *et al.* (2019a). In comparison to the OPE for the quasi-PDF, a crucial difference here is that the total derivative of operators can come into play, as it simply gives momentum transfer factors when sandwiched between nonforward external states, and therefore is nonvanishing. In other words, the local twist-2 operators in Eq. (97) will mix under renormalization with operators with total derivatives. The RGE that governs the mixing reads (Braun, Korchemsky, and Müller, 2003)

$$\mu^2 \frac{d}{d\mu^2} O^{\mu_0\mu_1\cdots\mu_n}(\mu)$$

$$= \sum_{m=0}^{[n/2]} \Gamma_{nm}[i\partial^{(\mu_1} \cdots i\partial^{\mu_{2m}}\bar{\psi}\gamma^{\mu_0}i\overleftrightarrow{D}^{\mu_{2m+1}} \cdots i\overleftrightarrow{D}^{\mu_n)}\psi - \text{trace}],$$

$$(136)$$

where Γ_{nm} is the anomalous dimension of the associated operators $\overleftrightarrow{D} = (\vec{D} - \overleftarrow{D})/2$, with $\vec{D}$ ($\overleftarrow{D}$) denoting the covariant derivative acting to the right (left). Equation (136) can be diagonalized by choosing an appropriate operator basis. Such an operator basis has been studied in the literature and is known as "renormalization group improved" conformal operators (Müller, 1994; Braun, Korchemsky, and Müller, 2003). In terms of the matrix elements of these operators, we have

FIG. 8. Parton interpretation of the GPDs in different kinematic regions.

$$\langle P'|O_{\gamma^0}(z)|P\rangle = 2P^0 \sum_{n=0}^{\infty} C_n(\mu^2 z^2)\mathcal{F}_n(-\lambda)\sum_{m=0}^{n}\mathcal{B}_{nm}(\mu)$$
$$\times \xi^n \int_{-1}^{1} dx\, C_m^{3/2}\left(\frac{x}{\xi}\right)F(x,\xi,t,\mu)+\cdots, \quad (137)$$

where $\mathcal{F}_n(-\lambda)$ are partial wave polynomials whose explicit forms are known in the conformal OPE of current-current correlators for hadronic light-cone DAs (Braun and Müller, 2008), $\mathcal{B}_{nm}$ was given by Müller (1994) and Braun, Korchemsky, and Müller (2003), and the ellipsis denotes the higher-twist contributions $\mathcal{O}(M^2/(\bar{P}^z)^2, t/(\bar{P}^z)^2, z^2\Lambda_{\mathrm{QCD}}^2)$.

Fourier transforming the lhs of Eq. (137) to momentum space and inverting it order by order in α_s, we obtain the following EFT expansion of the unpolarized quark GPD:

$$F(x,\xi,t,\mu) = \int_{-\infty}^{\infty}\frac{dy}{|\xi|}\bar{C}\left(\frac{x}{\xi},\frac{y}{\xi},\frac{\mu}{\xi\bar{P}^z}\right)\tilde{F}(y,\xi,t,\bar{P}^z,\mu)+\cdots$$
$$= \int_{-\infty}^{\infty}\frac{dy}{|y|}C\left(\frac{x}{y},\frac{\xi}{y},\frac{\mu}{y\bar{P}^z}\right)\tilde{F}(y,\xi,t,\bar{P}^z,\mu)+\cdots,$$
$$(138)$$

which has been organized in the same spirit as the earlier factorizations of PDFs. Both forms have been used in the literature (Ji, Schäfer *et al.*, 2015; Xiong and Zhang, 2015; Liu *et al.*, 2019a), with the matching coefficients related by

$$C\left(\frac{x}{y},\frac{\xi}{y},\frac{\mu}{y\bar{P}^z}\right) = \left|\frac{y}{\xi}\right|\bar{C}\left(\frac{x}{\xi},\frac{y}{\xi},\frac{\mu}{\xi\bar{P}^z}\right) \quad (139)$$

and the ellipsis denoting the higher-twist contributions that have the same power counting as in Eq. (137) except that z^2 is replaced by $1/(x\bar{P}^z)^2$. For the helicity and transversity quark quasi-GPDs, the factorization formula has the same form as Eq. (138) (Liu *et al.*, 2019a).

The matching coefficient can be obtained by replacing the hadron states in Eqs. (128) and (133) with the quark states carrying momenta $p+\Delta/2$ and $p-\Delta/2$, with $p^\mu = (p^0,0,0,p^z)$, and calculating the quark matrix element in perturbation theory. The explicit expression for the $\mathcal{O}(\alpha_s)$ matching coefficients was given by Liu *et al.* (2019a). An important feature of the result is that the quasi-GPDs do not vanish in the entire y range, but the collinear singularities show up only in DGLAP and ERBL regions at one loop. They are exactly the same as those in light-cone GPDs, and thus cancel out in the matching coefficient. Moreover, one can derive momentum RGEs for the quasi-GPDs, which are turned into RGEs for the scale dependence of the GPDs using the matching procedure.

To conclude this section, we make some remarks on the EFT formula for the previous quark GPD. First, at zero skewness $\xi = 0$ we have

$$F(x,0,t,\mu) = \int_{-\infty}^{\infty}\frac{dy}{|y|}C\left(\frac{x}{y},0,\frac{\mu}{yP^z}\right)\tilde{F}(y,0,t,P^z,\mu)+\cdots, \quad (140)$$

where the matching kernel $C(x/y,0,\mu/yP^z)$ is exactly the same as the matching coefficient for the quasi-PDF (Izubuchi

et al., 2018), even when $t \neq 0$. This can be understood as follows: At zero skewness, both the longitudinal-momentum transfer and the energy transfer vanish, and the momentum transfer is purely transverse and thus not affected by Lorentz boost along the longitudinal z direction. As a result, no extra matching related to t is required in the large-P^z limit, and the matching remains the same as in the quasi-PDF case. If we take the forward limit $\Delta \to 0$, then Eq. (140) reduces exactly to the EFT expansion formula for the PDF (Ji, Schäfer *et al.*, 2015; Izubuchi *et al.*, 2018).

Second, in the limit $\xi \to 1$ and $t \to 0$, the quasi-GPD reduces to the quasi-DA discussed in Sec. IV.B, and the corresponding matching kernel also reduces to that of the quasi-DA.

B. Hadronic distribution amplitudes

Within LaMET, the DAs of protons as well as other hadrons can also be extracted from lattice simulations of appropriately chosen quasi-DAs. In this section, we show how this can be done in practice. For illustration, we take the leading-twist pion DA as an example. The application to other hadrons (Wang, Wang *et al.*, 2019; Zhang, Jin *et al.*, 2019) is analogous.

The leading-twist DA of the pion is the simplest and most extensively studied hadronic DA. It represents the probability amplitude of finding the valence $q\bar{q}$ Fock state in the pion with the quark carrying a fraction x of the total pion momentum and is defined as

$$\phi_\pi(x) = \frac{1}{if_\pi}\int\frac{d\lambda}{2\pi P^+}e^{-i(x-1/2)\lambda}\langle 0|O_{\gamma^+\gamma_5}(\lambda n)|\pi(P)\rangle, \quad (141)$$

with normalization $\int_0^1 dx\phi_\pi(x) = 1$. Here f_π denotes the decay constant and $O_{\gamma^+\gamma_5}(\lambda n)$ has the same structure as Eq. (128), with γ^+ replaced by $\gamma^+\gamma_5$. The pion DA can be constrained by experimental measurements, such as $\gamma\gamma^* \to \pi^0$ from the *BABAR* and Belle collaborations (Aubert *et al.*, 2009; Uehara *et al.*, 2012), then used as an input to test QCD in other measurements such as the pion form factor (Farrar and Jackson, 1979; Efremov and Radyushkin, 1980). In the asymptotic limit, it is well known that the pion DA takes the form $6x(1-x)$ (Lepage and Brodsky, 1979; Efremov and Radyushkin, 1980). However, how it behaves at lower scales remains under debate; see Chernyak and Zhitnitsky (1982). Calculating the pion DA with controllable systematics in LaMET will enable us to shed new light on its shape, and thus on our understanding of the pion structure.

Following the same strategy as before, we can access the x dependence of the pion DA by studying the following quasi-DA (Ji, Schäfer *et al.*, 2015; Zhang *et al.*, 2017):

$$\tilde{\phi}_\pi(y,P^z) = \frac{1}{if_\pi}\int\frac{d\lambda}{2\pi P^z}e^{i(y-1/2)\lambda}\langle 0|O_{\gamma^z\gamma_5}(z)|\pi(P)\rangle. \quad (142)$$

The longitudinally and transversely polarized vector meson quasi-DAs can be defined analogously by replacing $\gamma^z\gamma_5$ in Eq. (142) with γ^0 and $\gamma^z\gamma_\perp$, respectively (Liu *et al.*, 2019b).

The quark bilinear operators defining quasi-DAs follow the same renormalization pattern as those defining the quasi-PDFs

or quasi-GPDs. In the literature, the Wilson-line mass-subtraction scheme was used in the first LaMET calculations of the meson DAs (Zhang *et al.*, 2017; Zhang, Jin *et al.*, 2019), and the RI/MOM scheme has been adopted in more recent work (R. Zhang *et al.*, 2020).

The LaMET expression for DAs takes the following form in the $\overline{\text{MS}}$ scheme (Ji, Schäfer *et al.*, 2015; Liu *et al.*, 2019b):

$$\phi_\pi(x,\mu) = \int_{-\infty}^{\infty} dy\, C_\pi(x,y,P^z/\mu)\tilde{\phi}_\pi(y,P^z,\mu) + \cdots. \quad (143)$$

The matching coefficient for the quasi-DAs can be obtained by replacing the meson state $|\pi(P)\rangle$ in Eqs. (141) and (142) with the lowest Fock state $|q(yP)\bar{q}[(1-y)P]\rangle$ and calculating the quark matrix elements, where yP and $(1-y)P$ are the momenta of the quark q and antiquark $\bar{q}$, respectively. Its one-loop results have been calculated in both the $\overline{\text{MS}}$ and RI/MOM schemes (Liu *et al.*, 2019b), which agrees with the matching coefficients for the quasi-GPDs (Ji, Schäfer *et al.*, 2015; Xiong and Zhang, 2015; Liu *et al.*, 2019a) in Eq. (138), with the replacement of $\xi \to 1/(2y-1)$, $x/\xi \to 2x-1$, and the external momentum p^z to $p^z/2$.

Apart from the LaMET approach in momentum space, the shape of the pion DA has also been studied using equal-time current-current correlation in the coordinate-space approach (Bali *et al.*, 2018; Bali, Braun *et al.*, 2018):

$$\langle 0|T\left\{J_\mu\left(\frac{z}{2}\right)J_\nu\left(-\frac{z}{2}\right)\right\}|\pi^0(P)\rangle = \frac{2if_\pi}{3\pi^2 z^4}\epsilon_{\mu\nu\alpha\beta}P^\alpha z^\beta \Phi_\pi(\lambda, z^2),$$
$$(144)$$

where $\Phi_\pi(\lambda, z^2)$ can be factorized as

$$\Phi_\pi(\lambda, z^2) = C_2(\lambda, z^2\mu^2, x) \otimes \phi_\pi(x,\mu) + \cdots. \quad (145)$$

In Eq. (145) the matching coefficient C_2 depends on the choice of the currents. Its explicit expression was given by Bali, Braun *et al.* (2018). This factorization is controlled by $\mathcal{O}(z^2\Lambda_{\text{QCD}}^2)$, with power corrections denoted by an ellipsis. Bali, Braun *et al.* (2018) performed a combined analysis of several current-current correlations where twist-4 contributions were also included using the model estimate of Braun and Filyanov (1990) and Ball, Braun, and Lenz (2006). The leading-twist pion DA was then extracted from a global fit to the data, and the second moment of the pion DA has been fitted with controlled precision, both of which favor a considerably broader shape than the asymptotic DA at a scale of 2 GeV. A large pion momentum is required to access information at large λ so that we can extract a wider range of x or higher moments of the pion DA (Bali *et al.*, 2018).

C. Higher-twist distributions

Higher-twist distributions are quantities of great interest because they describe the coherent quark-gluon correlations in the proton. Compared to the leading-twist distributions, our understanding of the higher-twist ones is rather poor. On the one hand, they often depend on more than one parton momentum fraction; on the other hand, there is no physical

intuition about what they may look like, in particular, about how they behave asymptotically at small and large x (Braun *et al.*, 2011). There have been studies on the higher-twist distributions in the context of their connection to the DIS structure function, the transverse single-spin asymmetries in various hadron productions, GPDs related to quark and gluon OAM, parton DAs, etc. LaMET will be able to shed new light by providing a possibility to access them from the lattice.

Higher-twist contributions also appear in the LaMET expansion, where the suppression is provided by powers of the hadron momentum squared. In all of the previously presented factorizations, only the leading-twist terms that capture the logarithmic dependence on hadron momentum were taken into account. The higher-twist contributions have been assumed to be small. If the hadron momentum is not sufficiently large and/or one is close to the end-point region ($x \to 0$ and $x \to 1$), the higher-twist contributions can become non-negligible; their structure and impact require understanding.

1. Higher-twist collinear-parton observables

Beyond leading twist, the three simplest twist-3 quark distributions $e(x)$, $g_T(x)$, and $h_L(x)$ related to unpolarized, transversely, and longitudinally polarized protons (Jaffe and Ji, 1992) are

$$e(x) = \frac{1}{2M}\int \frac{d\lambda}{2\pi} e^{ix\lambda}$$
$$\times \langle PS|\psi_+^\dagger(0)\gamma_0\psi_-(\lambda n)|PS\rangle + \text{H.c.}, \quad (146)$$

$$g_T(x) = \frac{1}{2M}\int \frac{d\lambda}{2\pi} e^{ix\lambda}$$
$$\times \langle PS_\perp|\psi_+^\dagger(0)\gamma_0\gamma_\perp\gamma_5\psi_-(\lambda n)|PS_\perp\rangle + \text{H.c.}, \quad (147)$$

$$h_L(x) = \frac{1}{2M}\int \frac{d\lambda}{2\pi} e^{ix\lambda}$$
$$\times \langle PS_z|\psi_+^\dagger(0)\gamma_0\gamma_5\psi_-(\lambda n)|PS_z\rangle + \text{H.c.}, \quad (148)$$

where we have again employed the decomposition of quark fields $\psi = \psi_+ + \psi_-$ from Sec. I.A and the light-cone gauge $A^+ = 0$ and H.c. stands for Hermitian conjugate.

The twist-3 distributions can contribute as leading effects in certain experimental observables. For example, $g_T(x)$ and $h_L(x)$ can be measured as the leading effects in the longitudinal-transverse-spin asymmetry in polarized Drell-Yan process.

Since ψ_- is a nondynamical component depending on ψ_+, all previously mentioned distributions can be shown to be related to more complicated quark-gluon correlation functions (Ji and Chou, 1990; Balitsky *et al.*, 1996). A complete set of such correlation functions was given by Qiu and Sterman (1991), Ji (1992), Ji and Osborne (2001), and Kang and Qiu (2009), where the quark-gluon correlations in a transversely polarized proton take the following form:

$$T_q(x_1, x_2) = \frac{1}{(P^+)^2} \int \frac{d\lambda d\zeta}{(2\pi)^2} e^{i\lambda x_1 + i\zeta(x_2 - x_1)}$$
$$\times \langle PS_\perp | \bar\psi(0)\gamma^+ \epsilon^{+-S_\perp i} gF^{+i}(\zeta n)\psi(\lambda n)|PS_\perp\rangle, \tag{149}$$

$$T_{\Delta q}(x_1, x_2) = \frac{1}{(P^+)^2} \int \frac{d\lambda d\zeta}{(2\pi)^2} e^{i\lambda x_1 + i\zeta(x_2 - x_1)}$$
$$\times \langle PS_\perp | \bar\psi(0)i\gamma^+\gamma_5 S_\perp^i gF^{+i}(\zeta n)\psi(\lambda n)|PS_\perp\rangle. \tag{150}$$

There are also correlations in an unpolarized and longitudinally polarized proton. Generalizing to off-forward kinematics, the resulting twist-3 GPDs are also related to quark and gluon OAM contributions to the proton spin (Hatta and Yoshida, 2012; Ji, Xiong, and Yuan, 2013).

One can also define twist-4 distributions in a manner similar to Eq. (149) by using ψ_- for both quark fields. More general twist-4 distributions will involve three light-cone variables that contribute to the $1/Q^2$ term in DIS (Jaffe and Soldate, 1982; Ellis, Furmanski, and Petronzio, 1983; Jaffe and Ji, 1992; Ji, 1993).

In principle, all of these higher-twist distributions, as well as others that are not listed here, can be computed using the LaMET approach by choosing appropriate quasi-LF correlations. For example, the first exploratory lattice calculation of $g_T(x)$ was done by Bhattacharya et al. (2020a), which we discuss in Sec. VI.C. However, extra complications are expected due to their complex structure. For instance, the light-cone zero modes that do not enter into dealing with leading-twist distributions come into play here. Recently Ji (2020) showed how to study the properties of these zero modes from lattice simulations in LaMET. In addition, the higher-twist distributions will have a more complex mixing pattern (Ji and Chou, 1990; Balitsky et al., 1996). Thus, their matching from the corresponding quasidistributions must take such mixings into account, making them more challenging to calculate than the twist-2 PDFs. One-loop studies of the matching for twist-3 distributions were carried out by Bhattacharya et al. (2020b, 2020c) and Braun, Ji, and Vladimirov (2021).

2. Higher-twist contributions to quasi-PDFs

We now turn to the power-suppressed higher-twist contributions appearing in the extraction of leading-twist quark PDFs using LaMET. Such contributions have two distinct origins. To understand them, we recall the OPE for the quasi-LF correlation in Eq. (98). For simplicity, we ignore the renormalization here. Recovering the leading-twist quark PDF requires one to remove the contributions of both trace terms in that equation. The trace terms on the rhs of Eq. (98), which lead to contributions suppressed by powers of $M^2/(P^z)^2$, are known as kinematic power contributions or target-mass corrections. In DIS, they can be accounted for by changing the scaling variable x to the Nachtmann variable (Nachtmann, 1973). In the case of LaMET, it behaves slightly differently, as shown later. The second type of power corrections come from the trace terms in the operators on the rhs of Eq. (97), and in general leads to contributions of $\mathcal{O}(\Lambda_{\rm QCD}^2/(P^z)^2)$. These are

genuine higher-twist contributions that involve multiparton correlations, sometimes also known as dynamical higher-twist contributions. The target-mass corrections have been computed to all orders in $M^2/(P^z)^2$ for the quark quasi-PDFs given by Chen et al. (2016) and Radyushkin (2017c). Genuine higher-twist contributions have been investigated using two different approaches (Chen et al., 2016; Braun, Vladimirov, and Zhang, 2019).

According to Chen et al. (2016), the $M^2/(P^z)^2$ corrections can be obtained from the ratio

$$K_m \equiv \frac{n_{(\mu_1} \cdots n_{\mu_m)}P^{\mu_1} \cdots P^{\mu_m}}{n_{\mu_1} \cdots n_{\mu_m}P^{\mu_1} \cdots P^{\mu_m}} = \sum_{i=0}^{i_{\rm max}} C_{m-i}^i c^i, \tag{151}$$

where $i_{\rm max} = (m - \mod[m, 2])/2$, C is the binomial function, and $c = -n^2 M^2/4(n \cdot P)^2 = M^2/4(P^z)^2$, with $n^\mu = (0, 0, 0, -1)$ and $n \cdot P = P^z$.

Plugged into the tree-level OPE formula in Eq. (98), these factors can then be converted into the following relation between an unpolarized PDF and a quasi-PDF (Chen et al., 2016):

$$q(x) = \sqrt{1 + 4c} \sum_{n=0}^\infty \frac{(4c)^n}{f_+^{2n+1}} \left[[1 + (-1)^n]\tilde q\left(\frac{f_+^{2n+1}x}{2(4c)^n}\right) \right.$$
$$\left. + [1 - (-1)^n]\tilde q\left(\frac{-f_+^{2n+1}x}{2(4c)^n}\right) \right], \tag{152}$$

where $f_+ = \sqrt{1 + 4c} + 1$. Note that quark number conservation is preserved in Eq. (152). The target-mass corrections for the longitudinally and transversely polarized quasi-PDFs can be derived analogously.

The trace part on the rhs of Eq. (97) is a genuine higher-twist effect. One may try to construct a nonlocal form of the higher-twist operators from the OPE. The leading trace term, which is a twist-4 effect, was studied by Chen et al. (2016) [see also Balitsky and Braun (1989)] and shown to give rise to a twist-4 PDF

$$q_4(x, P^z) = \int_{-\infty}^\infty \frac{d\lambda}{8\pi P^z} \Gamma_0(-ix\lambda)\langle P|O_{\rm tr}(z)|P\rangle, \tag{153}$$

with

$$O_{\rm tr}(z) = \int_0^z dz_1 \bar\psi(0)\left[\Gamma^\nu W(0, z_1)D_\nu W(z_1, z) \right.$$
$$\left. + \int_0^{z_1} dz_2 n \cdot \Gamma W(0, z_2)D^\nu W(z_2, z_1)D_\nu W(z_1, z)\right]$$
$$\times \psi(zn), \tag{154}$$

where one has $\Gamma^\mu = \gamma^\mu, \gamma^\mu\gamma^5, \gamma^\perp\gamma^\mu\gamma^5$ for the unpolarized, helicity, and transversity PDFs, respectively. Γ_0 is the incomplete gamma function

$$\Gamma_0(-ix) = \int_0^1 \frac{dt}{t} e^{ix/t}. \tag{155}$$

The previous twist-4 contribution needs to be removed from the quasi-PDF to recover the leading-twist PDF. It also

provides a possibility for practical computations on the lattice. However, as a multiparton correlation involving more gauge links and covariant derivatives, its lattice computation is challenging and has not been carried out in any existing work.

Another approach that has been used to estimate power corrections related to quark quasi-PDFs is the renormalon model; see Beneke (1999) for a comprehensive review. The model is based on the observation that the perturbative expansion of the matching coefficient for the quasi-PDF diverges factorially with the loop order, implying that it is only well defined up to a power accuracy. This is known as the renormalon ambiguity, which must be canceled out by terms in the higher-twist contributions.

Braun, Vladimirov, and Zhang (2019) showed that the cancellation of renormalon ambiguity requires the leading higher-twist or twist-4 contribution to take the following form:

$$q_4(y, P^z, \mu) = \mu^2 \int_{-1}^{1} \frac{dx}{|x|} D\left(\frac{y}{x}\right) q(x, \mu) + q_4'(y, P^z, \mu), \quad (156)$$

where the first term on the rhs cancels out the renormalon ambiguity from the leading-twist matching coefficient and q_4' depends on μ at most logarithmically. Since the first term is to merely cancel out similar contributions in the matching coefficient, it does not contribute to any physical observable. The renormalon model of power corrections (Beneke and Braun, 1995; Dasgupta and Webber, 1996, 1997; Dokshitzer, Marchesini, and Webber, 1996; Beneke, Braun, and Magnea, 1997; Braun, Gardi, and Gottwald, 2004) is based on the assumption that, by replacing μ with a suitable nonperturbative scale, this contribution reflects the order and the functional form of actual power-suppressed contributions. This was referred to as "ultraviolet dominance" by Braun (1995), Beneke (1999), and Beneke and Braun (2000). Under this assumption, we obtain the following estimate:

$$q_4(y, P^z, \mu) = \kappa \Lambda_{\text{QCD}}^2 \int_{-1}^{1} \frac{dx}{|x|} D\left(\frac{y}{x}\right) q(x, \mu), \quad (157)$$

where κ is a dimensionless coefficient of $\mathcal{O}(1)$ that cannot be fixed within theory and remains a free parameter.

A detailed analysis (Braun, Vladimirov, and Zhang, 2019) showed that for the quasi-PDF we have

$$
\begin{aligned}
q_4(y, P^z) = {} & \frac{\kappa \Lambda_{\text{QCD}}^2}{y^2(1-y)(P^z)^2} \\
& \times (1-y) \left[\int_{|y|}^{1} \frac{dx}{x} \left[\frac{x^2}{(1-x)_+} - 2x^2 \right] q\left(\frac{y}{x}\right) \right. \\
& \left. + 2q(y) - |y|q'(y) \right],
\end{aligned}
\quad (158)
$$

where the first term in the integral was reproduced in a recent analysis of the renormalon effects in the quasi-PDF (Liu and Chen, 2020). As one can see, the second row vanishes as $q(y)$ when $y \to 1$ if $\lim_{y \to 1} q(y) \sim (1-y)^a$ with $a > 0$. This gives an estimate of the twist-4 contribution on the rhs of Eq. (33), which implies that the higher-twist contributions are enhanced as $1/y^2$ and $1/(1-y)$ for $y \sim 0$ and $y \sim 1$, respectively.

A similar analysis can also be done for the pseudo-PDF. This result can be used as a way to model the twist-4 contribution with κ as the only parameter.

D. Orbital angular momentum of partons in the proton

Over the past three decades, much experimental and theoretical work has been done on the origin and structure of proton spin, which has been covered in depth in various reviews (Filippone and Ji, 2001; Bass, 2005; Aidala *et al.*, 2013; Leader and Lorcé, 2014; Ji, 2017; Deur, Brodsky, and Téramond, 2019; Ji, Yuan, and Zhao, 2020).

In addition to the spin-dependent PDFs and TMDs, the GCPOs (in particular, the GPDs) also play an important role in understanding the spin structure of the proton. Since GPDs describe the correlation between the transverse position and longitudinal momentum of quarks and gluons inside the proton, they offer a unique channel to study the OAM from experiments.

There are two widely known definitions of OAM in literature. One is the kinetic OAM in the gauge-invariant and frame-independent sum rule for the proton spin (Ji, 1997a, 1997b), which is related to the first moment of twist-2 GPDs and can be calculated from the form factors of the symmetric QCD energy-momentum tensor. A review of the lattice calculations of kinetic OAM was given by Ji, Yuan, and Zhao (2020). The other definition, which has a clear partonic interpretation relative to the kinetic OAM, is the canonical OAM in the naive partonic sum rule (Jaffe and Manohar, 1990) based on the following free-field form of the QCD angular momentum:

$$
\begin{aligned}
\vec{J} = {} & \int d^3\xi \, \psi^\dagger \frac{\vec{\Sigma}}{2} \psi + \int d^3\xi \, \psi^\dagger [\vec{\xi} \times (-i\vec{\nabla})]\psi \\
& + \int d^3\xi \, \vec{E} \times \vec{A} + \int d^3\xi \, E^i(\vec{\xi} \times \vec{\nabla})A^i,
\end{aligned}
\quad (159)
$$

where i is the spatial Lorentz index. The three operators other than the first one are gauge dependent, and their matrix elements are generally frame dependent. In high-energy scattering, there are one frame and one gauge that are special: the IMF and light-front gauge ($A^+ = 0$). Therefore, the naive partonic sum rule for proton spin can be expressed as (Jaffe and Manohar, 1990)

$$\tfrac{1}{2} = \tfrac{1}{2}\Delta\Sigma(\mu) + l_q^z(\mu) + \Delta G(\mu) + l_g^z(\mu), \quad (160)$$

where $l_q^z(\mu)$ and $l_g^z(\mu)$ are the canonical OAM of the quark and gluon partons, respectively. Both l_q^z and l_g^z can be related to twist-3 GPDs (Hatta, 2012; Hatta and Yoshida, 2012; Ji, Xiong, and Yuan, 2013), which can be accessed through spin asymmetries in hard exclusive processes (Bhattacharya, Metz, and Zhou, 2017; Hatta *et al.*, 2017; Ji, Yuan, and Zhao, 2017; Bhattacharya *et al.*, 2018); see the recent review by Ji, Yuan, and Zhao (2020).

To fully understand the partonic spin structure of the proton, one also needs to determine the quark and gluon canonical OAM (l_q^z and l_g^z). LaMET allows extraction of l_q^z and l_g^z from

the lattice calculation in the same way as the gluon helicity that was reviewed in Sec. III.E.

The quasipartonic OAM operators can be chosen as the free-field operators fixed in gauges that belong to the universality class (Hatta, Ji, and Zhao, 2014). Their matrix elements $\tilde{l}_q^z$ and $\tilde{l}_g^z$ can be calculated from the off-forward matrix elements of the relevant energy-momentum tensors (Zhao, Liu, and Yang, 2016):

$$\tilde{l}_q^z(2S^z) = \lim_{\Delta \to 0} \epsilon^{ij} \frac{\partial}{\partial i\Delta^i} \langle P'S|\psi^\dagger(0)i\partial^j\psi(0)|PS\rangle|_{\vec{\nabla}\cdot\vec{A}=0}, \quad (161)$$

where the kinematics is the same as in Eq. (130).

Along with ΔG, $\tilde{l}_q^z$ and $\tilde{l}_g^z$ can be matched to the partonic quantities defined in the Jaffe-Manohar sum rule through the following factorization formulas:

$$\begin{aligned} \tilde{l}_q^z(P^z, \mu) = &P_{qq}l_q^z(\mu) + P_{gq}l_g^z(\mu) \\ &+ p_{qq}\Delta\Sigma(\mu) + p_{gq}\Delta G(\mu) + \cdots, \end{aligned} \quad (162)$$

$$\begin{aligned} \tilde{l}_g^z(P^z, \mu) = &P_{qg}l_q^z(\mu) + P_{gg}l_g^z(\mu) \\ &+ p_{qg}\Delta\Sigma(\mu) + p_{gg}\Delta G(\mu) + \cdots, \end{aligned} \quad (163)$$

where the ellipses are power corrections suppressed by the momentum P^z, and the one-loop matching coefficients in front of each term on the rhs have been calculated in the Coulomb gauge (Ji, Zhang, and Zhao, 2015). Since the quasipartonic operators are gauge variant and need to be fixed in a particular gauge, they can mix with new operators that are not allowed in Lorentz or gauge symmetries. For example, the gauge-dependent potential angular momentum $\psi^\dagger(\vec{r} \times \vec{A})\psi$ comes into play (Wakamatsu, 2014; Ji *et al.*, 2016). Such mixings must be taken into account in lattice renormalization to have a controlled calculation of the canonical OAM.

In addition to this approach, it has also been proposed to calculate the ratio of l_q^z and the valence quark number from the derivatives of off-forward matrix elements of staple-shaped quark-Wilson-line operators (Engelhardt, 2017), whose definition is given in Eq. (195). The first lattice calculations with this approach, carried out by Engelhardt (2017) and Engelhardt *et al.* (2018), showed different sizes of effects between the kinetic and canonical OAM. For systematic improvement in this calculation, one should include the matching of such matrix elements to the physical l_q^z in the limit when the transverse separation of the quark fields approaches zero.

For the transverse polarization, it is natural to define a twist-2 partonic transverse angular momentum density of quarks (Hoodbhoy, Ji, and Lu, 1998; Ji, Xiong, and Yuan, 2012; Ji and Yuan, 2020; Ji, Yuan, and Zhao, 2020),

$$J_\perp^q(x) = x[q(x) + E_q(x)]/2, \quad (164)$$

and a similar approach is followed with gluons, where $q(x)$ is the unpolarized quark PDF and $E_{q,g}(x)$ are the GPDs defined earlier in this section. Thus, to get a simple partonic picture of

the proton transverse spin from first principles, it is important to calculate the GPD $E(x)$ using LaMET.

V. TRANSVERSE-MOMENTUM-DEPENDENT PDFs

The TMDPDFs are a natural generalization of the collinear PDFs including both longitudinal and transverse momenta of partons. They are in principle probability distributions $f_i(x, \vec{k}_\perp, \sigma)$ of finding a parton of a given species i, longitudinal and transverse momenta $(xP^+, \vec{k}_\perp)$, and polarization σ inside the hadron state. TMDPDFs are playing an increasingly important role in understanding the partonic structure of hadrons and high-energy scattering.

The TMD parton densities were introduced by Collins and Soper in the 1980s (Collins and Soper, 1981, 1982a; Collins, Soper, and Sterman, 1983, 1985a, 1985b; Bodwin, 1985) to understand the Drell-Yan (DY) and e^+e^- annihilation processes and generalized by Ji, Ma, and Yuan (2004, 2005) to the SIDIS process. The TMD factorization has been reanalyzed in the framework of SCET, in which modes are made manifest by effective fields (Bauer *et al.*, 2001; Bauer, Pirjol, and Stewart, 2002; Manohar and Stewart, 2007; Becher and Neubert, 2011; Chiu *et al.*, 2012; Echevarría, Idilbi, and Scimemi, 2012, 2013). Various TMD factorization formalisms finally converged to the standard one where a scheme-independent TMDPDF can be defined (Collins and Rogers, 2013, 2017; Echevarría, Idilbi, and Scimemi, 2013).

The TMD parton densities are important for understanding the experimental processes where the transverse momenta of final-state particles are measured. For example, in a DY pair and W, Z production it is known that the differential cross section $d\sigma/dQ_T^2$ normally peaks at relatively small transverse momentum. For $Q \sim 10$ GeV, the peak is typically located at $Q_\perp \sim 1$ GeV where nonperturbative effects are important (Collins, Soper, and Sterman, 1985b). Good knowledge of TMD parton densities is therefore crucial for the determination of the cross sections and a precise test of perturbative QCD predictions.

In addition to their importance for understanding the high-energy experimental data, the TMD parton densities are also important by themselves for their crucial role in describing hadron structures. With them, one can simultaneously study the fast-moving collinear physics through the longitudinal x dependencies, and the nonperturbative effect from the transverse $\vec{k}_\perp$ dependencies. Moreover, the TMDPDFs are sensitive to effects such as soft radiation. Therefore, the physics in the presence of transverse degrees of freedom is rich. This is particularly true in studies of spin-dependent phenomena where one can define various TMDPDFs through Lorentz decompositions; see Sec. V.B. One example is the Sivers function for a transversely polarized proton $\epsilon_{ij}k_\perp^i S_\perp^i f_{1T}^\perp(x, k_\perp)$, which is naive time reversal odd and is predicted to change sign between the DY and SIDIS processes (Collins, 2011a). Similar properties also exist in the Boer-Mulders function (Boer and Mulders, 1998) concerning a transversely polarized parton distribution in an unpolarized hadron. These two functions are related to the single transverse-spin asymmetry. If we generalize the TMDPDFs to include the impact parameter dependence, we can further

define the Wigner function, the parton orbital angular momentum distributions, etc. (Belitsky, Ji, and Yuan, 2004; Lorce *et al.*, 2012). Therefore, the TMDPDFs allow for a more complete and refined 3D description (or tomography) of the hadron structure (Burkardt, 2000; Boer *et al.*, 2011). The 3D tomography of the proton is a major physical goal of the EIC program. The TMDPDFs are also important for understanding small-*x* physics (Kuraev, Lipatov, and Fadin, 1977; Balitsky and Lipatov, 1978; Balitsky, 1996; Kovchegov, 1999; Kovchegov and Levin, 2012).

Our current knowledge on TMDPDFs comes mainly from fitting to the experimental data (Landry *et al.*, 2000; Konychev and Nadolsky, 2006; Echevarría *et al.*, 2014; Kang *et al.*, 2016; Bacchetta *et al.*, 2017, 2020; Scimemi and Vladmirov, 2018, 2019; Sun *et al.*, 2018; Bertone, Scimemi, and Vladimirov, 2019). This is, however, rather primitive due to the paucity of data. Although the future EIC will make up the gap and produce more data for TMD measurements, it is still important to develop first-principle methods for the determination of nonperturbative TMDPDFs, which can serve as a test or provide useful inputs to constrain the global fits. LaMET provides a systematic way to extract TMDPDFs from the lattice calculations. Early studies (Ji, Sun *et al.*, 2015; Ebert, Stewart, and Zhao, 2019a, 2019b; Ji *et al.*, 2019) tried to construct a quasi-TMDPDF on the lattice, but its relation to the physical TMDPDF is expected to be nonperturbative due to complications in the soft function (Ebert, Stewart, and Zhao, 2019b). Recently Ji, Liu, and Liu (2019, 2020) provided a formulation for calculating the soft function so that a perturbative matching formula can be established between the quasi-PDFs and physical TMDPDFs, allowing for a complete determination of the latter from lattice QCD. In this section we review the application of LaMET to the nonperturbative TMDPDFs. The investigation is still in its early stages and much remains to be explored, particularly in lattice calculations and matching.

In Sec. V.A we introduce the TMDPDFs and discuss the associated rapidity divergences. In Secs. V.B–V.D we define the quasi-TMDPDFs or TMD momentum distributions in a proton of finite momentum and study their momentum RGEs and UV renormalization properties. In the process, we introduce off-light-cone soft functions. We then present the factorization of the quasi-TMDPDFs into the light-cone TMDPDFs and the off-light-cone soft function, where various one-loop results and the relevant RGEs are also given. The properties of the off-light-cone soft-function are discussed in Sec. V.D, where they are shown to be related to the form factor of a pair of charged color sources, which paves the way for its calculation on a Euclidean lattice.

A. Introduction to TMDPDFs and rapidity divergence

As explained in Sec. II, we can define various TMDPDFs by choosing different gauge links between the quark or gluon bilinears. The one relevant to high-energy phenomena is defined by lightlike Wilson lines. The links represent the propagation of high-energy color-charged particles and are crucial in forming gauge-invariant nonlocal operators (Belitsky, Ji, and Yuan, 2003). As previously argued, such operators are the result of an EFT description (more explicitly

so in SCET) arising from taking the infinite-momentum limit of the proton. Thus, it is natural to expect that they require additional regularization and renormalization.

Take the nonsinglet quark unpolarized TMDPDF as an example. Without the field theoretical subtleties, the distribution is

$$
f(x, \vec{k}_\perp) = \frac{1}{2P^+} \int \frac{d\lambda}{2\pi} \frac{d^2 \vec{b}_\perp}{(2\pi)^2} e^{-i\lambda x + i\vec{k}_\perp \cdot \vec{b}_\perp}
$$
$$
\times \langle P| \bar{\psi}(\lambda n/2 + \vec{b}_\perp) \gamma^+ \mathcal{W}_n(\lambda n/2 + \vec{b}_\perp) \psi(-\lambda n/2)|P\rangle, \tag{165}
$$

where $\mathcal{W}_n(\lambda n + \vec{b}_\perp)$ is the staple-shaped gauge link of the form

$$
\mathcal{W}_n(\xi) = W_n^\dagger(\xi) W_\perp W_n(-\xi \cdot pn), \tag{166}
$$

$$
W_n(\xi) = \mathcal{P} \exp\left[-ig \int_0^{-\infty} d\eta \, n \cdot A(\xi + \eta n)\right] \tag{167}
$$

along the light-cone direction n^μ, as shown in Fig. 9. The $W_\perp$ is a transverse gauge link at light-cone infinity to maintain gauge invariance. If one uses LFQ and ignores the transverse gauge link, Eq. (167) is simply $\langle P|b^\dagger(x, \vec{k}_\perp) b(x, \vec{k}_\perp)|P\rangle$ for $x > 0$, as expected.

However, there are a number of qualifications in this definition. First, the lightlike gauge links $\mathcal{W}_n$ are chosen to be past pointing, in accordance with the DY kinematics, but for SIDIS they should be chosen as future pointing, as shown in Fig. 9. For unpolarized TMDPDFs there is no distinction between the two choices, but for spin-dependent TMDPDFs there are physical consequences associated with the direction of the gauge links.

Second, there is a new type of divergence associated with the infinitely long lightlike gauge links. These divergences are due to the radiation of gluons collinear to the lightlike gauge link and cannot be regularized using the standard UV
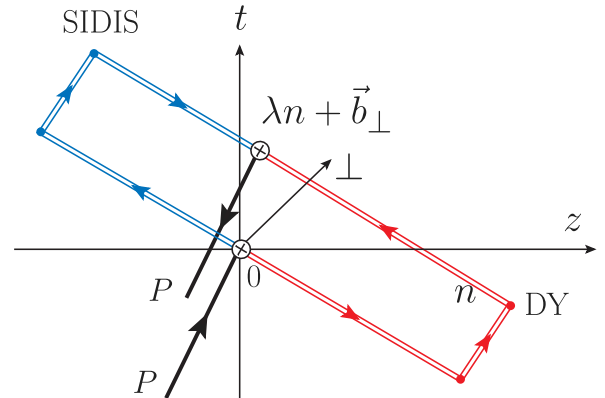

FIG. 9. Space-time picture of TMDPDF for DY and SIDIS processes. The circled crosses denote the quark-link vertices. Notice that the vertices are placed at $\lambda n + \vec{b}_\perp$ and 0, which gives the same result as the symmetric choice in Eq. (165).

regulators. An example is the following integral in DR (Ebert, Stewart, and Zhao, 2019b):

$$I = \int dk^+ dk^- \frac{f(k^+ k^-)}{(k^+ k^-)^{1+\epsilon}} = \frac{1}{2} \int \frac{dy}{y} \int dm^2 \frac{f(m^2)}{m^{2+2\epsilon}}, \quad (168)$$

where $m^2 = k^+ k^-$ and $y = k^+/k^-$ is the rapidity-related variable. The divergences in y arise from large and small y where the integral is unregulated. The contribution from $k^+ = 0$ is called the light-zero mode in LFQ, where it is also called light-cone divergence, which causes considerable problems.

To regulate the light-cone or rapidity divergence, a number of methods have been introduced in the literature; for a review see Ebert, Stewart, and Zhao (2019b). They can be put into two classes: on-light-cone regulators and off-light-cone regulators. In the former case, the gauge links are kept along the light-cone direction n^μ after regularization. For example, the so-called δ regulator (Echevarría, Scimemi, and Vladimirov, 2016a, 2016b) regularizes the gauge link as

$$W_n(\xi) \to W_n(\xi)|_{\delta^-}$$
$$= \mathcal{P} \exp\left[-ig \int_0^{-\infty} d\eta A^+(\xi + \eta n) e^{-\delta^-/(2p^+)|\eta|}\right], \quad (169)$$

and a similar approach is used for the conjugate direction. The δ regulator breaks gauge invariance but preserves the boost invariance $\delta^\pm \to e^{\pm Y}\delta^\pm$, where Y is the rapidity of the Lorentz boost. Other on-light-cone regulators include the exponential regulator (Li, Neill, and Zhu, 2020), η regulator (Chiu *et al.*, 2012), analytical regulator (Becher and Neubert, 2011), etc. In the remainder of this section, we use the δ regulator as a representative whenever we need an on-light-cone regulator.

The off-light-cone regulator was introduced by Collins and Soper (1981), Ji, Ma, and Yuan (2004, 2005), and Collins (2011a). This type of regulator chooses off-light-cone directions to avoid the rapidity divergence. One can choose to deform the gauge links into the spacelike region as follows:

$$n \to n_Y = n - e^{-2Y} \frac{p}{(p^+)^2}. \quad (170)$$

Here Y plays the role of a rapidity regulator, as when $Y \to \infty$, $n_Y \to n$. In certain cases one can also deform n_Y into the timelike region (Collins and Metz, 2004).

The on-light-cone regulators are consistent with the spirit of parton physics, and therefore are useful to define center-of-mass-momentum-independent parton densities. The off-light-cone regulators, on the other hand, have a similar spirit as LaMET, and therefore can be exploited for practical lattice QCD calculations, as we see in Sec. V.B.

To avoid light-cone divergences, from now on we include the rapidity regulator in the definition of the light-cone TMDPDFs. Using the same label f for the TMDPDFs in both momentum and coordinate spaces, we have

$$f(\lambda, b_\perp, \mu, \delta^-/P^+)$$
$$= \langle P|\bar{\psi}(\lambda n/2 + \vec{b}_\perp) \slashed{n} \mathcal{W}_n(\lambda n/2 + \vec{b}_\perp)|_{\delta^-} \psi(-\lambda n/2)|P\rangle, \quad (171)$$

where μ is the $\overline{\text{MS}}$ scale for UV renormalization. Because of rotational invariance, the previously defined bare TMDPDF is a function of $b_\perp = |\vec{b}_\perp|$, so we have omitted the vector arrow for $\vec{b}_\perp$ in f and do so throughout the discussion of the soft functions, quasi-TMDPDFs, etc. The subscript δ^- denotes that the staple-shaped gauge link $\mathcal{W}$ is regulated by the δ regulator in the light-cone minus direction. f diverges logarithmically as $\delta^- \to 0$, and the finite part also depends on the rapidity regulator. To define the physical TMDPDF, we need to remove all divergences and rapidity regularization scheme dependencies in f, in a manner similar to removing UV divergences in physical quantities.

The rapidity divergence for TMDPDFs can be removed by the soft function, which also plays an important role in TMD factorization. Intuitively, the soft function represents a cross section for fast-moving charged particles emitting soft gluons into final states. It has rapidity divergence associated with the light-cone direction, which is ultimately related to the mass singularity. The TMD soft function corresponding to the Drell-Yan process is defined as (Collins, 2011b; Echevarría, Scimemi, and Vladimirov, 2016b)

$$S(b_\perp, \mu, \delta^+, \delta^-) = \frac{\text{Tr}\langle 0|\bar{\mathcal{T}} W_p(\vec{b}_\perp)|_{\delta^+} W_n^\dagger(\vec{b}_\perp)|_{\delta^-} \mathcal{T} W_n(0)|_{\delta^-} W_p^\dagger(0)|_{\delta^+}|0\rangle}{N_c}$$
$$= \frac{\text{tr}\langle 0|\mathcal{W}_n(\vec{b}_\perp)|_{\delta^+} \mathcal{W}_p^\dagger(\vec{b}_\perp)|_{\delta^-}|0\rangle}{N_c}, \quad (172)$$

where $\mathcal{T}/\bar{\mathcal{T}}$ stands for time-antitime ordering. The first equality defines the soft function in terms of cut diagrams as an amplitude square. Since the soft function for the DY process is independent of time ordering, one can also define it with a single time ordering or no time ordering, leading to the second equality. The staple-shaped gauge link $\mathcal{W}_n$ is defined in Eq. (167), while the staple-shaped gauge link $\mathcal{W}_p$ is similarly defined as

$$\mathcal{W}_p(\xi) = W_p^\dagger(\xi) W_\perp W_p(0), \quad (173)$$

$$W_p(\xi) = \mathcal{P} \exp\left[-ig \int_0^{-\infty} d\eta\, p \cdot A(\xi + p\eta)\right]. \quad (174)$$

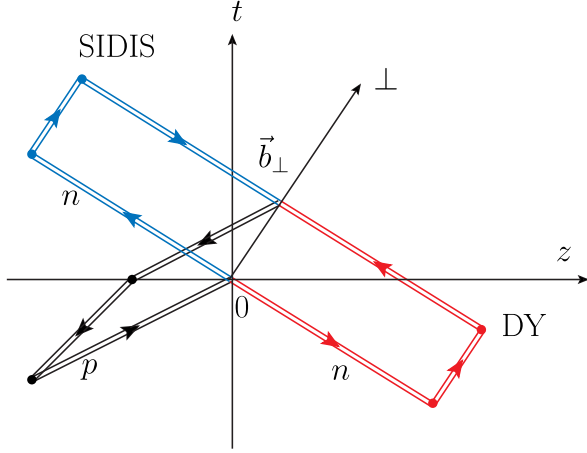The soft function is shown in Fig. 10 as a Wilson loop in Minkowski space.

FIG. 10. The soft function $S(b_\perp, \mu, \delta^+, \delta^-)$ as space-time Wilson loop arising in the factorization of DY and SIDIS processes.

If the rapidity divergences are multiplicative, one can use S as the rapidity renormalization factor for the TMDPDF defined in Eq. (165). In on-light-cone schemes such as the δ regularization, it was argued by Vladimirov (2018) based on conformal transformation that the rapidity divergences are indeed multiplicative in position space. For each of the staple-shaped lightlike gauge links, the rapidity divergence is proportional to $\exp\{-(1/2)K(b_\perp, \mu)\ln[\mu^2/2(\delta^\pm)^2]\}$, where $K(b_\perp, \mu)$ is the nonperturbative Collins-Soper evolution kernel (Collins and Soper, 1981). Thus, at small $\delta^\pm$ we can write

$$S(b_\perp, \mu, \delta^+, \delta^-) = e^{\ln(\mu^2/2\delta^+\delta^-)K(b_\perp,\mu) + \mathcal{D}_2(b_\perp,\mu)}, \quad (175)$$

where $\mathcal{D}_2(b_\perp, \mu)$ is a $b_\perp$-dependent but rapidity-independent function. Notice that our definitions of $\delta^\pm$ differ from those used by Echevarría, Scimemi, and Vladimirov (2016b) by a factor of $\sqrt{2}$ due to our normalization of light-cone vectors.

The soft function in δ regularization satisfies the renormalization group equation

$$\mu^2 \frac{d}{d\mu^2} \ln S(b_\perp, \mu, \delta^+, \delta^-)$$
$$= -\Gamma_{\text{cusp}}(\alpha_s) \ln \frac{\mu^2}{2\delta^+\delta^-} + \gamma_s(\alpha_s), \quad (176)$$

where $\Gamma_{\text{cusp}}(\alpha_s)$ is the lightlike cusp anomalous dimension (Polyakov, 1980; Korchemsky and Radyushkin, 1987) and $\gamma_s(\alpha_s)$ is the soft anomalous dimension (Korchemskaya and Korchemsky, 1992). The Collins-Soper kernel and the rapidity-independent part $\mathcal{D}_2$ satisfy the RGEs

$$\mu^2 \frac{d}{d\mu^2} K(b_\perp, \mu) = -\Gamma_{\text{cusp}}(\alpha_s), \quad (177)$$

$$\mu^2 \frac{d}{d\mu^2} \mathcal{D}_2(b_\perp, \mu) = \gamma_s(\alpha_s) - K(b_\perp, \mu). \quad (178)$$

At one loop, the soft function $S(b_\perp, \mu, \delta^+, \delta^-)$ is given by (Echevarría, Idilbi, and Scimemi, 2013)

$$S(b_\perp, \mu, \delta^+, \delta^-) = 1 + \frac{\alpha_s C_F}{2\pi}\left(L_b^2 - 2L_b \ln\frac{\mu^2}{2\delta^+\delta^-} + \frac{\pi^2}{6}\right), \quad (179)$$

where $L_b = \ln(\mu^2 b_\perp^2 e^{2\gamma_E}/4)$. Therefore, we have at the leading order

$$K(b_\perp, \mu) = -\frac{\alpha_s C_F}{\pi} L_b, \quad (180)$$

$$\mathcal{D}_2(b_\perp, \mu) = \frac{\alpha_s C_F}{2\pi}\left(L_b^2 + \frac{\pi^2}{6}\right), \quad (181)$$

$\Gamma_{\text{cusp}} = \alpha_s C_F/\pi + \mathcal{O}(\alpha_s^2)$, and $\gamma_s = \mathcal{O}(\alpha_s^2)$. Note that K (Li and Zhu, 2017; Vladimirov, 2017) and $\mathcal{D}_2$ (Li and Zhu, 2017) are known to three-loop order in the exponential regularization scheme.

For the previously mentioned soft function, we can take its square root to perform rapidity renormalization for the bare TMD correlator. The square root can be explained as follows: S contains two staples, while f contains one; thus, the rapidity divergences as well as scheme dependencies of S are twice those of f. This leads to the following definition of the renormalized physical TMDPDF (Collins and Rogers, 2013; Echevarría, Idilbi, and Scimemi, 2013):

$$f^{\text{TMD}}(x, b_\perp, \mu, \zeta) = \lim_{\delta^- \to 0} \frac{f(x, b_\perp, \mu, \delta^-/P^+)}{\sqrt{S(b_\perp, \mu, \delta^- e^{2y_n}, \delta^-)}}, \quad (182)$$

where the rapidity scale reads

$$\zeta = 2(xP^+)^2 e^{2y_n}. \quad (183)$$

The rapidity dependence in the numerator of the right-hand side of Eq. (182) has the form $\exp\{-(1/2)K(b_\perp, \mu) \times \ln[(\delta^-)^2/(xP^+)^2]\}$, while in the denominator it behaves as $\exp\{(1/2)K(b_\perp, \mu)\ln[\mu^2/2(\delta^-)^2 e^{2y_n}]\}$. The δ^- dependence thus cancels out in the ratio, leaving a dependence on the rapidity scale of $\exp\{-(1/2)K(b_\perp, \mu)\ln[\mu^2/2(xP^+)^2 e^{2y_n}]\}$, which is controlled by the following so-called Collins-Soper evolution equation:

$$2\zeta \frac{d}{d\zeta} \ln f^{\text{TMD}}(x, b_\perp, \mu, \zeta) = K(b_\perp, \mu). \quad (184)$$

The ζ dependence comes from the initial-state quark radiation and is intrinsically nonperturbative for large $b_\perp$. $f^{\text{TMD}}(x, b_\perp, \mu, \zeta)$ is the standard object to be matched to in LaMET.

We emphasize that although f^{TMD} is free from rapidity divergences, it does contain soft radiation from the charged particles in the initial state. This can be seen by considering Feynman diagrams for the unsubtracted f and applying soft approximation to gluons. One-half of the soft contribution in f is subtracted to define the physical f^{TMD} due to the requirement of factorization for physical processes. The remaining soft radiation also has a natural rapidity cutoff associated with $\ln(xP^+)$, which is reflected in the ζ dependence. What is noteworthy, however, is that f^{TMD} is rapidity regulator independent. Although a general proof to all orders in

perturbation theory is beyond the scope of this review, it is due to factorization and exponentiation of the soft physics in f, and thus the scheme cancellation can be done systematically in the exponent. In SCET-like approaches, one can define the "subtracted" TMDPDF or "beams function" that contains only collinear physics. However, they are generically scheme dependent and must be combined with an extrasoft function in factorization theorems. At one-loop level, the scheme-independent one-loop TMDPDF for an external quark state reads

$$
\begin{aligned}
f^{\text{TMD}}&(x, b_\perp, \mu, \zeta) \\
&= \delta(1-x) + \frac{\alpha_s C_F}{2\pi} F(x, \epsilon_{\text{IR}}, b_\perp, \mu)\theta(x)\theta(1-x) \\
&\quad + \frac{\alpha_s C_F}{2\pi}\delta(1-x)\left[-\frac{1}{2}L_b^2 + \left(\frac{3}{2} - \ln\frac{\zeta}{\mu^2}\right)L_b + \frac{1}{2} - \frac{\pi^2}{12}\right],
\end{aligned}
\tag{185}
$$

where

$$
F(x, \epsilon_{\text{IR}}, b_\perp, \mu) = \left[-\left(\frac{1}{\epsilon_{\text{IR}}} + L_b\right)\frac{1+x^2}{1-x} + 1 - x\right]_+. \tag{186}
$$

Two-loop order results for the TMDPDFs were given by Catani and Grazzini (2012), Catani *et al.* (2012), Gehrmann, Luebbert, and Yang (2014), Echevarría, Scimemi, and Vladimirov (2016c), Lübbert, Oredsson, and Stahlhofen (2016), and Luo *et al.* (2019) and three-loop order results were given by Luo *et al.* (2020).

The physical TMDPDF also satisfies the RG equation

$$
\begin{aligned}
\gamma_\mu(\mu, \zeta) &= \mu^2\frac{d}{d\mu^2}\ln f^{\text{TMD}}(x, b_\perp, \mu, \zeta) \\
&\equiv \frac{1}{2}\Gamma_{\text{cusp}}(\alpha_s)\ln\frac{\mu^2}{\zeta} - \gamma_H(\alpha_s),
\end{aligned}
\tag{187}
$$

where γ_H is called the hard anomalous dimension. At one loop, the cusp and hard anomalous dimensions read

$$
\Gamma_{\text{cusp}}(\alpha_s) = \frac{\alpha_s C_F}{\pi}, \qquad \gamma_H(\alpha_s) = -\frac{3\alpha_s C_F}{4\pi}. \tag{188}
$$

Recently the cusp anomalous dimension was calculated to four loops (Henn, Korchemsky, and Mistlberger, 2019; von Manteuffel, Panzer, and Schabinger, 2020).

Combining the RGE and the rapidity evolution equation for the TMDPDF, one obtains the following consistency condition:

$$
\mu^2\frac{d}{d\mu^2}K(b_\perp, \mu) = -2\zeta\frac{d}{d\zeta}\gamma_\mu(\mu, \zeta) = -\Gamma_{\text{cusp}}[\alpha_s(\mu)], \tag{189}
$$

from which one finds the following resummed form for the Collins-Soper kernel:

$$
K(b_\perp, \mu) = -2\int_{1/b_\perp}^\mu \frac{d\mu'}{\mu'}\Gamma_{\text{cusp}}[\alpha_s(\mu')] + K[\alpha_s(1/b_\perp)]. \tag{190}
$$

In Eq. (190) $K[\alpha_s(1/b_\perp)]$ contains both perturbative and nonperturbative contributions. The TMDPDFs at different scales are then related by

$$
\begin{aligned}
f^{\text{TMD}}&(x, b_\perp, \mu, \zeta) \\
&= f^{\text{TMD}}(x, b_\perp, \mu_0, \zeta_0)\exp\left[\int_{\mu_0}^\mu \frac{d\mu'}{\mu'}\gamma_\mu(\mu', \zeta_0)\right] \\
&\quad \times \exp\left[\frac{1}{2}K(b_\perp, \mu)\ln\frac{\zeta}{\zeta_0}\right].
\end{aligned}
\tag{191}
$$

The double-scale evolution in the μ-ζ plane for phenomenology was recently studied by Scimemi and Vladimirov (2018b). With the previously defined scheme-independent physical TMDPDF, the DY cross section at $s = (P_A + P_B)^2$ and small $Q_\perp$ can be factorized as

$$
\begin{aligned}
\frac{d\sigma}{dQ_\perp^2} &= \int dx_A dx_B d^2 b_\perp e^{i\vec{b}_\perp\cdot\vec{Q}_\perp}\hat\sigma(x_A x_B s, \mu) \\
&\quad \times f_A^{\text{TMD}}(x_A, b_\perp, \mu, \zeta_A)f_B^{\text{TMD}}(x_B, b_\perp, \mu, \zeta_B) \\
&\quad + \cdots.
\end{aligned}
\tag{192}
$$

The rapidity scales satisfy $\zeta_A\zeta_B = Q^4 \equiv (x_A x_B s)^2$. The remaining terms at large but finite Q^2 are called power corrections or "higher-twist" contributions. A detailed study of the power corrections to TMD factorization is beyond the scope of this review. We omit all the power corrections from the equations. The QCD part of the hard cross section $\hat\sigma$ at one-loop level reads

$$
\hat\sigma(x_A, x_B) = \sigma_0\left|1 + \frac{\alpha_s C_F}{4\pi}\left(-L_Q^2 + 3L_Q - 8 + \frac{\pi^2}{6}\right)\right|^2, \tag{193}
$$

where σ_0 is the Born cross section and $L_Q = \ln[(-Q^2 - i0)/\mu^2]$, and the result is now known up to three loops; see (Moch, Vermaseren, and Vogt (2005), Baikov *et al.* (2009), Gehrmann *et al.* (2010), and Lee, Smirnov, and Smirnov (2010) and the references therein. Similarly, for the SIDIS process we have

$$
\begin{aligned}
\frac{d\sigma}{dQ_\perp^2} &= \int dx dz d^2 b_\perp e^{i\vec{b}_\perp\cdot\vec{Q}_\perp}H(x, z, \mu, Q) \\
&\quad \times f^{\text{TMD}}(x, b_\perp, \mu, \zeta_A)d^{\text{TMD}}(z, b_\perp, \mu, \zeta_B),
\end{aligned}
\tag{194}
$$

where $d^{\text{TMD}}(z, b_\perp, \mu, \zeta_B)$ is the TMD-fragmentation function and H is the hard kernel.

B. Lattice quasi-TMDPDFs and matching

Before LaMET, there had been efforts to access TMD physics from lattice QCD by calculating the ratios of the x moments of TMDPDFs (Hagler *et al.*, 2009; Musch *et al.*, 2011, 2012; Engelhardt *et al.*, 2016; Yoon *et al.*, 2017), which are free from complications associated with the soft function and can be compared to certain experimental observables. In LaMET, we are more interested in obtaining the full x and $\vec{k}_\perp$

dependence of the TMDPDFs (Ji, Sun *et al.*, 2015; Ebert, Stewart, and Zhao, 2019a, 2019b; Ji, Liu, and Liu, 2019, 2020; Ji *et al.*, 2019). Therefore, a proper treatment of the soft-function subtraction and matching is essential. The earliest suggestion of a bent soft function, given by Ji, Sun *et al.* (2015) and in the follow-up work by Ebert, Stewart, and Zhao (2019b), has the correct IR logarithms at one-loop order, but this is expected to break down at higher-loop orders (Ji, Liu, and Liu, 2020), thus not allowing for a perturbative matching. Another suggestion that uses a naive rectangle-shaped Wilson loop (Ebert, Stewart, and Zhao, 2019b; Ji *et al.*, 2019) does not possess the correct IR physics either. Nevertheless, Ebert, Stewart, and Zhao (2019a) made important progress in calculating the nonperturbative Collins-Soper kernel $K(b_\perp, \mu)$ from the ratio of quasi-TMDPDFs at two different large momenta. Recently Ji, Liu, and Liu (2019, 2020) showed that the quasi-TMDPDF combined with a reduced soft function captures the correct IR physics to all orders and thus allows for a perturbative matching to the physical TMDPDF.

To construct such quasi-TMDPDFs, the collinear part can be treated in a manner similar to the collinear PDFs, while the soft piece is more challenging. Our starting point is that the physical f^{TMD} is independent of the rapidity regulator, so one can use a scheme in which the gauge links in both f and S are off the light cone, such as that used by Collins (2011a). In this case, one can use Lorentz symmetry to boost the staple-shaped gauge link $\mathcal{W}_n$ in f to a purely spacelike staple with no time dependence. However, one can use this trick for only one of the staples in S, say, $\mathcal{W}_n$, whereas the other one ($\mathcal{W}_p$) is still time dependent. In other words, there is no way to get rid of the time dependence in S entirely with Lorentz boost alone. This is natural because S in fact represents the square of an S matrix, which appears to be intrinsically Minkowskian. However, using the LaMET principle that time dependence of an operator can be simulated through external physical states at large momentum, we find that S can indeed be calculated on the lattice in the off-light-cone scheme as a form factor. A detailed discussion is given in Sec. V.C. Here we assume that this is true and discuss the matching between quasi-PDFs and physical TMDPDFs.

We first define the quasi-TMDPDF with a staple-shaped gauge link along the z direction (Ji, Sun *et al.*, 2015; Ebert, Stewart, and Zhao, 2019b; Ji, Liu, and Liu, 2019; Ji *et al.*, 2019) as

$$\tilde{f}(\xi^z, b_\perp, \mu, \zeta_z) = \lim_{L\to\infty} \frac{\langle P | \bar{\psi}(\xi^z n_z/2 + \vec{b}_\perp) \gamma^z \mathcal{W}_z(\xi^z n_z/2 + \vec{b}_\perp; L) \psi(-\xi^z n_z/2) | P \rangle}{\sqrt{Z_E(2L, b_\perp, \mu)}}, \tag{195}$$

where the $\overline{\mathrm{MS}}$ renormalization is implied and

$$\mathcal{W}_z(\xi; L) = W_z^\dagger(\xi; L) W_\perp W_z(-\xi^z n_z; L), \tag{196}$$

$$W_z(\xi; L) = \mathcal{P} \exp\left[-ig \int_{\xi^z}^L d\eta\, n_z \cdot A(\vec{\xi}_\perp + n_z\eta)\right]. \tag{197}$$

In Eqs. (196) and (197) $\xi^z = -\xi \cdot n_z$ and $\zeta_z = (2xP^z)^2$ is the Collins-Soper scale of the quasi-TMDPDF. $W_\perp$ is inserted at $z = L$ to maintain explicit gauge invariance. $\sqrt{Z_E(2L, b_\perp, \mu, 0)}$ is the square root of the vacuum expectation value of a flat rectangular Euclidean Wilson loop along the n_z direction with length $2L$ and width $b_\perp$:

$$Z_E(2L, b_\perp, \mu) = \frac{1}{N_c} \mathrm{Tr}\langle 0 | W_\perp \mathcal{W}_z(\vec{b}_\perp; 2L) | 0 \rangle. \tag{198}$$

Again γ^z can be replaced by γ^t as in the collinear quasi-PDF. For a depiction of $\tilde{f}$ and Z_E, see Fig. 11.

The purpose of the factor Z_E is as follows. At large L, the naive quasi-TMD correlator in the numerator of Eq. (195) contains divergences that go as $e^{-LE(b_\perp, \mu)}$, where $E(b_\perp)$ is the ground-state energy of a pair of static heavy quarks. $E(b_\perp, \mu) = 2\delta m + V(b_\perp, \mu)$ contains both the linear divergent mass corrections $2\delta m$ and the heavy-quark potential $V(b_\perp, \mu)$ due to mutual interactions. In the literature the $LV(b_\perp, \mu)$ part is sometimes called the "pinch-pole singularity." Therefore, we introduce the square root of a
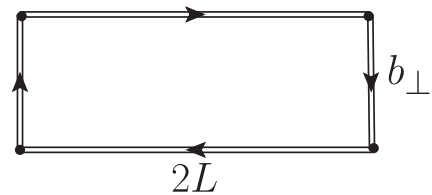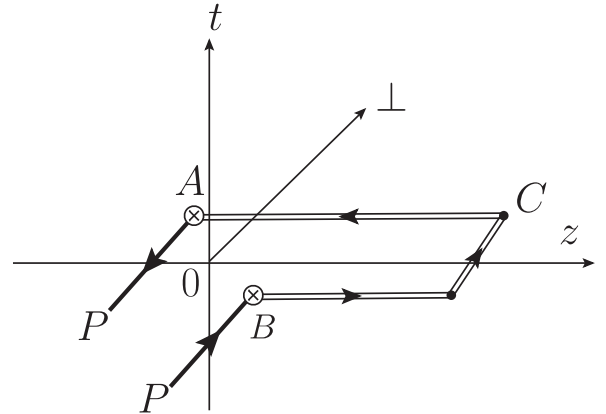

FIG. 11. Quasi-TMDPDF (upper panel) and Euclidean Wilson loop $Z_E(2L, b_\perp, \mu, 0)$ (lower panel). $A = \xi^z n_z/2 + \vec{b}_\perp/2$, $B = -\xi^z n_z/2 - \vec{b}_\perp/2$, and $C = L n_z + \vec{b}_\perp$. The crosses denote the quark-link vertices.

rectangular Wilson loop $Z_E(2L, b_\perp, \mu)$ with twice the length to cancel out all these divergences and guarantee the existence of the $L \to \infty$ limit after the subtraction. The introduction of $\sqrt{Z_E}$ also removes additional contributions from the transverse gauge link. An alternative approach to avoiding the pinch-pole singularity was proposed by Li (2016). We should mention that although the $\sqrt{Z_E}$ subtraction removes all the linear divergences, the logarithmic UV divergences are still present. Therefore, a nonperturbative renormalization of $\tilde{f}$ on the lattice is still required. It has been studied in the RI/MOM scheme (Shanahan, Wagman, and Zhao, 2019), and its matching to the $\overline{\rm MS}$ scheme has been calculated at one-loop order (Constantinou, Panagopoulos, and Spanoudes, 2019; Ebert, Stewart, and Zhao, 2020).

The previously defined quasi-TMDPDFs satisfy the following RGE (Collins and Soper, 1981; Ji, Sun *et al.*, 2015; Ji, Liu, and Liu, 2019):

$$\mu^2 \frac{d}{d\mu^2} \ln \tilde{f}(x, b_\perp, \mu, \zeta_z) = \gamma_F[\alpha_s(\mu)], \qquad (199)$$

where γ_F is the anomalous dimension for the heavy-to-light current in Sec. III.A. This is due to the fact that the quasi-TMDPDF, after the self-energy subtraction, contains only logarithmic UV divergences associated with quark-Wilson-line vertices. In the $\overline{\rm MS}$ scheme, the one-loop quasi-TMDPDF in an external quark state with momentum $(p^z, 0, 0, p^z)$ reads (Ebert, Stewart, and Zhao, 2019b; Ji *et al.*, 2019)

$$\tilde{f}(x, b_\perp, \mu, \zeta_z)$$
$$= \delta(1-x) + \frac{\alpha_s C_F}{2\pi} F(x, \epsilon_{\rm IR}, b_\perp, \mu)\theta(x)\theta(1-x) + \frac{\alpha_s C_F}{2\pi} \delta(1-x)$$
$$\times \left[-\tfrac{1}{2}L_b^2 + L_b(\tfrac{5}{2} - L_z) - \tfrac{3}{2} - \tfrac{1}{2}L_z^2 + L_z \right], \qquad (200)$$

where $L_z = \ln(\zeta_z/\mu^2)$. As expected, the L dependence has been canceled in the large-L limit.

As there is no lightlike gauge link in $\tilde{f}$, no additional rapidity regulator is needed. Instead, there is an explicit dependence on the hadron momentum (or energy), which is similar to the momentum RGE for collinear quasi-PDF. The momentum (rapidity) evolution equation for $\tilde{f}$ reads (Collins and Soper, 1981; Ji, Sun *et al.*, 2015; Ji, Liu, and Liu, 2019)

$$P^z \frac{d}{dP^z} \ln \tilde{f}(x, b_\perp, \mu, \zeta_z) = K(b_\perp, \mu) + \mathcal{G}\left(\frac{\zeta_z}{\mu^2}\right), \qquad (201)$$

where $\mathcal{G}(\zeta_z/\mu^2)$ is perturbative and $K(b_\perp, \mu)$ is the Collins-Soper kernel. A similar equation was proven for off-light-cone TMD-fragmentation functions by Collins and Soper (1981). From Eq. (201), it is clear that a correct matching to $f^{\rm TMD}(x, b_\perp, \mu, \zeta)$ with arbitrary ζ must include $K(b_\perp, \mu)$ to compensate for the P^z dependence.

There is actually one more requirement for the matching: there is a rapidity-scheme dependence that must be removed since the quasi-TMDPDF can be viewed as defined with an off-light-cone regulator along the z direction. To understand this dependence, we consider f again in the off-light-cone regularization, where there are rapidity divergences. The divergence is canceled out by the square root of an off-light-cone soft

function $S_{\rm DY}(b_\perp, \mu, Y, Y')$, with Y and Y' the rapidities of the off-light-cone spacelike vectors $p \to p_Y = p - e^{-2Y}(p^+)^2 n$ and $n \to n_{Y'} = n - e^{-2Y'} p/(p^+)^2$. Schematically, we have

$$S_{\rm DY}(b_\perp, \mu, Y, Y') = \frac{\text{tr}\langle 0|\mathcal{W}_{n_{Y'}}(\vec{b}_\perp)\mathcal{W}_{p_Y}^\dagger(\vec{b}_\perp)|0\rangle}{N_c \sqrt{Z_E}\sqrt{Z_E}}, \qquad (202)$$

where $\mathcal{W}_{n_{Y'}}(\vec{b}_\perp)$ and $\mathcal{W}_{p_Y}^\dagger(\vec{b}_\perp)$ are staple-shaped gauge links in the $n_{Y'}$ and p_Y directions, respectively. $\sqrt{Z_E}$ is introduced to subtract the pinch-pole singularities for the off-light-cone staple-shaped gauge links. In terms of $\ln \rho^2 = 2(Y + Y')$ sometimes we also write this soft function as $S_{\rm DY}(b_\perp, \mu, \rho)$. At large ρ, we have

$$S_{\rm DY}(b_\perp, \mu, Y, Y') = e^{(Y+Y')K(b_\perp,\mu) + \mathcal{D}(b_\perp,\mu)} + \cdots. \qquad (203)$$

We can perform a Lorentz boost of $\mathcal{W}_{n_{Y'}}(\vec{b}_\perp)\mathcal{W}_{p_Y}^\dagger(\vec{b}_\perp)$ in Eq. (202) such that one of the gauge links, say, $\mathcal{W}_{n_{Y'}}$, is boosted to the equal-time version $\mathcal{W}_z$ in $\tilde{f}$, whereas the other gauge link $\mathcal{W}_{n_Y}$ is boosted to $\mathcal{W}_{n_{Y+Y'}}$. The soft function becomes $S_{\rm DY}(b_\perp, \mu, Y + Y', 0)$, which contains a light-cone divergence for the $p_{Y+Y'}$ direction but is still the same $S_{\rm DY}(b_\perp, \mu, Y, Y')$ due to boost invariance. The square root of the finite part $e^{\mathcal{D}(b_\perp,\mu)}$ is exactly what is needed to cancel the rapidity-scheme dependence. We define the rapidity-independent part as the following reduced soft function:

$$S_r(b_\perp, \mu) \equiv e^{-\mathcal{D}(b_\perp,\mu)}. \qquad (204)$$

Based on the renormalization property of nonlightlike Wilson loops, the reduced soft function satisfies the RG equation

$$\mu^2 \frac{d}{d\mu^2} \ln S_r(b_\perp, \mu) = \Gamma_S(\alpha_s), \qquad (205)$$

where Γ_S is the constant part of the cusp anomalous dimension at large hyperbolic cusp angle $Y + Y'$ for the off-light-cone soft function

$$\mu^2 \frac{d}{d\mu^2} \ln S_{\rm DY}(b_\perp, \mu, Y, Y')$$
$$= -(Y + Y')\Gamma_{\rm cusp}(\alpha_s) - \Gamma_S(\alpha_s). \qquad (206)$$

At one-loop level (Ebert, Stewart, and Zhao, 2019b),

$$S_{\rm DY}^{(1)}(b_\perp, \mu, Y, Y') = \frac{\alpha_s C_F}{2\pi}[2 - 2(Y + Y')]L_b \qquad (207)$$

and $\Gamma_S^{(1)}(\alpha_s) = -\alpha_s C_F/\pi$. Based on RGE, at two-loop level $\mathcal{D}(b_\perp, \mu)$ can be predicted as

$$\mathcal{D}^{(2)}(b_\perp, \mu) = c_2 + \Gamma_S^{(2)} L_b - \frac{\alpha_s^2 \beta_0 C_F}{2\pi} L_b^2, \qquad (208)$$

where

$$\Gamma_S^{(2)} = -\frac{\alpha_s^2}{\pi^2}\left[C_F C_A\left(-\frac{49}{36} + \frac{\pi^2}{12} - \frac{\zeta_3}{2} \right) + C_F N_F \frac{5}{18} \right]$$

is the two-loop anomalous dimension for S_r, which can be extracted from Grozin *et al.* (2016), $\beta_0 = -[(11/3)C_A - (4/3)N_f T_F]/(2\pi)$ is the coefficient of the one-loop β function, and c_2 is a constant to be determined by explicit calculation.

After taking into account the reduced soft function, we can now write the following matching formula between the quasi-TMDPDF and the scheme-independent TMDPDF (Ji, Liu, and Liu, 2019):

$$
f^{\mathrm{TMD}}(x, b_\perp, \mu, \zeta)
$$
$$
= H\left(\frac{\zeta_z}{\mu^2}\right) e^{-\ln(\zeta_z/\zeta)K(b_\perp,\mu)} \tilde{f}(x, b_\perp, \mu, \zeta_z) S_r^{1/2}(b_\perp, \mu) + \cdots,
$$
$$(209)$$

where the power corrections of the order of $\mathcal{O}(\Lambda_{\mathrm{QCD}}^2/\zeta_z, M^2/(P^z)^2, 1/(b_\perp^2\zeta_z))$. Equation (209), except for the definition of $S_r(b_\perp, \mu)$, was argued to hold by Ebert, Stewart, and Zhao (2019b), where the unknown function g_q^S in their Eq. (5.3) should be identified as the reduced soft function here; this was also recently confirmed by Vladimirov and Schäfer (2020).

We now explain the individual factors of the formula.

(1) The factor $H(\zeta_z/\mu^2)$ is the perturbative matching kernel, which is a function of $\zeta_z/\mu^2 = (2xP^z)^2/\mu^2$. The kernel is responsible for the large logarithms of P^z generated by the $\mathcal{G}(\zeta_z/\mu^2)$ term of the momentum RG equation. Unlike the case of quasi-PDFs, the momentum fractions of the quasi-TMDPDF and the TMDPDF are the same. This is due to the fact that, at leading power in the $1/\zeta_z$ expansion, the $k_\perp$ integral is naturally cut off by the transverse separation around $k_\perp \sim 1/b_\perp \ll P^z$. Therefore, the momentum fraction can be modified only by collinear modes for which there is no distinction between $x = k^z/P^z$ and $x = k^+/P^+$. In comparison, for the $\vec{k}_\perp$-integrated quasi-PDF the $k_\perp \geq P^z$ region leads to nontrivial x dependence outside the physical region. This is also consistent with the fact that the momentum evolution equation for quasi-TMDPDF is local in x instead of being a convolution.

(2) The factor $\exp[\ln(\zeta_z/\zeta)K(b_\perp,\mu)]$ is the part involving the Collins-Soper evolution kernel. From the momentum evolution equation, it is clear that at large P^z there are logarithms of the form $K(b_\perp,\mu)\ln(\zeta_z/\mu^2)$, with ζ_z the natural Collins-Soper scale. Therefore, to match to the TMDPDF at arbitrary ζ, a factor $\exp[\ln(\zeta_z/\zeta)K(b_\perp,\mu)]$ is required to compensate for the difference. An implication of this property is that one can obtain the Collins-Soper kernel $K(b_\perp,\mu)$ by constructing the following ratio of quasi-TMDPDFs at two different momenta or ζ_z's (Ebert, Stewart, and Zhao, 2019a):

$$
\frac{\tilde{f}(x, b_\perp, \mu, \zeta_{z,1})}{\tilde{f}(x, b_\perp, \mu, \zeta_{z,2})} = \frac{H(\zeta_{z,2}/\mu^2)}{H(\zeta_{z,1}/\mu^2)}\left(\frac{\zeta_{z,1}}{\zeta_{z,2}}\right)^{K(b_\perp,\mu)}.
$$
$$(210)$$

Thus, given the $\tilde{f}$'s at the two rapidity scales the Collins-Soper kernel $K(b_\perp)$ can be obtained.

Combining the RGEs of the quasi-TMDPDF $\tilde{f}$, the reduced soft function S_r, and the physical TMDPDF f^{TMD}, we obtain the following RGE of the matching kernel $H(\zeta_z/\mu^2)$ (Ji, Liu, and Liu, 2019):

$$
\mu^2 \frac{d}{d\mu^2} \ln H^{-1}\left(\frac{\zeta_z}{\mu^2}\right) = \frac{1}{2}\Gamma_{\mathrm{cusp}}(\alpha_s) \ln \frac{\zeta_z}{\mu^2} + \frac{\gamma_C(\alpha_s)}{2}, \quad (211)
$$

where $\gamma_C(\alpha_s) = 2\gamma_F(\alpha_s) + \Gamma_S(\alpha_s) + 2\gamma_H(\alpha_s)$. The matching kernel is closely related to the perturbative part of the rapidity evolution kernel $\mathcal{G}(\zeta_z/\mu^2)$ through

$$
2\zeta_z \frac{d}{d\zeta_z} \ln H^{-1}\left(\frac{\zeta_z}{\mu^2}\right) = \mathcal{G}\left(\frac{\zeta_z}{\mu^2}\right).
$$
$$(212)$$

Again we can see that the anomalous dimension of $\mathcal{G}(\zeta_z/\mu^2)$ is $\Gamma_{\mathrm{cusp}}(\alpha_s)$.

It is convenient to write H in the exponential form $H = e^{-h}$. Collecting all the previous results, one obtains at one-loop level (Ebert, Stewart, and Zhao, 2019b; Ji *et al.*, 2019)

$$
h^{(1)}\left(\frac{\zeta_z}{\mu^2}\right) = \frac{\alpha_s C_F}{2\pi}\left(-2 + \frac{\pi^2}{12} - \frac{L_z^2}{2} + L_z\right). \quad (213)
$$

Similar as before, the two-loop contribution $h^{(2)}$ is predicted to be

$$
h^{(2)}\left(\frac{\zeta_z}{\mu^2}\right) = c_2' - \frac{1}{2}(\gamma_C^{(2)} - \alpha_s^2\beta_0 c_1) \ln \frac{\zeta_z}{\mu^2}
$$
$$
- \frac{1}{4}\left(\Gamma_{\mathrm{cusp}}^{(2)} - \frac{\alpha_s^2\beta_0 C_F}{2\pi}\right)\ln^2 \frac{\zeta_z}{\mu^2}
$$
$$
- \frac{\alpha_s^2\beta_0 C_F}{24\pi} \ln^3 \frac{\zeta_z}{\mu^2},
$$
$$(214)$$

where $c_1 = (C_F/2\pi)(-2 + \pi^2/12)$ and c_2' is again a constant to be determined in perturbation theory at two-loop level.

Finally, we compare the current formulation to previous approaches to lattice TMDPDF. First, we comment on the developments discussed by Hagler *et al.* (2009), Musch *et al.* (2011, 2012), Engelhardt *et al.* (2016), and Yoon *et al.* (2017), in which the x moments of the TMDPDF are extracted from the ratio of the quasi-TMDPDF. From Eq. (209), it is clear that both the matching kernel H and the exponential factor of the Collins-Soper kernel depends on x nontrivially. Therefore, simply taking the ratio of moments for quasi-TMDPDF will not be sufficient to reproduce the same ratio for TMDPDF, although the soft function does cancel. This observation was also made recently by Ebert *et al.* (2020). Second, the quasi-TMDPDF defined with the naive rectangle-shaped soft function, i.e., Z_E, is $\tilde{f}$ in Eq. (195), so it still needs the reduced soft function S_r to be matched to f^{TMD}. As for the other proposal made by Ji, Sun *et al.* (2015) and Ebert, Stewart, and Zhao (2019b), it replaces Z_E in $\tilde{f}$ with S_{bent}, which is the vacuum matrix element of a spacelike bent-shaped Wilson loop with angle $\pi/2$ at each junction, and does

not include the function $S_r^{1/2}$ in Eq. (209). Although $\sqrt{S_{\text{bent}}/Z_E}$ agrees with $S_r^{-1/2}$ at one-loop order (Ebert, Stewart, and Zhao, 2019b; Ji *et al.*, 2019), it is expected to be different at higher orders. In fact, for the anomalous dimension $\Gamma_{\pi/2}$ defined through

$$\Gamma_{\pi/2}(\alpha_s) \equiv \mu^2 \frac{d}{d\mu^2} \ln\left(\frac{S_{\text{bent}}(L, b_\perp, \mu)}{Z_E(2L, b_\perp, \mu)}\right), \qquad (215)$$

it starts to deviate from $\Gamma_S(\alpha_s)$ at two-loop order (Grozin *et al.*, 2016) as

$$-\Gamma_S(\alpha_s) = \frac{\alpha_s C_F}{\pi} + \frac{\alpha_s^2}{\pi^2}\left[C_F C_A\left(-\frac{49}{36} + \frac{\pi^2}{12} - \frac{\zeta_3}{2}\right) + C_F N_F \frac{5}{18}\right], \quad (216)$$

$$\Gamma_{\pi/2}(\alpha_s) = \frac{\alpha_s C_F}{\pi} + \frac{\alpha_s^2}{\pi^2}\left[C_F C_A\left(-\frac{49}{36} + \frac{\pi^2}{24}\right) + C_F N_F \frac{5}{18}\right]. \quad (217)$$

In Eq. (217), $\zeta_3 = \sum_{n=1}^\infty (1/n^3) \neq \pi^2/12$; therefore, the two anomalous dimensions are different. The differences in the anomalous dimension will result in different logarithmic behaviors in $b_\perp$, as the soft functions are dimensionless and depend on $b_\perp$ and μ only. At large $b_\perp$, it will lead to different IR physics that cannot be controlled by perturbation theory.

Combining the reduced soft function and the quasi-TMDPDF, one can effectively factorize the DY cross section as follows:

$$\sigma = \int dx_A dx_B d^2 b_\perp e^{i\vec{Q}_\perp \cdot \vec{b}_\perp} \hat{\sigma}(x_A, x_B, Q^2, \mu)$$
$$\times \tilde{f}(x_A, b_\perp, \mu, \zeta_A)\tilde{f}(x_B, b_\perp, \mu, \zeta_B) S_r(b_\perp, \mu), \qquad (218)$$

where all nonperturbative quantities do not involve the light cone and can be calculated on lattice.

Spin-dependent TMDPDFs are also physically important. They can be computed using LaMET theory (Ebert *et al.*, 2020). Again one can define quasidistributions just like the spin-independent ones. For a general proton target $|PS\rangle$ and the general spin structure Γ of the parton, the parent TMDPDF can be defined as

$$f_{[\Gamma]}^{\text{TMD}}(x, \vec{k}_\perp, \mu, \zeta)$$
$$= \frac{1}{2P^+} \int \frac{d\lambda}{2\pi} \int \frac{d^2\vec{b}_\perp}{(2\pi)^2} e^{-i\lambda x + i\vec{k}_\perp \cdot \vec{b}_\perp}$$
$$\times \lim_{\delta^- \to 0} \frac{\langle PS|\bar{\psi}(\lambda n + \vec{b}_\perp)\Gamma\mathcal{W}_n(\lambda n + \vec{b}_\perp)|_{\delta^-}\psi(0)|PS\rangle}{\sqrt{S(b_\perp, \mu, \delta^- e^{2y_n}, \delta^-)}}, \qquad (219)$$

where $\zeta = 2(P^+)^2 e^{2y_n}$ is the rapidity scale; see Sec. V for more details on the soft-function subtraction. The individual spin-dependent TMD distributions can then be obtained through Lorentz decompositions (Ralston and Soper, 1979;

Tangerman and Mulders, 1995; Mulders and Tangerman, 1996) as follows:

$$f_{[\gamma^+]}^{\text{TMD}} = f_1 - \frac{\epsilon^{ij} k^i S_\perp^j}{M} f_{1T}^\perp, \qquad (220)$$

$$f_{[\gamma^+\gamma_5]}^{\text{TMD}} = S^+ g_1 + \frac{\vec{k}_\perp \cdot \vec{S}_\perp}{M} g_{1T}, \qquad (221)$$

$$f_{[i\sigma^{i+}\gamma_5]}^{\text{TMD}} = S_\perp^i h_1 + \frac{(2k^i k^j - \vec{k}_\perp^2 \delta^{ij})S_\perp^j}{2M^2} h_{1T}^\perp$$
$$+ \frac{S^+ k^i}{M} h_{1L}^\perp + \frac{\epsilon^{ij} k^j}{M} h_1^\perp, \qquad (222)$$

where we suppress the arguments $(x, \vec{k}_\perp, \mu, \zeta)$ in all distributions; f_1, g_1, and h_1 are unpolarized, helicity, and transversity TMDPDFs, respectively; the indices i and j are in the transverse space of $\vec{k}_\perp$; S^+ and $S_\perp^i$ are longitudinal and transverse-spin components.

Note that the Sivers function $f_{1T}^\perp$ (Sivers, 1990) and the Boer-Mulders function $h_1^\perp$ (Boer and Mulders, 1998) are T odd. The orientation of the gauge link have important effects on these two functions (Collins, 2002, 2011a), such that they change sign between the DY and SIDIS processes. In the light-cone gauge, these contributions arise from the transversal gauge link at infinities (Belitsky, Ji, and Yuan, 2003). They are related to the phenomenologically interesting single transverse-spin asymmetry (Boer and Mulders, 1998; Collins *et al.*, 2005, 2006; Efremov *et al.*, 2005).

C. Off-light-cone soft function

The soft function was previously introduced to define rapidity-scheme-independent TMDPDFs. The major motivation of introducing the soft function is to capture nonperturbative effects due to soft-gluon radiation from fast-moving color charges. For many inclusive processes the soft radiations cancel out in the total cross section, but for certain processes where a small transverse momentum is measured such cancellation can be incomplete and result in measurable consequences. In such cases, the TMD soft function is introduced to account for the soft-gluon effects and appears in factorization theorems for the DY (Collins, Soper, and Sterman, 1985b, 1988) and SIDIS processes (Ji, Ma, and Yuan, 2004, 2005).

To calculate the TMD physics nonperturbatively, formulating a Euclidean version of the soft function is critical. Since the soft function is in fact a cross section and hence real and positive, it satisfies the necessary condition for a Monte Carlo simulation. In this section, we present an approach to calculate it in HQET (Ji, Liu, and Liu, 2020). There has also been another method proposed to extract the reduced soft function S_r from a light-meson form factor (Ji, Liu, and Liu, 2020), where many subtleties of HQET can be avoided. The first lattice calculation of the reduced soft function based on the light-meson formalism was performed recently by Q.-A. Zhang *et al.* (2020).

Because of the different space-time pictures of the DY and SIDIS processes, the soft functions for the two processes also

differ from each other, as shown in Fig. 10. To define the soft function, one also needs to specify a time-ordering prescription. Since it is a cross section, it involves a time order and an antitime order (or cut diagrams). However, in the light-cone limit the time order does not matter. What really matters is the rapidity regularization scheme. It was proven for the δ regulator of Vladimirov (2018) that the time ordering is not quite relevant up to overall phase factors, and the soft functions for the two processes are equal. The method therein can be modified to apply to the off-light-cone scheme too. Therefore, our first step is to convert the cut diagrams into Feynman diagrams by imposing just the single time order. In this way, the soft function can be viewed as a scattering amplitude.

In the off-light-cone scheme, there are further complications caused by the spacelike or timelike choices for off-light-cone vectors. One can show that in the light-cone limit the spacelike and timelike choices are equivalent up to overall phase factors (Ji, Liu, and Liu, 2021). Thus, we use the notation $S(b_\perp, \mu, Y, Y')$ to denote a generic off-light-cone soft function that satisfies our demands.

With these in mind, we show that the off-light-cone soft function $S(b_\perp, \mu, Y, Y')$ is equivalent to an equal-time form factor of fast-moving color sources and can be formulated on the Euclidean lattice. From the matching formula (209) in Sec. V.B, once the off-light-cone soft function is known we can combine it with the lattice calculated quasi-TMDPDF to obtain the physical TMDPDF. Therefore, the cross section of DY processes in the low-transverse-momentum region (Collins, Soper, and Sterman, 1985b) becomes predictable from first principles (Ji, Liu, and Liu, 2020).

To begin with, we define the scattering amplitude of a Wilson loop as shown in Fig. 12:

FIG. 12. The Wilson loop $\mathcal{W}$ showing a pairing of quark and antiquark scattering at $t = 0$.

$$W(t, t', b_\perp, Y, Y')$$
$$= \frac{1}{N_c}\mathrm{Tr}\langle 0|\mathcal{T}[\mathcal{W}_{v'}^\dagger(\vec{b}_\perp, t')\mathcal{W}_v(\vec{b}_\perp, t)]|0\rangle, \quad (223)$$

where $|0\rangle$ is the QCD vacuum state, N_c is the number of colors, and Tr is the color trace. Timelike four-vectors $v^\mu = \gamma(1, \beta, \vec{0}_\perp)$ and $v'^\mu = \gamma'(1, -\beta', \vec{0}_\perp)$ approach the light cone as β and $\beta' \to 1$. The rapidity Y and the speed β are related through $\beta = \tanh Y$ in terms of the light-cone vectors p and n, and the velocities read $v = (e^Y/\sqrt{2})(p/p^+ + e^{-2Y}p^+n)$ and $v' = (e^Y/\sqrt{2})[e^{-2Y}(p/p^+) + p^+n]$. $\mathcal{W}_v(\vec{b}_\perp, t)$ is a staple-shaped gauge link along v direction that is similar to those defined in Eqs. (173) and (196). t and t' are the lengths of the t components of the staples. The single time-order prescription for S allows physical interpretation as a chronological process. Like the quasi-TMDPDF, the Wilson loop in Eq. (223) contains pinch-pole singularities associated with time evolution of initial and final states at large t and t'. Therefore, we need to subtract them out in Eq. (223) with rectangular Wilson loops (Collins, 2008; Ji *et al.*, 2019). This leads to the following off-light-cone realization of the soft function:

$$S(b_\perp, \mu, Y, Y') = \lim_{\substack{t \to \infty \\ t' \to \infty}} \frac{W(t, t', b_\perp, \mu, Y, Y')}{\sqrt{Z(2t, b_\perp, \mu, Y)Z(2t', b_\perp, \mu, Y')}}, \quad (224)$$

where $Z(2t, b_\perp, Y)$ is the vacuum expectation value of the rectangular Wilson loop that is similar to W when one sets $v' = v$ and $t' = t$, i.e., $Z(2t, b_\perp, Y) = W(t, t, b_\perp, Y, -Y)$. The factor Z has a clear physical interpretation: It can be viewed as the wave-function renormalization for incoming or outgoing color sources. After the subtraction through Z, the only remaining UV divergences for $S(b_\perp, \mu, Y, Y')$ are the cusp divergences with hyperbolic angle $Y + Y'$.

A more common definition of the soft function $S_{\mathrm{DY}}(b_\perp, \mu, Y, Y')$ for the DY process was proposed by Collins (2011a, 2011b). The spacelike vectors $u^\mu = \gamma(\beta, 1, 0, 0)$ and $u'^\mu = \gamma'(-\beta', 1, 0, 0)$ were chosen instead of timelike vectors v and v' to define the soft function for the DY process. This soft function was defined in Sec. V.B in Eq. (202). u and u' are equal to p_Y and $n_{Y'}$ up to overall normalization factors.

While S and S_{DY} are defined differently, we can show that

$$S(b_\perp, \mu, Y, Y') = S_{\mathrm{DY}}(b_\perp, \mu, Y, Y') \quad (225)$$

using the analyticity property (Ji, Liu, and Liu, 2021). Here we focus on S in Eq. (224), which has a simple Euclidean realization.

After defining the soft function S, we now show that it is equal to a form factor. In HQET, the propagator of a color source is equivalent to a gauge link along its moving direction. Thus, $W(t, t', b_\perp, \mu, Y, Y')$ can be expressed by fields in HQET with the Lagrangian

$$\mathcal{L}_{\mathrm{HQET}} = Q_v^\dagger(x)(iv \cdot D)Q_v(x) + \bar{Q}_v^\dagger(x)(iv \cdot D)\bar{Q}_v(x), \quad (226)$$

where Q_v and $\bar{Q}_v$ are the quark and antiquark in the fundamental and antifundamental representations, respectively, $v^\mu = \gamma(1, \beta, \vec{0}_\perp)$ is the four-velocity, and D is the covariant derivative. Note that quarks in HQET can be viewed as color sources. If the gluon soft function is considered, the heavy quarks should be in the adjoint representation.

In HQET, a color-singlet heavy-quark pair separated by $\vec{b}$ generates a heavy-quark potential $V(|\vec{b}|)$ in the ground state, and the spectrum includes a gapped continuum above it. The state can also have a residual momentum $\delta\vec{P}$, which is arbitrary due to reparametrization invariance (Luke and Manohar, 1992; Manohar and Wise, 2000), and for simplicity we always consider $\delta\vec{P} = 0$. When the sources move with a velocity v, the ground state can be labeled by $|\bar{Q}Q, \vec{b}, \delta\vec{P}\rangle_v$, where the residue momentum $\delta\vec{P} = \vec{P}_{\text{total}} - 2m_Q \gamma \vec{\beta}$ is the difference between the total momentum $\vec{P}_{\text{total}}$ and the kinetic momentum of the heavy quarks. The residual energy of the state is $E = \gamma^{-1}V(|\vec{b}_\perp|) + \vec{\beta}\cdot\delta\vec{P}$.

Consider a process with incoming and outgoing states being heavy-quark pairs separated by $\vec{b}_\perp$ and at velocities v and v', respectively. Such a state is created by the interpolating fields

$$\mathcal{O}_v(t, \vec{b}_\perp) = \int d^3\vec{r}\, Q_v^\dagger(t, \vec{r})\mathcal{U}(\vec{r}, \vec{r}', t)\bar{Q}_v^\dagger(t, \vec{r}'), \quad (227)$$

where $\vec{r}' = \vec{r} + \vec{b}_\perp$ and $\mathcal{U}(\vec{r}, \vec{r}', t)$ is a gauge link connecting $\vec{r}'$ to $\vec{r}$ at time t. The heavy-quark pair created by $\mathcal{O}_v$ is forced to be at relative separation $\vec{b}_\perp$ and to have vanishing residual momentum $\delta\vec{P} = 0$. Between the incoming and outgoing states, a product of two local equal-time operators

$$J(v, v', \vec{b}_\perp) = \bar{Q}_{v'}^\dagger(\vec{b}_\perp)\bar{Q}_v(\vec{b}_\perp)Q_{v'}^\dagger(0)Q_v(0) \quad (228)$$

is inserted at $t = 0$. W can then be expressed in terms of HQET propagators that are gauge links in the v and v' directions. After integrating out the heavy-quark fields, we obtain up to an overall volume factor (Ji, Liu, and Liu, 2020)

$$W(t, t', b_\perp, \mu, Y, Y')$$
$$= \frac{1}{N_c}\langle 0|\mathcal{O}_{v'}^\dagger(t', \vec{b}_\perp)J(v, v', \vec{b}_\perp)\mathcal{O}_v(-t, \vec{b}_\perp)|0\rangle$$
$$\underset{t, t'\to\infty}{\longrightarrow} \frac{1}{N_c}\Phi^\dagger(b_\perp, \mu)S(b_\perp, \mu, Y, Y')\Phi(b_\perp, \mu)e^{-iE't'-iEt}, \quad (229)$$

where

$$\Phi(b_\perp, \mu) = \lim_{T\to\infty}{}_v\langle\bar{Q}Q, \vec{b}_\perp|\mathcal{O}_v(T, \vec{b}_\perp)|0\rangle,$$

$$S(b_\perp, \mu, Y, Y') = {}_{v'}\langle\bar{Q}Q, \vec{b}_\perp|J(v, v', \vec{b}_\perp)|\bar{Q}Q, \vec{b}_\perp\rangle_v. \quad (230)$$

In the last line of Eq. (229), we inserted a complete set of heavy-quark pair states before and after J. At large t and t', the contribution from the continuum spectrum is damped out due to the Riemann-Lebesgue lemma (Zuazo, 2001), while the contribution from $|\bar{Q}Q, \vec{b}_\perp, \delta\vec{P} = 0\rangle_v$ with residual energy $E = \gamma^{-1}V(|\vec{b}_\perp|)$ survives. As a result we obtain Eqs. (229)

and (230), where we have omitted the state label $\delta\vec{P} = 0$ for simplicity. Alternatively, we can also give t and t' a small negative imaginary part, which is consistent with the time order, to damp out all states except $|\bar{Q}Q, \vec{b}_\perp\rangle_v$ at large t and t'. Note that $\Phi(\vec{b}_\perp, \mu)$ is independent of Y because it is boost invariant.

Similarly, Z can be formulated in HQET as

$$Z(2t, b_\perp, Y) = \frac{1}{N_c}\langle 0|\mathcal{O}_{v'}^\dagger(t, \vec{b}_\perp)\mathcal{O}_v(-t, \vec{b}_\perp)|0\rangle$$
$$\underset{t\to\infty}{\longrightarrow} \frac{1}{N_c}\Phi^\dagger(\vec{b}_\perp, \mu)\Phi(\vec{b}_\perp, \mu)e^{-2iEt}, \quad (231)$$

whose t component has length $2t$. The Y dependence of Z is implicit in the energy E. Combining Eqs. (229) and (231), we obtain the S defined in Eq. (224). We emphasize that Eq. (224) can be seen as a Lehmann-Symanzik-Zimmermann reduction formula in which we amputate the external heavy-quark pair states $|\bar{Q}Q, \vec{b}_\perp\rangle_v$.

As an equal-time observable, $S(b_\perp, \mu, Y, Y')$ can be straightforwardly realized in Euclidean time as

$$S(b_\perp, \mu, Y, Y')$$
$$= \lim_{\substack{T\to\infty\\T'\to\infty}} \frac{W_E(T, T', b_\perp, \mu, Y, Y')}{\sqrt{Z_E(2T, b_\perp, \mu, Y)Z_E(2T', b_\perp, \mu, Y')}}, \quad (232)$$

where the subscript E indicates that the quantity is defined in Euclidean time, with corresponding variables T and T'. Because of boost invariance, the factor $Z_E(T, b_\perp, \mu, Y)$ relates to the rectangular Wilson loop defined in Eq. (198) along the n_z direction through the relation $Z_E(2T, b_\perp, \mu, Y) = Z_E(2\gamma^{-1}T, b_\perp, 0)$. The relevant matrix elements are now calculated using a lattice version of HQET with the Lagrangian (Aglietti, 1994; Hashimoto and Matsufuru, 1996; Horgan *et al.*, 2009)

$$\mathcal{L}_{\text{HQET}}^E = Q_v^\dagger(x)(i\tilde{v}\cdot D_E)Q_v(x) + \bar{Q}_v^\dagger(x)(i\tilde{v}\cdot D_E)\bar{Q}_v(x), \quad (233)$$

where the subscript E denotes the Euclidean space $i\tilde{v}\cdot D_E = \gamma(D^\tau - i\beta)D^z$, with $\tilde{v}^\mu = \gamma(-i, -\beta, \vec{0}_\perp)$. We have explicitly verified Eq. (232) in Euclidean perturbation theory to one-loop order.

The soft function cannot be calculated on the lattice by simply replacing the Minkowskian gauge links in Eq. (223) with a finite number of Euclidean gauge links. Through HQET, we find a time-independent formulation of the soft function, which creates the possibility of direct lattice calculations.

D. Light-front wave-function amplitudes and soft function from the meson form factor

The LFQ or light-front formalism is a natural language for parton physics in which partons are made manifest at all stages of the calculation. This favors a Hamiltonian approach to QCD as for a nonrelativistic quantum mechanical system, i.e., to diagonalize the Hamiltonian

$$\hat{P}^-|\Psi_n\rangle = \frac{M_n^2 + \vec{P}_\perp^{\ 2}}{2P^+}|\Psi_n\rangle, \qquad (234)$$

to obtain wave functions for the QCD bound states (Brodsky, Pauli, and Pinsky, 1998). The LFWFs thus obtained can, in principle, be used to calculate all the partonic densities and correlations functions. Moreover, like in condensed matter systems, knowing quantum many-body wave functions allows one to understand interesting aspects of quantum coherence and entanglement, as well as the fundamental nature of quantum systems. Therefore, a practical realization of the light-front quantization program would be a significant step forward in understanding the fundamental structure of the proton.

However, from a field theory point of view, wave functions are not the most natural objects to consider due to the nontrivial vacuum and UV divergences as well as the requirement of Lorentz symmetry, according to which the space and time should be placed on equal footing. The proton or other hadrons are excitations of the QCD vacuum, which by itself is complicated because of the well-known phenomena of chiral symmetry breaking and color confinement. To build a proton on top of this vacuum, one naturally wonders which part of the wave function reflects the property of the proton and which reflects the vacuum: It is the difference that yields the properties of the proton that are experimentally measurable. There is no clean way to make this separation unless one builds the proton out of elementary excitations or quasiparticles that do not exist in the vacuum, as is often done in condensed matter systems.

The partons in the IMF avoid the previously mentioned problems to a certain extent. In fact, owing to the kinematic effects, in the IMF all partons in the vacuum have longitudinal momentum $k^+ = 0$, and to some degree of accuracy the proton is made of partons with $k^+ \neq 0$. This natural separation of degrees of freedom (d.o.f.) is particularly welcome, making a wave-function description of the proton more natural and interesting in IMF than in any other frame.

To implement the previous d.o.f. separation, one possibility is to assume triviality of the light-front vacuum. The question as to what extent this holds has been continually debated over the years. One knows *a priori* that in relativistic QFT the vacuum state is boost invariant and frame independent. In fact, Nakanishi and Yabuki (1977) and Nakanishi and Yamawaki (1977) proved that not only can the vacuum not be trivial, even the Green's functions of the full theory cannot pose generic meaningful restrictions to the null planes $\xi^+ = c$. In fact, the vacuum zero modes do contain nontrivial dynamics and contribute to the properties of the proton (Ji, 2020). Nevertheless, one can adopt an effective theory point of view to simply cut off the zero modes and relegate their physics to renormalization constants. In some simple cases, these zero modes can be treated explicitly (Heinzl, Krusche, and Warner, 1991; Yamawaki, 1998).

By imposing an IR cutoff on the $k^+ \geq \epsilon$ in the effective Hilbert space, all physics below $k^+ = \epsilon$ are taken into account through renormalization constants. We then obtain the following effective LF theory with trivial vacuum:

$$a_{k\lambda}|0\rangle = b_{p\sigma}|0\rangle = d_{p\sigma}|0\rangle = 0, \qquad (235)$$

where $|0\rangle$ is the vacuum of LFQ. Therefore, the proton can be expanded as follows in terms of the superposition of Fock states in the LF gauge $A^+ = 0$ (Brodsky, Pauli, and Pinsky, 1998):

$$|P\rangle = \sum_{n=1}^{\infty} \int d\Gamma_n \psi_n^0(x_i, \vec{k}_{i\perp}) \prod a_i^\dagger(x_i, \vec{k}_{i\perp})|0\rangle, \qquad (236)$$

where $a^\dagger$ are generic quarks and gluon quanta on the light front and the phase-space integral reads $d\Gamma_n = \prod dk^+ d^2 k_\perp / 2k^+ (2\pi)^3$. $\psi_n(x_i, \vec{k}_{i\perp})$ are LFWF amplitudes or simply wave front (WF) amplitudes, where x_i denotes the set of momentum fractions from x_1 to x_n. It is a complete set of nonperturbative quantities that describe the partonic landscape of the proton. These amplitudes can in principle be calculated through Hamiltonian diagonalization. However, as explained in Sec. II.A, a direct systematic solution in LFQ is impractical.

LaMET offers an alternate route to calculate these WF amplitudes. Thanks to the triviality of the vacuum after the truncation $k^+ \geq \epsilon$, they can then be written in terms of the invariant matrix elements by inverting Eq. (236) as

$$\psi_n^0(x_i, \vec{k}_{i\perp}) = \langle 0| \prod a_i(x_i, \vec{k}_{i\perp})|P\rangle. \qquad (237)$$

After properly restoring gauge invariance and imposing regularizations, they become the matrix elements of light-cone correlators, the same type as those in the TMDPDFs. Therefore, the LaMET method applies to them, which allows one to effectively obtain the results of light-front quantization through instant quantization in a large-momentum frame.

To realize the goal, the LFWF amplitudes also need a rapidity renormalization, as in the case of TMDPDFs. In this section, we explain how the reduced soft function S_r can be obtained by combining the LFWF amplitudes and a special light-meson form factor, instead of as the form factor in HQET discussed in Sec. V.C. A lattice calculation based on the light-meson framework was performed by Q.-A. Zhang *et al.* (2020).

We now consider the following form factor of a pseudo-scalar light-meson state with constituents $\bar{\psi}\eta$:

$$F(b_\perp, P, P', \mu) = \langle P'|\bar{\eta}(\vec{b}_\perp)\Gamma'\eta(\vec{b}_\perp)\bar{\psi}(0)\Gamma\psi(0)|P\rangle, \qquad (238)$$

where ψ and η are light-quark fields of different flavors, $P^\mu = (P^t, 0, 0, P^z)$ and $P'^\mu = (P^t, 0, 0, -P^z)$ are two large momenta that approach two opposite lightlike directions in the limit $P^z \to \infty$, and Γ and Γ' are Dirac gamma matrices, which can be chosen as $\Gamma = \Gamma' = 1$, γ_5, or $\gamma_\perp$ and $\gamma_\perp \gamma_5$, so that the quark fields have leading components on the respective light cones.

At large momentum, the form factor factorizes through TMD factorization into LFWF amplitudes. To motivate the factorization, we need to consider the leading region of IR divergences in a similar way for SIDIS and Drell-Yan processes (Ji, Ma, and Yuan, 2005; Collins, 2011b); the result is shown in Fig. 13. There are two collinear subdiagrams responsible for collinear modes in the positive and negative
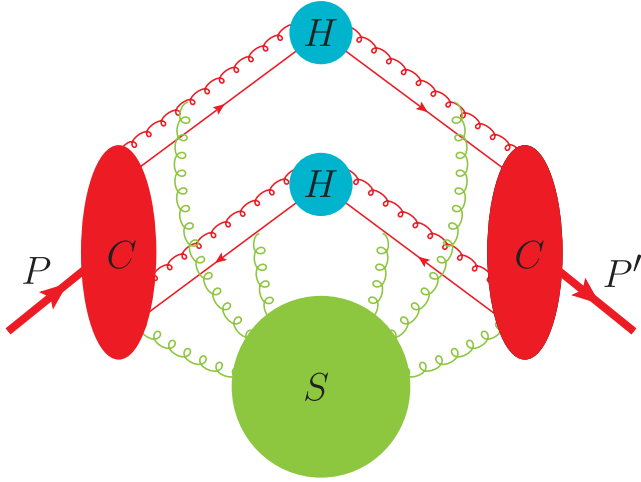
FIG. 13. The reduced diagram for the large-momentum form factor F of a meson. Two H denote the two hard cores separated in space by $\vec{b}_\perp$ and C are collinear subdiagrams and S denotes the soft subdiagram.

directions and a soft subdiagram responsible for soft contributions. In addition, there are two IR-free hard cores localized around $(0,0,0,0)$ and $(0,\vec{b}_\perp,0)$. In the covariant gauge, there are arbitrary numbers of longitudinally polarized collinear and soft gluons that can connect to the hard and collinear subdiagrams. Based on the region decomposition, we now follow the standard procedure to change the factorization into LF quantities (Collins, 2011b).

We first factorize the soft divergences. This can be done with the soft function $S(b_\perp,\mu,\delta^+,\delta^-)$. It resums the soft-gluon radiation from fast-moving color charges. Intuitively, soft gluons have no impact on the velocity of the fast-moving color-charged partons, and the propagators of the partons eikonalize to straight gauge links along their moving trajectory.

We then factorize the collinear divergences. For the incoming direction, the collinear divergence is captured as follows by the LFWF amplitude for the incoming parton $\psi_{\bar{q}q}(x,b_\perp,\mu,\delta'^-)$ defined with future-pointing gauge links:

$$\psi_{\bar{q}q}(x,b_\perp,\mu,\delta'^-) = \int \frac{d\lambda}{4\pi} e^{-ix\lambda} \langle 0|\bar{\psi}(\lambda n/2 + \vec{b}_\perp)\gamma^+ \mathcal{W}_n(\lambda n/2 + \vec{b}_\perp)|_{\delta'^-}\psi(-\lambda n/2)|P\rangle, \quad (239)$$

where the staple-shaped gauge link W_n is defined similar to that in Eq. (166), with the only exception being that the gauge links W_n should point to $+\infty$ instead of $-\infty$.

However, the naive LFWF amplitude contains soft divergences as well. To avoid double counting, we must subtract out the soft contribution from the bared collinear WF amplitude with the soft function $S(b_\perp,\mu,\delta^+,\delta^-)$. This leads to the following collinear function for the incoming direction: $\psi_{\bar{q}q}(x,b_\perp,\mu,\delta'^-)/S(b_\perp,\mu,\delta^+,\delta'^-)$. Similarly, for the outgoing direction one obtains the collinear function $\psi_{\bar{q}q}^\dagger(x',b_\perp,\mu,\delta'^+)/S(b_\perp,\mu,\delta'^+,\delta^-)$.

Here we comment on the choices for the gauge-link directions in the soft functions and the WF amplitudes. Naively, the gauge links along the p direction have to be past pointing. However, as in the arguments given by Collins and Metz (2004) for the SIDIS process, based on the space-time picture of collinear divergences one can chose future-pointing gauge links along the p direction as well. With all the gauge links future pointing, the soft function is equal to S, which is manifestly real, and the WF amplitudes for the incoming and outgoing hadrons are in complex conjugation with each other.

In addition to the collinear and soft functions, we still need the hard kernel $H_F(Q^2,\bar{Q}^2,\mu^2)$, where $Q^2 = xx'P\cdot P'$, $\bar{Q}^2 = \bar{x}\bar{x}'P\cdot P'$, and an integral over the momentum fractions x and x' is assumed. When these are taken together, we obtain the following TMD factorization of the form factor into hard, collinear, and soft functions:

$$F(b_\perp,P,P',\mu) = \int dx\,dx'\,H_F(Q^2,\bar{Q}^2,\mu^2)$$
$$\times \left[\frac{\psi_{\bar{q}q}^\dagger(x',b_\perp,\mu,\delta'^+)}{S(b_\perp,\mu,\delta'^+,\delta^-)}\right]\left[\frac{\psi_{\bar{q}q}(x,b_\perp,\mu,\delta'^-)}{S(b_\perp,\mu,\delta^+,\delta'^-)}\right]$$
$$\times S(b_\perp,\mu,\delta^+,\delta^-). \quad (240)$$

All the rapidity regulators in all the WF amplitudes and the soft functions are canceled out.

We now consider a one-loop example. The incoming hadron state consists of a free quark with momentum $x_0 P^+$ and a free antiquark with momentum $\bar{x}_0 P^+$. Similarly the outgoing state consists of a pairing of a free quark and an antiquark with momenta $x_0' P'^-$ and $\bar{x}_0' P'^-$, respectively. The spin projection operator for the incoming state is proportional to $\gamma^5\gamma^-$ and for the outgoing state is proportional to $\gamma^5\gamma^+$. The tree-level form factor is normalized to 1. At one-loop level, the pseudoscalar form factor with vector currents $\Gamma = \gamma^\mu$ and $\Gamma' = \gamma_\mu$, where a summation over μ is assumed, reads

$$F(b_\perp,P,P',\mu) = 1 + \frac{\alpha_s C_F}{2\pi} F^{(1)}(b_\perp,Q^2,\bar{Q}^2,\mu^2), \quad (241)$$

where $Q^2 = 2x_0 x_0' P^+ P'^-$, $\bar{Q}^2 = 2\bar{x}_0 \bar{x}_0' P^+ P'^-$, and

$$F^{(1)}(b_\perp,Q^2,\bar{Q}^2,\mu^2)$$
$$= -7 + [-\tfrac{1}{2}\ln^2 b_\perp^2 Q^2 + \tfrac{3}{2}\ln b_\perp^2 Q^2 + (Q\to\bar{Q})]. \quad (242)$$

This result can be obtained from the one-loop DY structure function (D'Alesio *et al.*, 2014) using the substitutions $\ln^2(-Q^2 b_\perp^2) \to (1/2)\ln^2 Q^2 b_\perp^2 + (1/2)\ln^2 \bar{Q}^2 b_\perp^2$ and $\ln(-Q^2 b_\perp^2) \to (1/2)\ln Q^2 b_\perp^2 + (1/2)\ln \bar{Q}^2 b_\perp^2$. As in the TMD factorization for SIDIS and DY processes, one should notice that the hard kernel $H_F(Q^2,\bar{Q}^2,\mu^2)$ can be obtained from that of the spacelike Sudakov form factor as follows:

$$H_F(Q^2,\bar{Q}^2,\mu^2) = H^{\text{Sud}}(-Q^2)H^{\text{Sud}}(-\bar{Q}^2), \quad (243)$$

where $H^{\text{Sud}}(-Q^2)$ is as given by Collins and Rogers (2017). At one-loop level, we then obtain

$$H_F(Q^2, \bar{Q}^2, \mu^2) = 1 + \frac{\alpha_s}{4\pi}\left(-16 + \frac{\pi^2}{3} + 3L_Q + 3L_{\bar{Q}} - L_Q^2 - L_{\bar{Q}}^2\right), \tag{244}$$

where $L_Q = \ln(Q^2/\mu^2)$ and $L_{\bar{Q}} = \bar{Q}^2/\mu^2$.

We now construct the Euclidean version of the factorization in terms of the quasi-WF amplitudes, the reduced soft function, and the hard contribution. The quasi-WF amplitudes are defined as in Eq. (195):

$$\tilde{\psi}_{\bar{q}q}(x, b_\perp, \mu, \zeta_z) = \int \frac{d\xi^z}{4\pi} e^{ix\xi^z P^z} \frac{\langle 0|\bar{\psi}(\xi^z n_z/2 + \vec{b}_\perp)\gamma^z \mathcal{W}_z(\xi^z n_z/2 + \vec{b}_\perp; L)\psi(-\xi^z n_z/2)|P\rangle}{Z_E(2L, b_\perp, \mu)}, \tag{245}$$

in which the staple-shaped gauge link $\mathcal{W}_z$ is as defined in Eq. (196). The gauge links should point in the $+z$ direction in accordance to the $+\infty$ choice on the light-cone side.

The factorization to the LFWF amplitude follows reasoning similar to that of the quasi-TMDPDFs presented earlier. Alternatively, we can factorize it as follows using quantities defined in the on-light-cone rapidity scheme:

$$\tilde{\psi}_{\bar{q}q}(x, b_\perp, \mu, \zeta_z) = H_1^+(\zeta_z/\mu^2, \bar{\zeta}_z/\mu^2)$$
$$\times \left[\frac{\psi_{\bar{q}q}(x, b_\perp, \mu, \delta^-)}{S(b_\perp, \mu, \delta^+, \delta^-)}\right] S(b_\perp, \mu, \delta^+). \tag{246}$$

Equation (246) is the result of applying a similar leading-region analysis to the quasi-WF amplitude. $\psi_{\bar{q}q}(x, b_\perp, \mu, \delta^-)/S(b_\perp, \mu, \delta^+, \delta^-)$ resums all the collinear divergences, while the soft function $S(b_\perp, \mu, \delta^+)$ contains an off-light-cone direction along n_z. It resums the soft divergences of the quasi-WF amplitude. The soft functions $S(b_\perp, \mu, \delta^+, \delta^-)$ and $S(b_\perp, \mu, \delta^+)$ subtract away the regulator dependencies introduced in the bare LFWF amplitude. The overall combination in the right-hand side of Eq. (246) is rapidity scheme independent. As in the case of the form factor, we can choose all the gauge links along the incoming collinear direction to be future pointing.

Combining Eqs. (240) and (246) and using the relation $\zeta\zeta' = \zeta_z\zeta_z'$, one obtains the form factor factorization

$$F(b_\perp, P, P', \mu)$$
$$= \int dx dx' H(x, x')\tilde{\psi}_{\bar{q}q}^\dagger(x', b_\perp)\tilde{\psi}_{\bar{q}q}(x, b_\perp)S_r(b_\perp, \mu), \tag{247}$$

where we have kept only the $x, b_\perp$ dependencies of the WF amplitudes, with other variables omitted, and the hard kernel H is given by

$$H(x, x') = H(\zeta_z, \zeta_z', \bar{\zeta}_z, \bar{\zeta}_z', \mu^2)$$
$$= \frac{H_F(Q^2, \bar{Q}^2, \mu^2)}{H_1^+(\zeta_z/\mu^2, \bar{\zeta}_z/\mu^2)H_1^+(\zeta_z'/\mu^2, \bar{\zeta}_z'/\mu^2)}, \tag{248}$$

where $Q^2 = \sqrt{\zeta_z\zeta_z'}$ and $\bar{Q}^2 = \sqrt{\bar{\zeta}_z\bar{\zeta}_z'}$. And the reduced soft function is

$$S_r(b_\perp, \mu) = \lim_{\delta^+, \delta^- \to 0} \frac{S(b_\perp, \mu, \delta^+, \delta^-)}{S(b_\perp, \mu, \delta^+)S(b_\perp, \mu, \delta^-)}. \tag{249}$$

It can be shown based on the properties of off-light-cone soft functions that the S_r defined here agrees with the one defined in Eq. (204).

Therefore, with nonperturbative quantities F and ψ^+, we obtain the reduced soft function

$$S_r(b_\perp, \mu) = \frac{F(b_\perp, P, P', \mu)}{\int dx dx' H(x, x')\tilde{\psi}_{\bar{q}q}^\dagger(x', b_\perp)\tilde{\psi}_{\bar{q}q}(x, b_\perp)}, \tag{250}$$

where H can be obtained perturbatively.

Based on the one-loop results for the form factor, the quasi-WF amplitudes and the reduced soft function, the one-loop matching kernel for the vector current can be extracted as

$$H(\zeta_z, \zeta_z', \bar{\zeta}_z, \bar{\zeta}_z', \mu^2)$$
$$= 1 + \frac{\alpha_s C_F}{2} i \ln \frac{\sqrt{\zeta_z \bar{\zeta}_z}}{\sqrt{\zeta_z' \bar{\zeta}_z'}}$$
$$+ \frac{\alpha_s C_F}{4\pi}\left(-8 + \ln^2 \frac{\sqrt{\zeta_z}}{\sqrt{\zeta_z'}} + \ln \frac{\sqrt{\zeta_z \zeta_z'}}{\mu^2} + (\zeta \to \bar{\zeta})\right), \tag{251}$$

and the renormalization group equation for H reads

$$\mu^2 \frac{d}{d\mu^2} \ln H(\zeta_z, \zeta_z', \bar{\zeta}_z, \bar{\zeta}_z', \mu^2) = -2\gamma_F(\alpha_s) - \Gamma_S(\alpha_s), \tag{252}$$

where γ_F and Γ_S are as previously defined.

Here we comment on the end-point behavior. As $x \sim 0$, the hard kernel diverges logarithmically near the end point as $1 + \alpha_s \ln^2 x$, but the quasi-WF amplitudes approach zero at large or small x linearly; thus, the end-point regions behave as $x \ln^2 x$, which is free from those problems for the k_T factorization for electromagnetic form factor (Li and Sterman, 1992). Moreover, we can fix the z-component momentum transfer at each of the vertices to be P^z, which indicates that $x + x' = 1$. In this case the end-point behavior is improved to $x^2 \ln^2 x$.

VI. LATTICE PARTON PHYSICS WITH LaMET

Lattice gauge theory simulates continuum QCD in imaginary time on a discretized 4D Euclidean lattice. The method is characterized by the finite lattice spacing a and volume $L_1 \times L_2 \times L_3 \times T$, as well as input parameters such as the strong coupling and quark masses. To calculate physical quantities, one usually expects to take the continuum ($a \to 0$) and infinite volume ($L_i, T \to \infty$) limits and tune the quark masses so that observables such as the pion mass m_π

agrees with the physical value of ∼140 MeV. There are different methods for implementing the fermions on the lattice (Rothe, 1992) that lead to different properties of the lattice action such as chiral symmetry breaking for Wilson fermions. In the lattice calculation of hadron matrix elements, the initial and final states are generated by acting the source and sink interpolation operators on the vacuum, and the ground-state contributions are filtered out by propagating over a sufficiently large Euclidean time. A boosted hadron state can be obtained by inserting momentum into the source and sink operators through a Fourier transform in the 3D spatial coordinates.

The lattice QCD calculations of parton physics using LaMET started with exploratory studies on the simplest PDFs and the gluon helicity (Alexandrou *et al.*, 2015; Lin *et al.*, 2015; Yang *et al.*, 2017) that yielded fairly encouraging results, demonstrating that LaMET is a viable approach. In subsequent studies, more attention has been paid to the systematics, including establishing a proper renormalization and matching procedure, simulating at the physical pion mass, removing the excited-state contamination, etc. Such studies have greatly improved the precision of the calculations, with the latest results exhibiting reasonable agreement with phenomenological PDFs (Alexandrou *et al.*, 2018a, 2018b; Lin, Chen *et al.*, 2018; Izubuchi *et al.*, 2019; Gao *et al.*, 2020). In the meantime, explorations have also been made on similar large-momentum data using coordinate-space factorization methods including the pseudo-PDF (Orginos *et al.*, 2017; Joó *et al.*, 2019a, 2019b, 2020) and current-current correlation (Bali *et al.*, 2019; Sufian *et al.*, 2019, 2020). Nevertheless, dedicated large-scale efforts with state-of-art resources have not yet been made. Lattice parton physics with LaMET is at its dawn. With EIC in the United States going forward, a new era of lattice calculations is to come.

In this section, we summarize the current status of lattice calculations using LaMET and discuss future prospects. We begin with a general discussion on the kind of lattice setups that are best suited for LaMET calculations, then summarize the relevant lattice techniques that facilitate such calculations. After that we review the lattice calculations that have been carried out thus far and point out future potential improvements. A complementary discussion about lattice calculations was conducted by Cichy and Constantinou (2019). Other reviews that summarize recent developments in the lattice calculation of PDFs were given by Monahan (2018a), Zhao (2020), and Constantinou (2021).

A. Special considerations for lattice calculations

In this section, we discuss the challenges for lattice calculations in LaMET and estimate the required lattice requirements while taking collinear PDFs as an example.

1. Challenges due to large momentum

In addition to common challenges with other lattice calculations, such as taking the continuum and infinite volume limits, simulating at or extrapolating to the physical pion mass, etc., LaMET applications require the generation of a large-momentum hadron on the lattice. For the LaMET expansion, $1/xP^z$ is the expansion parameter, and for the

coordinate-space factorizations large quasi-light-cone distance λ requires an even larger hadron momentum. However, this realization leads to a number of practical challenges. First, it was difficult to generate large-momentum hadron states on the lattice until the technique of momentum smearing (Bali *et al.*, 2016) was proposed. The conventional smearing method in coordinate space is designed to increase the overlap with a ground-state hadron at rest. Thus, it is not surprising that such a smearing is not efficient when the hadron has a large momentum. The momentum smearing technique introduces an extra phase factor $e^{i\vec{k}\cdot\vec{z}}$ to the quark field, such that it peaks at the nonzero momentum $\vec{k}$ in Fourier space, as shown in Fig. 14. In this way, the overlap with the high-momentum state is vastly increased after Euclidean time evolution. Recently the momentum smearing technique was incorporated into the framework of distillation (Egerer *et al.*, 2020) to improve the extraction of ground-state energy and matrix elements at momentum ≲3 GeV. Although there have been other proposed methods to generate large momentum (Wu *et al.*, 2018), momentum smearing has become a standard technique in LaMET applications.

Second, the proton size is frame dependent and changes with its momentum. In the proton's rest frame, simulating its structure requires the lattice spacing to be much smaller than the QCD confinement scale, i.e., $a \ll \Lambda_{QCD}^{-1}$. When the proton is moving fast, it undergoes Lorentz contraction by a boost factor γ in the momentum direction; thus, a finer lattice spacing $a \ll (\gamma\Lambda_{QCD})^{-1}$ is needed. If $a \leq 0.2$ fm is the minimum requirement to investigate a static proton, one will need at least $a \leq 0.04$ fm to have the same resolution for a proton at 5 GeV. A smaller lattice spacing is difficult to achieve with current computing resources, as it suffers from the well-known critical slowing down problem; i.e., the autocorrelation times of observables such as the topological
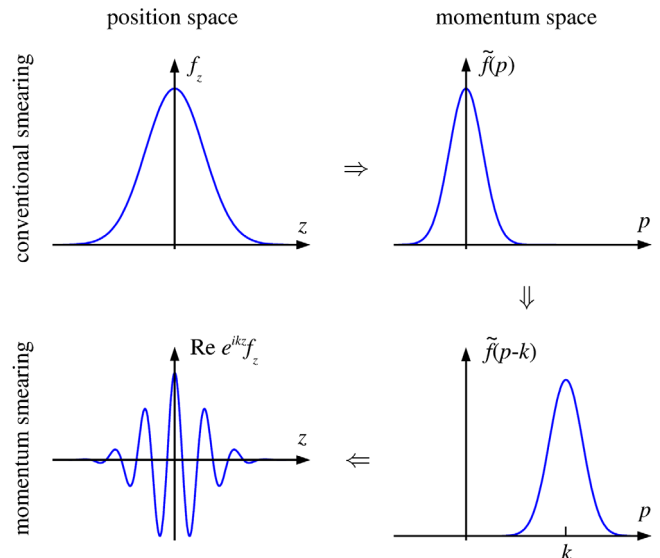

FIG. 14. Conventional smearing (top panels) vs momentum smearing (bottom panels) (Bali *et al.*, 2016). Conventional smearing has a small overlap with the high-momentum state. Momentum smearing shifts the momentum to its peak at the nonzero value in momentum space.

charge increase when approaching the continuum limit (Schaefer, Sommer, and Virotta, 2011), which can be much longer than the Monte Carlo simulation times. A lattice with the open (Neumann) boundary condition on gauge fields in the Euclidean time direction (Luscher and Schaefer, 2011), which allows topological charge to flow in and out at boundaries of time, may overcome this problem.

Third, the gaps between the ground-state and excited-state energies become smaller because of the time dilation effect. In the proton's rest frame, the excited-state contamination exponentially decays with the mass gap ΔM and evolution time τ in the form of $e^{-\Delta M \tau}$. In the boosted frame, the mass gap ΔM in the decay factor is replaced by the energy gap $\Delta E \sim \Delta M / \gamma$, and the decay changes as $e^{-\Delta M \tau} \to e^{-\Delta E \tau} = e^{-\Delta M \tau / \gamma}$ under Euclidean time evolution. Therefore, with a boosted state, a longer time evolution (source-sink separation) is needed. For example, if a source-sink separation of 1 fm is needed to separate the excited state of the proton with 2 GeV momentum, a proton with 5 GeV momentum will require a source-sink separation of 2.5 fm. Even if the two-state fit technique is used, a longer time evolution is still required so that only the ground and first excited states dominate.

Last, the lattice calculation requires $P^z \ll 1/a$ so that the discretization effects of $\mathcal{O}((aP^z)^n)$ are under control. Therefore, one has to use smaller lattice spacing in order to reach larger momentum. The quantification of $\mathcal{O}((aP^z)^n)$ effects alone in LaMET calculations has not been done, as all discretization errors are treated on equal footing in continuum extrapolation.

To summarize, to achieve a precise calculation of the boosted hadron structure on the lattice, a fine lattice spacing (at least in the longitudinal direction) and a large box size in the time direction are essential, which also requires one to have control of the signal-to-noise ratio at large Euclidean times.

2. Considerations for lattice setup

In practical calculations, a correlation function is first obtained on lattice in coordinate space, and then Fourier transformed to momentum space with the phase factor $e^{i\lambda x}$, where $\lambda = zP^z$. Therefore, the smallest x that one can reach can be estimated from the largest λ as $x \sim 1/\lambda$. However, a more stringent constraint comes from requiring the higher-twist contribution $\mathcal{O}(\Lambda_{\mathrm{QCD}}^2/(xP^z)^2)$ to be small so that the factorization is still valid, which implies $x \gg \Lambda_{\mathrm{QCD}}/P^z$. This also provides an estimate for the largest attainable x ($x \ll 1 - \Lambda_{\mathrm{QCD}}/P^z$) since the momentum fraction carried by other partons is $\sim (1 - x)$, which should be bounded from below by the previous estimate.

For the current state-of-the-art simulations, the lattice spacing can reach 0.04 fm (Fan *et al.*, 2020; Gao *et al.*, 2020), which implies $P_{\mathrm{max}}^z \sim 5$ GeV, and the effective resolution in the longitudinal direction is $\gamma a \sim 0.2$ fm. Thus, the valid x region that can be extracted from the lattice is roughly 0.1 to 0.9. On the other hand, to avoid finite volume effects, it is believed that $m_\pi L \gtrsim 4$. For the physical pion mass, the box size in the spatial direction L should be at least 6 fm, which means that the box size is 150 lattice spacings. Thus far the largest box size in LaMET calculations has been 5.8 fm (Lin, Chen *et al.*, 2018). As discussed in Sec. VI.A.1, a source-sink

separation of 2.5 fm is needed for $P^z = 5$ GeV. Therefore, the box size in the time direction T does not particularly need to be longer than L, and $T = L$ is sufficient in this lattice setup. In summary, with $a = 0.04$ fm at the physical pion mass one needs an $L^3 \times T = 150^3 \times 150$ lattice to reliably extract a $0.1 < x < 0.9$ region, which could be possible on an exascale computer.

There are potential tricks for reducing the computational cost. First, the required source-sink separation can be shorter if one uses a multistate instead of a two-state fit with enough statistics. However, since the number of fitting parameters in an n-state fit grows as n^2, such a fitting becomes infeasible for too large n. Second, note that the resolution required for transverse proton structures is not affected by the Lorentz boost, and one may use a coarse lattice in the transverse direction ($a_\perp = 0.1$ fm). The required box size is then $L_\parallel \times L_\perp^2 \times T = 150 \times 60^2 \times 150$. This asymmetric lattice can greatly reduce the resources needed for large momentum since the transverse box size is fixed. However, generating configurations and renormalization on such a lattice might bring new problems and should be further studied.

In the near future, exascale supercomputers may help us to reach higher momentum, as large as 5 GeV for the proton, and improve the precision of LaMET calculations. Further theoretical developments and new ideas on the technique and algorithms are also needed to overcome the simulation difficulties.

B. Nonsinglet PDFs

In this section, we review the current status of lattice calculations of flavor nonsinglet (isovector) PDFs in the proton and pion. The nonsinglet case has an advantage in that the mixing with gluons as well as the lattice calculation of disconnected diagrams can be avoided, thus greatly reducing the computational challenge. This is the most extensively studied parton observable with LaMET thus far.

1. Proton

Pioneering lattice studies for the isovector quark PDF in the proton were carried out by Alexandrou *et al.* (2015) and Lin *et al.* (2015). These were proof-of-principle studies, as the renormalization of quasi-PDFs was not well understood at the time. Nevertheless, their results encouraged the follow-up theoretical works on LaMET, including a proper renormalization and a matching suitable for lattice implementation.

Certain lattice artifacts have also been studied. For example, although there is no power-divergent mixing for the quasi-PDF operators on the lattice, additional operator mixings that are not seen in the continuum can still occur if a nonchiral lattice fermion such as the Wilson-type fermion is used. Constantinou and Panagopoulos (2017) and Chen *et al.* (2019) showed that at $\mathcal{O}(a^0)$ the operator for the unpolarized quark quasi-PDF $O_{\gamma^z}(z)$ can mix with the scalar operator $O_{\mathbf{1}}(z)$, whereas $O_{\gamma^t}(z)$ does not. To reduce the systematic uncertainty from such a mixing, $\Gamma = \gamma^t$ has been used since then for lattice calculations of the unpolarized quark PDF (Alexandrou, Cichy *et al.*, 2017; Chen *et al.*, 2018; Green, Jansen, and Steffens, 2018). Similarly, for helicity and transversity cases
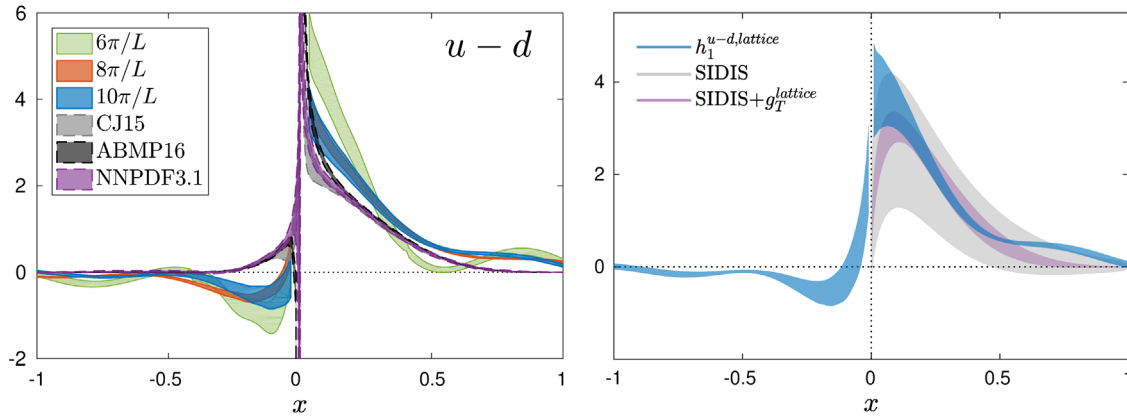
FIG. 15.   Proton isovector quark PDF (Alexandrou *et al.*, 2018a, 2018b). The unpolarized PDF with P^z from 0.82 to 1.4 GeV and the transversity PDF with $P^z = 1.4$ GeV are in left and right panels, respectively. CJ15 (Accardi, Brady *et al.*, 2016), ABMP16 (Alekhin *et al.*, 2017), and NNPDF3.1 (Ball *et al.*, 2017) are global fits. SIDIS is a global fit and SIDIS + g_T^{lattice} is global fit with a lattice constraint on tensor charge g_T^{lattice} (Lin, Melnitchouk *et al.*, 2018).

one should choose $\Gamma = \gamma^5 \gamma^z$ and $\Gamma = i\sigma^{z\perp} = \gamma^\perp \gamma^z$, respectively, in order to avoid the mixing. Note that at $\mathcal{O}(a)$ all $\tilde{O}_\Gamma(z)$'s can mix with others (Chen *et al.*, 2019). Nevertheless, a fine lattice spacing can reduce these effects.

Alexandrou, Cichy *et al.* (2017), Chen *et al.* (2018), and Green, Jansen, and Steffens (2018) studied the nonperturbative renormalization (NPR) of the quasi-PDFs in the RI/MOM scheme (Martinelli *et al.*, 1995). This scheme has several advantages: The lattice regularization scheme can be converted to the $\overline{\text{MS}}$ scheme through the RI/MOM renormalization condition, the computation cost is affordable, the systematic errors can be reduced or quantified more easily, etc. Work before 2018 did not include NPR and the systematics were not accurately quantified. More recent work has implemented the RI/MOM scheme and the corresponding perturbative matching (Constantinou and Panagopoulos, 2017; Stewart and Zhao, 2018; Liu *et al.*, 2020). The coordinate-space method was also developed in parallel by Orginos *et al.* (2017), Cichy, Debbio, and Giani (2019), Joó *et al.* (2019a, 2020), and Bhat *et al.* (2020). In Figs. 15 and 16, we select some of the most recent lattice results. The European Twisted Mass Collaboration (ETMC) published the proton unpolarized, helicity, and transversity PDFs with $P^z = 1.4$ GeV at the physical pion mass (Alexandrou *et al.*, 2018a, 2018b), and the LP^3 Collaboration published the proton helicity PDF with the unprecedented momentum $P^z = 3.0$ GeV at the physical pion mass (Lin, Chen *et al.*, 2018). Recently calculations on fine lattices (Alexandrou, Cichy, Constantinou, Green *et al.*, 2020; Fan *et al.*, 2020) and an extrapolation to the continuum limit (Alexandrou, Cichy, Constantinou, Green *et al.*, 2020) have become available. The finite volume effects, which were first studied in a model by Briceño *et al.* (2018), were investigated on the lattice recently by Lin and Zhang (2019), where no sizable volume dependence was observed at $P^z = 1.3$ and 2.6 GeV.

The PDFs extracted from LaMET can be useful for phenomenology by providing input in kinematic regions that are difficult to measure in experiments. This has attracted attention from the global fit community (Lin *et al.*, 2018; Hobbs *et al.*, 2019; Bringewatt *et al.*, 2020; Constantinou

et al., 2020). For example, it has been found that in the large-x region of unpolarized PDF the lattice result will lead to a significant improvement on the global fit result if it reaches an accuracy of about 10% (Lin *et al.*, 2018). It is now also possible to investigate the sea quark asymmetry (Geesaman and Reimer, 2019) directly on the lattice. For the transversity PDF, due to the difficulty of measurement in experiment, lattice results can have an impact on improving the global fit and even prediction making. In addition to the isovector cases, calculations of the strange and charm unpolarized distributions (Zhang, Lin, and Yoon, 2020), as well as the flavor separation of light quarks in the helicity PDF (Alexandrou, Constantinou *et al.*, 2020), have been carried out recently. From early exploratory results showing the qualitative behavior of PDFs to the latest results, which are comparable to global fits, we have come a long way in developing new techniques (momentum smearing, renormalization, matching, etc.) and the computation resources have steadily increased over time. Systematic uncertainties in the lattice calculation of PDFs have been thoroughly investigated by the ETMC
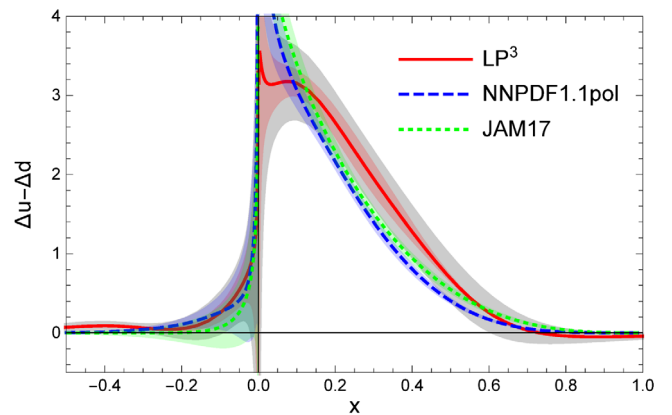

FIG. 16.   Proton isovector quark helicity PDF ($P^z = 3.0$ GeV) (Lin, Chen *et al.*, 2018) with a red band for the statistical error and a gray band for the statistical and systematic errors. NNPDF1.1pol (Nocera *et al.*, 2014) and JAM17 (Ethier, Sato, and Melnitchouk, 2017) are global fits.

(Alexandrou, Cichy *et al.*, 2019). Further studies on systematics such as the discretization effects and finite volume effects on various lattice ensembles are still necessary. In the future, lattice QCD is expected to make a significant impact on nucleon structure.

To conclude this section, we mention that there are also lattice studies of the isovector PDF of other baryons, Δ^+ to be specific, using LaMET (Chai *et al.*, 2020).

2. Pion

The pion valence quark distribution has been extracted from various Drell-Yan data for pion-nucleon and pion-nucleus scattering, while theoretical predictions do not yield results consistent with the experimental extraction, especially in the large-x region (Holt and Roberts, 2010). LaMET calculations will shed valuable light on how to resolve this disagreement, provided that all systematics are well under control.

In principle, calculating the pion valence PDF is easier than the proton PDF. First, the pion state is easier to produce and the quark contractions are fewer. Second, the energy gap between the first excited state and the ground state of the pion is much larger than the energy gap of the proton. Therefore, the excited-state contamination is easier to control. The simulation was first performed by Zhang, Chen *et al.* (2019) with the same lattice setup and procedure used in exploratory studies of the proton PDF. A more thorough study on the pion valence quark PDF was done by the lattice QCD group of BNL (Izubuchi *et al.*, 2019). Note that the excited-state contamination was thoroughly studied using multistate fits, with the ground and first excited states both agreeing with the expected dispersion relations, indicating that the excited contamination is well under control. The comparison of the lattice results from the quasi-PDF, pseudo-PDF, and current-current correlator approaches are shown in Fig. 17. Note that the LP^3 result (Zhang, Chen *et al.*, 2019) was obtained using a Fourier transformation and inversion of the factorization formula, while the other three groups used parametrization models to fit the lattice data. More dedicated effort is needed
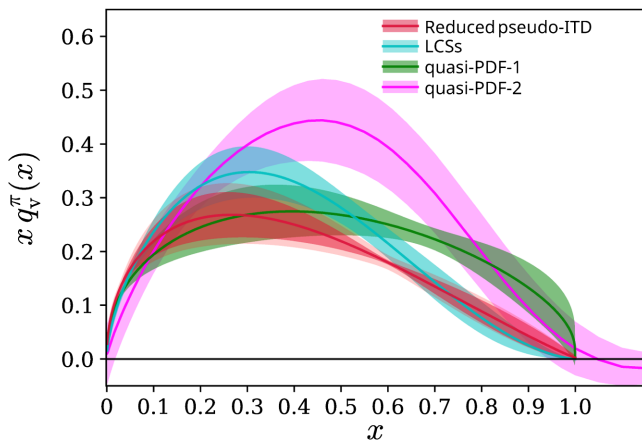
to reduce the errors, and a meaningful comparison between different operators and analysis methods should be made.

For other mesons, we mention that there is a study of the kaon valence quark PDF using MIMD Lattice Computation Collaboration configurations (Lin *et al.*, 2020).

C. Gluon helicity and other collinear-parton properties

In this section, we summarize the applications of LaMET to other collinear-parton observables, including the gluon helicity, the gluon PDFs, meson DAs, and GPDs.

1. Total gluon helicity

The total gluon helicity ΔG is a key component to understanding the proton spin structure. It has been intensively explored at RHIC and will be pursued at EIC in the future. However, a theoretical lattice calculation of ΔG was not possible until the proposal of LaMET.

The first such effort was made by the χQCD Collaboration (Yang *et al.*, 2017). The calculation was carried out with valence overlap fermions on $2+1$ flavor domain-wall fermion gauge configurations, using ensembles with multiple lattice spacings and volumes including one with physical pion mass. Yang *et al.* (2017) simulated proton matrix elements of the free-field operator $(\vec{E} \times \vec{A})^3$ in the Coulomb gauge at various momenta, then converted them to the $\overline{\text{MS}}$ scheme with one-loop lattice perturbation theory. The $\overline{\text{MS}}$ matrix elements at each lattice momentum are shown in Fig. 18. Although a LaMET matching is necessary to match the results to the physical gluon helicity, Yang *et al.* (2017) did not apply it due to concerns of perturbative convergence of the matching coefficient (Ji, Zhang, and Zhao, 2015). Instead, as the $\overline{\text{MS}}$ matrix elements showed mild momentum dependence up to the maximum momentum ~ 1.5 GeV, they extrapolated the results to infinite momentum, as well as physical pion mass and continuum limits, with a model motivated by chiral EFT. Their final result was $\Delta G(\mu^2 = 10 \text{ GeV}^2) = 0.251(47)(16)$, or 50%(9%)(3%) of the total proton spin, which agrees with
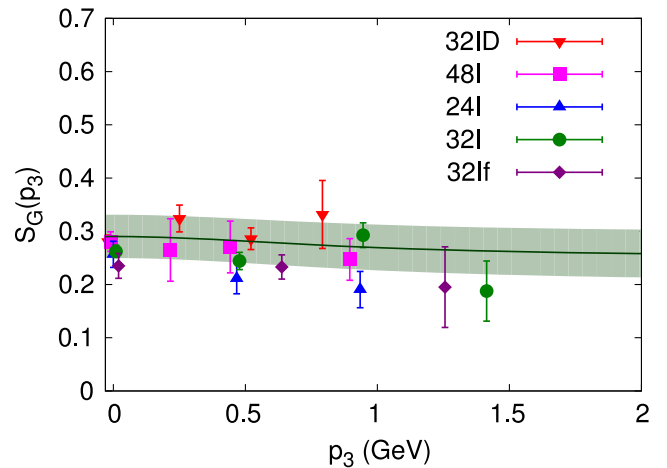

FIG. 17. Pion valence quark PDFs in various approaches. Compare the results of pesudo-PDF [reduced pseudo-ITD (Joó *et al.*, 2019b)], quasi-PDF [quasi-PDF-1 (Izubuchi *et al.*, 2019) and quasi-PDF-2 (Zhang, Chen *et al.*, 2019)], and the current-current correlator approach [LCSs (Sufian *et al.*, 2019)].

FIG. 18. Total gluon helicity. The results are extrapolated to the physical pion mass and continuum as a function of the proton momentum p_3 on all five ensembles and indicated by different colors for the data points. From Yang *et al.*, 2017.

the truncated moment of $\Delta g(x)$ (de Florian *et al.*, 2014; Nocera *et al.*, 2014) within uncertainties.

Despite such progress, one should be cautious and acknowledge that this calculation still needs further improvement in the future. Among others, the most important required improvements are simulations at larger proton momentum, performance of an NPR, and investigation of the perturbative convergence of LaMET matching and its implementation.

2. Gluon PDF

The gluon PDF is of great interest not only for precise physics at LHC but also for understanding the gluonic structure of the proton and nuclei, as well as the small-x dynamics, at the future EIC. With the recent progress on the renormalization and matching of gluon quasi-PDFs (Wang and Zhao, 2018; Wang, Zhao, and Zhu, 2018; Li, Ma, and Qiu, 2019; Wang, Zhang *et al.*, 2019; Zhang, Ji *et al.*, 2019) and coordinate-space "pseudodistributions" (Balitsky, Morris, and Radyushkin, 2019), a systematic lattice calculation of the gluon PDFs can be carried out in principle.

Before the previously mentioned theoretical developments, an exploratory lattice study of the proton and pion unpolarized gluon PDFs was carried out by Fan *et al.* (2018). They calculated quasigluon LF correlations and compared them to the LF correlations for the gluon PDFs. Later, based on the multiplicative renormalizability of a certain choice of the quasigluon LF correlator (Zhang, Ji *et al.*, 2019), Fan *et al.* used the ratio scheme (Balitsky, Morris, and Radyushkin, 2019) in coordinate space to renormalize the lattice matrix elements and fitted the proton unpolarized gluon PDF with a simple two-parameter model (Fan, Zhang, and Lin, 2021). Although the results show agreement with the global analyses in the large-x region, the systematics from the model dependence of the fit remains to be quantified for a controlled calculation of the gluon PDF.

3. DA

According to Sec. IV.B, LaMET can be readily applied to calculating DAs, and the lattice resource needed is expected to be cheaper than that for PDFs since there is one fewer external state, which reduces the number of contractions for the quark propagators. Thus far there have been a few exploratory investigations on meson DAs, in particular, on pion (Zhang *et al.*, 2017) and kaon DAs (Zhang, Jin *et al.*, 2019). The lattice calculations of pion (Zhang *et al.*, 2017) and kaon DAs (Zhang, Jin *et al.*, 2019) were first explored without the NPR and the corresponding matching. Recently the pion and kaon DAs from the RI/MOM scheme analysis were extrapolated to the continuum limit by R. Zhang *et al.* (2020), who eventually adopted a two-parameter model to fit the final result. The results are shown in Fig. 19. Apart from LaMET, the current-current correlation methods (Detmold and Lin, 2006; Braun and Müller, 2008; Braun *et al.*, 2015) have also reflected much progress on the pion DA (Bali *et al.*, 2019; Detmold *et al.*, 2018, 2020).

4. GPD

As discussed in Sec. IV, the global fitting of GPDs still faces challenges from their complicated kinematic dependence and
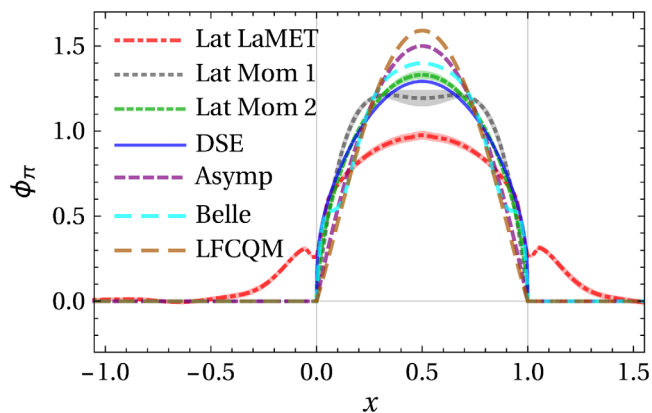
FIG. 19. Pion DA (Zhang, Jin *et al.*, 2019). Comparison of ϕ_π (Lat LaMET) to previous determinations in the literature. Lat Mom 1 and 2 are parametrized fits to the lattice moments (Braun *et al.*, 2015); DSE represents Dyson-Schwinger equation calculations (Chang *et al.*, 2013); Asymp is the asymptotic form $6x(1-x)$; Belle is a fit to the Belle data (Agaev *et al.*, 2012); LFCQM is the light-front constituent quark model (de Melo, Ahmed, and Tsushima, 2016).

limited information from the experimental observables despite the progress made (Favart *et al.*, 2016; Kumericki, Liuti, and Moutarde, 2016). On the other hand, the previously mentioned lattice QCD method is able to calculate only the lowest few moments of the GPDs (Hagler, 2010), which is far from sufficient for reconstructing their full kinematic dependence. Applying LaMET to GPD calculations will provide important information on the GPDs, especially in kinematic regions that are not accessible in currently available experiments. In addition, on the lattice one can study the GPD dependence on one kinematic variable by fixing the others. All these will help differentiate commonly used models in GPD parametrization.

Calculating quasi-GPDs requires more resources than calculating quasi-PDFs but does not need further techniques in principle. In addition, the lattice renormalization factors for the quasi-PDFs can be used here, as argued in Sec. IV. The first lattice calculation of the pion unpolarized isovector quark GPD was carried out by Chen, Lin, and Zhang (2019), although the results cannot yet be used to differentiate among models or make a comparison to experiments. Recently ETMC completed the first proof-of-principle calculation of the proton unpolarized and helicity GPDs (Alexandrou, Cichy, Constantinou, Hadjiyiannakou *et al.*, 2020), as shown in Fig. 20, which demonstrates that it is feasible to extract the GPDs with controlled systematics on available computational resources.

5. Higher-twist PDFs

The higher-twist PDFs probe multiparton correlations, and their contribution at $x = 0$, can shed light on the LF zero modes (Ji, 2020). As we discussed in Sec. IV, such distributions can also be calculated on the lattice with the LaMET approach.

The first attempt to calculate the isovector twist-3 PDF $g_T(x)$ was carried out by ETMC (Bhattacharya *et al.*, 2020a) using the one-loop matching coefficient that they computed in
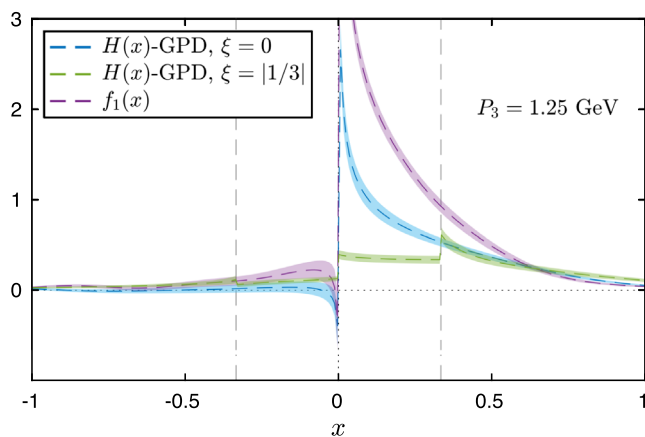
FIG. 20. Proton unpolarized isovector quark GPD $H(x, \xi, t)$ for $t = -0.69$ GeV^2 extracted from quasi-GPDs at $P_3 = 1.25$ GeV, which is compared to the unpolarized PDF $f_1(x)$. From Alexandrou, Cichy, Constantinou, Hadjiyiannakou *et al.*, 2020.

Bhattacharya *et al.* (2020b, 2020c). Their results show agreement with the Wandzura-Wilczeck approximation (Wandzura and Wilczek, 1977), which ignores the contribution from dynamical twist-3 contributions, and the Burkhardt-Cottingham sum rule (Burkhardt and Cottingham, 1970). Nevertheless, the mixing between $g_T(x)$ and other twist-3 distributions was not considered, and further study is still required for an accurate matching to the light-cone PDF.

D. TMDs

With tremendous experimental focus on the TMDPDFs for studying 3D proton structures and gluon saturation at EIC, their first-principle calculation from lattice QCD will significantly boost this direction by providing useful nonperturbative inputs for all the phenomenological analyses.

In this section, we discuss the status and prospects of calculating the quasi-TMDPDF and the soft function with LaMET. In addition, we note that before LaMET there had already been efforts to extract information of TMDs by studying ratios of the lattice correlators (Hagler *et al.*, 2009; Musch *et al.*, 2011, 2012; Engelhardt *et al.*, 2016; Yoon *et al.*, 2017), which has resulted in substantial progress in the past decade. We begin with a review of the lattice correlators.

1. Pre-LaMET study: The ratio of lattice correlators

By employing Lorentz covariance, the x moments of TMDPDFs are related to the form factors of spacelike staple-shaped gauge-link operators, which can be directly simulated on the lattice. Although the lattice calculation of the soft function was not available during that time, ratios of the spin-dependent and unpolarized matrix elements were formed to cancel it, thus providing useful information on different TMDPDFs. For example, the time-reversal odd TMDPDFs can be studied with the staple-shaped gauge-link operator in a transversely polarized proton state, thus helping us to understand properties related to single-spin asymmetry, which was

measured experimentally at STAR (Adamczyk *et al.*, 2016) and COMPASS (Aghasyan *et al.*, 2017). Musch *et al.* (2012) and Engelhardt *et al.* (2016) studied the Sivers and Boer-Mulders functions of proton and pion. Other time-reversal-even functions, such as the worm-gear function g_{1T} (Tangerman and Mulders, 1995), were also studied (Yoon *et al.*, 2017).

2. Quasi-TMDPDF and Collins-Soper kernel

The lattice calculation of the quasi-TMDPDF defined in Eq. (195) is straightforward. The matrix element of the staple-shaped quark-Wilson-line operator can be simulated the same way as the quasi-PDF case, except that the geometry of the gauge link is different, while the calculation of the Wilson loop Z_E is standard practice in lattice QCD. The more challenging part, however, is the renormalization of the quasi-TMDPDF and its matching to the $\overline{\text{MS}}$ scheme.

Using the auxiliary field theory formalism, one can argue that the staple-shaped quark-Wilson-line operator is also multiplicatively renormalizable (Ebert, Stewart, and Zhao, 2020; Green, Jansen, and Steffens, 2020). On a nonchiral lattice, it suffers from finite mixing with other quark bilinear operators, as was predicted by one-loop lattice perturbation theory (Constantinou, Panagopoulos, and Spanoudes, 2019). The full mixing pattern for such operators with different Dirac matrices have been studied in the RI/MOM scheme on three quenched lattice ensembles with different spacings (Shanahan, Wagman, and Zhao, 2019), and a diagonalization of the mixing matrix is adopted to renormalize these operators. Meanwhile, the one-loop conversion factors that convert the RI/MOM matrix elements to the $\overline{\text{MS}}$ scheme have been calculated in continuum perturbation theory for both the $z = 0$ (Constantinou, Panagopoulos, and Spanoudes, 2019) and $z \neq 0$ (Ebert, Stewart, and Zhao, 2020) cases.

Although the soft function is still needed to fully determine the physical TMDPDF, the $\overline{\text{MS}}$ quasi-TMDPDF can already be used to extract the Collins-Soper kernel according to Eq. (210) (Ebert, Stewart, and Zhao, 2019a, 2019b; Ji, Sun *et al.*, 2015). Since the Collins-Soper kernel can be defined from both the bare TMDPDF and the soft function, it is independent of the external state and can be calculated in a pion, which is the least expensive on the lattice. Up to the mass corrections suppressed by the momentum in Eq. (209), this calculation also allows one to use an unphysical valence pion mass as long as the sea quark masses are physical.

With the method developed by Ebert, Stewart, and Zhao (2019a), the first exploratory lattice calculation of the Collins-Soper kernel was performed by Shanahan, Wagman, and Zhao (2020) on a quenched lattice with the heavy valence pion mass $m_\pi \sim 1.2$ GeV, and the result is shown in Fig. 21. As one can see, the lattice prediction is robust for $0.1 < b_\perp < 0.8$ fm, which covers the nonperturbative region that is important for TMD evolution in global analyses. In addition, at small $b_\perp$ the perturbative calculation can serve as a calibration for estimating the systematic uncertainties, as there are power corrections of $\mathcal{O}(1/(P^z b_\perp))$ that can be reduced only with larger P^z. Q.-A. Zhang *et al.* (2020) also extracted the Collins-Soper kernel from a pion quasi-TMD DA, where the lattice
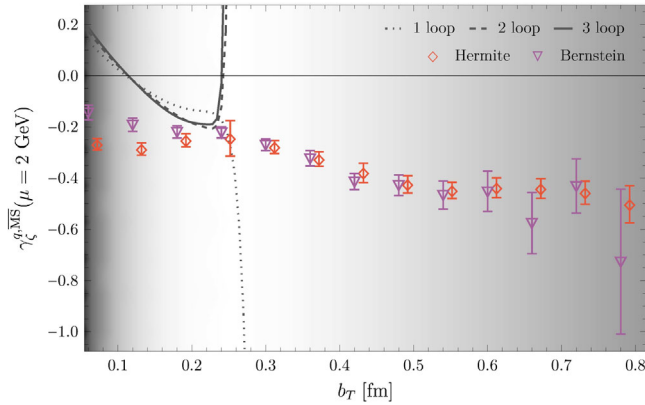
FIG. 21. Collins-Soper kernel from the first exploratory calculation on a quenched lattice (Vladimirov and Schäfer, 2020). The results are obtained by using fits to the $\overline{\text{MS}}$ unsubtracted quasi-TMDPDFs with Hermite and Bernstein polynomial bases. The solid and dashed lines are the perturbative predictions (Li and Zhu, 2017; Vladimirov, 2018), which hit the Landau pole near $b_\perp \sim 0.25$ fm. The background shading density is proportional to a naive estimate of the power corrections $1/(b_\perp P^z) + b_\perp/L$.

FIG. 22. Reduced soft factor as a function of $b_\perp$ extracted from the light-meson form factor in Sec. V (Q.-A. Zhang *et al.*, 2020). The results were obtained with quasi-TMD DAs at different pion momenta P^z, with perturbative matching and power corrections ignored. The dashed line is the one-loop prediction in perturbation theory, which hits the Landau pole at $b_\perp \sim 0.3$ fm, and the gray band is the error that results when μ is varied by a factor of $1/\sqrt{2}$ and $\sqrt{2}$.

renormalization was left out. The result is in agreement with Shanahan, Wagman, and Zhao (2020) within errors for a wide range of $b_\perp$. With improved lattice ensembles and systematic corrections in the future, it is promising that there will be a precise determination of the Collins-Soper kernel for TMD phenomenology.

3. Soft function

As the remaining piece toward physical TMDPDFs, the soft function must be calculated in lattice QCD. In particular, the reduced soft function in Eq. (204) eliminates the regulator-scheme dependence of the off-the-light-cone quasi-TMDPDF, so its calculation alone has great physical significance. According to Secs. V.C and V.D, two methods have been proposed to calculate the off-the-light-cone soft function or reduced soft function on the lattice (Ji, Liu, and Liu, 2020), as we discuss in the following. One relies on simulating HQET on the lattice, while the other requires calculating a light-meson form factor of transversely separated current products.

The latter method has been implemented in the first exploratory lattice calculation of the reduced soft function (Q.-A. Zhang *et al.*, 2020), which includes simulations of the pion form factor in two external states with opposite large momenta, as well as the pion quasi-TMD DA. The results for the reduced soft function, which were obtained with tree-level matching and omission of lattice renormalization, are shown in Fig. 22. As one can see, the results agree with the perturbative prediction for small $b_\perp$ within errors, as expected, and start to deviate when $b_\perp$ becomes large. Since the quasi-TMD DA depends on the momentum P^z, the stability of results at different P^z suggests the validity of Eq. (250). In the future, larger statistics and improved systematics in both lattice and perturbative matching will be necessary to achieve a precise calculation of this quantity.

VII. CONCLUSION AND OUTLOOK

Since Feynman proposed the parton model more than 50 years ago, our understanding of the partonic structure of the proton has been greatly advanced. On the one hand, a number of high-energy experiments carried out at facilities worldwide including SLAC, DESY, CERN, Fermi Lab, JLab, and BNL have allowed us to probe various aspects of hadronic structures at different energies and polarizations. On the other hand, many parton observables have been proposed in parallel that provide a multidimensional description of the proton structure, including the collinear PDFs, TMDPDFs, GPDs, parton DAs, and LFWFs.

Although QCD factorization theorems with RG improvement allow us to extract these parton observables through their connection to experimental observables, it is desirable to predict them from *ab initio* calculations such as lattice QCD. Developments along these lines have been slow due to difficulties in simulating real-time dynamics. The situation, however, has changed since the proposal of LaMET a few years ago, which provides a systematically improvable method to calculate parton physics from first principles.

In this review, we give an overview of the LaMET formalism and its applications to observables, which can be accessed using lattice QCD and other nonperturbative methods. By investigating the frame dependence of the structure of bound-state hadrons, we explain how the IMF physics or parton physics naturally arises as an EFT description of the proton structure. Such an EFT description is most naturally formulated in SCET and LFQ, but practical nonperturbative calculations of the proton matrix elements have been difficult. LaMET in effect provides what is needed to realize LFQ. This is achieved by forming appropriate quasiparton observables in a large-momentum state and matching them to the true parton observables on the LF through factorization. In the case of PDFs, the former corresponds to finite-momentum distributions whose running is controlled by the momentum RGE,

whereas the latter corresponds to IMF PDFs whose running is controlled by the usual RGE. We point out that LaMET is a general framework that can be applied to large-momentum physical quantities calculated with any nonperturbative methods, either Euclidean (with imaginary time) or Minkowskian (with real time). Moreover, given a large-momentum state, the same parton physics can be determined from different quasiobservables that form a universality class.

We then present how to calculate the parton observables in practice, with a particular focus on the collinear PDFs, GPDs, DAs, TMDPDFs, and LFWFs. We also discuss the proton spin structure and show how the partonic contributions to proton spin can be obtained by following the same approach. We finally summarize the lattice studies carried out thus far with LaMET which, on the one hand, demonstrate that LaMET is a promising approach for computing partonic structures of the proton and, on the other hand, indicate that many improvements are still required to reach a level of accuracy such that the lattice results can have a considerable impact on phenomenology.

We complete this review with a few comments on improvements of lattice calculations for the future. See Alexandrou, Cichy *et al.* (2019) for additional systematic discussion of some of the issues, such as the continuum, the infinite volume, and physical pion mass limits.

- *Large hadron momentum.*—Since the future of LaMET lies in larger momenta, which naturally require smaller lattice spacings, it will be critical to address the challenges of using large momenta and small spacings for exascale computations, such as the excited-state contamination or topological charge freezing problem.

- *Renormalization.*—As discussed in Sec. III.D, the mass renormalization of Wilson-line operators is favored, as it is gauge invariant and does not introduce extra higher-twist effects or large statistical errors at long distance. However, its matching to the $\overline{\text{MS}}$ scheme, especially the renormalon ambiguities, still needs to be resolved for a full systematic application. Moreover, alternative schemes that include the previously mentioned features are also desirable.

- *Higher-order perturbative matching.*—In current LaMET calculations, one-loop perturbative matching has brought considerable corrections. Higher-order matching kernels will be necessary to control the systematics from this procedure.

- *Power corrections.*—These are important if the hadron momentum is not large or if x is close to 0 or 1. Scant progress has been made toward a model-independent determination of power corrections thus far. One contingent strategy is to extrapolate to the $P^z \to \infty$ limit after implementing matching and target-mass corrections, but the ultimate solution relies on the lattice calculation of higher-twist distributions that was discussed in Sec. IV.C.

The previous discussion of systematics is generic and applies to all quasiobservables. The rich theoretical developments in recent years have paved the way for calculating a wide range of parton observables using LaMET. With the rapid increase in computing resources and progress in developing new techniques and algorithms, we expect to see these

systematics kept under control step by step in the future. That would be important for establishing LaMET as a systematic approach to computing parton physics, and for making lattice calculations play a crucial role in the EIC era.

LIST OF SYMBOLS AND ABBREVIATIONS

Here we list some acronyms, abbreviations, and terminologies used throughout this review.

AM	angular momentum
BRST	Becchi-Rouet-Stora-Tyutin
DA	distribution amplitude
DGLAP	Dokshizer-Gribov-Lipatov-Altarelli-Parisi
DIS	deep-inelastic scattering
DR	dimensional regularization
DVCS	deeply virtual Compton scattering
DVMP	deeply virtual meson production
DY	Drell-Yan
EFT	effective field theory
EIC	Electron-Ion Collider
EOM	equation of motion
ERBL	Efremov-Radyushkin-Brodsky-Lepage
GCPO	generalized collinear-parton observable
GPD	generalized parton distribution
GTMD	generalized transverse-momentum-dependent distribution
HQET	heavy-quark effective field theory
IMF	infinite-momentum frame
IR	infrared
LaMET	large-momentum effective theory
LC	light cone
LF	light front
LFWF	light-front wave function
$\overline{\text{MS}}$	modified minimal subtraction
NPR	nonperturbative renormalization
OAM	orbital angular momentum
OPE	operator product expansion
PDF	parton distribution function
QCD	quantum chromodynamics
QED	quantum electrodynamics
QFT	quantum field theory
RGE	renormalization group equation
RI/MOM	regularization-independent momentum subtraction
SCET	soft-collinear effective theory
SIDIS	semi-inclusive deep-inelastic scattering
TMD	transverse momentum dependent
UV	ultraviolet

Parton model.—Model proposed by R. Feynman in which hadrons are viewed as a collection of pointlike quasifree partons.

Parton distribution function.—Probability function describing how the longitudinal momentum is distributed among the partons (quarks and gluons) in a hadron.

Factorization theorem.—Theorem that separates hadronic observables into process-dependent short-distance partonic observables and universal long-distance functions characterizing the hadron structure.

Light-front quantization.—Quantization program that is carried out at equal light-front time and yields a relativistic description of QCD bound states in terms of light-front wave functions.

Bjorken x_B.—Variable proposed by J. D. Bjorken to characterize the kinematics in DIS. Its definition is given prior to Eq. (1).

Scaling.—Behavior in which an observable is independent of the scale at which it is probed.

Effective field theory.—Theoretical framework that describes physical phenomena at a given length scale using only active degrees of freedom at that scale while integrating out degrees of freedom at other length scales.

Renormalization group equation.—Equation that describes how a physical system can be viewed and interpreted at different scales.

HQET.—An effective field theory obtained from QCD by taking the infinite heavy-quark mass limit.

Gauge link or Wilson line.—Nonlocal quantity constructed as exponentials of integrals of gauge fields along a given path used to connect fields at different space-time points to maintain gauge invariance.

Compton amplitude.—The quantum amplitude for scattering of a virtual photon by the proton.

Auxiliary field approach.—Approach in which the nonlocal gauge link can be replaced by the two-point function of the auxiliary field.

Matching.—A procedure used to relate full theory operators to effective field theory operators.

Nonsinglet.—Combination accounting for the difference between quark distributions such as the *u-d* isovector combination discussed extensively in the context of this review.

Universality class.—Collection of operators that flow into the same fixed point under momentum renormalization group running.

Quasi-light-front correlations.—Spatial correlations defining the finite-momentum distributions.

Collinear divergence.—Divergence in a Feynman diagram when loop momentum of the internal line is collinear to that of the external massless particle.

Two-particle-irreducible diagram.—Feynman diagram that cannot be divided into disconnected parts by cutting two internal lines.

Wilson fermion.—A way to discretize the QCD fermion action on the lattice, which breaks down the chiral symmetry.

Generalized parton distribution.—Generalization of PDFs to nonforward kinematics; i.e., the initial and final states have different momenta.

Skewness.—Defined to characterize the longitudinal-momentum transfer in GPDs.

Distribution amplitude.—Transition matrix element between vacuum and hadron state representing the probability amplitude of finding a given Fock state in the hadron.

Twist.—Defined as dimension spin of the operator. Leading twist (higher twist) denotes the leading (nonleading) power behavior in the quantity under investigation.

Zero-mode.—Degrees of freedom with zero longitudinal momentum in LFQ.

TMDPDF.—Defined in Eq. (220), the distribution function of both longitudinal and transverse momentum for partons.

Staple-shaped gauge link.—Pair of gauge links separated along transverse directions that appear in the definition of TMDPDFs. They are defined in Eqs. (166), (173), and (196).

Rapidity divergence.—Divergence of TMDPDF and soft functions due to the presence of infinite rapidity scale introduced by the infinitely long gauge links.

Light-cone regulator.—Regulates the rapidity divergence. First mentioned upon the introduction of Eq. (168).

On light cone.—Rapidity regulator that maintains the presence of lightlike separations in the gauge link.

Off light cone.—Rapidity regulator that makes the separations of the gauge link nonlightlike.

Soft function.—Functions that capture the factorable soft radiation of TMDPDF. Defined in Eq. (172) for on-light-cone regulators and Eq. (202) for off-light-cone regulators.

Collins-Soper kernel.—Kernel for rapidity evolution of TMDPDF; see Eq. (191).

Quasi-TMDPDF.—Defined in Eq. (195), it is similar to the TMDPDF but with lightlike separations replaced by space-like ones.

Pinch-pole singularity.—Divergence due to an infinitely long gauge-link pair in the quasi-TMDPDF. It can be subtracted out by the factor Z_E; see the discussion following Eq. (198).

Off-light-cone soft function.—Soft function using an off-light-cone regulator defined in Eqs. (202) and (224). It is required to match a quasi-TMDPDF to a TMDPDF.

Reduced soft function.—Rapidity-independent part of an off-light-cone soft function; see Eq. (204).

Light-front wave function.—Wave function for a hadron state in light-front quantization that is expanded in the free-Fock state.

Reduced diagram.—Diagram showing the power-leading region of IR divergences. All the IR safe propagators are shrunk to blobs.

Momentum smearing.—Lattice technique to increase the overlap of the field and nonzero-momentum state.

Nonsinglet.—Transforms under the fundamental representation of $\mathrm{SU}(N_f)$, with N_f the quark flavor number.

ACKNOWLEDGMENTS

APPENDIX: CONVENTIONS

We use the following convention for the metric tensor:

$$g^{\mu\nu} = \text{diag}(1, -1, -1, -1). \tag{A1}$$

The space-time indices are labeled $(0, 1, 2, 3)$ or (t, x, y, z) or some combination of the two.

In ordinary coordinates, a generic four-vector is denoted as $v^\mu = (v^0, v^x, v^y, v^z)$ or $v^\mu = (v^0, \vec{v}_\perp, v^z)$. For example, the spacelike and timelike direction vectors are written as $n_z = (0, 0, 0, 1)$ and $n_t = (1, 0, 0, 0)$, respectively. In the light-cone coordinates $\xi^\pm = (1/\sqrt{2})(\xi^0 \pm \xi^3)$, a vector is denoted as $v^\mu = (v^+, v^-, \vec{v}_\perp)$.

The hadron state $|P\rangle$ is normalized as

$$\langle P'|P\rangle = (2\pi)^3 2P^0 \delta^{(3)}(\vec{P} - \vec{P}'). \tag{A2}$$

The covariant derivative and the Wilson-line gauge link in the fundamental representation are defined as

$$D^\mu \psi = (\partial^\mu + igA^\mu)\psi = (\partial^\mu + igt^a A_a^\mu)\psi \tag{A3}$$

and

$$W(x_2, x_1)$$
$$= \exp\left[-ig \int_0^1 dt(x_2 - x_1)_\mu A^\mu[x_1 + (x_2 - x_1)t]\right]. \tag{A4}$$

The gauge links in the adjoint representation are completely analogous.

We use $O_\Gamma(s)$ to generically denote an operator defining the corresponding (quasi)parton observable, where s can be a lightlike separation (for parton observables) or a spacelike separation (for quasiparton observables) and Γ is a Dirac structure. The momentum fraction in a quasiobservable is denoted as y, while that in the usual parton observable is denoted as x.

The light-cone operator that defines the quark parton observable is

$$O_\Gamma(\lambda n) = \bar{\psi}(0)\Gamma W(0, \lambda n)\psi(\lambda n), \tag{A5}$$

with Γ denoting a Dirac matrix. If we take $\Gamma = \slashed{n} \equiv \gamma^+$, the unpolarized quark PDF is then given by

$$q(x) = \frac{1}{2P^+} \int \frac{d\lambda}{2\pi} e^{ix\lambda} \langle P|O_{\gamma^+}(\lambda n)|P\rangle, \tag{A6}$$

with $n^\mu = (1/\sqrt{2})(1/P^+, 0, 0, -1/P^+)$.

Accordingly, the quark quasiobservable is defined as

$$O_\Gamma(z) = \bar{\psi}(zn_z/2)\Gamma W(zn_z/2, -zn_z/2)\psi(-zn_z/2). \tag{A7}$$

If we choose $\Gamma = \gamma^t$, the unpolarized quark quasi-PDF is then defined as

$$\tilde{q}(y) = \frac{1}{2P^0} \int \frac{d\lambda}{2\pi} e^{iy\lambda} \langle P|O_{\gamma^t}(z)|P\rangle, \tag{A8}$$

with the quasi-light-cone distance $\lambda = zP^z$.

The staple-shaped gauge link required for the TMDPDFs is defined as

$$\mathcal{W}_n(\lambda n/2 + \vec{b}_\perp) = W_n^\dagger(\lambda n/2 + \vec{b}_\perp)W_\perp W_n(-\lambda n/2), \tag{A9}$$

where

$$W_n(\xi) = W(\xi + \infty n, \xi). \tag{A10}$$

The unsubtracted unpolarized quark TMDPDF is then defined as

$$f(x, \vec{k}_\perp, \mu, \delta^-/P^+) = \frac{1}{2P^+} \int \frac{d\lambda}{2\pi} \frac{d^2\vec{b}_\perp}{(2\pi)^2} e^{-i\lambda x + i\vec{k}_\perp \cdot \vec{b}_\perp}$$
$$\times \langle P|\bar{\psi}(\lambda n/2 + \vec{b}_\perp)\slashed{n}\mathcal{W}_n(\lambda n/2 + \vec{b}_\perp)|_{\delta^-}$$
$$\times \psi(-\lambda n/2)|P\rangle, \tag{A11}$$

and the TMD soft function for the DY process is defined as

$$S(b_\perp, \mu, \delta^+, \delta^-)$$
$$= \frac{\text{Tr}\langle 0|\bar{\mathcal{T}}W_p(\vec{b}_\perp)|_{\delta^+}W_n^\dagger(\vec{b}_\perp)|_{\delta^-}\mathcal{T}W_n(0)|_{\delta^-}W_p^\dagger(0)|_{\delta^+}|0\rangle}{N_c}$$
$$= \frac{\text{Tr}\langle 0|\mathcal{W}_n(\vec{b}_\perp)|_{\delta^+}\mathcal{W}_p^\dagger(\vec{b}_\perp)|_{\delta^-}|0\rangle}{N_c}, \tag{A12}$$

where $|_{\delta^\pm}$ denotes the rapidity regulator for the gauge links involved. In terms of those, the physical scheme-independent TMDPDF is defined as

$$f^{\text{TMD}}(x, b_\perp, \mu, \zeta) = \lim_{\delta^- \to 0} \frac{f(x, b_\perp, \mu, \delta^-/P^+)}{\sqrt{S(b_\perp, \mu, \delta^- e^{2y_n}, \delta^-)}}, \tag{A13}$$

where $\zeta \equiv 2(xP^+)^2 e^{2y_n}$ is the rapidity scale.

The staple-shaped gauge link for the quasi-TMDPDF is defined as

$$\mathcal{W}_z(\xi; L) = W_z^\dagger(\xi; L)W_\perp \mathcal{W}_z(-\xi^z n_z; L), \qquad (A14)$$

where

$$W_z(\xi) = W(\xi + (L - \xi^z)n_z, \xi). \qquad (A15)$$

The quasi-TMDPDF is then defined as follows using $\mathcal{W}_z(\xi^z n_z/2 + \vec{b}_\perp; L)$ in exactly the same way as in the unsubtracted TMDPDF:

$$\tilde{f}(\xi^z, b_\perp, \mu, \zeta_z) = \lim_{L\to\infty} \frac{\langle P|\bar{\psi}(\xi^z n_z/2 + \vec{b}_\perp)\gamma^z \mathcal{W}_z(\xi^z n_z/2 + \vec{b}_\perp; L)\psi(-\xi^z n_z/2)|P\rangle}{\sqrt{Z_E(2L, b_\perp, \mu)}}, \qquad (A16)$$

where $Z_E(2L, b_\perp, \mu)$ is a flat rectangular Euclidean Wilson loop along the n_z direction with length $2L$ and width $b_\perp$:

$$Z_E(2L, b_\perp, \mu) = \frac{1}{N_c}\mathrm{Tr}\langle 0|W_\perp \mathcal{W}_z(\vec{b}_\perp; 2L)|0\rangle. \qquad (A17)$$

The staple-shaped operators for LFWFs and quasi-LFWFs are the same as those for TMDPDFs and quasi-TMDPDFs and are given in Sec. V.D.

REFERENCES

Abada, A., Philippe Boucaud, G. Herdoiza, J. P. Leroy, J. Micheli, O. Pene, and J. Rodriguez-Quintero, 2001, "Preliminaries on a lattice analysis of the pion light cone wave function: A partonic signal?," Phys. Rev. D **64**, 074511.

Abdel-Rehim, A., *et al.*, 2015, "Nucleon and pion structure with lattice QCD simulations at physical value of the pion mass," Phys. Rev. D **92**, 114513; **93**, 039904(E) (2016).

Accardi, A., L. T. Brady, W. Melnitchouk, J. F. Owens, and N. Sato, 2016, "Constraints on large-*x* parton distributions from new weak boson production and deep-inelastic scattering data," Phys. Rev. D **93**, 114017.

Accardi, A., *et al.*, 2016, "Electron Ion Collider: The next QCD frontier," Eur. Phys. J. A **52**, 268.

Adamczyk, L., *et al.* (STAR Collaboration), 2016, "Measurement of the Transverse Single-Spin Asymmetry in $p^\uparrow + p \to W^\pm/Z^0$ at RHIC," Phys. Rev. Lett. **116**, 132301.

Agaev, S. S., V. M. Braun, N. Offen, and F. A. Porkert, 2012, "BELLE data on the $\pi^0\gamma * \gamma$ form factor: A game changer?," Phys. Rev. D **86**, 077504.

Aghasyan, M., *et al.* (COMPASS Collaboration), 2017, "First Measurement of Transverse-Spin-Dependent Azimuthal Asymmetries in the Drell-Yan Process," Phys. Rev. Lett. **119**, 112002.

Aglietti, U., 1994, "Consistency and lattice renormalization of the effective theory for heavy quarks," Nucl. Phys. **B421**, 191–216.

Aglietti, U., Marco Ciuchini, G. Corbo, E. Franco, G. Martinelli, and L. Silvestrini, 1998, "Model independent determination of the light cone wave functions for exclusive processes," Phys. Lett. B **441**, 371–375.

Aidala, Christine A., Steven D. Bass, Delia Hasch, and Gerhard K. Mallot, 2013, "The spin structure of the nucleon," Rev. Mod. Phys. **85**, 655–691.

Alekhin, S., J. Blümlein, S. Moch, and R. Placakyte, 2017, "Parton distribution functions, α_s, and heavy-quark masses for LHC run II," Phys. Rev. D **96**, 014011.

Alexandrou, C., S. Bacchio, M. Constantinou, J. Finkenrath, K. Hadjiyiannakou, K. Jansen, G. Koutsou, and A. Vaquero Aviles-Casco, 2019, "The nucleon axial, tensor and scalar charges and σ-terms in lattice QCD," arXiv:1909.00485.

Alexandrou, C., M. Constantinou, K. Hadjiyiannakou, K. Jansen, C. Kallidonis, G. Koutsou, A. Vaquero Avilés-Casco, and C. Wiese, 2017, "Nucleon Spin and Momentum Decomposition Using Lattice QCD Simulations," Phys. Rev. Lett. **119**, 142002.

Alexandrou, C., M. Constantinou, K. Hadjiyiannakou, K. Jansen, and F. Manigrasso, 2020, "Flavor decomposition for the proton helicity parton distribution functions," arXiv:2009.13061.

Alexandrou, C., *et al.*, 2020, "Moments of nucleon generalized parton distributions from lattice QCD simulations at physical pion mass," Phys. Rev. D **101**, 034519.

Alexandrou, Constantia, Krzysztof Cichy, Martha Constantinou, Jeremy R. Green, Kyriakos Hadjiyiannakou, Karl Jansen, Floriano Manigrasso, Aurora Scapellato, and Fernanda Steffens, 2020, "Lattice continuum-limit study of nucleon quasi-PDFs," arXiv:2011.00964.

Alexandrou, Constantia, Krzysztof Cichy, Martha Constantinou, Kyriakos Hadjiyiannakou, Karl Jansen, Haralambos Panagopoulos, and Fernanda Steffens, 2017, "A complete non-perturbative re-normalization prescription for quasi-PDFs," Nucl. Phys. **B923**, 394–415.

Alexandrou, Constantia, Krzysztof Cichy, Martha Constantinou, Kyriakos Hadjiyiannakou, Karl Jansen, Aurora Scapellato, and Fernanda Steffens, 2019, "Systematic uncertainties in parton distribution functions from lattice QCD simulations at the physical point," Phys. Rev. D **99**, 114504.

Alexandrou, Constantia, Krzysztof Cichy, Martha Constantinou, Kyriakos Hadjiyiannakou, Karl Jansen, Aurora Scapellato, and Fernanda Steffens, 2020, "Unpolarized and helicity generalized parton distributions of the proton within lattice QCD," arXiv:2008.10573.

Alexandrou, Constantia, Krzysztof Cichy, Martha Constantinou, Karl Jansen, Aurora Scapellato, and Fernanda Steffens, 2018a, "Light-Cone Parton Distribution Functions from Lattice QCD," Phys. Rev. Lett. **121**, 112001.

Alexandrou, Constantia, Krzysztof Cichy, Martha Constantinou, Karl Jansen, Aurora Scapellato, and Fernanda Steffens, 2018b, "Transversity parton distribution functions from lattice QCD," Phys. Rev. D **98**, 091503.

Alexandrou, Constantia, Krzysztof Cichy, Vincent Drach, Elena Garcia-Ramos, Kyriakos Hadjiyiannakou, Karl Jansen, Fernanda Steffens, and Christian Wiese, 2015, "Lattice calculation of parton distributions," Phys. Rev. D **92**, 014502.

Altarelli, Guido, and G. Parisi, 1977, "Asymptotic freedom in parton language," Nucl. Phys. **B126**, 298–318.

Aoki, S., *et al.* (Flavour Lattice Averaging Group), 2020, "FLAG review 2019," Eur. Phys. J. C **80**, 113.

Aoki, Yasumichi, Tom Blum, Huey-Wen Lin, Shigemi Ohta, Shoichi Sasaki, Robert Tweedie, James Zanotti, and Takeshi Yamazaki, 2010, "Nucleon isovector structure functions in $(2+1)$-flavor QCD with domain wall fermions," Phys. Rev. D **82**, 014501.

Aprahamian, Ani, *et al.*, 2015, "Reaching for the horizon: The 2015 long range plan for nuclear science" (unpublished), https://www.osti.gov/biblio/1296778-reaching-horizon-long-range-plan-nuclear-science.

Arefeva, I. Ya., 1980, "Quantum contour field equations," Phys. Lett. **93B**, 347–353.

Aubert, Bernard, *et al.* (*BABAR* Collaboration), 2009, "Measurement of the $\gamma\gamma^* \to \pi^0$ transition form factor," Phys. Rev. D **80**, 052002.

Bacchetta, Alessandro, Valerio Bertone, Chiara Bissolotti, Giuseppe Bozzi, Filippo Delcarro, Fulvio Piacenza, and Marco Radici, 2020, "Transverse-momentum-dependent parton distributions up to N³LL from Drell-Yan data," J. High Energy Phys. 07, 117.

Bacchetta, Alessandro, Filippo Delcarro, Cristian Pisano, Marco Radici, and Andrea Signori, 2017, "Extraction of partonic transverse momentum distributions from semi-inclusive deep-inelastic scattering, Drell-Yan and Z-boson production," J. High Energy Phys. 06, 081; 06 (2019) 051(E).

Bagan, E., and P. Gosdzinsky, 1994, "Renormalizability of the heavy quark effective theory," Phys. Lett. B **320**, 123–129.

Baikov, P. A., K. G. Chetyrkin, A. V. Smirnov, V. A. Smirnov, and M. Steinhauser, 2009, "Quark and Gluon Form Factors to Three Loops," Phys. Rev. Lett. **102**, 212002.

Bali, Gunnar S., Vladimir M. Braun, Simon Bürger, Meinulf Gückeler, Michael Gruber, Fabian Hutzler, Piotr Korcyl, Andreas Schäfer, André Sternbeck, and Philipp Wein, 2019, "Light-cone distribution amplitudes of pseudoscalar mesons from lattice QCD," J. High Energy Phys. 08, 065.

Bali, Gunnar S., Vladimir M. Braun, Benjamin Gläßle, Meinulf Göckeler, Michael Gruber, Fabian Hutzler, Piotr Korcyl, Andreas Schäfer, Philipp Wein, and Jian-Hui Zhang, 2018, "Pion distribution amplitude from Euclidean correlation functions: Exploring universality and higher-twist effects," Phys. Rev. D **98**, 094507.

Bali, Gunnar S., Sara Collins, Benjamin Gläßle, Meinulf Göckeler, Johannes Najjar, Rudolf H. Rüdl, Andreas Schäfer, Rainer W. Schiel, André Sternbeck, and Wolfgang Süldner, 2014, "The moment $\langle x \rangle_{u-d}$ of the nucleon from $N_f = 2$ lattice QCD down to nearly physical quark masses," Phys. Rev. D **90**, 074510.

Bali, Gunnar S., Bernhard Lang, Bernhard U. Musch, and Andreas Schäfer, 2016, "Novel quark smearing for hadrons with high momenta in lattice QCD," Phys. Rev. D **93**, 094515.

Bali, Gunnar S., *et al.*, 2018, "Pion distribution amplitude from Euclidean correlation functions," Eur. Phys. J. C **78**, 217.

Balitsky, I., 1996, "Operator expansion for high-energy scattering," Nucl. Phys. **B463**, 99–160.

Balitsky, I. I., and Vladimir M. Braun, 1989, "Evolution equations for QCD string operators," Nucl. Phys. **B311**, 541–584.

Balitsky, I. I., Vladimir M. Braun, Y. Koike, and K. Tanaka, 1996, "Q^2 Evolution of Chiral Odd Twist-3 Distributions $h_L(x, Q^2)$ and $e(x, Q^2)$ in Large-N_c QCD," Phys. Rev. Lett. **77**, 3078–3081.

Balitsky, I. I., and L. N. Lipatov, 1978, "The Pomeranchuk singularity in quantum chromodynamics," Yad. Fiz. **28**, 1597 [Sov. J. Nucl. Phys. **28**, 822–829 (1978), https://www.osti.gov/biblio/6180758].

Balitsky, Ian, Wayne Morris, and Anatoly Radyushkin, 2019, "Gluon pseudo-distributions at short distances: Forward case," arXiv:1910.13963.

Ball, Patricia, V. M. Braun, and A. Lenz, 2006, "Higher-twist distribution amplitudes of the K meson in QCD," J. High Energy Phys. 05, 004.

Ball, Richard D., *et al.* (NNPDF Collaboration), 2017, "Parton distributions from high-precision collider data," Eur. Phys. J. C **77**, 663.

Barone, Vincenzo, Alessandro Drago, and Philip G. Ratcliffe, 2002, "Transverse polarisation of quarks in hadrons," Phys. Rep. **359**, 1–168.

Bars, I., and Michael B. Green, 1978, "Poincaré and gauge invariant two-dimensional QCD," Phys. Rev. D **17**, 537.

Bass, Steven D., 2005, "The spin structure of the proton," Rev. Mod. Phys. **77**, 1257–1302.

Bauer, Christian W., Sean Fleming, Dan Pirjol, and Iain W. Stewart, 2001, "An effective field theory for collinear and soft gluons: Heavy to light decays," Phys. Rev. D **63**, 114020.

Bauer, Christian W., Dan Pirjol, and Iain W. Stewart, 2002, "Soft collinear factorization in effective field theory," Phys. Rev. D **65**, 054022.

Bauer, Christian W., and Iain W. Stewart, 2001, "Invariant operators in collinear effective theory," Phys. Lett. B **516**, 134–142.

Becher, Thomas, and Matthias Neubert, 2011, "Drell-Yan production at small q_T, transverse parton distributions and the collinear anomaly," Eur. Phys. J. C **71**, 1665.

Belitsky, A. V., and A. V. Radyushkin, 2005, "Unraveling hadron structure with generalized parton distributions," Phys. Rep. **418**, 1–387.

Belitsky, Andrei V., X. Ji, and F. Yuan, 2003, "Final state interactions and gauge invariant parton distributions," Nucl. Phys. **B656**, 165–198.

Belitsky, Andrei V., Xiangdong Ji, and Feng Yuan, 2004, "Quark imaging in the proton via quantum phase space distributions," Phys. Rev. D **69**, 074014.

Beneke, M., 1999, "Renormalons," Phys. Rep. **317**, 1–142.

Beneke, M., and Vladimir M. Braun, 1994, "Heavy quark effective theory beyond perturbation theory: Renormalons, the pole mass and the residual mass term," Nucl. Phys. **B426**, 301–343.

Beneke, M., and Vladimir M. Braun, 1995, "Power corrections and renormalons in Drell-Yan production," Nucl. Phys. **B454**, 253–290.

Beneke, M., and Vladimir M. Braun, 2000, "Renormalons and power corrections," in *At the Frontier of Particle Science*, edited by M. Shifman (World Scientific, Singapore), pp. 1719–1773.

Beneke, M., Vladimir M. Braun, and Lorenzo Magnea, 1997, "Phenomenology of power corrections in fragmentation processes in $e^+ e^-$ annihilation," Nucl. Phys. **B497**, 297–333.

Bertone, Valerio, Ignazio Scimemi, and Alexey Vladimirov, 2019, "Extraction of unpolarized quark transverse momentum dependent parton distributions from Drell-Yan/Z-boson production," J. High Energy Phys. 06, 028.

Bhat, Manjunath, Krzysztof Cichy, Martha Constantinou, and Aurora Scapellato, 2020, "Parton distribution functions from lattice QCD at physical quark masses via the pseudo-distribution approach," arXiv:2005.02102.

Bhattacharya, Shohini, Krzysztof Cichy, Martha Constantinou, Andreas Metz, Aurora Scapellato, and Fernanda Steffens, 2020a, "New insights on proton structure from lattice QCD: The twist-3 parton distribution function $g_T(x)$," arXiv:2004.04130.

Bhattacharya, Shohini, Krzysztof Cichy, Martha Constantinou, Andreas Metz, Aurora Scapellato, and Fernanda Steffens, 2020b, "One-loop matching for the twist-3 parton distribution $g_T(x)$," Phys. Rev. D **102**, 034005.

Bhattacharya, Shohini, Krzysztof Cichy, Martha Constantinou, Andreas Metz, Aurora Scapellato, and Fernanda Steffens, 2020c,

"The role of zero-mode contributions in the matching for the twist-3 PDFs $e(x)$ and $h_L(x)$," arXiv:2006.12347.

Bhattacharya, Shohini, Christopher Cocuzza, and Andreas Metz, 2019a, "Exploring twist-2 GPDs through quasi-distributions in a diquark spectator model," arXiv:1903.05721.

Bhattacharya, Shohini, Christopher Cocuzza, and Andreas Metz, 2019b, "Generalized quasi parton distributions in a diquark spectator model," Phys. Lett. B **788**, 453–463.

Bhattacharya, Shohini, Andreas Metz, Vikash Kumar Ojha, Jeng-Yuan Tsai, and Jian Zhou, 2018, "Exclusive double quarko-nium production and generalized TMDs of gluons," arXiv: 1802.10550.

Bhattacharya, Shohini, Andreas Metz, and Jian Zhou, 2017, "Generalized TMDs and the exclusive double Drell-Yan process," Phys. Lett. B **771**, 396–400.

Bigi, Ikaros I. Y, Mikhail A. Shifman, N. G. Uraltsev, and A. I. Vainshtein, 1994, "Pole mass of the heavy quark: Perturbation theory and beyond," Phys. Rev. D **50**, 2234–2246.

Bjorken, J. D., and Emmanuel A. Paschos, 1969, "Inelastic electron proton and gamma proton scattering, and the structure of the nucleon," Phys. Rev. **185**, 1975–1982.

Bloom, Elliott D., *et al.*, 1969, "High-Energy Inelastic e-p Scattering at 6° and 10°," Phys. Rev. Lett. **23**, 930–934.

Bodwin, Geoffrey T., 1985, "Factorization of the Drell-Yan cross section in perturbation theory," Phys. Rev. D **31**, 2616; **34**, 3932(E) (1986).

Boer, Daniel, and P. J. Mulders, 1998, "Time reversal odd distribution functions in leptoproduction," Phys. Rev. D **57**, 5780–5786.

Boer, Daniel, *et al.*, 2011, "Gluons and the quark sea at high energies: Distributions, polarization, tomography," arXiv:1108.1713.

Braun, V., P. Gornicki, and L. Mankiewicz, 1995, "Ioffe-time distributions instead of parton momentum distributions in description of deep inelastic scattering," Phys. Rev. D **51**, 6036–6051.

Braun, V., and Dieter Müller, 2008, "Exclusive processes in position space and the pion distribution amplitude," Eur. Phys. J. C **55**, 349–361.

Braun, V. M., 2006, "Nucleons on the light-cone: Theory and phenomenology of baryon distribution amplitudes," in *Proceedings of the 7th Workshop on Continuous Advances in QCD (QCD 2006), Minneapolis, 2006*, pp. 42–57.

Braun, V. M., K. G. Chetyrkin, and B. A. Kniehl, 2020, "Renorm-alization of parton quasi-distributions beyond the leading order: Spacelike vs. timelike," arXiv:2004.01043.

Braun, V. M., S. Collins, M. Gückeler, P. Pérez-Rubio, A. Schäfer, R. W. Schiel, and A. Sternbeck, 2015, "Second moment of the pion light-cone distribution amplitude from lattice QCD," Phys. Rev. D **92**, 014504.

Braun, V. M., Y. Ji, and A. Vladimirov, 2021, "QCD factorization for twist-three axial-vector parton quasidistributions," J. High Energy Phys. 05, 086.

Braun, V. M., G. P. Korchemsky, and Dieter Müller, 2003, "The uses of conformal symmetry in QCD," Prog. Part. Nucl. Phys. **51**, 311–398.

Braun, V. M., T. Lautenschlager, A. N. Manashov, and B. Pirnay, 2011, "Higher twist parton distributions from light-cone wave functions," Phys. Rev. D **83**, 094023.

Braun, Vladimir M., 1995, "QCD renormalons and higher twist effects," in *Proceedings of the XXXth Rencontres de Moriond, "QCD and High Energy Hadronic Interactions" ('95 QCD), Les Arcs, France, 1995* (Editions Frontières, Gif-sur-Yvette, France), pp. 271–278.

Braun, Vladimir M., and I. E. Filyanov, 1990, "Conformal invariance and pion wave functions of nonleading twist," Z. Phys. C **48**, 239–248.

Braun, Vladimir M., Einan Gardi, and Stefan Gottwald, 2004, "Renormalon approach to higher twist distribution amplitudes and the convergence of the conformal expansion," Nucl. Phys. **B685**, 171–226.

Braun, Vladimir M., Alexey Vladimirov, and Jian-Hui Zhang, 2019, "Power corrections and renormalons in parton quasidistributions," Phys. Rev. D **99**, 014013.

Briceño, Raúl A., Jozef J. Dudek, and Ross D. Young, 2018, "Scattering processes and resonances from lattice QCD," Rev. Mod. Phys. **90**, 025001.

Briceño, Raúl A., Juan V. Guerrero, Maxwell T. Hansen, and Christopher J. Monahan, 2018, "Finite-volume effects due to spatially nonlocal operators," Phys. Rev. D **98**, 014511.

Briceño, Raúl A., Maxwell T. Hansen, and Christopher J. Monahan, 2017, "Role of the Euclidean signature in lattice calculations of quasidistributions and other nonlocal matrix elements," Phys. Rev. D **96**, 014502.

Bringewatt, J., N. Sato, W. Melnitchouk, Jian-Wei Qiu, F. Steffens, and M. Constantinou, 2020, "Confronting lattice parton distribu-tions with global QCD analysis," arXiv:2010.00548.

Broadhurst, David J., and A. G. Grozin, 1991, "Two loop renorm-alization of the effective field theory of a static quark," Phys. Lett. B **267**, 105–110.

Brodsky, S. J., 2002, "Perspectives on exclusive processes in QCD," in *Exclusive Processes at High Momentum Transfer*, edited by P. Stoler and A. Radyushkin (World Scientific, Singapore), pp. 1–33.

Brodsky, Stanley J., Hans-Christian Pauli, and Stephen S. Pinsky, 1998, "Quantum chromodynamics and other field theories on the light cone," Phys. Rep. **301**, 299–486.

Brodsky, Stanley J., and G. Peter Lepage, 1989, "Exclusive processes in quantum chromodynamics," in *Perturbative Quantum Chromo-dynamics*, edited by A. H. Mueller, Advanced Directions in High Energy Physics Vol. 5 (World Scientific, Singapore), pp. 93–240.

Broniowski, Wojciech, and Enrique Ruiz Arriola, 2017, "Nonper-turbative partonic quasidistributions of the pion from chiral quark models," Phys. Lett. B **773**, 385–390.

Broniowski, Wojciech, and Enrique Ruiz Arriola, 2018, "Partonic quasidistributions of the proton and pion from transverse-momentum distributions," Phys. Rev. D **97**, 034031.

Bunce, Gerry, Naohito Saito, Jacques Soffer, and Werner Vogelsang, 2000, "Prospects for spin physics at RHIC," Annu. Rev. Nucl. Part. Sci. **50**, 525–575.

Burkardt, M., 1989, "The virial theorem and the structure of the deuteron in $(1 + 1)$-dimensional QCD on the light cone," Nucl. Phys. **A504**, 762–776.

Burkardt, Matthias, 1993, "Light front quantization of the sine-Gordon model," Phys. Rev. D **47**, 4628–4633.

Burkardt, Matthias, 2000, "Impact parameter dependent parton distributions and off forward parton distributions for $\zeta \to 0$," Phys. Rev. D **62**, 071503; **66**, 119903(E) (2002).

Burkhardt, Hugh, and W. N. Cottingham, 1970, "Sum rules for forward virtual Compton scattering," Ann. Phys. (N.Y.) **56**, 453–463.

Cammarota, Justin, Leonard Gamberg, Zhong-Bo Kang, Joshua A. Miller, Daniel Pitonyak, Alexei Prokudin, Ted C. Rogers, and Nobuo Sato, 2020, "The origin of single transverse-spin asymme-tries in high-energy collisions," arXiv:2002.08384.

Capitani, S., M. Gockeler, R. Horsley, H. Oelrich, D. Petters, Paul E. L. Rakow, and G. Schierholz, 1999, "Towards a nonperturbative

calculation of DIS Wilson coefficients," Nucl. Phys. B, Proc. Suppl. **73**, 288–290.

Capitani, S., M. Gockeler, R. Horsley, D. Petters, D. Pleiter, Paul E. L. Rakow, and G. Schierholz, 1999, "Higher twist corrections to nucleon structure functions from lattice QCD," Nucl. Phys. B, Proc. Suppl. **79**, 173–175.

Carlson, Carl E., and Michael Freid, 2017, "Lattice corrections to the quark quasidistribution at one loop," Phys. Rev. D **95**, 094504.

Catani, S., and M. Grazzini, 2012, "Higgs boson production at hadron colliders: Hard-collinear coefficients at the NNLO," Eur. Phys. J. C **72**, 2013; **72**, 2132(E) (2012).

Catani, Stefano, Leandro Cieri, Daniel de Florian, Giancarlo Ferrera, and Massimiliano Grazzini, 2012, "Vector boson production at hadron colliders: Hard-collinear coefficients at the NNLO," Eur. Phys. J. C **72**, 2195.

Chadwick, J., 1932, "Possible existence of a neutron," Nature (London) **129**, 312.

Chai, Yahui, *et al.*, 2020, "Parton distribution functions of Δ^+ on the lattice," arXiv:2002.12044.

Chambers, A. J., R. Horsley, Y. Nakamura, H. Perlt, P. E. L. Rakow, G. Schierholz, A. Schiller, K. Somfleth, R. D. Young, and J. M. Zanotti, 2017, "Nucleon Structure Functions from Operator Product Expansion on the Lattice," Phys. Rev. Lett. **118**, 242001.

Chang, C. C., *et al.*, 2018, "A per-cent-level determination of the nucleon axial coupling from quantum chromodynamics," Nature (London) **558**, 91–94.

Chang, Lei, I. C. Cloet, J. J. Cobos-Martinez, C. D. Roberts, S. M. Schmidt, and P. C. Tandy, 2013, "Imaging Dynamical Chiral Symmetry Breaking: Pion Wave Function on the Light Front," Phys. Rev. Lett. **110**, 132001.

Chang, Shau-Jin, and Shang-Keng Ma, 1969, "Feynman rules and quantum electrodynamics at infinite momentum," Phys. Rev. **180**, 1506–1513.

Chang, Wen-Chen, and Jen-Chieh Peng, 2014, "Flavor structure of the nucleon sea," Prog. Part. Nucl. Phys. **79**, 95–135.

Chen, Jiunn-Wei, Saul D. Cohen, Xiangdong Ji, Huey-Wen Lin, and Jian-Hui Zhang, 2016, "Nucleon helicity and transversity parton distributions from lattice QCD," Nucl. Phys. **B911**, 246–273.

Chen, Jiunn-Wei, Tomomi Ishikawa, Luchang Jin, Huey-Wen Lin, Yi-Bo Yang, Jian-Hui Zhang, and Yong Zhao, 2018, "Parton distribution function with nonperturbative renormalization from lattice QCD," Phys. Rev. D **97**, 014505.

Chen, Jiunn-Wei, Tomomi Ishikawa, Luchang Jin, Huey-Wen Lin, Jian-Hui Zhang, and Yong Zhao (LP3 Collaboration), 2019, "Symmetry properties of nonlocal quark bilinear operators on a lattice," Chin. Phys. C **43**, 103101.

Chen, Jiunn-Wei, Xiangdong Ji, and Jian-Hui Zhang, 2017, "Improved quasi parton distribution through Wilson line renormalization," Nucl. Phys. **B915**, 1–9.

Chen, Jiunn-Wei, Huey-Wen Lin, and Jian-Hui Zhang, 2019, "Pion generalized parton distribution from lattice QCD," arXiv:1904.12376.

Chen, Long-Bin, Wei Wang, and Ruilin Zhu, 2020a, "Next-to-next-to-leading order corrections to quark quasi parton distribution functions," arXiv:2006.14825.

Chen, Long-Bin, Wei Wang, and Ruilin Zhu, 2020b, "Quasiparton distribution functions at NNLO: Flavor nondiagonal quark contributions," Phys. Rev. D **102**, 011503.

Chen, Long-Bin, Wei Wang, and Ruilin Zhu, 2020c, "Master integrals for two-loop QCD corrections to quark quasi PDFs," J. High Energy Phys. 10, 079.

Chen, Xiang-Song, Wei-Min Sun, Fan Wang, and T. Goldman, 2011, "Proper identification of the gluon spin," Phys. Lett. B **700**, 21–24.

Chernyak, V. L., and A. R. Zhitnitsky, 1982, "Exclusive decays of heavy mesons," Nucl. Phys. **B201**, 492; **B214**, 547(E) (1983).

Chetyrkin, K. G., and A. G. Grozin, 2003, "Three loop anomalous dimension of the heavy light quark current in HQET," Nucl. Phys. **B666**, 289–302.

Chiu, Jui-Yu, Ambar Jain, Duff Neill, and Ira Z. Rothstein, 2012, "A formalism for the systematic treatment of rapidity logarithms in quantum field theory," J. High Energy Phys. 05, 084.

Christ, Norman H., B. Hasslacher, and Alfred H. Mueller, 1972, "Light cone behavior of perturbation theory," Phys. Rev. D **6**, 3543.

Cichy, Krzysztof, and Martha Constantinou, 2019, "A guide to light-cone PDFs from lattice QCD: An overview of approaches, techniques and results," Adv. High Energy Phys. 3036904.

Cichy, Krzysztof, Luigi Del Debbio, and Tommaso Giani, 2019, "Parton distributions from lattice data: The nonsinglet case," J. High Energy Phys. 10, 137.

Collins, J. C., A. V. Efremov, K. Goeke, M. Grosse Perdekamp, S. Menzel, B. Meredith, A. Metz, and P. Schweitzer, 2005, "Sivers effect in semi-inclusive deeply inelastic scattering and Drell-Yan," in *Proceedings of the International Workshop on Transverse Polarisation Phenomena in Hard Processes (Transversity 2005), Villa Olmo, Como, Italy, 2005*, edited by P. Ratcliffe, pp. 212–219, https://inspirehep.net/conferences/977010?ui-citation-summary=true.

Collins, J. C., A. V. Efremov, K. Goeke, S. Menzel, A. Metz, and P. Schweitzer, 2006, "Sivers effect in semi-inclusive deeply inelastic scattering," Phys. Rev. D **73**, 014021.

Collins, John, 2011a, *Foundations of Perturbative QCD*, Cambridge Monographs on Particle Physics, Nuclear Physics and Cosmology Vol. 32 (Cambridge University Press, Cambridge, England), pp. 1–624.

Collins, John, 2011b, "New definition of TMD parton densities," Int. J. Mod. Phys. Conf. Ser. **04**, 85–96.

Collins, John, 2008, "Rapidity divergences and valid definitions of parton densities," Proc. Sci. LC2008, 028 [arXiv:0808.2665].

Collins, John, and Ted C. Rogers, 2017, "Connecting different TMD factorization formalisms in QCD," Phys. Rev. D **96**, 054011.

Collins, John C., 1986, *Renormalization*, Cambridge Monographs on Mathematical Physics Vol. 26 (Cambridge University Press, Cambridge, England).

Collins, John C., 1993, "Fragmentation of transversely polarized quarks probed in transverse momentum distributions," Nucl. Phys. **B396**, 161–182.

Collins, John C., 2002, "Leading twist single transverse-spin asymmetries: Drell-Yan and deep inelastic scattering," Phys. Lett. B **536**, 43–48.

Collins, John C., and Andreas Metz, 2004, "Universality of Soft and Collinear Factors in Hard-Scattering Factorization," Phys. Rev. Lett. **93**, 252001.

Collins, John C., and Ted C. Rogers, 2013, "Equality of two definitions for transverse momentum dependent parton distribution functions," Phys. Rev. D **87**, 034018.

Collins, John C., and Randall J. Scalise, 1994, "Renormalization of composite operators in Yang-Mills theories using general covariant gauge," Phys. Rev. D **50**, 4117–4136.

Collins, John C., and Davison E. Soper, 1981, "Back-to-back jets in QCD," Nucl. Phys. **B193**, 381; **B213**, 545(E) (1983).

Collins, John C., and Davison E. Soper, 1982a, "Back-to-back jets: Fourier transform from b to k_T," Nucl. Phys. **B197**, 446–476.

Collins, John C., and Davison E. Soper, 1982b, "Parton distribution and decay functions," Nucl. Phys. **B194**, 445–492.

Collins, John C., Davison E. Soper, and George F. Sterman, 1983, "Factorization for one-loop corrections in the Drell-Yan process," Nucl. Phys. **B223**, 381–421.

Collins, John C., Davison E. Soper, and George F. Sterman, 1985a, "Factorization for short distance hadron-hadron scattering," Nucl. Phys. **B261**, 104–142.

Collins, John C., Davison E. Soper, and George F. Sterman, 1985b, "Transverse momentum distribution in Drell-Yan pair and W and Z boson production," Nucl. Phys. **B250**, 199–224.

Collins, John C., Davison E. Soper, and George F. Sterman, 1988, "Soft gluons and factorization," Nucl. Phys. **B308**, 833–856.

Constantinou, Martha, 2021, "The x-dependence of hadronic parton distributions: A review on the progress of lattice QCD," Eur. Phys. J. A **57**, 77.

Constantinou, Martha, and Haralambos Panagopoulos, 2017, "Perturbative renormalization of quasi-parton distribution functions," Phys. Rev. D **96**, 054506.

Constantinou, Martha, Haralambos Panagopoulos, and Gregoris Spanoudes, 2019, "One-loop renormalization of staple-shaped operators in continuum and lattice regularizations," Phys. Rev. D **99**, 074508.

Constantinou, Martha, *et al.*, 2020, "Parton distributions and lattice QCD calculations: Toward 3D structure," arXiv:2006.08636.

Courtoy, Aurore, Gary R. Goldstein, J. Osvaldo Gonzalez Hernandez, Simonetta Liuti, and Abha Rajan, 2014, "On the observability of the quark orbital angular momentum distribution," Phys. Lett. B **731**, 141–147.

Craigie, N. S., and Harald Dorn, 1981, "On the renormalization and short distance properties of hadronic operators in QCD," Nucl. Phys. **B185**, 204–220.

Curci, G., W. Furmanski, and R. Petronzio, 1980, "Evolution of parton densities beyond leading order: The nonsinglet case," Nucl. Phys. **B175**, 27–92.

D'Alesio, Umberto, Miguel G. Echevarría, Stefano Melis, and Ignazio Scimemi, 2014, "Non-perturbative QCD effects in q_T spectra of Drell-Yan and Z-boson production," J. High Energy Phys. 11, 098.

Dasgupta, M., and B. R. Webber, 1996, "Power corrections and renormalons in deep inelastic structure functions," Phys. Lett. B **382**, 273–281.

Dasgupta, M., and B. R. Webber, 1997, "Power corrections and renormalons in e^+e^- fragmentation functions," Nucl. Phys. **B484**, 247–264.

Dawson, C., G. Martinelli, G. C. Rossi, Christopher T. Sachrajda, Stephen R. Sharpe, M. Talevi, and M. Testa, 1998, "New lattice approaches to the $\Delta I = 1/2$ rule," Nucl. Phys. **B514**, 313–335.

de Florian, Daniel, Rodolfo Sassot, Marco Stratmann, and Werner Vogelsang, 2014, "Evidence for Polarization of Gluons in the Proton," Phys. Rev. Lett. **113**, 012001.

Deka, M., T. Streuer, T. Doi, S. J. Dong, T. Draper, K. F. Liu, N. Mathur, and A. W. Thomas, 2009, "Moments of nucleon's parton distribution for the sea and valence quarks from lattice QCD," Phys. Rev. D **79**, 094502.

Del Debbio, Luigi, Tommaso Giani, Joseph Karpie, Kostas Orginos, Anatoly Radyushkin, and Savvas Zafeiropoulos, 2020, "Neural-network analysis of parton distribution functions from Ioffe-time pseudodistributions," arXiv:2010.03996.

Del Debbio, Luigi, Tommaso Giani, and Christopher J. Monahan, 2020, "Notes on lattice observables for parton distributions: Non-gauge theories," J. High Energy Phys. 09, 021.

de Melo, J. P. B. C., Isthiaq Ahmed, and Kazuo Tsushima, 2016, "Parton distribution in pseudoscalar mesons with a light-front constituent quark model," AIP Conf. Proc. **1735**, 080012.

Dennison, David M., 1927, "A note on the specific heat of the hydrogen molecule," Proc. R. Soc. A **115**, 483–486, https://www.jstor.org/stable/94849.

Detmold, William, and C. J. David Lin, 2006, "Deep-inelastic scattering and the operator product expansion in lattice QCD," Phys. Rev. D **73**, 014501.

Detmold, William, Anthony V. Grebe, Issaku Kanamori, C.-J. David Lin, Santanu Mondal, Robert J. Perry, and Yong Zhao, 2020, "A preliminary determination of the second Mellin moment of the pion's distribution amplitude using the heavy quark operator product expansion," arXiv:2009.09473.

Detmold, William, Issaku Kanamori, C. J. David Lin, Santanu Mondal, and Yong Zhao, 2018, "Moments of pion distribution amplitude using operator product expansion on the lattice," Proc. Sci. LATTICE2018, 106 [arXiv:1810.12194].

Deur, Alexandre, Stanley J. Brodsky, and Guy F. De Téramond, 2019, "The spin structure of the nucleon," Rep. Prog. Phys. **82**, 076201.

Diehl, M., 2003, "Generalized parton distributions," Phys. Rep. **388**, 41–277.

Dirac, Paul A. M., 1949, "Forms of relativistic dynamics," Rev. Mod. Phys. **21**, 392–399.

Dokshitzer, Yuri L., 1977, "Calculation of the structure functions for deep inelastic scattering and e^+e^- annihilation by perturbation theory in quantum chromodynamics," Zh. Eksp. Teor. Fiz. **73**, 1216 [Sov. Phys. JETP **46**, 641–653 (1977)].

Dokshitzer, Yuri L., G. Marchesini, and B. R. Webber, 1996, "Dispersive approach to power behaved contributions in QCD hard processes," Nucl. Phys. **B469**, 93–142.

Dolgov, D., *et al.* (LHPC and SESAM Collaborations), 2002, "Moments of nucleon light cone quark distributions calculated in full lattice QCD," Phys. Rev. D **66**, 034506.

Dorn, Harald, 1986, "Renormalization of path ordered phase factors and related hadron operators in gauge field theories," Fortschr. Phys. **34**, 11–56.

Dotsenko, V. S., and S. N. Vergeles, 1980, "Renormalizability of phase factors in non-abelian gauge theory," Nucl. Phys. **B169**, 527–546.

Drell, S. D., and Tung-Mow Yan, 1971, "Partons and their applications at high energies," Ann. Phys. (N.Y.) **66**, 578.

Ebert, Markus A., Stella T. Schindler, Iain W. Stewart, and Yong Zhao, 2020, "One-loop matching for spin-dependent quasi-TMDs," J. High Energy Phys. 09, 099.

Ebert, Markus A., Iain W. Stewart, and Yong Zhao, 2019a, "Determining the nonperturbative Collins-Soper kernel from lattice QCD," Phys. Rev. D **99**, 034505.

Ebert, Markus A., Iain W. Stewart, and Yong Zhao, 2019b, "Towards quasi-transverse momentum dependent PDFs computable on the lattice," J. High Energy Phys. 09, 037.

Ebert, Markus A., Iain W. Stewart, and Yong Zhao, 2020, "Renormalization and matching for the Collins-Soper kernel from lattice QCD," J. High Energy Phys. 03, 099.

Echevarría, Miguel G., Ahmad Idilbi, Zhong-Bo Kang, and Ivan Vitev, 2014, "QCD evolution of the Sivers asymmetry," Phys. Rev. D **89**, 074013.

Echevarría, Miguel G., Ahmad Idilbi, and Ignazio Scimemi, 2012, "Factorization theorem for Drell-Yan at low q_T and transverse momentum distributions on-the-light-cone," J. High Energy Phys. 07, 002.

Echevarría, Miguel G., Ahmad Idilbi, and Ignazio Scimemi, 2013, "Soft and collinear factorization and transverse momentum dependent parton distribution functions," Phys. Lett. B **726**, 795–801.

Echevarría, Miguel G., Ignazio Scimemi, and Alexey Vladimirov, 2016a, "Transverse momentum dependent fragmentation function at next-to-next-to-leading order," Phys. Rev. D **93**, 011502; **94**, 099904(E) (2016).

Echevarría, Miguel G., Ignazio Scimemi, and Alexey Vladimirov, 2016b, "Universal transverse momentum dependent soft function at NNLO," Phys. Rev. D **93**, 054004.

Echevarría, Miguel G., Ignazio Scimemi, and Alexey Vladimirov, 2016c, "Unpolarized transverse momentum dependent parton distribution and fragmentation functions at next-to-next-to-leading order," J. High Energy Phys. 09, 004.

Efremov, A. V., K. Goeke, S. Menzel, A. Metz, and P. Schweitzer, 2005, "Sivers effect in semi-inclusive DIS and in the Drell-Yan process," Phys. Lett. B **612**, 233–244.

Efremov, A. V., and A. V. Radyushkin, 1980, "Asymptotical behavior of pion electromagnetic form factor in QCD," Theor. Math. Phys. **42**, 97–110.

Egerer, Colin, Robert G. Edwards, Kostas Orginos, and David G. Richards, 2020, "Distillation at high-momentum," arXiv:2009.10691.

Ellis, R. Keith, W. Furmanski, and R. Petronzio, 1983, "Unraveling higher twists," Nucl. Phys. **B212**, 29.

Engelhardt, M., 2017, "Quark orbital dynamics in the proton from lattice QCD—From Ji to Jaffe-Manohar orbital angular momentum," Phys. Rev. D **95**, 094505.

Engelhardt, M., J. Green, N. Hasan, S. Krieg, S. Meinel, J. Negele, A. Pochinsky, and S. Syritsyn, 2018, "Quark orbital angular momentum in the proton evaluated using a direct derivative method," Proc. Sci. LATTICE2018, 115 [arXiv:1901.00843].

Engelhardt, M., P. Hägler, B. Musch, J. Negele, and A. Schäfer, 2016, "Lattice QCD study of the Boer-Mulders effect in a pion," Phys. Rev. D **93**, 054501.

Estermann, I., R. Frisch, and O. Stern, 1933, "Magnetic moment of the proton," Nature (London) **132**, 169–170.

Ethier, J. J., N. Sato, and W. Melnitchouk, 2017, "First Simultaneous Extraction of Spin-Dependent Parton Distributions and Fragmentation Functions from a Global QCD Analysis," Phys. Rev. Lett. **119**, 132001.

Fan, Zhouyou, Xiang Gao, Ruizi Li, Huey-Wen Lin, Nikhil Karthik, Swagato Mukherjee, Peter Petreczky, Sergey Syritsyn, Yi-Bo Yang, and Rui Zhang, 2020, "Isovector parton distribution functions of the proton on a superfine lattice," Phys. Rev. D **102**, 074504.

Fan, Zhouyou, Rui Zhang, and Huey-Wen Lin, 2021, "Nucleon gluon distribution function from $2 + 1 + 1$-flavor lattice QCD," Int. J. Mod. Phys. A **36**, 2150080.

Fan, Zhou-You, Yi-Bo Yang, Adam Anthony, Huey-Wen Lin, and Keh-Fei Liu, 2018, "Gluon Quasi-Parton-Distribution Functions from Lattice QCD," Phys. Rev. Lett. **121**, 242001.

Farrar, Glennys R., and Darrell R. Jackson, 1979, "Pion Form Factor," Phys. Rev. Lett. **43**, 246.

Favart, L., M. Guidal, T. Horn, and P. Kroll, 2016, "Deeply virtual meson production on the nucleon," Eur. Phys. J. A **52**, 158.

Feynman, R. P., 1972, *Photon-Hadron Interactions* (CRC Press, Boca Raton).

Feynman, Richard P., 1969, "Very High-Energy Collisions of Hadrons," Phys. Rev. Lett. **23**, 1415–1417.

Filippone, B. W, and Xiangdong Ji, 2001, "The spin structure of the nucleon," in *Advances in Nuclear Physics*, Vol. 26, edited by J. W. Negele and E. W. Vogt (Springer, New York), pp. 1.

Fritzsch, H., Murray Gell-Mann, and H. Leutwyler, 1973, "Advantages of the color octet gluon picture," Phys. Lett. **47B**, 365–368.

Gamberg, Leonard, Zhong-Bo Kang, Ivan Vitev, and Hongxi Xing, 2015, "Quasi-parton distribution functions: A study in the diquark spectator model," Phys. Lett. B **743**, 112–120.

Gao, Jun, Lucian Harland-Lang, and Juan Rojo, 2018, "The structure of the proton in the LHC precision era," Phys. Rep. **742**, 1–121.

Gao, Xiang, Luchang Jin, Christos Kallidonis, Nikhil Karthik, Swagato Mukherjee, Peter Petreczky, Charles Shugert, Sergey Syritsyn, and Yong Zhao, 2020, "Valence parton distribution of pion from lattice QCD: Approaching continuum," arXiv:2007.06590.

Geesaman, D. F., and P. E. Reimer, 2019, "The sea of quarks and antiquarks in the nucleon," Rep. Prog. Phys. **82**, 046301.

Gehrmann, T., E. W. N. Glover, T. Huber, N. Ikizlerli, and C. Studerus, 2010, "Calculation of the quark and gluon form factors to three loops in QCD," J. High Energy Phys. 06, 094.

Gehrmann, Thomas, Thomas Luebbert, and Li Lin Yang, 2014, "Calculation of the transverse parton distribution functions at next-to-next-to-leading order," J. High Energy Phys. 06, 155.

Gervais, Jean-Loup, and A. Neveu, 1980, "The slope of the leading Regge trajectory in quantum chromodynamics," Nucl. Phys. **B163**, 189–216.

Gockeler, M., R. Horsley, D. Pleiter, Paul E. L. Rakow, A. Schafer, G. Schierholz, and W. Schroers (QCDSF Collaboration), 2004, "Generalized Parton Distributions from Lattice QCD," Phys. Rev. Lett. **92**, 042002.

Gong, Ming, Yi-Bo Yang, Jian Liang, Andrei Alexandru, Terrence Draper, and Keh-Fei Liu (χQCD Collaboration), 2017, "Strange and charm quark spins from the anomalous Ward identity," Phys. Rev. D **95**, 114509.

Green, J. R., M. Engelhardt, S. Krieg, J. W. Negele, A. V. Pochinsky, and S. N. Syritsyn, 2014, "Nucleon structure from lattice QCD using a nearly physical pion mass," Phys. Lett. B **734**, 290–295.

Green, Jeremy, Karl Jansen, and Fernanda Steffens, 2018, "Nonperturbative Renormalization of Nonlocal Quark Bilinears for Parton Quasidistribution Functions on the Lattice Using an Auxiliary Field," Phys. Rev. Lett. **121**, 022004.

Green, Jeremy R., Karl Jansen, and Fernanda Steffens, 2020, "Improvement, generalization, and scheme conversion of Wilson-line operators on the lattice in the auxiliary field approach," arXiv:2002.09408.

Gribov, V. N., and L. N. Lipatov, 1972, "Deep inelastic ep scattering in perturbation theory," Yad. Fiz. **15**, 781 [Sov. J. Nucl. Phys. **15**, 438–450 (1972), https://www.osti.gov/biblio/4621331].

Gross, David J., and Frank Wilczek, 1973, "Ultraviolet Behavior of Non-Abelian Gauge Theories," Phys. Rev. Lett. **30**, 1343–1346.

Grozin, Andrey, Johannes M. Henn, Gregory P. Korchemsky, and Peter Marquard, 2016, "The three-loop cusp anomalous dimension in QCD and its supersymmetric extensions," J. High Energy Phys. 01, 140.

Grozin, Andrey G., 2005, "B-meson distribution amplitudes," Int. J. Mod. Phys. A **20**, 7451–7484.

Gupta, Rajan, David Daniel, and Jeffrey Grandy, 1993, "Bethe-Salpeter amplitudes and density correlations for mesons with Wilson fermions," Phys. Rev. D **48**, 3330–3339.

Hagler, Ph., 2010, "Hadron structure from lattice quantum chromodynamics," Phys. Rep. **490**, 49–175.

Hagler, Ph., B. U. Musch, J. W. Negele, and A. Schafer, 2009, "Intrinsic quark transverse momentum in the nucleon from lattice QCD," Europhys. Lett. **88**, 61001.

Hagler, Ph., *et al.* (LHPC Collaboration), 2008, "Nucleon generalized parton distributions from full lattice QCD," Phys. Rev. D **77**, 094502.

Hannaford-Gunn, A., R. Horsley, Y. Nakamura, H. Perlt, P. E. L. Rakow, G. Schierholz, K. Somfleth, H. Stüben, R. D. Young, and J. M. Zanotti, 2020, "Scaling and higher twist in the nucleon Compton amplitude," Proc. Sci. LATTICE2019, 278 [arXiv:2001.05090].

Harada, Koji, Atsushi Okazaki, and Masa-aki Taniguchi, 1996, "Mesons in the massive Schwinger model on the light cone," Phys. Rev. D **54**, 7656–7663.

Harindranath, A., and J. P. Vary, 1987, "Solving two-dimensional φ^4 theory by discretized light front quantization," Phys. Rev. D **36**, 1141–1147.

Harland-Lang, L. A., A. D. Martin, P. Motylinski, and R. S. Thorne, 2015, "Parton distributions in the LHC era: MMHT 2014 PDFs," Eur. Phys. J. C **75**, 204.

Hashimoto, Shoji, and Hideo Matsufuru, 1996, "Lattice heavy quark effective theory and the Isgur-Wise function," Phys. Rev. D **54**, 4578–4584.

Hatta, Yoshitaka, 2012, "Notes on the orbital angular momentum of quarks in the nucleon," Phys. Lett. B **708**, 186–190.

Hatta, Yoshitaka, Xiangdong Ji, and Yong Zhao, 2014, "Gluon helicity ΔG from a universality class of operators on a lattice," Phys. Rev. D **89**, 085030.

Hatta, Yoshitaka, Yuya Nakagawa, Feng Yuan, Yong Zhao, and Bowen Xiao, 2017, "Gluon orbital angular momentum at small x," Phys. Rev. D **95**, 114032.

Hatta, Yoshitaka, and Shinsuke Yoshida, 2012, "Twist analysis of the nucleon spin in QCD," J. High Energy Phys. 10, 080.

Heinzl, Th., St. Krusche, and E. Warner, 1991, "Non-trivial vacuum structure in light-cone quantum field theory," Nucl. Phys. **A532**, 429–434.

Henn, Johannes M., Gregory P. Korchemsky, and Bernhard Mistlberger, 2019, "The full four-loop cusp anomalous dimension in $\mathcal{N} = 4$ super Yang-Mills and QCD," arXiv:1911.10174.

Hobbs, T. J., 2018, "Quantifying finite-momentum effects in the quark quasidistribution functions of mesons," Phys. Rev. D **97**, 054028.

Hobbs, T. J., Bo-Ting Wang, Pavel M. Nadolsky, and Fredrick I. Olness, 2019, "Charting the coming synergy between lattice QCD and high-energy phenomenology," Phys. Rev. D **100**, 094040.

Hofstadter, Robert, 1956, "Electron scattering and nuclear structure," Rev. Mod. Phys. **28**, 214–254.

Holt, Roy J., and Craig D. Roberts, 2010, "Distribution functions of the nucleon and pion in the valence region," Rev. Mod. Phys. **82**, 2991–3044.

Hoodbhoy, Pervez, Xiangdong Ji, and Wei Lu, 1999, "Implications of color gauge symmetry for nucleon spin structure," Phys. Rev. D **59**, 074010.

Hoodbhoy, Pervez, Xiangdong Ji, and Wei Lu, 1998, "Quark orbital-angular-momentum distribution in the nucleon," Phys. Rev. D **59**, 014013.

't Hooft, Gerard, 1974, "A two-dimensional model for mesons," Nucl. Phys. **B75**, 461–470.

Horgan, R. R., *et al.*, 2009, "Moving NRQCD for heavy-to-light form factors on the lattice," Phys. Rev. D **80**, 074505.

Horsley, Roger, Yoshifumi Nakamura, Holger Perlt, Paul E. L. Rakow, Gerrit Schierholz, Kim Somfleth, Ross D. Young, and James M. Zanotti (QCDSF, UKQCD, and CSSM Collaborations), 2020, "Structure functions from the Compton amplitude," Proc. Sci. LATTICE2019, 137 [arXiv:2001.05366].

Hou, Tie-Jiun, *et al.*, 2019, "New CTEQ global analysis of quantum chromodynamics with high-precision data from the LHC," arXiv:1912.10053.

Ishikawa, Tomomi, Yan-Qing Ma, Jian-Wei Qiu, and Shinsuke Yoshida, 2016, "Practical quasi parton distribution functions," arXiv:1609.02018.

Ishikawa, Tomomi, Yan-Qing Ma, Jian-Wei Qiu, and Shinsuke Yoshida, 2017, "Renormalizability of quasiparton distribution functions," Phys. Rev. D **96**, 094019.

Izubuchi, Taku, Xiangdong Ji, Luchang Jin, Iain W. Stewart, and Yong Zhao, 2018, "Factorization theorem relating euclidean and light-cone parton distributions," Phys. Rev. D **98**, 056004.

Izubuchi, Taku, Luchang Jin, Christos Kallidonis, Nikhil Karthik, Swagato Mukherjee, Peter Petreczky, Charles Shugert, and Sergey Syritsyn, 2019, "Valence parton distribution function of pion from fine lattice," Phys. Rev. D **100**, 034516.

Jaffe, R. L., and Xiangdong Ji, 1991, "Chiral-Odd Parton Distributions and Polarized Drell-Yan Process," Phys. Rev. Lett. **67**, 552–555.

Jaffe, R. L., and Xiangdong Ji, 1992, "Chiral odd parton distributions and Drell-Yan processes," Nucl. Phys. **B375**, 527–560.

Jaffe, R. L., and Aneesh Manohar, 1990, "The g_1 problem: Fact and fantasy on the spin of the proton," Nucl. Phys. **B337**, 509–546.

Jaffe, R. L., and M. Soldate, 1982, "Twist-4 effects in electroproduction: Canonical operators and coefficient functions," Phys. Rev. D **26**, 49–68.

Ji, Xiangdong, 1992, "Gluon correlations in the transversely polarized nucleon," Phys. Lett. B **289**, 137–142.

Ji, Xiangdong, 1993, "The nucleon structure functions from deep inelastic scattering with electroweak currents," Nucl. Phys. **B402**, 217–250.

Ji, Xiangdong, 1995, "Infrared renormalons and power corrections in deep inelastic sum rules," Nucl. Phys. **B448**, 51–66.

Ji, Xiangdong, 1997a, "Deeply virtual Compton scattering," Phys. Rev. D **55**, 7114–7125.

Ji, Xiangdong, 1997b, "Gauge-Invariant Decomposition of Nucleon Spin," Phys. Rev. Lett. **78**, 610–613.

Ji, Xiangdong, 1998, "Off-forward parton distributions," J. Phys. G **24**, 1181–1205.

Ji, Xiangdong, 2003, "Viewing the Proton through 'Color' Filters," Phys. Rev. Lett. **91**, 062001.

Ji, Xiangdong, 2004, "Generalized parton distributions," Annu. Rev. Nucl. Part. Sci. **54**, 413–450.

Ji, Xiangdong, 2013, "Parton Physics on a Euclidean Lattice," Phys. Rev. Lett. **110**, 262002.

Ji, Xiangdong, 2014, "Parton physics from large-momentum effective field theory," Sci. China Phys. Mech. Astron. **57**, 1407–1412.

Ji, Xiangdong, 2017, "Proton tomography through deeply virtual Compton scattering," Natl. Sci. Rev. **4**, 213–223.

Ji, Xiangdong, 2020, "Fundamental properties of the proton in light-front zero modes," arXiv:2003.04478.

Ji, Xiangdong, and Chi-hong Chou, 1990, "QCD radiative corrections to the transverse spin structure function $g_2(x, Q^2)$: Nonsinglet operators," Phys. Rev. D **42**, 3637–3644.

Ji, Xiangdong, Lu-Chang Jin, Feng Yuan, Jian-Hui Zhang, and Yong Zhao, 2019, "Transverse momentum dependent parton quasidistributions," Phys. Rev. D **99**, 114006.

Ji, Xiangdong, and Chul-woo Jung, 2001, "Studying Hadronic Structure of the Photon in Lattice QCD," Phys. Rev. Lett. **86**, 208.

Ji, Xiangdong, Yizhuang Liu, and Yu-Sheng Liu, 2021 (to be published).

Ji, Xiangdong, Yizhuang Liu, and Yu-Sheng Liu, 2019, "Transverse-momentum-dependent PDFs from large-momentum effective theory," arXiv:1911.03840.

Ji, Xiangdong, Yizhuang Liu, and Yu-Sheng Liu, 2020, "TMD soft function from large-momentum effective theory," Nucl. Phys. **B955**, 115054.

Ji, Xiangdong, Yizhuang Liu, Andreas Schäfer, Wei Wang, Yi-Bo Yang, Jian-Hui Zhang, and Yong Zhao, 2020, "A hybrid renormalization scheme for quasi light-front correlations in large-momentum effective theory," arXiv:2008.03886.

Ji, Xiangdong, Yizhuang Liu, and Ismail Zahed, 2019, "Quasiparton distribution functions: Two-dimensional scalar and spinor QCD," Phys. Rev. D **99**, 054008.

Ji, Xiangdong, Jian-Ping Ma, and Feng Yuan, 2004, "QCD factorization for spin-dependent cross sections in DIS and Drell-Yan processes at low transverse momentum," Phys. Lett. B **597**, 299–308.

Ji, Xiangdong, Jian-Ping Ma, and Feng Yuan, 2005, "QCD factorization for semi-inclusive deep-inelastic scattering at low transverse momentum," Phys. Rev. D **71**, 034005.

Ji, Xiangdong, and M. J. Musolf, 1991, "Sub-leading logarithmic mass-dependence in heavy-meson form-factors," Phys. Lett. B **257**, 409–413.

Ji, Xiangdong, and Jonathan Osborne, 2001, "An analysis of the next-to-leading order corrections to the $g_T(=g_1+g_2)$ scaling function," Nucl. Phys. **B608**, 235–278.

Ji, Xiangdong, Andreas Schäfer, Xiaonu Xiong, and Jian-Hui Zhang, 2015, "One-loop matching for generalized parton distributions," Phys. Rev. D **92**, 014039.

Ji, Xiangdong, Andreas Schäfer, Feng Yuan, Jian-Hui Zhang, and Yong Zhao, 2016, "Spin decomposition of the electron in QED," Phys. Rev. D **93**, 054013.

Ji, Xiangdong, Peng Sun, Xiaonu Xiong, and Feng Yuan, 2015, "Soft factor subtraction and transverse momentum dependent parton distributions on the lattice," Phys. Rev. D **91**, 074009.

Ji, Xiangdong, Xiaonu Xiong, and Feng Yuan, 2012, "Proton Spin Structure from Measurable Parton Distributions," Phys. Rev. Lett. **109**, 152005.

Ji, Xiangdong, Xiaonu Xiong, and Feng Yuan, 2013, "Probing parton orbital angular momentum in longitudinally polarized nucleon," Phys. Rev. D **88**, 014041.

Ji, Xiangdong, and Feng Yuan, 2020, "Transverse spin sum rule of the proton," Phys. Lett. B **810**, 135786.

Ji, Xiangdong, Feng Yuan, and Yong Zhao, 2017, "Hunting the Gluon Orbital Angular Momentum at the Electron-Ion Collider," Phys. Rev. Lett. **118**, 192004.

Ji, Xiangdong, Feng Yuan, and Yong Zhao, 2020, "Proton spin after 30 years: What we know and what we don't," arXiv:2009.01291.

Ji, Xiangdong, and Jian-Hui Zhang, 2015, "Renormalization of quasiparton distribution," Phys. Rev. D **92**, 034006.

Ji, Xiangdong, Jian-Hui Zhang, and Yong Zhao, 2013, "Physics of the Gluon-Helicity Contribution to Proton Spin," Phys. Rev. Lett. **111**, 112002.

Ji, Xiangdong, Jian-Hui Zhang, and Yong Zhao, 2015, "Justifying the naive partonic sum rule for proton spin," Phys. Lett. B **743**, 180–183.

Ji, Xiangdong, Jian-Hui Zhang, and Yong Zhao, 2017, "More on large-momentum effective theory approach to parton physics," Nucl. Phys. **B924**, 366–376.

Ji, Xiangdong, Jian-Hui Zhang, and Yong Zhao, 2018, "Renormalization in Large Momentum Effective Theory of Parton Physics," Phys. Rev. Lett. **120**, 112001.

Jia, Shaoyang, and James P. Vary, 2019, "Valence structures of light and strange mesons from the basis light-front quantization framework," in," *Proceedings of the 18th International Conference on Hadron Spectroscopy and Structure (HADRON 2019), Guilin, Guangxi, China, 2019* (World Scientific, Singapore), https://doi.org/10.1142/9789811219313_0110.

Jia, Yu, Shuangran Liang, LiuJi Li, and Xiaonu Xiong, 2017, "Solving the Bars-Green equation for moving mesons in two-dimensional QCD," J. High Energy Phys. 11, 151.

Jia, Yu, Shuangran Liang, Xiaonu Xiong, and Rui Yu, 2018, "Partonic quasidistributions in two-dimensional QCD," Phys. Rev. D **98**, 054011.

Jia, Yu, and Xiaonu Xiong, 2016, "Quasidistribution amplitude of heavy quarkonia," Phys. Rev. D **94**, 094005.

Joó, Bálint, Joseph Karpie, Kostas Orginos, Anatoly Radyushkin, David Richards, and Savvas Zafeiropoulos, 2019a, "Parton distribution functions from Ioffe time pseudo-distributions," J. High Energy Phys. 12, 081.

Joó, Bálint, Joseph Karpie, Kostas Orginos, Anatoly V. Radyushkin, David G. Richards, Raza Sabbir Sufian, and Savvas Zafeiropoulos, 2019b, "Pion valence structure from Ioffe-time parton pseudodistribution functions," Phys. Rev. D **100**, 114512.

Joó, Bálint, Joseph Karpie, Kostas Orginos, Anatoly V. Radyushkin, David G. Richards, and Savvas Zafeiropoulos, 2020, "Parton distribution functions from Ioffe time pseudodistributions from lattice caclulations: Approaching the physical point," arXiv:2004.01687.

Kang, Zhong-Bo, Alexei Prokudin, Peng Sun, and Feng Yuan, 2016, "Extraction of quark transversity distribution and Collins fragmentation functions with QCD evolution," Phys. Rev. D **93**, 014009.

Kang, Zhong-Bo, and Jian-Wei Qiu, 2009, "Evolution of twist-3 multi-parton correlation functions relevant to single transverse-spin asymmetry," Phys. Rev. D **79**, 016003.

Karpie, Joseph, Kostas Orginos, Alexander Rothkopf, and Savvas Zafeiropoulos, 2019, "Reconstructing parton distribution functions from Ioffe time data: From Bayesian methods to neural networks," J. High Energy Phys. 04, 057.

Karpie, Joseph, Kostas Orginos, and Savvas Zafeiropoulos, 2018, "Moments of Ioffe time parton distribution functions from non-local matrix elements," J. High Energy Phys. 11, 178.

Kiptily, D. V., and M. V. Polyakov, 2004, "Genuine twist-3 contributions to the generalized parton distributions from instantons," Eur. Phys. J. C **37**, 105–114.

Kock, Arthur, Yizhuang Liu, and Ismail Zahed, 2020, "Pion and kaon parton distributions in the QCD instanton vacuum," arXiv:2004.01595.

Kogut, John B., and Davison E. Soper, 1970, "Quantum electrodynamics in the infinite momentum frame," Phys. Rev. D **1**, 2901–2913.

Konychev, Anton V., and Pavel M. Nadolsky, 2006, "Universality of the Collins-Soper-Sterman nonperturbative function in gauge boson production," Phys. Lett. B **633**, 710–714.

Korchemskaya, I. A., and G. P. Korchemsky, 1992, "On lightlike Wilson loops," Phys. Lett. B **287**, 169–175.

Korchemsky, G. P., and A. V. Radyushkin, 1987, "Renormalization of the Wilson loops beyond the leading order," Nucl. Phys. **B283**, 342–364.

Kovchegov, Yuri V., 1999, "Small-x F_2 structure function of a nucleus including multiple Pomeron exchanges," Phys. Rev. D **60**, 034008.

Kovchegov, Yuri V., and Eugene Levin, 2012, *Quantum Chromodynamics at High Energy*, Cambridge Monographs on Particle Physics, Nuclear Physics and Cosmology Vol. 33 (Cambridge University Press, Cambridge, England), pp. 1–350.

Kronfeld, Andreas S., and Douglas M. Photiadis, 1985, "Phenomenology on the lattice: Composite operators in lattice gauge theory," Phys. Rev. D **31**, 2939.

Kumericki, Kresimir, Simonetta Liuti, and Herve Moutarde, 2016, "GPD phenomenology and DVCS fitting," Eur. Phys. J. A **52**, 157.

Kuraev, E. A., L. N. Lipatov, and Victor S. Fadin, 1977, "Pomeranchuk singularity in non-Abelian gauge theories," Zh. Eksp. Teor. Fiz. **72**, 377 [Sov. Phys. JETP **45**, 199–204 (1977), https://www.osti.gov/biblio/5273201].

Lan, Jiangshan, Chandan Mondal, Shaoyang Jia, Xingbo Zhao, and James P. Vary, 2019, "Parton Distribution Functions from a Light Front Hamiltonian and QCD Evolution for Light Mesons," Phys. Rev. Lett. **122**, 172001.

Landry, F., R. Brock, G. Ladinsky, and C. P. Yuan, 2000, "New fits for the nonperturbative parameters in the CSS resummation formalism," Phys. Rev. D **63**, 013004.

Langnau, Alex, and M. Burkardt, 1993, "Ultraviolet regularization of light-cone Hamiltonian perturbation theory: Application to the anomalous magnetic moment of the electron $(g-2)$ in the light-cone gauge," Phys. Rev. D **47**, 3452–3464.

Leader, E., and C. Lorcé, 2014, "The angular momentum controversy: What's it all about and does it matter?," Phys. Rep. **541**, 163–248.

Lee, R. N., A. V. Smirnov, and V. A. Smirnov, 2010, "Analytic results for massless three-loop form factors," J. High Energy Phys. 04, 020.

Lenz, F., M. Thies, K. Yazaki, and S. Levit, 1991, "Hamiltonian formulation of two-dimensional gauge theories on the light cone," Ann. Phys. (N.Y.) **208**, 1–89.

Lepage, G. Peter, and Stanley J. Brodsky, 1979, "Exclusive processes in quantum chromodynamics: Evolution equations for hadronic wave functions and the form factors of mesons," Phys. Lett. **87B**, 359–365.

Lepage, G. Peter, and Paul B. Mackenzie, 1993, "On the viability of lattice perturbation theory," Phys. Rev. D **48**, 2250–2264.

Li, Hsiang-nan, 2016, "Nondipolar Wilson links for quasiparton distribution functions," Phys. Rev. D **94**, 074036.

Li, Hsiang-nan, and George F. Sterman, 1992, "The perturbative pion form factor with Sudakov suppression," Nucl. Phys. **B381**, 129–140.

Li, Ye, Duff Neill, and Hua Xing Zhu, 2020, "An exponential regulator for rapidity divergences," Nucl. Phys. **B960**, 115193.

Li, Ye, and Hua Xing Zhu, 2017, "Bootstrapping Rapidity Anomalous Dimensions for Transverse-Momentum Resummation," Phys. Rev. Lett. **118**, 022004.

Li, Zheng-Yang, Yan-Qing Ma, and Jian-Wei Qiu, 2019, "Multiplicative Renormalizability of Operators Defining Quasiparton Distributions," Phys. Rev. Lett. **122**, 062002.

Li, Zheng-Yang, Yan-Qing Ma, and Jian-Wei Qiu, 2020, "Extraction of next-to-next-to-leading-order PDFs from lattice QCD calculations," arXiv:2006.12370.

Lin, Huey-Wen, Jiunn-Wei Chen, Saul D. Cohen, and Xiangdong Ji, 2015, "Flavor structure of the nucleon sea from lattice QCD," Phys. Rev. D **91**, 054510.

Lin, Huey-Wen, Jiunn-Wei Chen, Zhouyou Fan, Jian-Hui Zhang, and Rui Zhang, 2020, "The valence-quark distribution of the kaon from lattice QCD," arXiv:2003.14128.

Lin, Huey-Wen, Jiunn-Wei Chen, Xiangdong Ji, Luchang Jin, Ruizi Li, Yu-Sheng Liu, Yi-Bo Yang, Jian-Hui Zhang, and Yong Zhao, 2018, "Proton Isovector Helicity Distribution on the Lattice at Physical Pion Mass," Phys. Rev. Lett. **121**, 242003.

Lin, Huey-Wen, W. Melnitchouk, Alexei Prokudin, N. Sato, and H. Shows, 2018, "First Monte Carlo Global Analysis of Nucleon Transversity with Lattice QCD Constraints," Phys. Rev. Lett. **120**, 152502.

Lin, Huey-Wen, and Rui Zhang, 2019, "Lattice finite-volume dependence of the nucleon parton distributions," Phys. Rev. D **100**, 074502.

Lin, Huey-Wen, *et al.*, 2018, "Parton distributions and lattice QCD calculations: A community white paper," Prog. Part. Nucl. Phys. **100**, 107–160.

Liu, K. F., S. J. Dong, Terrence Draper, D. Leinweber, J. H. Sloan, W. Wilcox, and R. M. Woloshyn, 1999, "Valence QCD: Connecting QCD to the quark model," Phys. Rev. D **59**, 112001.

Liu, Keh-Fei, 2000, "Parton degrees of freedom from the path integral formalism," Phys. Rev. D **62**, 074501.

Liu, Keh-Fei, 2017, "Evolution equations for connected and disconnected sea parton distributions," Phys. Rev. D **96**, 033001.

Liu, Keh-Fei, 2020, "Parton degrees of freedom in PDFs from the hadronic tensor and large momentum effective theory," Phys. Rev. D **102**, 074502.

Liu, Keh-Fei, and Shao-Jing Dong, 1994, "Origin of Difference between u^- and d^- Partons in the Nucleon," Phys. Rev. Lett. **72**, 1790–1793.

Liu, Keh-Fei, 2016, "Parton distribution function from the hadronic tensor on the lattice," Proc. Sci. LATTICE2015, 115 [arXiv:1603.07352].

Liu, Wei-Yang, and Jiunn-Wei Chen, 2020, "Renormalon effects in quasi parton distributions," arXiv:2010.06623.

Liu, Yu-Sheng, Jiunn-Wei Chen, Luchang Jin, Ruizi Li, Huey-Wen Lin, Yi-Bo Yang, Jian-Hui Zhang, and Yong Zhao, 2018, "Nucleon transversity distribution at the physical pion mass from lattice QCD," arXiv:1810.05043.

Liu, Yu-Sheng, Wei Wang, Ji Xu, Qi-An Zhang, Jian-Hui Zhang, Shuai Zhao, and Yong Zhao, 2019a, "Matching generalized parton quasidistributions in the RI/MOM scheme," Phys. Rev. D **100**, 034006.

Liu, Yu-Sheng, Wei Wang, Ji Xu, Qi-An Zhang, Shuai Zhao, and Yong Zhao, 2019b, "Matching the meson quasidistribution amplitude in the RI/MOM scheme," Phys. Rev. D **99**, 094036.

Liu, Yu-Sheng, *et al.* (Lattice Parton Collaboration), 2020, "Unpolarized isovector quark distribution function from lattice QCD: A systematic analysis of renormalization and matching," Phys. Rev. D **101**, 034020.

Lorce, Cedric, Barbara Pasquini, Xiaonu Xiong, and Feng Yuan, 2012, "The quark orbital angular momentum from Wigner distributions and light-cone wave functions," Phys. Rev. D **85**, 114006.

Lübbert, Thomas, Joel Oredsson, and Maximilian Stahlhofen, 2016, "Rapidity renormalized TMD soft and beam functions at two loops," J. High Energy Phys. 03, 168.

Luke, Michael E., and Aneesh V. Manohar, 1992, "Reparametrization invariance constraints on heavy particle effective field theories," Phys. Lett. B **286**, 348–354.

Luo, Ming-xing, Tong-Zhi Yang, Hua Xing Zhu, and Yu Jiao Zhu, 2020, "Quark Transverse Parton Distribution at the Next-to-Next-to-Next-to-Leading Order," Phys. Rev. Lett. **124**, 092001.

Luo, Ming-Xing, Xing Wang, Xiaofeng Xu, Li Lin Yang, Tong-Zhi Yang, and Hua Xing Zhu, 2019, "Transverse parton distribution and fragmentation functions at NNLO: The quark case," J. High Energy Phys. 10, 083.

Luscher, Martin, and Stefan Schaefer, 2011, "Lattice QCD without topology barriers," J. High Energy Phys. 07, 036.

Ma, Yan-Qing, and Jian-Wei Qiu, 2018a, "Exploring Partonic Structure of Hadrons Using *Ab Initio* Lattice QCD Calculations," Phys. Rev. Lett. **120**, 022003.

Ma, Yan-Qing, and Jian-Wei Qiu, 2018b, "Extracting parton distribution functions from lattice QCD calculations," Phys. Rev. D **98**, 074021.

Ma, Zhi-Lei, Jia-Qing Zhu, and Zhun Lu, 2019, "Quasi parton distribution function and quasi generalized parton distribution of the pion meson in a spectator model," arXiv:1912.12816.

Mannel, Thomas, Winston Roberts, and Zbigniew Ryzak, 1992, "A derivation of the heavy quark effective Lagrangian from QCD," Nucl. Phys. **B368**, 204–217.

Manohar, Aneesh V., 1991, "Polarized Parton Distribution Functions," Phys. Rev. Lett. **66**, 289–292.

Manohar, Aneesh V., and Iain W. Stewart, 2007, "The zero-bin and mode factorization in quantum field theory," Phys. Rev. D **76**, 074002.

Manohar, Aneesh V., and Mark B. Wise, 2000, *Heavy Quark Physics*, Cambridge Monographs on Particle Physics, Nuclear Physics and Cosmology Vol. 10 (Cambridge University Press, Cambridge, England), pp. 1–191.

Maris, Pieter, and Craig D. Roberts, 2003, "Dyson-Schwinger equations: A tool for hadron physics," Int. J. Mod. Phys. E **12**, 297–365.

Martinelli, G., 1999, "Hadronic weak interactions of light quarks," Nucl. Phys. B, Proc. Suppl. **73**, 58–71.

Martinelli, G., C. Pittori, Christopher T. Sachrajda, M. Testa, and A. Vladikas, 1995, "A general method for nonperturbative renormalization of lattice operators," Nucl. Phys. **B445**, 81–108.

Martinelli, G., and Christopher T. Sachrajda, 1987, "A lattice calculation of the second moment of the pion's distribution amplitude," Phys. Lett. B **190**, 151–156.

McCartor, Gary, 1994, "Schwinger model in the light-cone representation," Z. Phys. C **64**, 349–354.

Messiah, A., 1979, *Quantum Mechanics*, Vol. 2 (North-Holland, Amsterdam).

Miller, Gerald A., 2007, "Charge Density of the Neutron," Phys. Rev. Lett. **99**, 112001.

Moch, S., J. A. M. Vermaseren, and A. Vogt, 2005, "Three-loop results for quark and gluon form factors," Phys. Lett. B **625**, 245–252.

Monahan, Christopher, and Kostas Orginos, 2017, "Quasi parton distributions and the gradient flow," J. High Energy Phys. 03, 116.

Monahan, Christopher, 2018a, "Recent developments in x-dependent structure calculations," Proc. Sci. LATTICE2018, 018 [arXiv: 1811.00678].

Monahan, Christopher, 2018b, "Smeared quasidistributions in perturbation theory," Phys. Rev. D **97**, 054507.

Mueller, Alfred H., 1985, "On the structure of infrared renormalons in physical processes at high energies," Nucl. Phys. **B250**, 327–350.

Mueller, Alfred H., 1994, "Soft gluons in the infinite momentum wave function and the BFKL Pomeron," Nucl. Phys. **B415**, 373–385.

Mulders, P. J., and R. D. Tangerman, 1996, "The complete tree-level result up to order $1/Q$ for polarized deep-inelastic leptoproduction," Nucl. Phys. **B461**, 197–237; **B484**, 538(E) (1997).

Müller, Dieter, 1994, "Conformal constraints and the evolution of the nonsinglet meson distribution amplitude," Phys. Rev. D **49**, 2525–2535.

Müller, Dieter, D. Robaschik, B. Geyer, F. M. Dittes, and J. Hořejši, 1994, "Wave functions, evolution equations and evolution kernels from light ray operators of QCD," Fortschr. Phys. **42**, 101–141.

Musch, B. U., Ph. Hagler, M. Engelhardt, J. W. Negele, and A. Schafer, 2012, "Sivers and Boer-Mulders observables from lattice QCD," Phys. Rev. D **85**, 094510.

Musch, Bernhard U., Philipp Hagler, John W. Negele, and Andreas Schafer, 2011, "Exploring quark transverse momentum distributions with lattice QCD," Phys. Rev. D **83**, 094507.

Nachtmann, Otto, 1973, "Positivity constraints for anomalous dimensions," Nucl. Phys. **B63**, 237–247.

Nakanishi, Noboru, and Haruichi Yabuki, 1977, "Null-plane quantization and Haag's theorem," Lett. Math. Phys. **1**, 371–374.

Nakanishi, Noboru, and Koichi Yamawaki, 1977, "A consistent formulation of the null-plane quantum field theory," Nucl. Phys. **B122**, 15–28.

Nam, Seung-il, 2017, "Quasi-distribution amplitudes for pion and kaon via the nonlocal chiral-quark model," Mod. Phys. Lett. A **32**, 1750218.

Nocera, Emanuele R., Richard D. Ball, Stefano Forte, Giovanni Ridolfi, and Juan Rojo (NNPDF Collaboration), 2014, "A first unbiased global determination of polarized PDFs and their uncertainties," Nucl. Phys. **B887**, 276–308.

Orginos, Kostas, Anatoly Radyushkin, Joseph Karpie, and Savvas Zafeiropoulos, 2017, "Lattice QCD exploration of parton pseudo-distribution functions," Phys. Rev. D **96**, 094503.

Pauli, Hans Christian, and Stanley J. Brodsky, 1985, "Discretized light-cone quantization: Solution to a field theory in one space and one time dimension," Phys. Rev. D **32**, 2001.

Penttinen, M., Maxim V. Polyakov, A. G. Shuvaev, and M. Strikman, 2000, "DVCS amplitude in the parton model," Phys. Lett. B **491**, 96–100.

Perry, Robert J., Avaroth Harindranath, and Kenneth G. Wilson, 1990, "Light-Front Tamm-Dancoff Field Theory," Phys. Rev. Lett. **65**, 2959–2962.

Politzer, H. David, 1973, "Reliable Perturbative Results for Strong Interactions?," Phys. Rev. Lett. **30**, 1346–1349.

Politzer, H. David, and Mark B. Wise, 1988, "Leading logarithms of heavy quark masses in processes with light and heavy quarks," Phys. Lett. B **206**, 681–684.

Polyakov, Alexander M., 1980, "Gauge fields as rings of glue," Nucl. Phys. **B164**, 171–188.

Qiu, Jian-wei, and George F. Sterman, 1991, "Single Transverse Spin Asymmetries," Phys. Rev. Lett. **67**, 2264–2267.

Radici, Marco, and Alessandro Bacchetta, 2018, "First Extraction of Transversity from a Global Analysis of Electron-Proton and Proton-Proton Data," Phys. Rev. Lett. **120**, 192001.

Radyushkin, A. V., 1998, "Double distributions and evolution equations," Phys. Rev. D **59**, 014030.

Radyushkin, A. V., 2017a, "Quasi-parton distribution functions, momentum distributions, and pseudo-parton distribution functions," Phys. Rev. D **96**, 034025.

Radyushkin, A. V., 2017b, "Nonperturbative evolution of parton quasi-distributions," Phys. Lett. B **767**, 314–320.

Radyushkin, A. V., 2017c, "Target mass effects in parton quasi-distributions," Phys. Lett. B **770**, 514–522.

Radyushkin, A. V., 2017d, "Pion distribution amplitude and quasi-distributions," Phys. Rev. D **95**, 056020.

Radyushkin, A. V., 2018a, "Quark pseudodistributions at short distances," Phys. Lett. B **781**, 433–442.

Radyushkin, A. V., 2018b, "One-loop evolution of parton pseudo-distribution functions on the lattice," Phys. Rev. D **98**, 014019.

Radyushkin, A. V., 2019a, "Theory and applications of parton pseudodistributions," arXiv:1912.04244.

Radyushkin, A. V., 2019b, "Structure of parton quasi-distributions and their moments," Phys. Lett. B **788**, 380–387.

Radyushkin, A. V., 2019c, "Generalized parton distributions and pseudodistributions," Phys. Rev. D **100**, 116011.

Ralston, John P., and Davison E. Soper, 1979, "Production of dimuons from high-energy polarized proton proton collisions," Nucl. Phys. **B152**, 109.

Rossi, G. C., and M. Testa, 2017, "Note on lattice regularization and equal-time correlators for parton distribution functions," Phys. Rev. D **96**, 014507.

Rossi, Giancarlo, and Massimo Testa, 2018, "Euclidean versus Minkowski short distance," Phys. Rev. D **98**, 054028.

Rothe, H. J., 1992, *Lattice Gauge Theories: An Introduction*, World Scientific Lecture Notes in Physics Vol. 43 (World Scientific, Singapore), https://doi.org/10.1142/1268.

Rutherford, E., 1919, "Collision of α particles with light atoms. IV. An anomalous effect in nitrogen," Philos. Mag. **37**, 581–587.

Samuel, Stuart, 1979, "Color zitterbewegung," Nucl. Phys. **B149**, 517–524.

Schaefer, Stefan, Rainer Sommer, and Francesco Virotta (ALPHA Collaboration), 2011, "Critical slowing down and error analysis in lattice QCD simulations," Nucl. Phys. **B845**, 93–119.

Schäfer, Thomas, and Edward V. Shuryak, 1998, "Instantons in QCD," Rev. Mod. Phys. **70**, 323–426.

Scimemi, Ignazio, and Alexey Vladimirov, 2018a, "Analysis of vector boson production within TMD factorization," Eur. Phys. J. C **78**, 89.

Scimemi, Ignazio, and Alexey Vladimirov, 2018b, "Systematic analysis of double-scale evolution," J. High Energy Phys. 08, 003.

Scimemi, Ignazio, and Alexey Vladimirov, 2019, "Non-perturbative structure of semi-inclusive deep-inelastic and Drell-Yan scattering at small transverse momentum," arXiv:1912.06532.

Shanahan, Phiala, Michael L. Wagman, and Yong Zhao, 2019, "Nonperturbative renormalization of staple-shaped Wilson line operators in lattice QCD," arXiv:1911.00800.

Shanahan, Phiala, Michael Wagman, and Yong Zhao, 2020, "Collins-Soper kernel for TMD evolution from lattice QCD," arXiv:2003.06063.

Shifman, Mikhail A., and M. B. Voloshin, 1987, "On annihilation of mesons built from heavy and light quark and $\bar{B}^0 \Leftrightarrow B^0$ oscillations," Yad. Fiz. **45**, 463 [Sov. J. Nucl. Phys. **45**, 292 (1987), https://inis.iaea.org/search/search.aspx?orig_q=RN:18034311#].

Shugert, Charles, Xiang Gao, Taku Izubichi, Luchang Jin, Christos Kallidonis, Nikhil Karthik, Swagato Mukherjee, Peter Petreczky, Sergey Syritsyn, and Yong Zhao, 2020, "Pion valence quark PDF from lattice QCD," in *Proceedings of the 37th International Symposium on Lattice Field Theory (Lattice 2019), Wuhan, Hubei, China, 2019*, edited by Heng-Tong Ding, https://inspirehep.net/conferences/1700247?ui-citation-summary=true.

Sivers, Dennis W., 1990, "Single spin production asymmetries from the hard scattering of point-like constituents," Phys. Rev. D **41**, 83.

Son, Hyeon-Dong, Asli Tandogan, and Maxim V. Polyakov, 2020, "Nucleon quasi-parton distributions in the large N_c limit," Phys. Lett. B **808**, 135665.

Srivastava, Prem P., and Stanley J. Brodsky, 2001, "Light-front-quantized QCD in the light-cone gauge: The doubly transverse gauge propagator," Phys. Rev. D **64**, 045006.

Stefanis, N. G., 1984, "Gauge-invariant quark two-point Green's function through connector insertion to $O(\alpha_s)$," Nuovo Cimento Soc. Ital. Fis. **83A**, 205.

Sterman, George F., 1993, *An Introduction to Quantum Field Theory* (Cambridge University Press, Cambridge, England).

Stewart, Iain W., and Yong Zhao, 2018, "Matching the quasiparton distribution in a momentum subtraction scheme," Phys. Rev. D **97**, 054512.

Sufian, Raza Sabbir, Colin Egerer, Joseph Karpie, Robert G. Edwards, Bálint Joó, Yan-Qing Ma, Kostas Orginos, Jian-Wei Qiu, and David G. Richards, 2020, "Pion valence quark distribution at large x from lattice QCD," arXiv:2001.04960.

Sufian, Raza Sabbir, Joseph Karpie, Colin Egerer, Kostas Orginos, Jian-Wei Qiu, and David G. Richards, 2019, "Pion valence quark distribution from matrix element calculated in lattice QCD," Phys. Rev. D **99**, 074507.

Sun, Peng, Joshua Isaacson, C. P. Yuan, and Feng Yuan, 2018, "Nonperturbative functions for SIDIS and Drell-Yan processes," Int. J. Mod. Phys. A **33**, 1841006.

Tanabashi, M., *et al.* (Particle Data Group), 2018, "Review of particle physics," Phys. Rev. D **98**, 030001.

Tangerman, R. D., and P. J. Mulders, 1995, "Intrinsic transverse momentum and the polarized Drell-Yan process," Phys. Rev. D **51**, 3357–3372.

Thomas, Anthony William, and Wolfram Weise, 2001, *The Structure of the Nucleon* (Wiley, Weinheim).

Uehara, S., *et al.* (Belle Collaboration), 2012, "Measurement of $\gamma\gamma^* \to \pi^0$ transition form factor at Belle," Phys. Rev. D **86**, 092007.

Vary, J. P., H. Honkanen, Jun Li, P. Maris, S. J. Brodsky, A. Harindranath, G. F. de Teramond, P. Sternberg, E. G. Ng, and C. Yang, 2010, "Hamiltonian light-front field theory in a basis function approach," Phys. Rev. C **81**, 035205.

Vladimirov, Alexey, 2018, "Structure of rapidity divergences in multi-parton scattering soft factors," J. High Energy Phys. 04, 045.

Vladimirov, Alexey A., 2017, "Correspondence between Soft and Rapidity Anomalous Dimensions," Phys. Rev. Lett. **118**, 062001.

Vladimirov, Alexey A., and Andreas Schäfer, 2020, "Transverse momentum dependent factorization for lattice observables," arXiv:2002.07527.

von Manteuffel, Andreas, Erik Panzer, and Robert M. Schabinger, 2020, "Analytic four-loop anomalous dimensions in massless QCD from form factors," arXiv:2002.04617.

Wakamatsu, Masashi, 2014, "Is gauge-invariant complete decomposition of the nucleon spin possible?," Int. J. Mod. Phys. A **29**, 1430012.

Wandzura, S., and Frank Wilczek, 1977, "Sum rules for spin dependent electroproduction: Test of relativistic constituent quarks," Phys. Lett. **72B**, 195–198.

Wang, Wei, Yu-Ming Wang, Ji Xu, and Shuai Zhao, 2019, "B-meson light-cone distribution amplitude from lattice QCD," arXiv:1908.09933.

Wang, Wei, Jian-Hui Zhang, Shuai Zhao, and Ruilin Zhu, 2019, "Complete matching for quasidistribution functions in large momentum effective theory," Phys. Rev. D **100**, 074509.

Wang, Wei, and Shuai Zhao, 2018, "On the power divergence in quasi gluon distribution function," J. High Energy Phys. 05, 142.

Wang, Wei, Shuai Zhao, and Ruilin Zhu, 2018, "Gluon quasidistribution function at one loop," Eur. Phys. J. C **78**, 147.

Weinberg, Steven, 1966, "Dynamics at infinite momentum," Phys. Rev. **150**, 1313–1318.

West, Geoffrey B., 1975, "Electron scattering from atoms, nuclei and nucleons," Phys. Rep. **18**, 263–323.

Wilson, Kenneth G., 1974, "Confinement of quarks," Phys. Rev. D **10**, 2445–2459.

Wilson, Kenneth G., Timothy S. Walhout, Avaroth Harindranath, Wei-Min Zhang, Robert J. Perry, and Stanislaw D. Glazek, 1994, "Nonperturbative QCD: A weak coupling treatment on the light front," Phys. Rev. D **49**, 6720–6766.

Wu, J. J., W. Kamleh, D. B. Leinweber, R. D. Young, and J. M. Zanotti, 2018, "Accessing high-momentum nucleons with dilute stochastic sources," J. Phys. G **45**, 125102.

Xiong, Xiaonu, Xiangdong Ji, Jian-Hui Zhang, and Yong Zhao, 2014, "One-loop matching for parton distributions: Nonsinglet case," Phys. Rev. D **90**, 014051.

Xiong, Xiaonu, Thomas Luu, and Ulf-G. Meißner, 2017, "Quasi-parton distribution function in lattice perturbation theory," arXiv:1705.00246.

Xiong, Xiaonu, and Jian-Hui Zhang, 2015, "One-loop matching for transversity generalized parton distribution," Phys. Rev. D **92**, 054037.

Xu, Shu-Sheng, Lei Chang, Craig D. Roberts, and Hong-Shi Zong, 2018, "Pion and kaon valence-quark parton quasidistributions," Phys. Rev. D **97**, 094014.

Yamawaki, Koichi, 1998, "Zero mode problem on the light front," in *Proceedings of the 10th Nuclear Summer School and Symposium (NuSS '97), Seoul, 1997*, pp. 116–199, https://inspirehep.net/conferences/970471.

Yang, Yi-Bo, Raza Sabbir Sufian, Andrei Alexandru, Terrence Draper, Michael J. Glatzmaier, Keh-Fei Liu, and Yong Zhao, 2017, "Glue Spin and Helicity in the Proton from Lattice QCD," Phys. Rev. Lett. **118**, 102001.

Yoon, Boram, Michael Engelhardt, Rajan Gupta, Tanmoy Bhattacharya, Jeremy R. Green, Bernhard U. Musch, John W. Negele, Andrew V. Pochinsky, Andreas Schäfer, and Sergey N. Syritsyn, 2017, "Nucleon transverse momentum-dependent parton distributions in lattice QCD: Renormalization patterns and discretization effects," Phys. Rev. D **96**, 094508.

Zhang, Jian-Hui, Jiunn-Wei Chen, Xiangdong Ji, Luchang Jin, and Huey-Wen Lin, 2017, "Pion distribution amplitude from lattice QCD," Phys. Rev. D **95**, 094514.

Zhang, Jian-Hui, Jiunn-Wei Chen, Luchang Jin, Huey-Wen Lin, Andreas Schäfer, and Yong Zhao, 2019, "First direct lattice-QCD calculation of the *x*-dependence of the pion parton distribution function," Phys. Rev. D **100**, 034505.

Zhang, Jian-Hui, Jiunn-Wei Chen, and Christopher Monahan, 2018, "Parton distribution functions from reduced Ioffe-time distributions," Phys. Rev. D **97**, 074508.

Zhang, Jian-Hui, Xiangdong Ji, Andreas Schäfer, Wei Wang, and Shuai Zhao, 2019, "Accessing Gluon Parton Distributions in Large Momentum Effective Theory," Phys. Rev. Lett. **122**, 142001.

Zhang, Jian-Hui, Luchang Jin, Huey-Wen Lin, Andreas Schäfer, Peng Sun, Yi-Bo Yang, Rui Zhang, Yong Zhao, and Jiunn-Wei Chen (LP3 Collaboration), 2019, "Kaon distribution amplitude from lattice QCD and the flavor SU(3) symmetry," Nucl. Phys. **B939**, 429–446.

Zhang, Qi-An, *et al.* (Lattice Parton Collaboration), 2020, "Lattice-QCD calculations of TMD soft function through large-momentum effective theory," arXiv:2005.14572.

Zhang, Rui, Carson Honkala, Huey-Wen Lin, and Jiunn-Wei Chen, 2020, "Pion and kaon distribution amplitudes in the continuum limit," arXiv:2005.13955.

Zhang, Rui, Huey-Wen Lin, and Boram Yoon, 2020, "Probing nucleon strange and charm distributions with lattice QCD," arXiv:2005.01124.

Zhao, Yong, 2018, "Unraveling high-energy hadron structures with lattice QCD," Int. J. Mod. Phys. A **33**, 1830033.

Zhao, Yong, 2020, "Theoretical developments of the LaMET approach to parton physics," Proc. Sci. LATTICE2019, 267.

Zhao, Yong, Keh-Fei Liu, and Yibo Yang, 2016, "Orbital angular momentum and generalized transverse momentum distribution," Phys. Rev. D **93**, 054006.

Zuazo, J. D., 2001, *Fourier Analysis*, Graduate Studies in Mathematics Vol. 29 (American Mathematical Society, Providence).